A Chemical Model to Investigate the Risk of Kidney Stone Formation in Humans in Terms of Urinary Supersaturation

Michael Geoffrey Hill

BSc(Hons) MSc

This thesis is presented for the degree of

Doctor of Philosophy

of

Murdoch University

2019

I declare that this thesis is my own account of my research and contains as its main content work which has not previously been submitted for a degree at any tertiary education institution.

Michael Hill

Abstract

The formation of kidney stones is a significant human health problem. Despite much research, the processes involved in calcium oxalate and calcium phosphate stone formation remain poorly understood and hence reliable procedures to prevent their formation have yet to be discovered.

A model has been developed to investigate the solution chemistry of the kidney filtration process. The model simulates both long and short nephrons and illustrates the different properties of the fluid in the nephrons of different lengths. It can be used to examine the effects of different physiologic conditions on nephron fluid properties. An important function of the model is its ability to calculate nephron fluid concentrations given a specified urine composition. The substance concentrations calculated by the model have been used as input for the Joint Expert Speciation System. The resultant log(SI) values and speciation profiles allow the behaviour of the fluid in the nephron to be assessed and changes in stone formation risk to be evaluated. A new criterion based on Ostwald's Rule of Stages is developed, indicating that brushite is the solid phase most likely to precipitate in the loop of Henle.

The model has been used to analyse for the first time fluid concentration variations and associated changes in stone formation risk for different values of blood and urine concentrations, hormone fluctuations and some pathological changes in reabsorption. These developments will help researchers

better understand the pathogenesis of kidney stone formation which may in turn lead to further improvements in the methodology of treatment of this disease.

Publication arising from this work:

Hill MG, Königsberger E, and May PM. Mineral precipitation and dissolution in the kidney. American Mineralogist, 2017. 102, 701 – 710. doi:10.2138/am-2016-5778.

Contents

List of Figures

List of Tables

Acknowledgements

I would like to express my gratitude to my supervisors, Professor Peter May and Dr Erich Königsberger. I would also like to thank Mr Kris Parker for technical assistance with computing issues and Professor John Bolton for spending time with me to explain various complexities of renal physiology.

Chapter 1

Introduction

1.1 Kidney Stones

Kidney stones are the result of the pathological formation of solid structures composed of crystalline or amorphous material within the urinary tract. Kidney stone formation is a worldwide problem, which is a painful condition for those who suffer from it [86LiL, 98GCG, 05ThH, 11Tis1, 11KLL]. About 10 % of the population will develop a kidney stone [98GCG, 98Pak]. There is a high associated economic cost, mainly as a result of the time taken off work and the hospital treatment required [81RSB, 86LiL, 98GCG, 06GrC, 11Tis1]. It has been estimated that for every 1000 hospital admissions, seven to ten are due to kidney stones [02BGS]. There is still a high and increasing incidence of the condition [86Ros, 93DBJ, 06Rob, 11Tis1, 12Rob1] so, although surgical treatments have improved, new non-surgical treatments are highly desirable.

1.2 Motivation for the Research

Despite scientific and clinical research for over a century, the fundamental mechanisms involved in the formation of some types of kidney stones are not well understood [94LBF, 95SoG, 98GCG, 06GrC, 14Mor, 15Tis]; thus, reliable methods of prevention have not been developed [95SoG, 98GCG, 06GrC, 15Tis, 15EWC]. An identifiable metabolic disorder that can be linked to stone formation is only found in around one in three stone formers; the rest are idiopathic [08LRA]. The mechanisms of development of uric acid, infection (struvite) and cystine stones are understood and methods to successfully treat them are available [11Tis1] but, the majority of calcium-based stone cases are idiopathic and their cause remains elusive.

The formation of a kidney stone involves the production of solid substances from the liquid that flows through the urinary tract. Such processes of precipitation from solutions are the domain of solution chemistry. Solution chemistry has made considerable progress in recent years. The problems of solubility and activity coefficients are now better understood, leading to the development of more powerful and accurate computer models of complex solutions [15May, 17MaR]. Such models are increasingly being applied to the investigation of biological fluids [06KoK, 17HKM]. Urine is particularly well suited, as it contains a large number of ionic substances in a complex solution.

While the location of clinically significant stones is normally in the calyx, it is widely assumed that the formation of calcium based stones has its origin in the nephron [11RAJ, 09TLF, 99HoT, 97Tis, 97Kok]. A detailed investigation of the changes in fluid composition throughout the length of the nephron may thus be helpful in understanding the processes taking place.

1.3 Objectives of the Research

Apply Physicochemical Techniques to the Kidney Stone Problem

The problem of kidney stone formation is investigated here by performing metal–ligand speciation calculations with the Joint Expert Speciation System (JESS). The objective is to improve understanding of the kidney stone formation process from a physicochemical point of view.

Identify Relevant Physiological Aspects

A description of the physiology suitable for translating into computer-processable form is developed. Data from the literature regarding concentrations of different substances found in the fluid within the kidney and urine (with specific reference to the differences seen between values for those who form kidney stones and those who do not) is collated and analysed.

Model Development

An extended computer model to put the kidney filtration process into the context of solution chemistry is developed. The particular aim is to investigate both long and short nephrons, in contrast to previous models which have been based on nephrons of a single length [11RAJ, 15Rob]. An enlarged set of substances is also considered.

Model Coupling

A novel filtration simulation model to calculate the changes in concentrations of dissolved substances in the fluid as it passes through the kidney is constructed. By altering various parameters of the model, different situations are investigated, corresponding to deviations from normal filtration and reabsorption processes which may lead to the formation of kidney stones. The sets of concentration data generated are then used as input to JESS generate speciation and supersaturation data.

Data Analysis

The sets of data generated are analysed for changes in supersaturation in order to gain insight into the stone formation process.

Chapter 2

Literature Review

2.1 Urolithiasis

Urolithiasis is defined as the formation of stones anywhere in the urinary tract [07PCC]. The term nephrolithiasis is more specific, as it refers to a stone within the kidney. Urolithiasis is the result of uncontrolled crystal formation when one or more substances precipitate from the urine solution during part of the urine formation process, creating a harmful solid structure. Urolithiasis is different to most other forms of biomineralization in that the healthy condition is characterized by the inhibition of deposition [92BrP]. A biological balance is required to ensure the biologically-controlled production of highly ordered solid structures where they are required, but prevent their formation where they would be damaging. For example, hydroxyapatite is an important component of bones and teeth [11SoG] and as a result of the requirement to form these structures, many biofluids, including blood plasma

Table 2.1: Mineral Names of Calculus Forming Substances

$Ca_5(PO_4)_3(OH)$	Hydroxyapatite
$CaHPO_4 \cdot 2\,H_2O$	Brushite
$Ca_8H_2(PO_4)_6 \cdot 5\,H_2O$	Octacalcium Phosphate
$CaC_2O_4 \cdot H_2O$	Whewellite
$CaC_2O_4 \cdot 2\,H_2O$	Weddellite
$MgNH_4PO_4 \cdot 6\,H_2O$	Struvite
$Ca_3(PO_4)_2$	Whitlockite

and urine, are supersaturated with respect to hydroxyapatite (HAP)[11SoG]. Thus HAP is also found in kidney stones.

2.2 Types of Kidney Stones

Classification of stones is a complex subject [93DBJ] as there are many charactistics that have been used to define the type of stone. A number of different substances are typically found in these solid structures, known as *calculi*, including calcium oxalate, hydroxyapatite, struvite, uric acid, cystine, brushite, whewellite and monosodium urate [78Fin]. Table 2.1 lists stone forming substances which are classified as minerals and gives their mineralogical names. Brushite is also known as dicalcium phosphate dihydrate, or, DCPD. Organic material makes up 2 % to 5 % of the mass of most stones [10BGK]. Urinary components present in trace amounts can dramatically modify the calculogenesis process [99GSC]. Tables 2.2, 2.3 and 2.4 show some ways by which the types of stones and stone forming patients have been categorized.

The following sections provide an overview of the main types of stones, including some approximate figures of their prevalence. Adding up the percentage

Table 2.2: Stone Type Classification [02GCR, 12GCG]

Type	Description
1	COM (attached)
2	COM (unattached)
3	COD
4	COD/HAP
5	HAP
6	Struvite
7	Brushite
8	Uric Acid
9	COM/Uric Acid
10	Cystine
11	Other

Table 2.3: Stone Classification from Daudon *et al.* (1993) [93DBJ]

Type	Description
I	Whewellite
II	Weddellite
III	Uric Acid
IV	Calcium and Magnesium Phosphates
V	Cystine
VI	Protein Rich
VII	Miscellaneous

figures shown here results in a figure greater than one hundred, due mainly to the fact that almost all stones contain more than substance, and thus may be put into more than one stone type category.

2.2.1 Calcium Based Stones

About 85 % of all kidney stones in humans are calcium-based [11Fav]. Such stones have a high recurrence rate [09TLF]. Of these calcium based stones, 30 % to 35 % are typically calcium oxalate, 60 % to 65 % are mixed calcium

Table 2.4: Stone Former Pheno-Types [15EWC]

Type	Pheno-Type
1	Idiopathic
2	Hydroxyapatite
3	Brushite
4	Small Bowel Resection
5	Ileostomy
6	Primary Hyperparathyroidism
7	Obesity Bypass
8	Renal Tubule Acidosis
9	Cystine
10	Primary Hyperoxaluria Type 1

oxalate and calcium phosphate and less than 5 % are pure calcium phosphate. In the case of many of the the mixed calcium oxalate and calcium phosphate stones, the calcium phosphate only makes up a small proportion of the stone [11Tis1], and it has been found that **almost all calcium oxalate stones contain at least a small amount of calcium phosphate** [84SmW, 93DBJ].

Calcium Oxalate Hydrates

At least 70 % of all stones have calcium oxalate as the main constituent [98GCG, 09TLF] and calcium phosphate makes up 1 % to 10 % of the stone. Calcium oxalate in kidney stones occurs in two forms, the monohydrate (COM) and the dihydrate (COD). The monohydrate is the major component of most calcium oxalate calculi [06KoK]. The solubility of calcium oxalate monohydrate is lower than that of calcium oxalate dihydrate and is essentially pH independent within the pH range of urine. It depends on ions that form complexes with calcium or oxalate, particularly citrate and

magnesium [06KoK, 98STK].

Calcium Phosphate

Calcium phosphate stones not only tend to form in the presence of increased calcium concentration but also as a result of an increase in pH, which decreases the solubility [76RoN]. The formation of pure calcium phosphate stones requires persistent alkaline urine [11Tis1]. Calcium phosphate becomes progressively more soluble as the pH decreases below 6 [95SoG, 12GCG], as lowering urinary pH reduces urinary PO_4^{3-} and OH^- in their unbound form [77Fin], reducing the ion product $(Ca^{2+})^5(OH^-)(PO_4^{3-})^3$. Types of calcium phosphates found in stones are hydroxyapatite ($Ca_5OH(PO_4)_3$), carbonate apatite ($Ca_{10}(PO_4CO_3OH)_6(OH)_2$), brushite ($CaHPO_4 \cdot 2\,H_2O$) and whitlockite ($Ca_3(PO_4)_2$) [97KoT]. Octacalcium phosphate and brushite have both been identified as a possible precusor in the formation of HAP stones [90Nan, 97KoT]. Macromolecules present may have an important influence on the type of calcium phosphate phase that precipitates [97Tis]. Around 10 % of stones are mainly hydroxyapatite, and 2 % mainly brushite [98GCG].

2.2.2 Magnesium Ammonium Phosphate

Magnesium ammonium phosphate, or struvite ($MgNH_4PO_4 \cdot 6\,H_2O$), stones are a common complication of urinary tract infections. This is because of urea-splitting bacteria, which increase the pH and NH_4^+ concentration [76RoN]. Typically, this type of stone also contains significant amounts of or-

ganic matter, hydroxyapatite [06GrC] and carbonate apatite [97BrK, 11Tis1, 16PrM]. Only around 15 % of stones are found to be composed mainly of struvite [98GCG].

2.2.3 Uric Acid and Urates

About 4 % to 15 % of stones are composed predominantly of uric acid [98GCG, 05CJR, 06GrC, 06Moe, 12GCG]. Uric acid stones form as a result of increased uric acid concentration and lower pH values [76RoN, 08Pak, 12GCG]. Uric acid becomes progressively less soluble at pH below 5.5 [82DeS, 95SoG, 12GCG].

2.2.4 Cystine

The formation of cystine stones is generally the result of genetic factors [06GrC]. Usual cystine excretion is around 0.05 g per 24 hours, while in cases of cystinuria, it may be in excess of 1 g [77Met]. Cystine-based stones account for about 1 % to 4 % of stones [98GCG, 00KWK, 06GrC, 06Moe]. Increasing the pH to above 7.5 using potassium citrate increases cystine solubility, but, at these pH levels, the formation of calcium phosphate stones becomes a risk [00KWK].

2.3 Stone Formation Promoters

Stone formation is not a continuous process, resulting from excretions exceeding static limits, but the result of relative combinations of factors, that increase the risk to a point where an event starts a pathological crystallization,

ultimately ending in the formation of a stone [08LRA, 11Tis1, 17Rob, 17Rod]. In the case of calcium oxalate crystal formation, urinary supersaturation with calcium oxalate monohydrate is in general never high enough to result in homogeneous nucleation so heterogeneous nucleation on a nucleating substrate is considered much more likely [95SoG, 12GCG]. Hydroxyapatite, brushite, uric acid and glycoproteins can readily serve as substrates for calcium oxalate monohydrate nucleation [81RSB, 95SoG, 97Tis, 99HoT, 09TLF, 12GCG]. Of these, the calcium phosphates have the highest capacity to enhance nucleation, with uric acid less so but greater than glycoproteins [12GCG]. Calcium phosphate is thus a principal promoter of calcium oxalate precipitation [81RSB, 97Tis]. The build up of calcium phosphate in the renal interstitial tissue is known as Randall's plaque. Section 2.9.7 gives further details. There is strong evidence that in many cases Randall's plaque is the primary agent underlying calcium oxalate kidney stone formation [08MGW, 09TLF, 11Tis1, 11CEW].

Almost all calcium oxalate stones show signs of having developed while attached to a surface within the kidney [11CEW]. In most cases the point of attachment is the papilla [95SoG, 09TLF]. An anti-adherent protective layer of glycosaminoglycans covering the internal renal walls is the most important factor controlling any papillary calculogenic process [95SoG]. Hence, most calcium oxalate stones seem to be formed on Randall's plaque, at places where the epithelial layer has been damaged. The mechanism of formation is thought to be as follows. A particle of COM, or a substance having compatible structure to COM, becomes attached to the papilla, where the covering

layer is damaged. Crystals then grow by nucleation and aggregation or agglomeration [95SoG]. Aggregates are groups of primary particles joined at their faces, while in agglomerates, the primary particles are joined at the edges or corners [90Nan]. As as a result of the configuration difference, aggregates have significantly less surface area than the sum of the surface areas of the consitiuent particles, but the surface area of an agglomeration is not much less than the sum of the surface areas of the constituent components. Thus, those crystals formed by agglomeration tends to have a higher rate of growth.

2.4 Stone Formation Inhibitors

Urine is a strong inhibitor of crystal growth and aggregation [81RSB]. The common constituents of urine increase the solubility of calcium oxalate over that in water [32Med, 58MVM]. Citrate [07PCC, 99ABG, 11Slo], glycosaminoglycans [99APC, 07PCC, 11Slo], hippuric acid [91GAB, 13AtG], phytate and phytic acid [98MSG, 11Slo], pyrophosphate [11Slo] and Tamm-Horsfall protein [81RSB, 11Tis1], have all been found to inhibit the formation of stones. Citrate is a particularly strong inhibitor of calcium oxalate formation through chelation of free calcium ions [08LRA]. Likewise, it is an inhibitor of crystal nucleation and growth [81Tis, 04KYY, 09ZuA]. Inorganic pyrophosphate, found in both blood plasma and urine, is also known to be an inhibitor of calcium phosphate precipitation [77FlR]. Phytate has been observed in substantially reduced amounts in stone formers urine [99GSC] and therefore is also sometimes said to be an inhibitor of stone formation.

Inhibitors are often more effective in preventing the formation of the thermodynamically more stable phases of a precipitating substance [90Nan]. This may enhance the formation of a less stable phase, for example in the formation of COD due to the supression of the formation of COM. This may explain why COD has been found in kidney stones, despite the fact that it is not considered to be a stable phase of calcium oxalate [80ToN, 98GCG, 11RAJ].

Rodgers *et al.* [06RAJ] have shown that the administration of a complex containing sodium, citrate, bicarbonate and tartrate reduces the calcium oxalate stone formation risk. Using a chemical speciation simulation, it was demonstrated that a $CaCitPO_4^{4-}$ species formed as the higher pH deprotonated $H_2PO_4^-$ and HPO_4^{2-} species. Thus, the therapeutic action of citrate in this case is due to the combination of the presence of citrate and raised pH. These factors allow the formation of this $CaCitPO_4^{4-}$ complex and simultaneously lower the available calcium ion concentration [06RAJ]. The administration of alkali reduces citrate reabsorption and thus increases urinary citrate [81BDF, 08Pak] and augments the inhibitory power of urinary macromolecules opposing crystal formation [11Tis1]. Potassium citrate reduces calcium excretion by increasing proximal tubule calcium reabsorption via reduction of net acid load and so can be used to treat hypocitraturia. This is of value as citrate inhibits apatite nucleation and growth [11Tis2] but the resultant increase in urinary pH increases calcium phosphate supersaturation. Thus, a recommended dosage is only enough to reduce urine ammonia by one half to two thirds [11CEW].

2.5 The Chemical Composition of Blood

Approximately half of the volume of blood is occupied by the three types of blood cells, the red blood cells, the white blood cells and the platelets. The liquid portion is called blood plasma. This fluid is made up of 90 % water and 10 % solutes. The composition of plasma is very complex. It contains a large variety of proteins, lipoproteins, hormones, nutrients, metabolites, waste products and inorganic ions. Proteins make up over 70 % of the solid residue [93LNC]. Appendix A gives data about the concentrations of substances dissolved in blood plasma.

2.6 Urine Composition

Urine is produced from blood plasma, via the filtration, reabsorption and secretion processes within the kidney. However, unlike blood plasma, the composition of urine varies greatly [07SAR]. Another major difference between urine and blood plasma, is that urine contains almost no proteins. Urine is typically about 95 % water [99Ker]. Appendix B provides data about urine composition.

2.7 The Kidney Filtration Process

Since the details of the changes in composition of the fluid as it undergoes the process of conversion from blood plasma to urine are not well known,

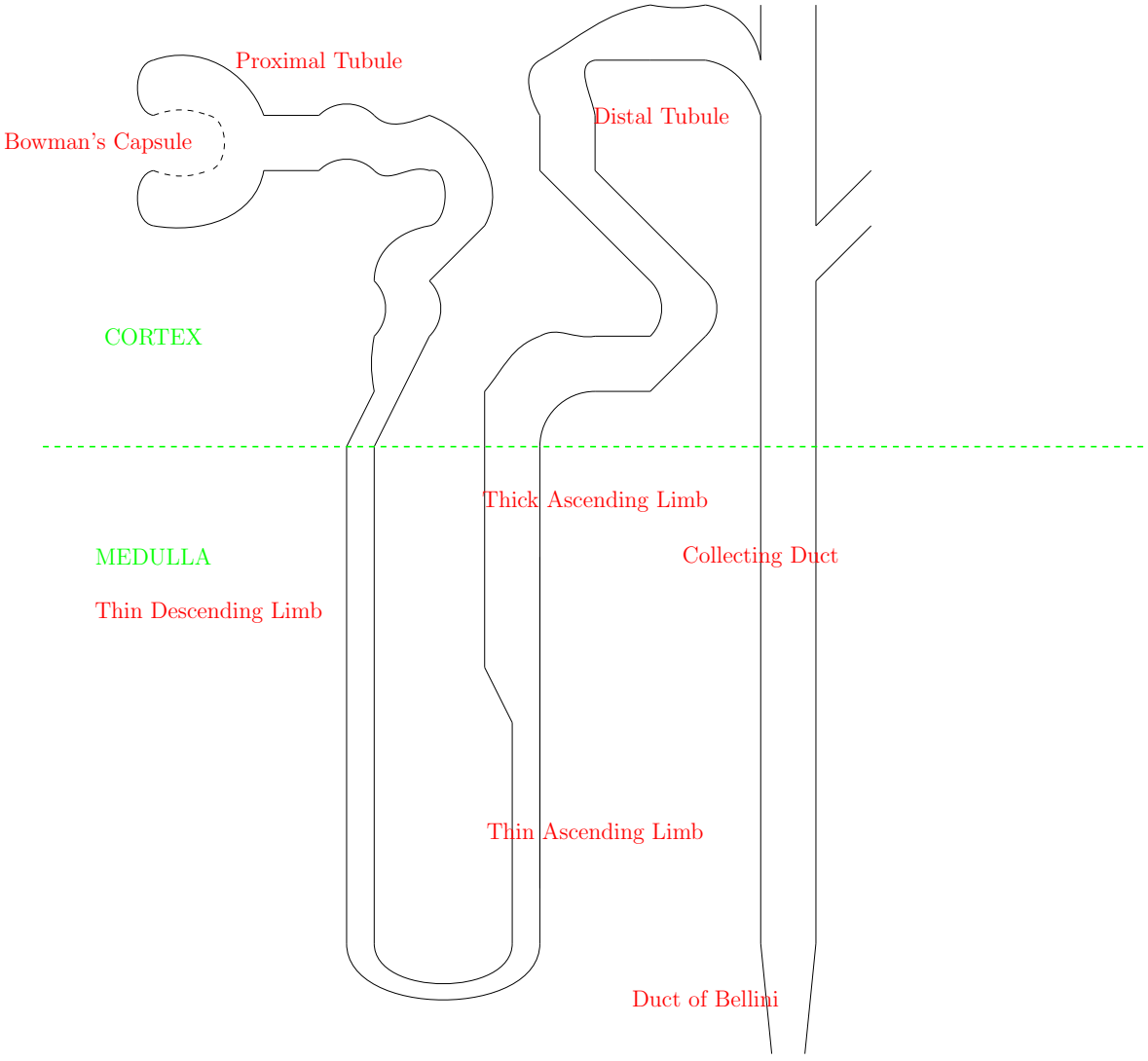

Figure 2.1: Schematic Diagram of a Nephron.

a literature review has been undertaken to assemble data about this process. The values collected have been used to build a model that describes how the chemical composition of the fluid changes as it passes through the kidney. Appendix C describes the anatomy and physiology of the kidney. This information is necessary to achieve the objective of this research. The development of the kidney-flow model developed in this work is described in Chapter 3.

2.7.1 Filtration, Reabsorption and Secretion

The kidney contains a large number of tubules, called nephrons, which perform the filtration process. See Appendix C for a description of the anatomy of the kidney and the details of nephron structure. At the start of each nephron, an ultrafiltration process separates the water and small molecule components of blood plasma and channels this fluid, called glomerular filtrate, into the tubule. Blood cells and larger molecules cannot generally pass into the nephron tubule. A nephron is made up of a number of sections (See Figure 2.1), each with different properties and functions. Table 2.5 lists the sections of the nephron and abbreviations that are commonly used when referring to them.

There is a large difference between the volume of fluid filtered through the kidneys and the volume of urine produced. Values are around 140 to 184 L per day (100 to 120 mL per minute) for glomerular filtration rate (GFR), 178.5 L per day for tubular reabsorption whereas only about 1.5 L per day of urine

Table 2.5: Nephron Sections and their Abbreviations

Bowman's Capsule	BC
Proximal Tubule	PT
Proximal Convoluted Tubule	PCT
Pars Recta	PR
Thin Descending Limb	tDL
Thin Ascending Limb	tAL
Thick Ascending Limb	TAL
Macula Densa	MD
Distal Tubule	DT
Distal Convoluted Tubule	DCT
Distal Section of the Distal Tubule	DTD
Connecting Tubule	CT
Collecting Duct	CD
Cortical Collecting Duct	CCD
Medullary Collecting Duct	MCD
Calyx	CX

is excreted [06GuH]. In other words, much of the water in the initial filtrate is reabsorbed. Thus, during the process of converting glomerular filtrate into urine, the fluid passing through the nephron undergoes significant changes in terms of the concentrations of the substances dissolved within it [06Ath2]. Although the main function of the tubular cells is to reabsorb substances that have passed through the glomerular filtration process, there are some substances that are actively secreted into the lumen. Examples of these are amino-hippuric acid, Tamm-Horsfall Protein, penicillin, creatinine, K^+ and H^+ ions [68BDS]. Secretion accounts for significant amounts of potassium and hydrogen ions found in the urine [00GuH]. The cells in different sections of the nephron have different sets of ion channels to perform these transport functions [12KuE]. Glomerular filtration is not regulated but is selective in terms of molecular size and charge. Tubular reabsorption is highly selective.

Most reabsorption takes place in the cortex [68BDS]. Tubular reabsorption includes passive and active mechanisms. Water is always reabsorbed by the passive mechanism of osmosis [68BDS]. Some substances are subject to a limit of how much the kidney can reabsorb so any amount over this limit will be excreted in the urine. Table 2.6 lists the transport maxima for some substances. Figure 2.2 illustrates the movement of substances into and out of the tubule in the different nephron sections.

Urinary Excretion =
Glomerular Filtration − *Tubular Reabsorption* + *Tubular Secretion* [06GuH]

Renal clearance is the amount of a substance removed from the plasma by the kidneys [68BDS]. The renal clearance of a solute x, C_x is defined as the volume of plasma passing through the kidneys from which all the solute has been removed in a unit of time.

Tables 2.7, 2.8, 2.9, 2.10, 2.11 and 2.12 illustrate some other estimates for changes in the fluid flowing through the nephron.

Table 2.6: Transport Maxima [06GuH]

Substance	Transport Maximum (min^{-1})
Glucose	375 mg
Phosphate	0.10 mmol
Sulfate	0.06mmol
Amino Acids	15mmol
Urate	15mg
Lactate	75mg
Plasma Protein	30mg

Table 2.7: Flow Rates [68BDS]

Blood Flow through Kidneys	1200 mL/min
Plasma Flow through Kidneys	700mL/min
Glomerular Filtrate	125 mL/min
Filtration Fraction	18 %

Table 2.8: Reabsorption (Approximate) Percentages of Filtered Load [68BDS]

Section	Water	Sodium	Urea
PT	80	80	50
LH	2	25	0
DT	20	5	5
CD	1	0	2

Table 2.9: Approximate Reabsorption Percentages ([1]:high ADH, [2]:low ADH) [99Ker]

	H_2O[1]	H_2O[2]	Na^+	K^+	PO_4^{2-}	Urea[1]	Urea[2]
PT	70	70	70	80	95	50	50
LH	5	4	20	5	–	–	–
DT,CD	24	13	9	5	–	–	–
Total	99	87	99	90	95	30	65

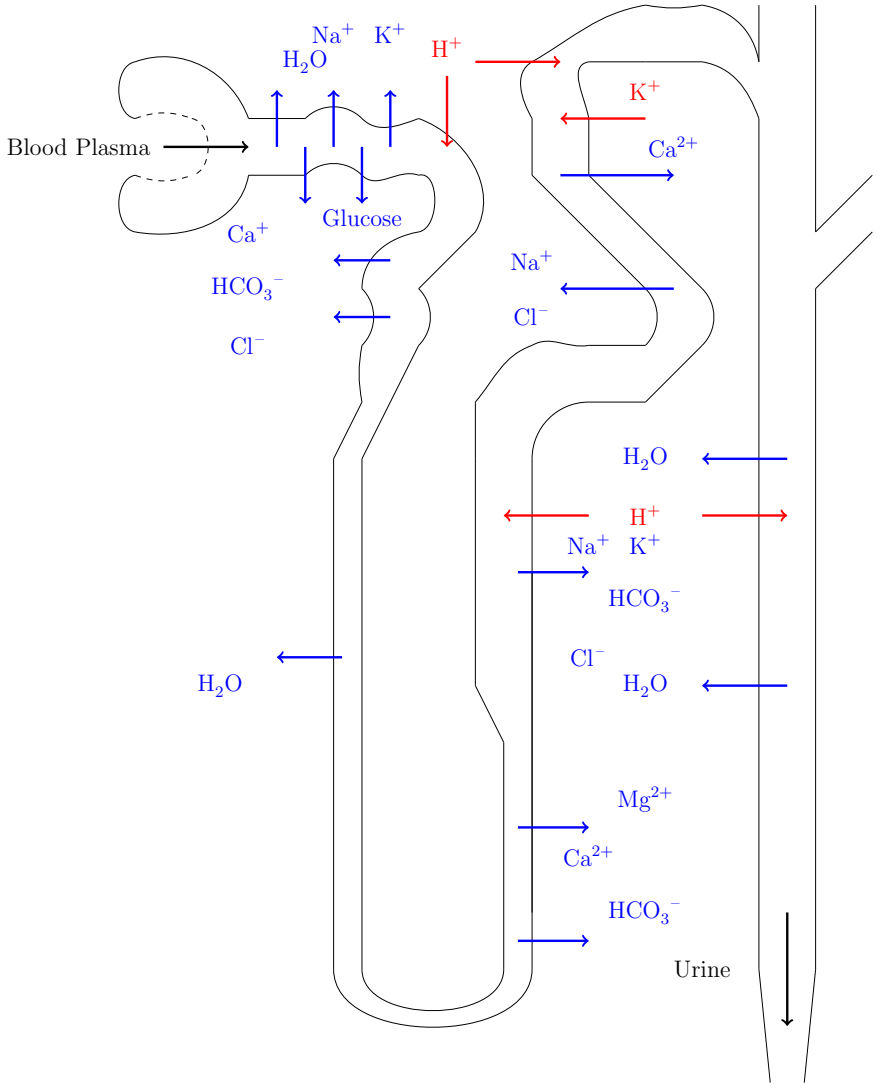

Figure 2.2: Main Nephron Substance Flows

Table 2.10: Filtration and Reabsorption of Different Substances, from [06GuH]

Substance	Filtered	Reabsorbed	Excreted
Glucose (g/day)	180	180	0
Bicarbonate (mEq/day)	4320	4318	2
Sodium (mEq/day)	25560	25410	150
Chloride (mEq/day)	19440	19260	180
Urea (g/day)	46.8	23.4	23.4
Creatinine (g/day)	1.8	0	1.8

Table 2.11: Composition Comparison[68BDS]

Substance	g/100mL Plasma	g/100mL Urine
Water	90 to 93	95
Proteins and other colloids	7 to 8	0
Urea	0.03	2
Uric acid	0.002	0.03
Glucose	0.1	0
Creatinine	0.001	0.1
Ammonia	0.0001	0.05
Sodium	0.32	0.6
Potassium	0.02	0.15
Calcium	0.01	0.015
Magnesium	0.0025	0.001
Chloride	0.37	0.6
Phosphate (inorganic)	0.003	0.012
Sulfate	0.003	0.18

Table 2.12: Difference per Day: Urine and Glomerular Filtrate [68BDS]

Substance	GF	Urine
Water (L)	180	1.5
Urea (g)	60	35
Glucose (g)	200	0
Sodium (g)	600	6
Potassium (g)	35	2
Calcium (g)	5	0.2

2.8 Processing of Different Substances

2.8.1 Volume Control via Water Reabsorption

The passive reabsorption of water is coupled mainly to the active transport of sodium [06GuH]. Peritubular reabsorption is dependent on ADH level (See Section C.5), and is around 124 mL/min [06GuH]. The figures given in Bell *et al.* [68BDS] are, 75 % of the filtered water is reabsorbed in the proximal tubule, 5 % in the loop of Henle and 20 % in the distal tubules. Other suggested values are: 65 % of the water is reabsorbed in the proximal tubule, 10 % to 15 % reabsorbed in the loop of Henle, 10 % in the distal convoluted tubule and 8 % to 9 % in the collecting tubule and collecting duct [09Kar].

Table 2.13: Water Volume (Litres) along the Nephron

Seg	[94LBF]	[97Kok]
BC	180	167
PT	–	58.5
tDL	36	8.4-33
tAL	–	–
TAL	–	8.4-33
MD	28.8	–
DT	8.6	8.4-33
CCD	–	–
MCD	–	–
CX	1.44	0.6-7.5

From the data in Table 2.12, 0.8 % of the filtered water is excreted. More data are given in Tables 2.8, 2.9 and 2.13. Where multiple published values that differ from each other have been found, an average value has been used

in the development of this model.

2.8.2 Sodium, Na^+

Sodium is the most abundant ion in the extracellular compartment. Plasma sodium concentration is normally between 140 to 145 mmol/L. Sodium and associated anions bicarbonate and chloride make up about 94 % of extracellular osmoles with glucose and urea contributing 3 to 5 % [06GuH].

Tables 2.9 and 2.14 show some literature data on sodium reabsorption. Up to 65 % [06GuH], 67 % [12KuE] or 75 % [68BDS] of the filtered sodium is reabsorbed in the proximal tubule. Around 20 % of Na^+ is reabsorbed in the thick ascending limb of the loop of Henle [12KuE]. Sodium is also reabsorbed in the connecting tubules and collecting ducts [12KuE]. From the values in Table 2.10, 99.4 % of the filtered sodium is reabsorbed and 0.6 % is excreted.

Table 2.14: Sodium Concentration along the Nephron (mmol/L)

Seg	[09TLF]	[11RAJ]	[94LBF]	[96AMC]	[97Kok]
BC	–	135	–	143	136-145
PT	–	135	139	146	140-150
tDL	–	–	–	–	300-870
tAL	–	278	–	355	–
TAL	–	–	–	–	73
MD	–	79	82	–	–
DT	–	93	96	49	30-50
CCD	–	94	–	164	–
MCD	94	109	106	73	–
CX	109	–	–	164	45-582

From the data in Table 2.12, 1 % of the filtered sodium is excreted. The

values from the paper by Asplin *et al.* [96AMC] shown in Table 2.14 are for rats.

2.8.3 Potassium, K^+

Potassium is reabsorbed in the proximal tubule and excreted into the distal tubule [68BDS]. As with sodium, up to 80 % is reabsorbed in the proximal convoluted tubule and 20 % is reabsorbed in the thick ascending limb of the loop of Henle [12KuE]. Plasma contains 4.2 mmol/L potassium. Glomerular filtration produces 756 mmol per day. Of this, 65 %, or 491 mmol, is reabsorbed in the proximal tubule, 27 %, 204 mmol, is reabsorbed in the ascending limb of the loop of Henle. Twelve percent of the amount filtered, or 92 mmol is excreted [06GuH].

Table 2.15: Potassium Concentration along the Nephron (mmol/L)

Segment	[09TLF]	[11RAJ]	[94LBF]	[99HoT]	[97Kok]
BC	–	3.8	–	–	3.6-4.8
PT	–	3.0	3.2	3.20	4-5.3
tDL	–	–	–	–	36-43
tAL	–	13.8	–	–	–
TAL	–	–	–	–	36-43
MD	–	0.90	0.95	0.95	–
DT	–	58.0	22.5	22.5	1-2
CCD	–	53.0	–	–	–
MCD	53	63.7	63.7	63.7	–
CX	63.7	–	–	–	20-260

The distal and collecting tubules can excrete or reabsorb potassium depending on whether there is too much or too little in the diet [00GuH]. Principal

cells (See Section C.2.4) make up 90 % of the epithelial cells in these regions and are responsible for potassium secretion. Acidosis decreases potassium secretion and alkalosis increases potassium secretion [06Ath2]. Having been transported into the cells by the ATPase pump, the potassium ions will passively diffuse into the lumen. The luminal membrane is highly permeable to potassium. Four percent, or 31 mmol, is on average excreted in the distal tubule and collecting tubule [06GuH]. Thus, from the data in Tables 2.9, 2.12 and 2.15, 5.7 % to 12 % of the filtered potassium is excreted.

2.8.4 Calcium, Ca^{2+}

Of the total amount of calcium in the body, 0.1 % occurs in the extracellular fluid, 1 % in cells and the rest in the bones [06GuH]. Extracellular calcium concentration is very tightly regulated [06GuH]. Plasma calcium concentration is ≈2.5 mmol/L, of which about 50 % is in ionised form, 40 % is bound to proteins and 10 % in the form of complexes with citrate and phosphate and similar ligands [06GuH]. Thus, about 50 % of plasma calcium is filterable by the glomerulus. Calcium reabsorption along the nephron is similar to the case of sodium. Around 95 % to 99 % is reabsorbed and about 1 % to 5 % excreted. Sixty-five percent of that is reabsorbed in the proximal tubule, 20 % to 30 % in the loop of Henle, 4 % to 9 % in the distal tubule or collecting duct. The descending and thin ascending limbs of the loop of Henle have low calcium permeability [90BuL, 92YaL]. Another set of estimates is 65 % is reabsorbed in the proximal tubule, 20 % in the thick ascending limb and 10 % in the distal tubule [93FrG]. About 10 % of the filtered calcium is re-

absorbed in the distal convoluted tubule, and together with the reabsorption in the thick ascending limb these two sites fine tune the regulation of calcium concentrations [90BuL]. By the end of the thick ascending limb of the loop of Henle, 90 % of the filtered amount of calcium has been reabsorbed [12KuE].

From the data in Tables 2.12 and 2.16, 4 % of the filtered calcium is excreted.

Table 2.16: Calcium Concentration along the Nephron (mmol/L)

Seg	[09TLF]	[11RAJ]	[94LBF]	[96AMC]	[97Kok]
BC	–	1.50	–	1.58	1.45
PT	–	2.78	2.78	1.75	1.8
tDL	–	–	–	–	3.0 - 3.7
tAL	–	3.47	–	3.03	–
TAL	–	–	–	–	0.92
MD	–	1.32	1.32	–	–
DT	–	0.94	1.04	0.5	0.21 - 0.5
CCD	–	1.60	–	0.84	–
MCD	1.6	4.50	4.50	0.77	–
CX	4.5	–	–	0.66	0.5 - 7.5

Idiopathic calcium oxalate stone formers have lower proximal tubule calcium reabsorption, hence the fluid in the thin limb of the loop of Henle has a higher calcium concentration [11CEW].

About 1.5 % of the filtered calcium is reabsorbed in the collecting duct [93FrG]. Calcium concentration in the collecting duct is estimated to be 1.48 times that of in final urine [97Tis]. Parathyroid hormone (PTH) increases calcium reabsorption in the thick ascending limb, distal convoluted tubule and cortical segment of the collecting duct [90BuL, 92YaL, 06GuH]. Increased phosphate levels stimulate PTH secretion, thus increasing calcium

reabsorption and reducing urinary calcium levels [92YaL]. An increase in protein intake increases urinary calcium, partially due to lowering pH. This protein effect is increased in stone forming patients [92YaL]. Lower pH reduces calcium reabsorption [00GuH]. An increase in sodium intake increases calcium excretion [05AlR]. Metabolic acidosis increases calcium excretion, and metabolic alkalosis decreases calcium excretion, the effects here take place in the distal part of the nephron, and are as a result of the link between calcium and bicarbonate transport [92YaL]. Chronic metabolic acidosis results in hypercalciuria [67LLL, 79SWD, 89LGP, 90CBK]. Increased plasma magnesium concentration results in an increase in calcium, magnesium and sodium excretion. Calcium transport in the loop of Henle is reduced with higher magnesium concentrations [92YaL]. Urinary calcium excretion is not constant throughout the day, but peaks around midday [92YaL] so, stone formation risk will be higher then.

2.8.5 Magnesium, Mg^{2+}

Magnesium plasma concentration is around 0.9 mmol/L, but only about 0.4 mmol/L is not bound to proteins. Of that filtered by the glomerulus, 25 % is reabsorbed in the proximal tubule, 65 % in the loop of Henle and less than 5 % in the distal and collecting tubules. Regulation is achieved by changing the rate of absorption [00GuH]. Magnesium is also reabsorbed in the collecting duct. Magnesium concentration in the collecting duct is estimated to be 1.1 times that of in final urine [97Tis]. Some estimates for magnesium concentration changes are shown in Table 2.17.

Table 2.17: Magnesium Concentration along the Nephron (mmol/L)

Seg	[09TLF]	[11RAJ]	[94LBF]	[96AMC]	[97Kok]
BC	–	0.54	–	–	0.45-1.00
PT	–	0.19	0.09	–	0.8-1.8
tDL	–	–	–	–	5.2-7
tAL	–	0.24	–	2.03	–
TAL	–	–	–	–	0.3-0.7
MD	–	0.12	0.12	–	–
DT	–	0.40	0.41	–	0.13-0.7
CCD	–	1.45	–	–	–
MCD	1.45	3.85	3.85	–	–
CX	3.85	–	–	–	0.5-12.5

2.8.6 Chloride, Cl^-

The negative chloride ions, are transported passively through the paracellular pathway, as a result of sodium reabsorption and also reabsorbed as a result of a concentration gradient that results from tubule water reabsorption [97GuH]. The amount of chloride reabsorbed in the proximal tubule is slightly less than the 65 % value for sodium [97GuH]. Chloride variations along the nephron are shown in Table 2.18. Chloride follows sodium, but the values are typically a little lower. The amount of chloride plus the amount of bicarbonate is approximately equal to the amount of sodium. In other words, tubule chloride concentration is approximately the sum of the potassium and sodium concentrations less the bicarbonate concentration [96AMC]. From the data in Table 2.10, 99.07 % of the filtered chloride is reabsorbed and 0.93 % is excreted.

Table 2.18: Chloride Concentration along the Nephron (mmol/L)

Seg	[11RAJ]	[96AMC]
BC	139	–
PT	139	–
tDL	–	–
tAL	293	377
TAL	–	–
MD	101	–
DT	145	–
CCD	–	–
MCD	–	–
CX	–	–

2.8.7 Phosphate, PO_4^{3-}

Of the total amount of phosphate in the body, 85 % occurs in the bones, 14 % in the cells and 1 % in the extracellular fluid [06GuH]. Unlike in the case of calcium, extracellular phosphate concentration is not as closely regulated [06GuH]. Plasma phosphate appears mainly in the two forms HPO_4^{2-} and $H_2PO_4^-$, with the ratio between the two around 4 so $[HPO_4^{2-}] \approx 1.05$ mmol/L and $[H_2PO_4^-] \approx 0.26$ mmol/L [92YaL, 06GuH]. Phosphate excretion takes place via an overflow mechanism due to a transport maximum of around 0.1 mmol/min. An extracellular concentration of 0.8 mmol/L results in a tubular load of 0.1 mmol/min (at a glomerular filtration rate of 125 mL/min). Thus a value above 0.8 leads to phosphate excretion [06GuH]. Around 20 % of the filtered load of phosphate is excreted [84NTM, 92YaL]. Eighty percent of the filtered phosphate is reabsorbed in the proximal tubule [84NTM]. Most of the reabsorption is within the early part of the proximal convoluted tubule, it continues in the pars recta, but at a rate in proportion

to that of sodium and water [92YaL]. The descending and thin ascending limbs of the loop of Henle have low phosphate permeability [90BuL]. Phosphate excretion is around 140 mmol per 24 hours [94LBF].

Table 2.19: Phosphate Concentration along the Nephron (mmol/L)

Seg	[09TLF]	[11RAJ]	[94LBF]	[96AMC]	[97Kok]
BC	–	0.80	–	2.1	0.85-3.3
PT	–	0.80	1.00	2.2	1.3-2.2
tDL	–	–	–	–	0.8-48
tAL	–	1.00	–	4.3	–
TAL	–	–	–	–	0.8-18
MD	–	1.00	1.25	–	–
DT	–	3.34	4.17	8.2	0.8-18
CCD	–	12.1	–	–	–
MCD	12.1	32.3	32.3	–	–
CX	32.3	–	–	219	5-75

Parathyroid hormone increases phosphate excretion by reducing the maximal transport rate [92YaL]. An increase in the plasma concentration of phosphate will cause an increase in the level of parathyroid hormone [06GuH], thus reducing the plasma concentration via urinary excretion. In the absence, or at low levels, of parathyroid hormone, phosphate is reabsorbed in the distal convoluted tubule and collecting duct [92YaL]. Some phosphate nephron concentrations from the literature are shown in Table 2.19.

2.8.8 Oxalate, $C_2O_4^{2-}$

As well as being absorbed from food, oxalate (like uric acid) is a metabolic end product [78Wil, 02BGS, 06KJA]. Dietary intake only accounts for about

10 % of normal urinary output [02BGS]. Vitamin D promotes intestinal absorption of oxalate, and protein and vitamin D increases calcium absorption [77Fin]. There is evidence that some calcium oxalate stone formers both hyperabsorb and under-produce oxalate [77Fin]. Oxalate is reabsorbed in the early proximal tubule and resecreted in the late proximal tubule [04Rob, 15Rob]. It is assumed that there is no reabsorption or secretion of oxalate after the proximal tubule [96AMC]. Some published estimates of oxalate nephron concentrations are shown in Table 2.20.

Table 2.20: Oxalate Concentration along the Nephron (mmol/L)

Seg	[04Rob]	[09TLF]	[11RAJ]	[94LBF]	[99HoT]	[97Kok]
BC	0.002	–	0.0015	–	–	0.0007-0.004
PT	0.007	–	0.01	0.010	0.01	0.0017-0.017
tDL	–	–	–	–	–	0.003-0.119
tAL	0.022	–	0.013	–	–	–
TAL	–	–	–	–	–	0.003-0.119
MD	–	0.013	0.013	–	0.013	–
DT	0.022	–	0.04	0.04	0.04	0.003-0.119
CCD	0.022	–	0.12	–	–	–
MCD	–	0.12	0.32	0.32	0.32	–
CX	0.22	0.32	–	–	–	0.1-1.0

2.8.9 Sulfate, SO_4^{2-}

Sulfate is mainly reabsorbed in the proximal tubule. Only 5 % to 20 % of the filtered load of sulfate is excreted in the urine. The reabsorption mechanism normally works close to the maximal rate and thus if plasma sulfate concentration increases, this is exceeded and the extra sulfate is excreted [01BeS]. As with urea, some sulfate diffuses back through the tubule cells,

along with the reabsorption of water [32HaJ]. In the proximal tubule, 80 to 90 mmol per 24 hours are reabsorbed [94LBF]. Some published sulfate nephron concentrations are shown in Table 2.21.

Table 2.21: Sulfate Concentration along the Nephron (mmol/L)

Seg	[09TLF]	[11RAJ]	[94LBF]	[96AMC]
BC	–	1.4	–	0.5
PT	–	3.1	3.3	0.34
tDL	–	–	–	–
tAL	–	3.9	–	0.603
TAL	–	–	–	–
MD	–	3.9	4.2	–
DT	–	13.0	13.8	0.34
CCD	–	7.8	–	1.16
MCD	7.8	20.8	20.8	1.34
CX	20.8	–	–	7.0

2.8.10 Citrate, $C_6H_5O_7^{3-}$

Citrate reabsorption in the proximal tubule is around 75 % [94LBF] to 78 % [96AMC]. In humans, 65 % to 90 % of the filtered citrate is reabsorbed, therefore 10 % to 35 % is excreted [90Ham]. Citrate reabsorption is increased by acidosis [09ZuA], thus, urinary citrate levels are higher at higher urinary pH levels [11Tis2]. It is assumed that there is no reabsorption or secretion of citrate after the proximal tubule [96AMC]. Some citrate nephron concentrations found in the literature are shown in Table 2.22.

2.8.11 Creatinine

Creatinine is filtered and not reabsorbed [97GuH].

Table 2.22: Citrate Concentration along the Nephron (mmol/L)

Seg	[09TLF]	[11RAJ]	[94LBF]	[96AMC]	[97Kok]
BC	–	0.07	–	–	0.09
PT	–	0.09	0.08	–	0.002-0.14
tDL	–	–	–	–	0.003-0.87
tAL	–	0.11	–	0.13	–
TAL	–	–	–	–	0.003-0.87
MD	–	0.11	0.10	–	–
DT	–	0.37	0.35	–	0.003-0.87
CCD	–	1.21	–	–	–
MCD	1.21	3.21	3.21	–	–
CX	3.21	–	–	–	0.1-7.5

2.8.12 Urea, $CO(NH_2)_2$

Renal nitrogen excretion is mainly via urea and ammonia; other forms make up less than 1 % of excreted nitrogen [15WMS]. Urea is the dominant urinary contributor to osmolarity [12BaY]. Urea is passively reabsorbed, as a result of the concentration gradient formed by water reabsorption and the electroneutral nature of this chemical species in solution. As the tubule is less permeable to urea than it is to water, somewhere between 50 % and 70 % of the urea that is filtered is reabsorbed, the remainder remains in the tubule and is excreted in the urine [97GuH, 15WMS]. The concentration of urea in urine can be up to 100 times that in plasma [12BaY]. The data in Tables 2.10 and 2.12, indicate that about 50 % of the filtered urea is reabsorbed and 50 % is excreted.

2.8.13 Urate, $C_5H_3N_4O_3^-$

Less than 5 % of the urate in plasma is bound to proteins so most of it is filterable [05CJR]. Most of the urate reabsorption takes place in the proximal convoluted tubule [77Fan] where, at first, almost all (99 %) is reabsorbed. Then about 50 % of that filtered is secreted, followed by around 80 % of the amount secreted being reabsorbed again [05CJR]. Ten to 12 % of the filtered urate is excreted [77Fan, 05CJR]. Table 2.23 shows some urate concentration ranges from the literature.

Table 2.23: Urate Concentrations along the Nephron (mmol/L)

Seg	[96AMC]	[97Kok]
BC	0.034–0.055	0.17-0.30
PT	0.027 –0.047	0.03-0.12
tDL	–	0.14-0.84
tAL	0.067–0.143	0.14-0.84
TAL	–	–
MD	–	–
DT	0.072–0.287	0.14-0.84
CCD	0.499–2.307	–
MCD	0.539–2.947	–
CX	0.636–5.0	2-10

2.8.14 Ammonium, NH_4^+

Ammonium is a substance that is generated by the kidneys. Figure 2.6 illustrates the mechanism of ammonium generation in a renal tubule cell. While a proportion of that which is generated is excreted, some leaves via the renal veins and enters the general circulation of blood [15WMS]. The proximal tubule is the main site of ammonium production [09Hye]. This

Table 2.24: Ammonia Quantity along the Nephron (in rats) [85GoK]

Seg	% of Excreted Ammonia
tDL	109
TAL	160
DT	46
CCD	53
MCD	93
CX	100

production is increased during acidosis. Ammonium is produced from glutamine in the proximal tubule, thick ascending limb and distal tubule before being excreted into the lumen. It is then reabsorbed in the thick ascending limb into the medullary interstitium and excreted again in the collecting duct [85GoK, 97GuH, 09Hye]. Ammonium reabsorption in the thick ascending limb is reduced by hyperkalemia [09Hye]. This is an important cyclic mechanism for the overall renal excretion of hydrogen ions. In the cortical collecting duct, NH_3 is transported into the lumen, while in the medullary collecting duct NH_4^+ is transported [09Hye]. Relative amounts of ammonia in the rat nephron are shown in Table 2.24. The basal (baseline) rate of renal ammoniagenesis is around 60 to 80 mmol per day but can increase up to as much as 400 mmol per day when metabolic acidosis requires the kidneys to increase acid excretion [15WMS].

The relationship between the concentration of NH_4^+ and NH_3 at a given pH is given by the Henderson-Hasselbalch equation:

$$\mathrm{pH} = \mathrm{pK_a} + \log([\mathrm{NH_3}]/[\mathrm{NH_4^+}])$$

which can also be written as:

$$[H^+] = K_a[NH_4{}^+]/[NH_3]$$

where $pK_a = -\log(K_a)$

The value of pK_a is approximately 9, so in most physiologic solutions, the ammonia occurs as $NH_4{}^+$ [85GoK, 09Hye]. The nitrogen excreted in the form of ammonium is around 10 % of that excreted in the form of urea in basal conditions, but ammonium excretion can increase 5 to 10-fold if required [15WMS].

2.8.15 Bicarbonate and the Regulation of pH

Bicarbonate reabsorption and excretion is closely related to the corresponding processes for the hydrogen ion and hence to the regulation of acid-base balance. The kidneys secrete hydrogen ions and reabsorb bicarbonate ions, as well as produce additional bicarbonate. The concentration of hydrogen ions in extracellular fluid can vary from 10 to 160 nEq/L and is usually around 0.00004 mmol/L ($-\log(0.00000004) = 7.4$). The normal pH of arterial blood is 7.40 and for venous blood and interstitial fluid it is 7.35 [97GuH].

Normal plasma P_{CO_2} is 40 mmHg and normal plasma bicarbonate concentration is 24 mmol/L [06GuH]. The kidneys filter 4320 mmol of $HCO_3{}^-$ per day (180L/day x 24 mmol/L). The proximal tubule reabsorbs 85 % of this, or 3672 mmol. The thick ascending limb reabsorbs, 10 %, or 432 mmol and the distal and collecting tubule 4.9 %, or 215 mmol. Thus, the excreted

Table 2.25: Bicarbonate Concentrations along the Nephron (mmol/L)

Seg	[96AMC]
BC	22
PT	8
tDL	–
tAL	20
TAL	–
MD	–
DT	6
CCD	3
MCD	1
CX	1.2

amount is 1 mmol/day [06GuH]. Bicarbonate reabsorption in the thick ascending limb is dependent on acid-base status and the thick ascending limb reabsorbs approximately 15 % of the filtered bicarbonate [14Mou].

From the data in Table 2.10, 99.95 % of the filtered bicarbonate is reabsorbed and only 0.05 % is excreted.

A bicarbonate ion must react with a hydrogen ion to form aqueous carbonic acid, H_2CO_3 before it can be reabsorbed. Thus, 4320 mmol of H^+ must be excreted each day to reabsorb the filtered bicarbonate. Figure 2.3 and Figure 2.4 show the mechanism of bicarbonate reabsorption in the proximal tubule and the distal and collecting tubules.

The reaction between gaseous carbon dioxide and water to produce carbonic acid is slow and thus only small amounts of carbonic acid are produced by the equilibrium.

Table 2.26: pH Values along the Nephron

Seg	[09TLF]	[11RAJ]	[94LBF]	[96AMC]	[97Kok]	[99HoT]
BC	–	7.40	–	7.38	7.25	–
PT	–	6.75	6.75	6.78	6.7	6.75
tDL	–	–	–	–	7.4	–
tAL	–	6.50-7.30	–	7.39	–	–
TAL	–	–	–	–	6.7	–
MD	–	6.38-7.00	–	6.59	–	6.45
DT	–	6.45-7.00	6.45	–	–	6.45
CCD	–	5.00-6.25	6.45	6.24	–	–
MCD	5.0 - 6.25	5.50-6.70	5.75	6.12	–	5.80
CX	5.5 - 6.7	–	–	6.09	4.86 - 7.20	–

$$CO_2(g) + H_2O \rightleftharpoons H_2CO_3(aq)$$

However, the enzyme carbonic anhydrase enhances the rate of this reaction. Carbonic anhydrase is found mainly in the lung alveoli and the renal tubules, where it is crucial that this equilibrium is attainded rapidly.

$$CO_2 + H_2O \overset{carbonic\ anhydrase}{\rightleftharpoons} H_2CO_3$$

The ionisation of carbonic acid is weak and thus the resultant hydrogen ion concentration is small.

$$H_2CO_3 \rightleftharpoons H^+ + HCO_3^-$$

An increase in the hydrogen ion concentration causes more carbonic acid to be formed:

$$\uparrow H^+ + HCO_3^- \longrightarrow H_2CO_3 \longrightarrow CO_2(g) + H_2O$$

The presence of the bicarbonate ions results in the removal of the hydrogen ions from the solution. Thus, the sodium bicarbonate acts as a buffer. The pH for a bicarbonate buffer system is given approximately by the Henderson-Hasselbalch equation:

$$\text{pH} = 6.1 + \log\left(\frac{[\text{HCO}_3{}^-]}{0.03P_{\text{CO}_2}}\right)$$

$$= 6.1 + \log\left(\frac{24}{0.03 \times 40}\right) = 7.4$$

where

$[\text{HCO}_3{}^-]$ is in mEq

and P_{CO_2} is in mmHg.

An extra 80 mmol of H^+ needs to be excreted to rid the body of non-volatile acids, giving a total of 4400 mmol H^+ secreted into the tubular fluid each day. Acids other than H_2CO_3 are termed non-volatile (because they cannot be exhaled as CO_2) [06GuH] so have transport properties which are easier to model.

H^+ secretion and $\text{HCO}_3{}^-$ reabsorption takes place in almost all parts of the tubule, except the thin descending and thin ascending limbs of the loop of Henle. This is important because it determines the pH of the fluid as it passes through the kidney, which is an over-arching factor in the precipitation of solids. In the proximal tubule and thick ascending limb, hydrogen ions are secreted using secondary active transport via the sodium-hydrogen counter transport mechanism and the secretion of H^+ ions is accompanied by the reabsorption of sodium bicarbonate. The H^+ ions pass into the fluid in exchange for Na^+ ions, which together with bicarbonate ions within the cells then move into the blood [68BDS]. In this process, almost all of the bicar-

bonate of the glomerular filtrate is reabsorbed [68BDS, 06GuH]. This is illustrated in Figure 2.3. From the late distal tubules, the secretion mechanism is primary active transport in the intercalating cells by hydrogen-transporting ATPase, as shown in Figure 2.4.

The variation of the pH of urine is dependent mainly on secretion of H^+ in the proximal tubule and the production of ammonia in the distal and collecting tubules. The proximal tubule is responsible for 80 % to 90 % of H^+ secretion. The pH of urine falls by about 0.3 to 0.5 units in the proximal and distal tubule and 1 to 2 units in the collecting ducts.

In the proximal tubule, the hydrogen ion concentration can be increased 3 to 4 times but, in the collecting duct, it can be increased as much as 900 times. The pH of the tubular fluid can be decreased to about 4.5 (*i.e.* a hydrogen ion concentration of 0.03 mmol per litre), which is the lower limit achievable by normal kidneys [00GuH]. To excrete up to 500 mmol per day, the extra H^+ ions are normally excreted with urinary buffers, such as phosphate and ammonia. Much of the filtered phosphate is reabsorbed, but some is available for buffering and the acid salt NaH_2PO_4 is excreted. This is illustrated in Figure 2.5.

In the quantitavely larger ammonia buffer, the acid salt NH_4Cl is excreted. Here, glutamine is actively transported into the epithelial cells of the proximal tubule, thick ascending limb and distal tubule. Glutamine ($C_5H_{10}N_2O_3$) can be metabolised to form 2 NH_4^+ and 2 HCO_3^- ions. Increased extracellu-

lar H^+ concentration stimulates renal glutamine metabolism [06GuH]. This mechanism is illustrated in Figure 2.6.

In Cell:

$CO_2 + H_2O \longrightarrow H^+ + HCO_3^-$

In Lumen:

$H^+ + Na^+ + HCO_3^- - Na^+ \longrightarrow H^+ + HCO_3^- \longrightarrow CO_2 + H_2O$

The CO_2 is then reabsorbed into the cell.

The unabsorbed phosphate in the lumen takes part in the following reaction:

$Na^+ + Na^+ + HPO_4^{2-} - Na^+ + H^+$

$\longrightarrow Na^+ + H^+ + {HPO_4}^{2-}$

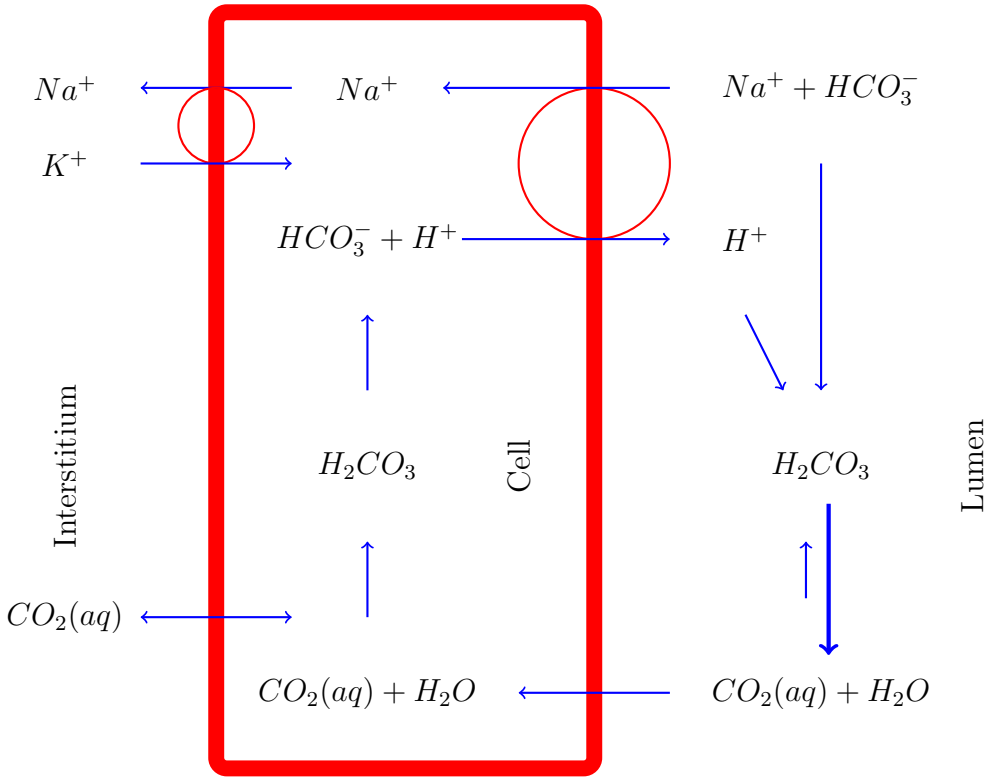

Figure 2.3: Cellular Mechanism of Hydrogen Ion Secretion and Bicarbonate Ion Reabsorption in the Proximal Tubule Cells (Redrawn from Fig.23-3 in [97GuH])

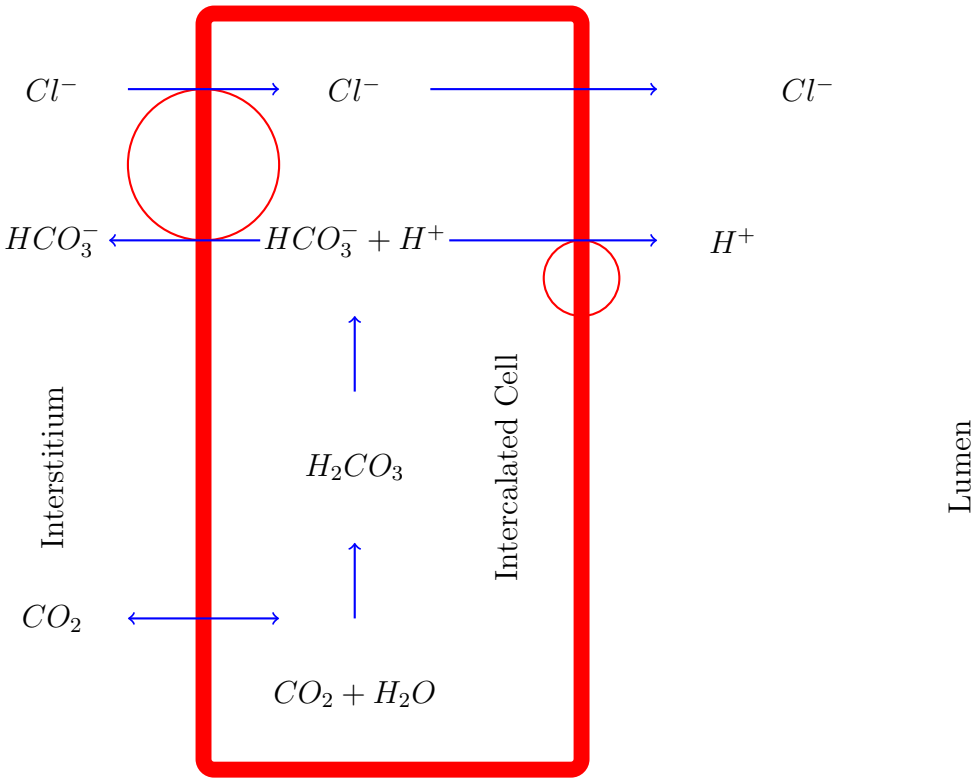

Figure 2.4: Hydrogen Ion Secretion in the Intercalated Cells of the Distal and Collecting Tubule Cells(Redrawn from Fig.23-4 in [97GuH])

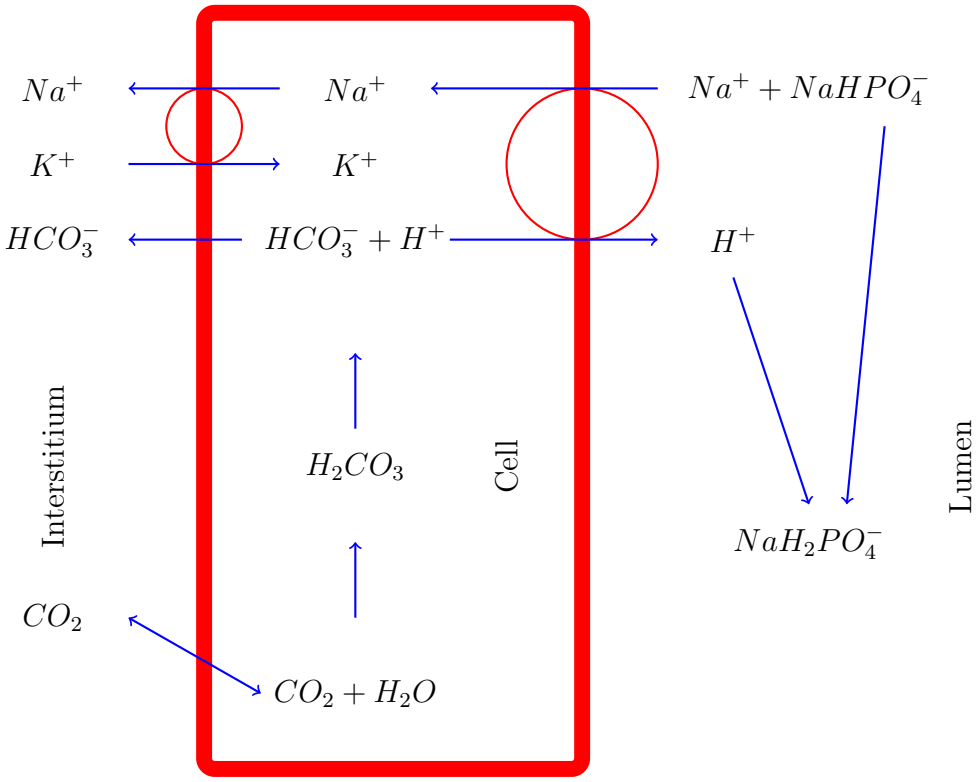

Figure 2.5: Phosphate Buffering (Redrawn from Fig.23-5 in [97GuH])

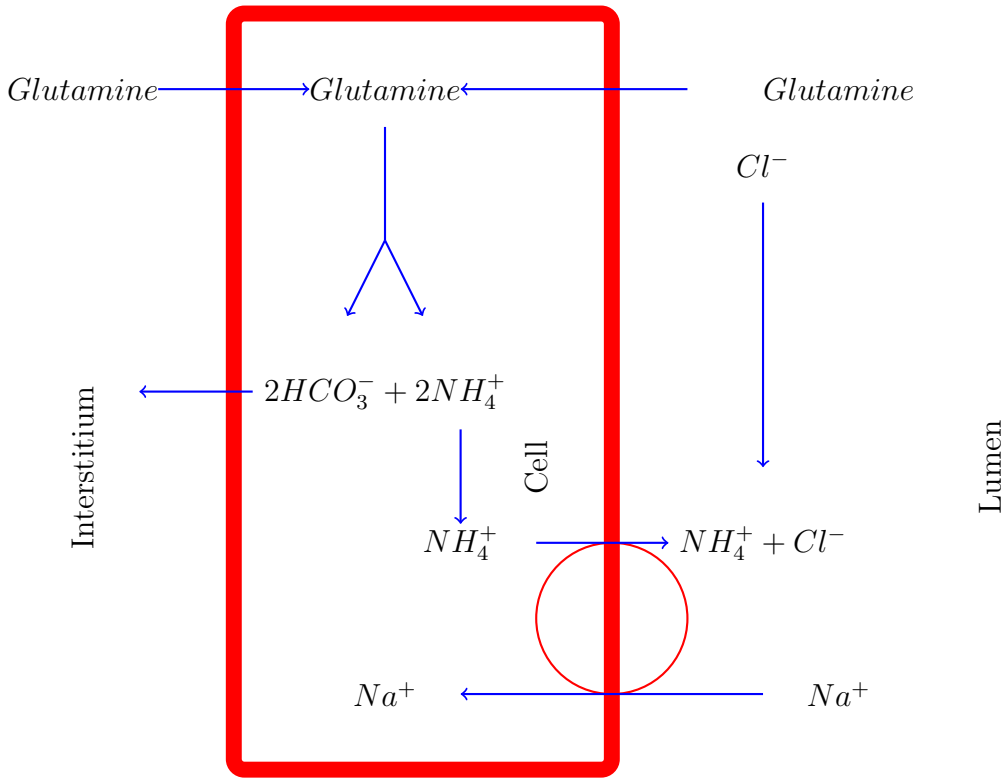

Figure 2.6: Ammonium Generation from Glutamine (Redrawn from Fig.23-6 in [97GuH])

2.9 Factors Affecting Kidney Stone Formation

2.9.1 Risk Factors

It is well known that kidney stone formation is a multifactorial disease [12Rob1, 17ARI]. Risk factors include, diet, drinking habits, climate, concomitant diseases, medication and genetics [11Tis1]. Risk is also age and gender dependent, being twice as common in males than in females [81RSB, 86HCK, 11Tis1], with a peak age of presentation between 20 and 50 years [81RSB, 86HCK]. It is important to remember this multi-causal nature as a limitation when applying the results of chemical speciation models to clinical applications. In particular, it is critical to appreciate that the computer calculations developed in this work are just one of many tools that can be used in diagnosis. Comparisons against other risk indices described in the literature are unfortunately less useful in general than may be supposed. Nevertheless, medical progress can rightly be expected from a better quantitative understanding of mineral supersaturation and how this relates to a variety of clinical observations, as described in this section.

The weightlessness experienced during space travel causes the loss of calcium and phosphate from the bones, as well as the loss of bone mass, due to the absence of the normal stresses of gravity required to stimulate bone deposition [92YaL, 06GuH, 07Bas]. This results in increased plasma con-

centrations of calcium and phosphate and hence an increased risk of stone formation. Computer models such as those developed in this work are therefore valuable tools for use by space agencies concerned with urolithiasis in long space flights.

Dietary factors are significant in increasing risk, especially high animal protein [81RSB, 05Abd, 05CJR, 11Tis1, 12Rob2] and high fat intakes [11Tis1]. Animal protein can stimulate bone resorption to buffer the resulting acid load, thus increasing calcium excretion [03Sch]. Insufficient fluid intake, resulting in a more concentrated urine also increases risk [11Tis1]. Obesity is another known risk factor [05Abd, 07Hug, 10RAA, 11Tis1, 13RDD]. However, reliable predictions for individuals are not yet possible [95SoG, 11Tis1].

2.9.2 The Bonn Risk Index

The *Bonn Risk Index* (BRI) has been defined as a measure of risk for calcium oxalate stone formation [12Rob1]. It is defined as the ratio $[Ca^{2+}]/(Ox^{2-})$, where the calcium ion concentration is that determined in the urine and the oxalate value is found from the quantity of ammonium oxalate that has to be added to produce crystals in the urine sample [00LSH]. A BRI value of $> 1/1$ is in the 'at risk' category and a BRI $\leq 1/1$ is 'without risk'.

2.9.3 Differences Between Stone Formers and Normal Subjects

There are important differences in kidney filtration processes and urine biochemistry between those who form stones and normal individuals, as shown in Appendix D. Disorders which can result in stone formation include hyperparathyroidism, cystinuria, infection with urease producing microorganisms, hyperoxaluria, hypercalciuria and hypocitraturia [93DBJ, 08LRA, 11Tis1, 13WBG, 16PrM].

Tables D.2, D.3, D.4, D.5, D.6, D.7, D.8 and D.9 show some data comparing stone forming patients and some normal controls. (See Appendix D.) Table D.6 shows data for normal subjects and for calcium oxalate or calcium phosphate stone formers from the UK (SF 1) and calcium oxalate stone formers from Saudi Arabia (SF 2).

2.9.4 Calcium

The mean value of calcium excretion by stone formers is double that of normal individuals [11CEW]. Reduced calcium reabsorption in the proximal tubule has been noted in calcium oxalate stone formers [11CEW, 13WBG, 15EWC].

Calcium phosphate stone formers have decreased calcium reabsorption as well as lower bicarbonate reabsorption [11CEW]. It is assumed that in the case of the calcium phosphate stone formers, the reduction of calcium reabsorp-

tion occurs mainly in the medullary thick ascending limb, rather than in the proximal tubule [11CEW], which is the case in calcium oxalate stone formers. The reduction in the reabsorption of bicarbonate is in both the proximal tubule and the thick ascending limb, thus increasing both calcium concentration and pH in the distal portions of the nephron [11CEW]. Calcium phosphate stone formers have higher urine calcium excretion than calcium oxalate stone formers [11CEW].

Hyperparathyroidism is another condition that can increase urinary calcium levels. In primary hyperparathyroidism, the ultrafiltrable plasma calcium concentration will be around 2.8 mmol/L [15Rob]. Higher post-prandial plasma calcium increase has been seen in stone formers than normals [13WBG]. It has been found that in idiopathic stone formers PTH levels are more sensitive to plasma calcium changes [13WBG]. This sensitivity will result in a greater fall in calcium reabsorption in the situation of a post-prandial calcium load, enhancing the stone formation process, which may explain this observation.

Computer models such as those developed in this thesis can be used to investigate the effects of such changes on the mineral solubilities.

2.9.5 Oxalate

Stone formers have been seen to have higher levels of oxalate absorption in the gut, absorbing 5 % to 10 % more of the ingested oxalate [82MFB, 15Rob].

In the kidney, there is a difference in oxalate reabsorption in the proximal tubule, normal males show an average fractional excretion of 0.84 (indicating net reabsorption) while in stone formers the value is up to 1.43 and in primary hyperoxaluria it is 2.29 [97Kok] showing net secretion, a result suggested by more than one study [11BZA].

2.9.6 Citrate

Lower urinary citrate concentrations are common in stone formers [81Tis, 90CRG, 11Tis2]. Table D.7 shows average concentrations in 24 hour urine for a group of healthy controls and two groups of stone formers. Group A are patients without metabolic alterations, while Group B are patients with hyperoxaluria and/or hypercalciuria. The data here show that the urine citrate values for stone formers are typically only about 2/3 normal values.

2.9.7 Randall's Plaque

Randall's Plaque is a calcification of the interstitial tissue at the end of the nephron, named after Dr Alexander Randall who discovered the association between kidney stones and calcium salt deposits in the papilla, in the 1930s [96DCM, 14Mor]. Calcium phosphate apatite and amorphous carbonated calcium phosphate are the major components of most Randall's plaques [15EWC, 10CBJ].

Such calcification in the interstitium is assumed to result from the calcium concentration gradient that is produced during the kidney filtration process.

In the papillae, each thin limb is surrounded by 3 or 4 capilliaries. The calcium concentration of the thin limb fluid exceeds that of the blood in the capilliaries due to water extraction. The epithelium has low calcium permeability and does not transport calcium, but since the fluid in the thin limb is in contact with the epithelium, calcium will move into the basement membrane at a higher concentration than blood, especially in the ascending portion, where extensive water movement is not permitted. The outer side of the basement membrane can lose calcium into the interstitium at a rate related inversely to the calcium concentration of the interstitial fluid. This will be dominated by the calcium concentration of the blood in the capilliaries. In the outer medulla, the descending vasa recta are surrounded by thick ascending limbs. The thick ascending limbs reabsorb calcium, but not water and hence increase the inner medulla calcium concentration and thus also raise the calcium concentration of the blood in the descending vasa recta. This means that the basement membrane of the papillary thin limbs have fluid with a calcium concentration higher than that of the blood both on the side of the lumen and the interstitial fluid on the other side. Thus, calcium will move into the basement membranes. The increased concentration results in a greater propensity to exceed solubility limits. This is the condition that leads to the formation of the Randall's plaque [11CEW].

The decreased calcium reabsorption in the proximal tubule of calcium oxalate stone formers results in high calcium concentrations within the loop of Henle and hence increased entry of calcium into the medullary interstitium. This increases the likelihood of calcium crystal nucleation in the thin limb

basement membranes. The formation of Randall's plaque begins in the basement membranes of the papillary thin limbs of the loops of Henle and then spreads into the interstitium and eventually spreads beneath the urothelium and the basement membranes of the inner medullary collecting ducts and ducts of Bellini [11CEW].

It can reasonably be expected that greater insight into the state of mineral supersaturation will assist in better understanding of Randall's plaque formation and its consequences.

2.10 The Calcium Phosphate Hypothesis

Urinary supersaturation with calcium oxalate monohydrate is apparently never high enough to result in homogeneous nucleation; thus, heterogeneous nucleation must be taking place on some nucleating substrate [95SoG, 12GCG]. Hydroxyapatite, brushite, and uric acid may all serve as substrates for calcium oxalate monohydrate nucleation [81RSB, 95SoG, 97Tis, 99HoT, 09TLF, 12GCG]. This important fact must be considered whenever the results of supersaturation modelling calculations are applied to clinical problems, as described below.

The "*Calcium Phosphate Hypothesis*" explains a mechanism where calcium oxalate stones are formed as the result of an initial precipitation of calcium phosphate. This is supported by findings that calcium phosphate activity products have been found to be significantly higher in calcium oxalate stone

formers [15RWH]. **Most calcium oxalate stones contain a small proportion of calcium phosphate, often in the core of the stone, indicating that calcium phosphate is a common initial crystal phase** [11Tis1, 99HoT]. Recent work has suggested that calcium oxalate stone formation is based on calcium phosphate precipitation higher up in the nephron. This highlights the importance of understanding the mechanisms underlying the processes [11Tis2, 11CEW] and the contribution that can be made by chemical speciation models. High levels of supersaturation of calcium phosphate and higher pH can be found in the loop of Henle and the distal tubule, resulting in the precipitation of calcium phosphate [97Kok, 11Tis2, 11RAJ]. Precipitated calcium phosphate may then either continue along in the nephron tubule, or be internalized by the nephron cells and build up in the interstitial tissue [11Tis2]. The internalization of calcium phosphate by the tubular cells may be a defense mechanism to prevent blockage of the lumen [11Tis2]. As outlined in the previous section, the precipitated calcium phosphate in the interstitial tissue acts as a precursor of Randall's Plaque [11Tis2]. For the crystals transported further along in the nephron tubule, the influence of change in pH becomes important. If the pH is sufficiently low in the collecting duct, the calcium phosphate which has remained within the nephron tubule, dissolves, bringing about sufficient levels of calcium and oxalate concentration for crystal nucleation or additional growth of an existing stone to occur [97Kok, 99HoT, 09TLF]. It is reasonable to think that in the case where all of the calcium phosphate crystals dissolve, the resultant stone will be a calcium oxalate stone and when some of the calcium phosphate remains undissolved, a mixed stone results. Whether, and how, the initial

calcium phosphate precipitation can be counteracted is not yet known but is now an active focus of research [11Tis1]. However, avoiding low pH in these late nephron sections is known to prevent the dissolution of calcium phosphate. The increase in citrate associated with the administration of alkali also increases urinary citrate [81BDF, 08Pak, 09ZuA] and augments urinary macromolecule inhibitory power [11Tis1].

It is known that hydroxyapatite is supersaturated throughout the length of the nephron [11RAJ] and that there is a risk of calcium phosphate precipitation both in the ascending limb of the loop of Henle and the distal tubule [11Tis1]. Locations where nucleation is most likely to occur are the end of the descending loop of Henle and the end of the collecting ducts [14BaA]. Calculations have shown that precipitation of hydroxyapatite can cause the other salts to become undersaturated [11RAJ]. However, it is not known which phase of calcium phosphate is the first to precipitate [97Tis, 11SoG]. It has thus been suggested that the first substance to precipitate in the formation of hydroxyapatite would likely be amorphous calcium phosphate, having the formula $Ca_xH_y(PO_4)_z \cdot nH_2O$, octacalcium phosphate, $Ca_8H_2(PO_4)_6 \cdot 5\,H_2O$, or brushite, $CaHPO_4 \cdot 2\,H_2O$ [94LBF, 96AMC, 97Tis, 97GVS, 11SoG]. Identification of this initially-formed phase would obviously be important in determining how the kidney stone formation process begins. While magnesium ions have been shown to inhibit the crystallization and growth of HAP and OCP, the same effect is not seen in the case of brushite [92JoN]. Pak, Coe and Rabadjieva, and co-workers [69Pak, 81Pak, 08PRP, 92CPN, 16RTS] consider brushite to the phase that initially precipitates, based on observations that

this phase has the highest nucleation rate amongst the calcium phosphates.

2.11 Physicochemical Aspects of Kidney Stone Formation

Physicochemical calculations and computer models have been applied to the study of urolithiasis at least since the late 1960s [69Rob]. The main chemical modelling packages currently used in this field are EQUIL (and the later versions EQUIL2 and EQUIL93) [85WBS, 94BAP, 97Tis, 98MBB, 09PMR, 14Rod, 17ARI] and JESS [97GVS, 06RAJ, 09PMR, 11RAJ, 17HKM]. The application of physicochemical principles to biological systems is complicated by a number of theoretical and practical factors [86Ros] and raises questions, some of which are difficult, or even impossible to answer adequately. However, a model is a representation of reality that cannot encompass everything [08CoC]. A good model should be an approximation of the system being studied representing those aspects of the system most relevant to the questions that the model is trying to answer. For example, using JESS to model the behaviour of a biological system does not involve information about organic macromolecules [14Rod]. Similarly, protein binding of calcium ions is not well characterised [94BAP, 13HLN], calcium buffering and the coating of seeds by proteins can cause other overlooked effects, such as inhibition of crystal growth [58MVM, 98STK]. It is hoped that as this data becomes available and is included in the modelling, the calculations will become more

accurate [17RoJ]. More importantly, the art of good modelling is to build new insights based on the key determining factors and despite the unavoidable simplifications.

Crystal growth inhibitors that work by being absorbed onto the surface are also not considered in the current model. The thermodynamic data in the database only relates to complexation equilibria between metal ions and ligands. However, by the application of certain modelling techniques it is possible to gain better insight into the processes involved by considering the quantitative consequences of physicochemical aspects.

2.11.1 Supersaturation and Metastability

The formation of kidney stones requires the precipitation of solid phases from substances dissolved in the fluid in the nephron [00GCK]. The maximum amount of a compound that can remain in equilibrium with a stable solution is determined by its solubility product (SP). When the actual activities in solution exceed this quantity the solution is said to be 'supersaturated' [02Kok]. Supersaturation is the driving factor which causes stone formation [90FKH]. However, new crystals do not readily develop in solutions that are just saturated [76RoN] as the so-called activation energy required to form stable particles is not available [14BaA]. Spontaneous homogeneous nucleation is dependent on kinetic factors. Between saturation and labile supersaturation is the metastable zone of supersaturation, where homogeneous nucleation will not take place but heterogeneous nucleation may occur in the presence

of a suitable nucleating substrate [90Nan] and growth of existing crystals can take place [14BaA]. Once precipitation has occured, crystal growth can generally take place more rapidly at any concentration level above saturation. Crystallization depends on a balance between thermodynamic and kinetic factors. Most urines remain in a metastable supersaturation state and do not form crystals [00GCK].

The composition of stones have been found to correspond to the supersaturation levels of those substances in the urine of the patient [97PCC, 10Eva] and supersaturation with respect to the stone constituents is a requirement for stone formation [76RoN, 78Fin, 99GSC, 11Tis2]. It is widely considered that the driving force for crystallization is supersaturation (a thermodynamic factor) [90Nan, 00GCK]. Thus, estimation of free ion concentrations, as described in Section 3.2, are important for the assessment of stone formation risk so speciation calculations are a powerful tool in the determination of risk factors [90Nan].

The four physicochemical features of urolithiasis are [78Fin]:

- supersaturation, as the driving force;
- nucleation, as the initiator;
- rate of growth of individual crystals and particles; and
- aggregation.

The driving force, is expressed as Gibbs Energy change, ΔG [78Fin].

$$\Delta G = RT \ln \left(\frac{a_i}{a_0} \right) \tag{2.1}$$

where

R is the gas constant

T is the temperature

a_i is the activity of the unionised salt in solution at any given condition

a_0 is the activity of the unionised salt in solution at equilibrium

The activity, a, is related to concentration, c, via an activity coefficient γ:

$$a = \gamma c$$

If

$$\frac{a_i}{a_0} < 1$$

for any given stone salt, then $\Delta G < 0$, the urine is undersaturated with respect to that stone salt. Hence, stones that are present can dissolve.

When

$$\frac{a_i}{a_0} = 1$$

then $\Delta G = 0$ and the urine is saturated. Stones will not dissolve and new ones will not form.

When

$$\frac{a_i}{a_0} > 1$$

then $\Delta G > 0$ and the urine is supersaturated. Here, there is available free energy, stones can grow and precipitation can occur, when a_i/a_0 exceeds the metastable limit.

The ion activity represents the effective concentration as a thermodynamic driver in the crystallization process. The effect of ionic strength on ionic activities is significant. The solubility product of calcium oxalate monohydrate at 37° C in water at pH 6.0 is 2.82×10^{-9}, but at an ionic strength of 0.35 M it is increased to 4.6×10^{-8} [02Kok]. Thus with a decrease in urine volume, the increase in driving force for crystallization due to the increased concentration can be offset by the increase in ionic strength.

Urine contains much higher concentrations of calcium and oxalate in solution than are present in a saturated solution of calcium oxalate in water. This can be attributed to the salting-in effect due to the other electrolytes present in urine and the formation of the soluble complexes calcium citrate and magnesium oxalate, as well as the activity of inhibitors [80Hod]. Similarly, most urines are supersaturated with respect to all three of the calcium oxalate hydrates [80Hod, 97KoT].

In order to calculate saturation of a dissolved substance, values for the ion activity coefficients as a function of ionic strength have to be determined. There are a number of models that have been used for this purpose. The Davies Equation (Equation 2.2) [62Dav] is an empirical extension of Debye-Hückel theory and is sometimes claimed to work fairly well for ionic strengths up to 0.1 mol per kg [97GPS], although it has no sound theoretical foundation.

$$\log_{10} \gamma_i = -0.51 Z_i^2 \left(\frac{\sqrt{I_m}}{1 + \sqrt{I_m}} - 0.3 I_m \right) \tag{2.2}$$

where:

γ_i is the activity coefficient of ion i

Z is the charge of the ion

More accurate methods include the Specific Ion Interaction (SIT), or Brønsted-Guggenheim-Scatchard (BES), models (Equation 2.3), which are semi-empirical models that contain a number of parameters with some theoretical basis [97GPS].

$$\log_{10} \gamma_i = -\frac{Z_i^2 A \sqrt{I_m}}{1 + 1.5\sqrt{I_m}} + \sum_k \epsilon(i,k) m_k \tag{2.3}$$

where:

A is the limiting Debye-Hückel law slope of the activity coefficient

$\epsilon(i,k)$ is an aqueous species interaction coefficient

The problem with the above (and other) methods of estimating the effects of ionic strength is that they refer to individual ionic species, which lie outside the realm of thermodynamics and are unmeasurable. It is therefore preferable

instead to use the equlibrium constants themselves which, as quotients of activities are thermodynamically well defined and experimentally accessible. The method used by JESS has a mathematical form similar to the Specific Ion Interaction model and is shown in Equation 2.4 [00May].

$$\log_{10} K' = \log_{10} K^0 + \left(\frac{-\Delta Z^2 A \sqrt{I}}{1 + 1.5\sqrt{I}} \right) + BI \tag{2.4}$$

where:

K^0 is the equilibrium constant at infinite dilution

K' is the conditional equilibrium constant at finite ionic strength

A and ΔZ^2 are the usual Debye-Hückel factors

B is a temperature dependent parameter

$$K^0 = \frac{\{ML\}}{\{M\}\{L\}} = \frac{\gamma_{ML}.[ML]}{\gamma_M.[M].\gamma_L.[L]} = \frac{\gamma_{ML}}{\gamma_M.\gamma_L}.\frac{[ML]}{[M][L]} = \frac{\gamma_{ML}}{\gamma_M.\gamma_L}.K'$$

Different numerical scales are used to express the degree of saturation of a solid. EQUIL calculates relative saturation ratio, RSR [96AMC]:

$$RSR = \frac{Concentration\ of\ Salt}{Solubility\ at\ 37°C}$$

The JESS software package calculates log(SI) values:

$$\log(\mathrm{SI}) = \log \frac{IAP}{K^0_{sp}}$$

where

IAP is the ion activity product

K^0_{sp} is the solubility product at infinite dilution

Chapter 3

Methodology

3.1 Modelling Concentration Changes in the Kidney Filtration Process

A model of the kidney filtration process has been constructed in this work based on the physiological processes described in the previous chapter and quantitative data collected from various sources. The values shown in this chapter describe an average scenario, where substance concentrations in the resultant urine are related to those values shown as the normal urine values in Appendix B. It should be noted that in some cases the final values in the tables illustrating the reabsorption calculations are not exactly the same as the reference values shown, due to approximations made by the model in the simulation process.

The model has been set up so that changes can be made to the input parameters to allow the investigation of the effects of these changes. The parameters which can be altered are: the blood plasma composition, variations to how much of a substance is reabsorbed in a particular nephron segment and changes in the levels of the hormones included in the model.

3.2 Changes in Concentration along the Nephron

Functions to describe the changes in concentration of substances in the filtrate have been developed, based on values in Section 2.8 about reabsorption and excretion of different substances along the length of the nephron. The range of x from 0 to 10 represents compartments along the path through the nephron, with 0 corresponding to the Bowman's capsule and 10 to the duct of Bellini at the end of the collecting duct (See Figure 3.1).

$[x = 0]$ Bowman's Capsule

$[0 < x < 2]$ Proximal Tubule

$[0 < x < 1]$ Proximal Convoluted Tubule

$[1 < x < 2]$ Pars Recta

$[x = 2]$ Start of the Loop of Henle

$[2 < x < 3]$ Thin Descending Limb

$[x = 3]$ Turn Around Point of the Loop of Henle

$[3 < x < 4]$ Thin Ascending Limb

$[x = 4]$ Change from Thin to Thick

$[4 < x < 5]$ Thick Ascending Limb

$[x = 5]$ Macula Densa

$[5 < x < 6]$ Distal Tubule (Convoluted Section)

$[6 < x < 7]$ Distal Tubule (Distal Section)

$[7 < x < 8]$ Collecting Tubule

$[x = 8]$ Junction of Collecting Tubules (where nephrons converge)

$[8 < x < 9]$ Cortical Collecting Duct

$[9 < x < 10]$ Medullary Collecting Duct

$[x = 10]$ Duct of Bellini/Calyx

In the functions below, x is the distance along the nephron (as described above) and y, is the amount of the filtered substance remaining in the lumen at that point along the path.

If, in a given section of the nephron, $x = a$ to $x = b$, $y(a)$ is the amount of the substance remaining in the lumen at the start of this section and $y(b)$ is the amount of the substance remaining in the lumen at the end of the section, then:

$$y(b) = y(a) - \frac{P}{100}y(0)$$

where:
a is the start of the interval under consideration
b is the end of the interval under consideration
P is the percentage of the substance reabsorbed in the interval under consideration

P is the percentage of the total amount of the substance that is filtered into the Bowman's capsule that is reabsorbed in that section of the nephron. P will be a positive value where the substance is being reabsorbed, and a negative value when it is being secreted.

For example, looking at the reabsorption of water in the pars recta, x is between 1 and 2, the initial value is that at point 1 and the value for the water amount in this segment will be given by:

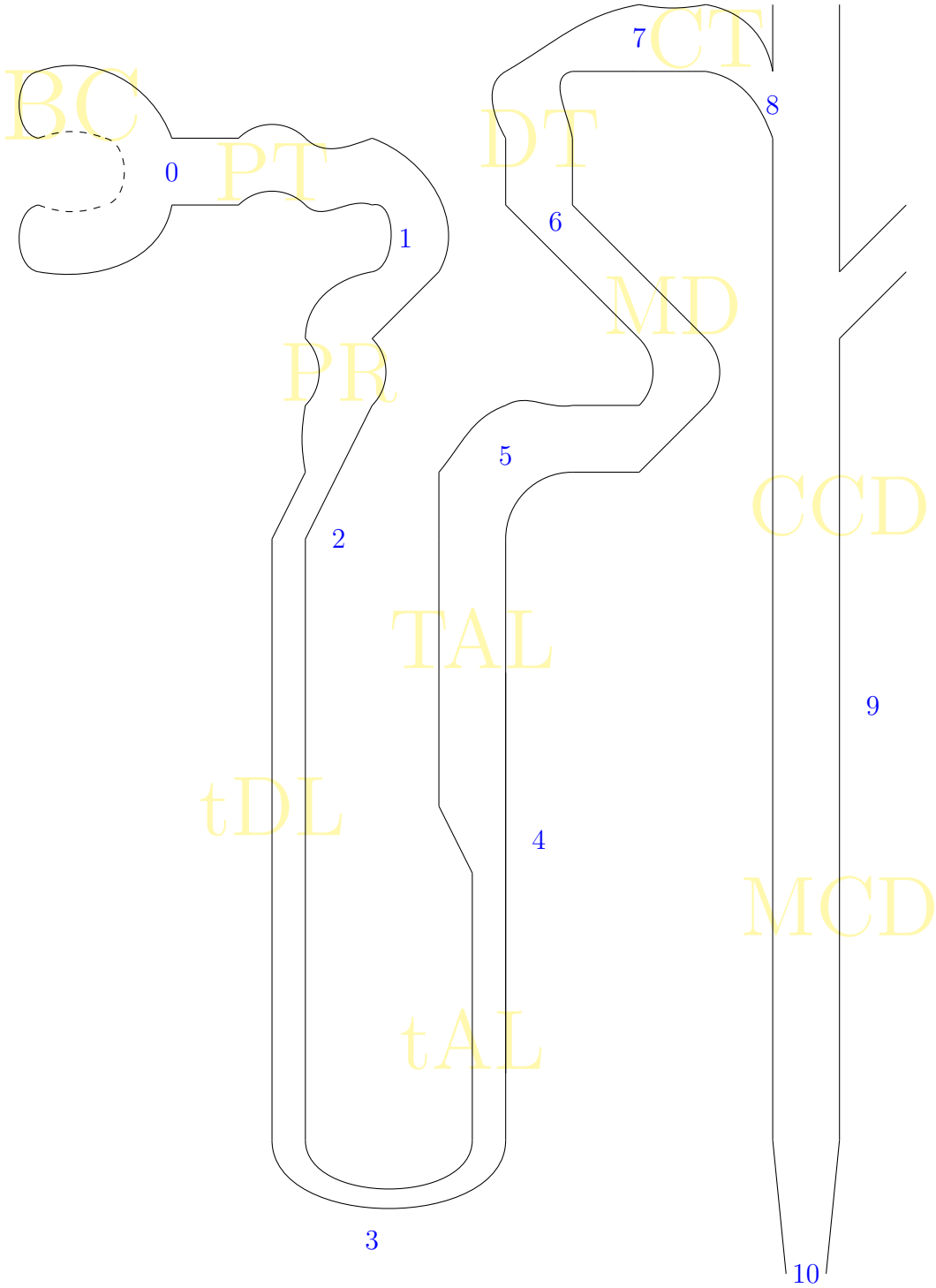

Figure 3.1: Nephron Coordinates used in Calculations

$$y(2) = y(1) - \frac{P}{100} y(0)$$

$y(1) = 0.54$

$P = 24$ (24 % of the water that was filtered into the Bowman's capsule is reabsorbed here)

So,

$y(2) = 0.54 - 0.24 \times 1.0$

$= 0.30$

This means that 0.3 litres of the 1.0 litres filtered into the Bowman's capsule remains in the lumen at the end of the pars recta.

The 19 substances considered are: water, sodium, potassium, calcium, magnesium, chloride, phosphate, oxalate, sulfate, citrate, creatinine, urea, urate, ammonia, bicarbonate, hydrogen ions (pH), glucose, amino acids and proteins. In comparison, Rodgers and co-workers [13RAJ, 14Rod] considers 13 variables (calcium, magnesium, sodium, potassium, oxalate, citrate, phosphate, sulphate, chloride, uric acid, ammonium, pH and volume) as being required for modelling calculations that take into account the important complexes determining the supersaturation state of the salts of interest in urolithiasis. The present set includes these but also includes bicarbonate and urea. While glucose, amino acids and proteins are included in the list of substances for completeness, their values are not used in the chemical speciation calculations as they are removed from the nephron fluid early in the nephron.

Table 3.1: SRAU Values and Model Urine Values

Substance	Concentration (mmol/L)	
Sodium	150	125
Potassium	24	30.4
Urea	180	338.3
Magnesium	2	2.1
Creatinine	5.3	7.4
Phosphate	11.6	19.9
Calcium	2	2.025
Urate	0.3	1.86
Iron	0.007	0.0
Ammonia	20.3	18.6
Citric Acid	0.98	1.8

The values for the concentrations of the substances in normal urine for the model are the selected average values indicated in Appendix B. The set of substance concentrations chosen to represent the Standard Reference Artificial Urine (SRAU) [97BrK], which has been developed for pathogen growth experiments, is shown for comparison with the values used here (Table 3.1). Model output of substance concentrations along the length of the nephron plotted against published values are shown in Section E.5.3. These comparisons show that the values produced by the model are reasonable.

Further details of the implementation of the model are given in Appendix E.

3.3 A JESS Model of Urine

JESS, the Joint Expert Speciation System, is a software package, which can be used to perform calculations concerned with chemical species in solution [91MaM1, 08MuM, 13MRM, 15May, 17MaR, JESS]. Speciation, which is the identity and relative abundance of different chemical entities, is an important property of a multicomponent chemical solution, as it generally determines the behaviour of the system. Chemical speciation calculations are non-trivial and a large amount of information is required to perform them correctly. JESS has been designed to achieve this by providing a comprehensive knowledge base including default rules to aid in decision-making.

3.4 The 'Rodgers Model' of Speciation in the Nephron

3.4.1 Overview

Rodgers *et al.* [11RAJ] have investigated changes in concentration and saturation index of stone forming salts along the nephron, using JESS. The salts considered were calcium oxalate, brushite, hydroxyapatite and octacalcium phosphate. As detailed information about the concentration of the different substances along the path of the nephron was not available, a number of assumptions and extrapolations had to be made to derive the values that these authors used in their calculations.

Table 3.2: Nephron Points used by Rodgers *et al.*

Location	GF	PT	LH	DTp	DTd	CDm	CDd
Coordinate	0	2	3	5	7	8	10

Table 3.3: Concentrations (Rodgers *et al.* [11RAJ]) (mmol/L)

Substance	GF	PT	LH	DTp	DTd	CDm	CDm
Na+1	135	135	278	79	93	94	109
K+1	3.8	3.0	13.8	0.90	58.0	53.0	63.7
Ca+2	1.50	2.78	3.47	1.32	0.94	1.60	4.50
Mg+2	0.54	0.19	0.24	0.12	0.40	1.45	3.85
PO4-3	0.80	0.80	1.00	1.00	3.34	12.1	32.3
Oxalic-2	0.0015	0.01	0.013	0.013	0.04	0.12	0.32
Citric-3	0.07	0.09	0.11	0.11	0.37	1.21	3.21
SO4-2	1.4	3.1	3.9	3.9	13.0	7.8	20.8
Cl-1	139	139	293	101	145	–	–

Concentrations are given and calculations are made at seven points along the nephron. Table 3.2 shows how these locations map onto the coordinates used in the model developed in this work, as described in Section 3.2. The concentrations that were used are shown in Table 3.3. The results are shown in Table 3.4.

3.4.2 Results

Using the input data given by Rodgers *et al.* [11RAJ], as shown in Table 3.3, and running the model through JESS, produces similar, but not exactly the same results. Some of the values obtained from the model are shown in Table 3.5 and Table 3.6. In Table 3.5, the log(SI) values are shown for all of the salts under consideration at the different parts along the nephron, and Table 3.6 shows calcium speciation, where both sets of values use the calculated

Table 3.4: Results from Rodgers *et al.* [11RAJ] (The figures are log(SI) values read off from Figures 1, 2, 3 and 4 of the article)

Section	pH	log(SI) CaOx	log(SI) HAP	log(SI) Bru	log(SI) OCP
GF	7.4	–	8.0	-0.4	1.1
PT	6.75	-0.3	6.3	-0.3	0.5
LH	6.50	-0.7	4.0	-0.5	-1.2
LH	7.30	-0.7	7.5	-0.5	0.8
DTp	6.38	-0.3	3.8	-0.3	-1.2
DTp	7.00	-0.3	7.0	-0.2	0.8
DTd	6.45	-0.3	4.0	-0.3	-0.9
DTd	7.00	-0.3	6.5	-0.2	0.7
CDm	5.00	0.6	-1.5	-0.5	-3.8
CDm	6.25	0.5	5.9	0.04	1.1
CDd	5.50	1.1	4.0	0.1	0.4
CDd	6.70	0.7	8.5	0.4	3.2

ionic strength and include the calcium chloride species. (See Section 3.6.)

Ostwald's Rule of Stages states that the formation of the least stable phases precedes the thermodynamically stable phase [11SoG, 97Saw]. In accord with a prediction based on this rule, the first solid to precipitate will be the one that is least supersaturated [11RAJ]. The results in Table 3.5 indicate that brushite is the supersaturated substance with the lowest SI value under the conditions in the ascending loop of Henle and thus, brushite is predicted to be the substance most likely to precitate [17HKM]. This is in agreement with the findings of Rodgers *et al.* [11RAJ], Grases *et al.* [97GVS] and Pak [69Pak]. Thus, for the purposes of analysis of the results of the calculations that follow, it has been assumed that brushite is the phase of calcium phosphate that will be the first to precipitate, accordingly, the risk of calcium phosphate precipitation has been based on the log(SI) values for brushite.

3.5 Ionic Strength and Redox Potential

When running JESS models the ionic strength values are, in the current circumstances, best fixed and not set to the value calculated at equilibrium by JESS (May PM, personal communication, August 2014). The average ionic strength of urine is ≈ 0.33 mol/L [95SoG]. The values are shown in Table 3.7 and graphically in Figure 3.2. The differences in results between using ionic strength set to zero (shown as the plain dashed lines) and the fixed values are shown for the long nephron in Figure 3.3 and for the short nephron in Figure 3.4. It can be seen from these figures that setting the ionic strength

Table 3.5: Calculated log(SI) Values for the Stone Forming Salts using input data from Rodgers *et al.* [11RAJ]

		Salt			
	pH	log(SI) COM	log(SI) Bru	log(SI) HAP	log(SI) OCP
GF	7.40	-1.423	-0.693	8.337	1.351
PT	6.75	-0.354	-0.572	6.630	0.680
LH	6.50	-0.615	-0.950	4.187	-1.022
LH	7.30	-0.617	-0.765	7.939	1.133
DTp	6.38	-0.347	-0.819	3.865	-1.099
DTp	7.30	-0.352	-0.548	7.144	0.947
DTd	6.45	-0.298	-0.674	3.993	-0.776
DTd	7.00	-0.327	-0.503	6.648	0.808
CDm	5.00	0.358	-1.081	-2.527	-4.649
CDm	6.25	0.298	-0.087	5.281	0.747
CDd	5.50	0.987	0.072	3.604	0.174
CDd	6.70	0.746	0.625	9.550	3.990

Table 3.6: Calcium Speciation

		Ca Speciation (%)					
	pH	Ca^{2+}	$CaCl_2$	$CaCl^+$	$CaSO_4$	Ca(Citric)	$Ca_4H(PO_4)$
GF	7.40	51	36	8	2	1	1
PT	6.75	51	35	8	4	1	1
LH	6.50	28	60	10	2	1	0
LH	7.30	28	60	10	2	1	0
DTp	6.38	56	25	7	7	4	1
DTp	7.00	56	25	7	7	4	2
DTd	6.45	42	30	7	12	8	2
DTd	7.00	40	28	7	11	7	0
CDm	5.00	44	31	7	8	8	0
CDm	6.25	38	27	6	7	17	0
CDd	5.50	36	22	6	14	19	0
CDd	6.70	20	12	0	8	7	0

Table 3.7: Calculated and Fixed Ionic Strengths (mol/L)

	Calculated		Value Used		
	Long	Short	Long	Common	Short
0BC	0.149	0.149	–	0.15	–
1PT	0.160	0.160	–	0.15	–
2PR	0.130	0.130	–	0.15	–
3DLH	0.295	0.177	0.30	–	0.15
4LH	0.295	0.176	0.30	–	0.15
5DCT	0.149	0.0617	0.15	–	0.05
6MD	0.159	0.0564	0.15	–	0.05
7DCT	0.156	0.0393	0.15	–	0.05
8CT	0.052	0.0520	–	0.05	–
9CCD	0.0346	0.0346	–	0.05	–
aUR	0.327	0.327	–	0.33	–

to the fixed values shown in Table 3.7, and in Figure 3.2, makes a significant difference to the results of the calculations.

The redox potential has been set to a pe value of 0.5 in all sections of the nephron. Changing the value resulted in no difference to the results. While the redox potential of urine does vary, and can be measured [14GCF], the species that have been assessed in the present study do not have redox activity.

3.6 Weakly Interacting Species

The species $CaCl^+$ and $CaCl_2{}^0$ are weakly interacting species [15May]. They may, or may not, exist and there are disadvantages associated with both removing them from calculations and with leaving them in [17MaR]. Calculations are made with data in the database that are based on them. If they

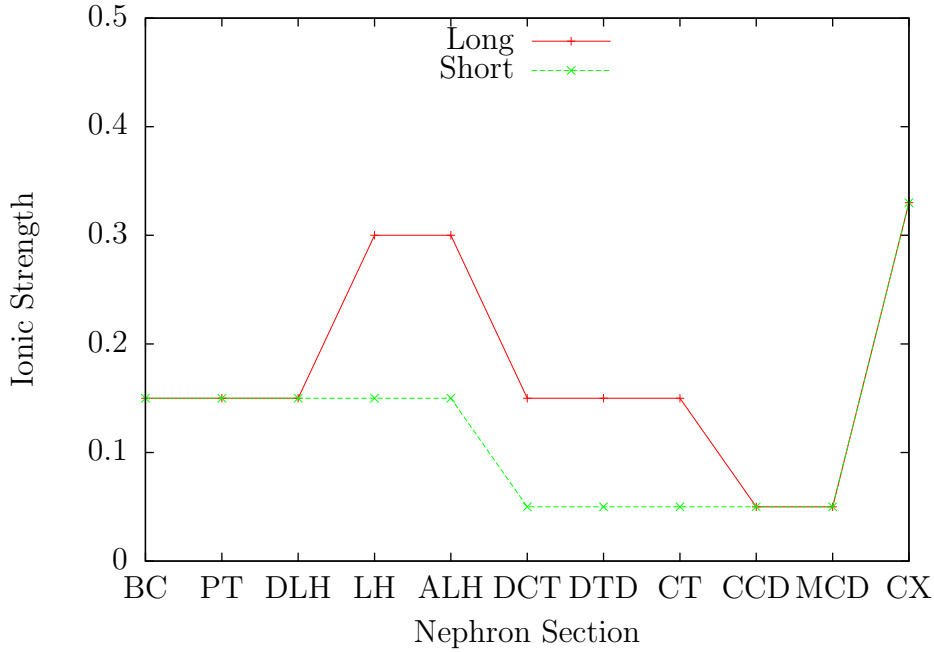

Figure 3.2: Fixed Ionic Strength Values along the Nephron (mol/L)

are removed then calculations are being made under conditions different to those the functions were set up for. If they are kept in then they alter the results by producing an effect that is not likely to be real. In this work the calculations have been performed without excluding these two species.

3.7 Modelling Normal and Pathological Variations in the Kidney Filtration Process

There are multiple factors affecting the composition of the fluid in the nephron at each stage of the kidney filtration process. The model developed in this work has been set up with a number of input values and parameters

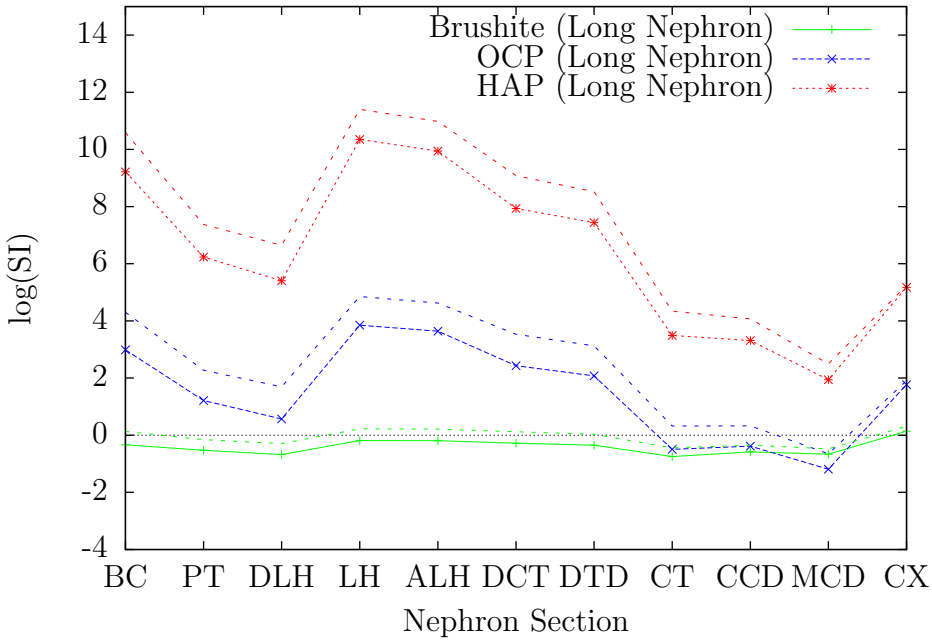

Figure 3.3: Long Nephron: Fixed vs Zero Ionic Strength. The results for the log(SI) values in the case where ionic strength is set to zero are significantly higher for all three substances (shown as the plain dashed lines).

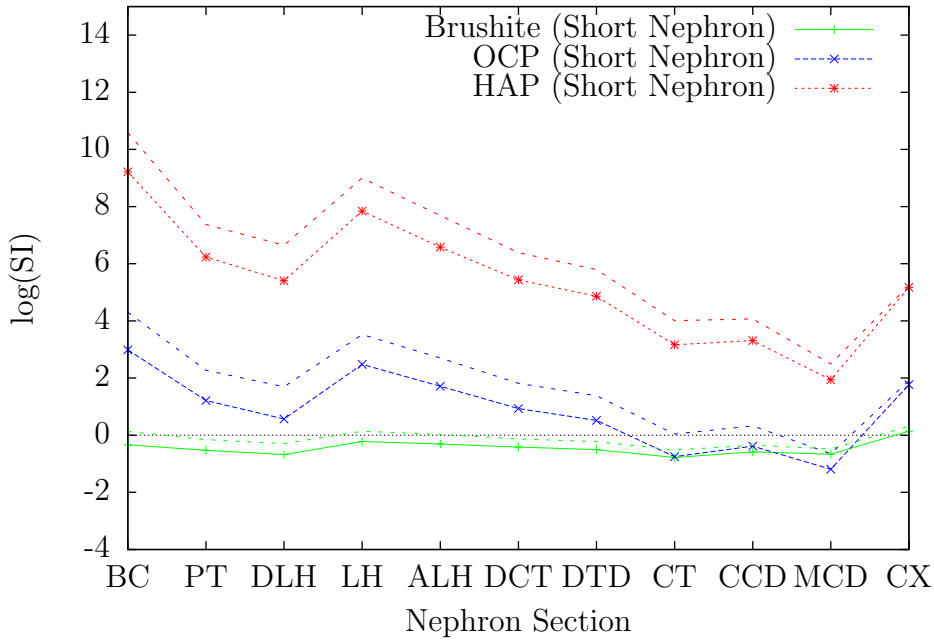

Figure 3.4: Short Nephron: Fixed vs Zero Ionic Strength. The results for the log(SI) values in the case where ionic strength is set to zero are significantly higher for all three substances (shown as the plain dashed lines).

which can be adjusted to simulate different situations. The model developed and used here is an extension of those described by Rodgers *et al.* [11RAJ] and Robertson [15Rob] in that it implements a larger set of substances and includes changes in hormone levels that alter the reabsorption processes, the simulation of malabsorption pathologies in different nephron sections and takes into account the differences between long and short nephrons.

Concentrations in the nephron are dynamic and changes can be significant [11RAJ, 11Tis2, 15Rob], but the concentrations found in urine show an average over a period of time. Thus, transient concentration variations within the nephron will be much greater than indicated by the changes observed in the urine. It seems very likely that the event that initiates a stone formation process results from simultaneous peaks of multiple risk factors [11Tis1]. People who form stones do not form them all the time and there is often no significant difference found in bio-analysis results between stone formers and those who do not form stones. The formation of a stone requires the unlikely event of the combination of a number of small differences resulting in a big difference taking place. The model developed here allows combinations of changes to be investigated to see how they change the level of risk for stone formation. In order to represent transient peaks that can occur in concentrations [97Kok] some input values have been set slightly higher than the usual upper limit of a range, such as those shown in Appendix A. For example, 2.8 mmol/L has been listed as a high level of plasma calcium (hypercalcaemia), and a value of 3.0 mmol/L has been used in some calculations. In modelling the effects of sulfate, Rodgers *et al.* used values of 10 %, 200 % and 500 % of

the normal urine value in calculations, and 100× for thiosulfate concentration [14RGE]. Their study determined that while increasing sulfate concentration reduced calcium salt supersaturation, thiosulfate had no effect. Thus, models considering larger variations in substance values than those considered to be normal need to be investigated.

The mechanism of formation of uric acid, struvite and cystine stones are understood. This means that reliable treatments are available for these types of stones. The majority of stones are calcium-based and calcium-based stone formation is not well understood. The focus of this research is therefore on these types of stones. The calculations performed are therefore looking at the log(SI) values of calcium oxalate and calcium phosphate with reference to the formation of stones composed of these substances. As described in Section 3.4.2, the risk of precipitation of calcium phosphate has been based on log(SI) values for brushite. Uric acid stone formation has also been included as a test of the model, as the conditions required for the formation of uric acid stones is well documented.

A number of profiles were defined to represent different changes to the kidney filtration process. See Appendix F for the list of scenarios investigated. The profiles are numbered, starting with Profile 0, which is the default "normal" situation. In each subsequent profile, some model input parameters are changed to simulate variations in the process. Profiles 1 to 351 consider calcium based stones. In Profiles 1 to 98 the variations are changes in hormone levels and concentrations of a selected set of substances in blood

plasma. Profiles 100 to 198 are based on the reduced early nephron calcium reabsorption associated with calcium oxalate stone formation. Profiles 200 to 298 are based on the reduced calcium reabsorption further along in the nephron associated with calcium phosphate stone formation. Profiles 101 to 198, and, 201 to 298 duplicate the variations of Profiles 1 to 98 in addition to the associated malabsorption pathology. Profiles 400 to 468 are concerned with stones composed of uric acid and the other relevant urate compounds. Profiles 511, 512 and 513 illustrate another mode of using the model. Here, the composition of the final urine is fixed, and the model produces the corresponding concentrations through the nephron tubules associated with that urine composition.

The supersaturation state (log(SI) values) of following substances have been investigated:

$CaHPO_4 \cdot 2\,H_2O$ Brushite

$Ca_8H_2(PO_4)_6 \cdot 5\,H_2O$ Octacalcium Phosphate

$Ca_5OH(PO_4)_3$ Hydroxyapatite

$CaC_2O_4 \cdot H_2O$ Calcium Oxalate Monohydrate

$CaC_2O_4 \cdot 2\,H_2O$ Calcium Oxalate Dihydrate

$CaC_2O_4 \cdot 3\,H_2O$ Calcium Oxalate Trihydrate

$C_5H_4N_4O_3$ Uric Acid

$Ca(C_5H_3N_4O_3)_2 \cdot 6\,H_2O$ Calcium Hydrogen Urate Hexahydrate

$NH_4C_5H_3N_4O_3$ Ammonium Hydrogen Urate

$NaC_5H_3N_4O_3$ Sodium Hydrogen Urate

Chapter 4

Results

The simulation and calculation of the log(SI) values was performed for all of the profiles described in Appendix F. Plots of the results were produced and viewed to discover significant changes in values. Analysis of the log(SI) data produced by JESS was performed by plotting changes in the value along the nephron, for the different substances, and comparing them against a reference plot. Details of the observations are contained in Appendix F. This chapter contains a selection of interesting results and discusses some general conclusions.

4.1 Normal Kidney Filtration

Figures 4.1, 4.2, 4.3, 4.4, 4.5, 4.6, 4.7 and 4.8 show the log(SI) values for the substances under consideration for both a long and a short nephron for the case of normal kidney filtration (Profile 0). Although brushite is included

in the plots for the three calcium phosphates, plots for brushite have been redrawn alone to show the changes more clearly. It can be seen in Figures 4.1 and 4.2 that there is a significant difference between the log(SI) values for brushite compared to those for octacalcium phosphate and hydroxyapatite. This effect is readily explained by the high powers of concentration appearing in the solubility products of octacalcium phosphate and hydroxyapatite.

$$K_{sp}(Bru) = [\mathrm{Ca}^{2+}][\mathrm{HPO_4}^{2-}]$$
$$K_{sp}(OCP) = [\mathrm{Ca}^{2+}]^8[\mathrm{H}^{+}]^2[\mathrm{PO_4}^{3-}]^6$$
$$K_{sp}(HAP) = [\mathrm{Ca}^{2+}]^{10}[\mathrm{PO_4}^{3-}]^6[\mathrm{OH}^{-}]^2$$

Figures 4.1 and 4.2 show that hydroxyapatite is supersaturated throughout the length of the nephron, and octacalcium phosphate is supersaturated for most of the nephron, but falls below supersaturation towards the end of the distal tubule and returns to above supersaturation in the medullary collecting duct. Brushite remains below supersaturation for most of the nephron, only becoming supersaturated at the end of the medullary collecting duct, as can be seen in Figures 4.3 and 4.4. These results produced by the present model are in accord with the earlier results of Rodgers et al [11RAJ].

The calcium oxalates remain below supersaturation until the end of the nephron, as shown in figures 4.5 and 4.6. COM becomes supersaturated as the fluid enters the collecting duct, while COD and COT only exceed saturation at the end of the medullary collecting duct.

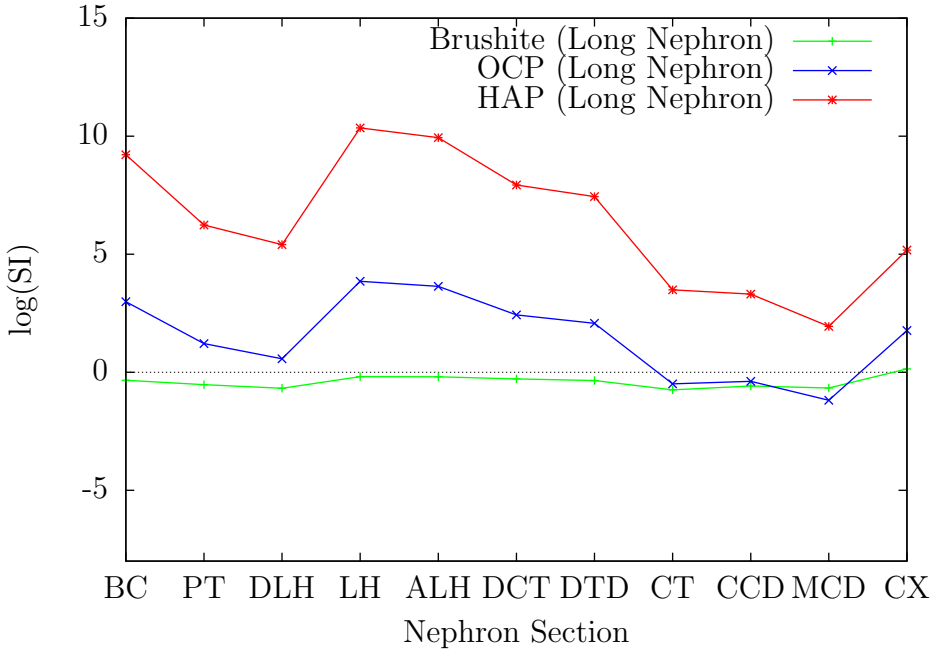

Figure 4.1: Profile 0: log(SI) Calcium Phosphates Long Nephron

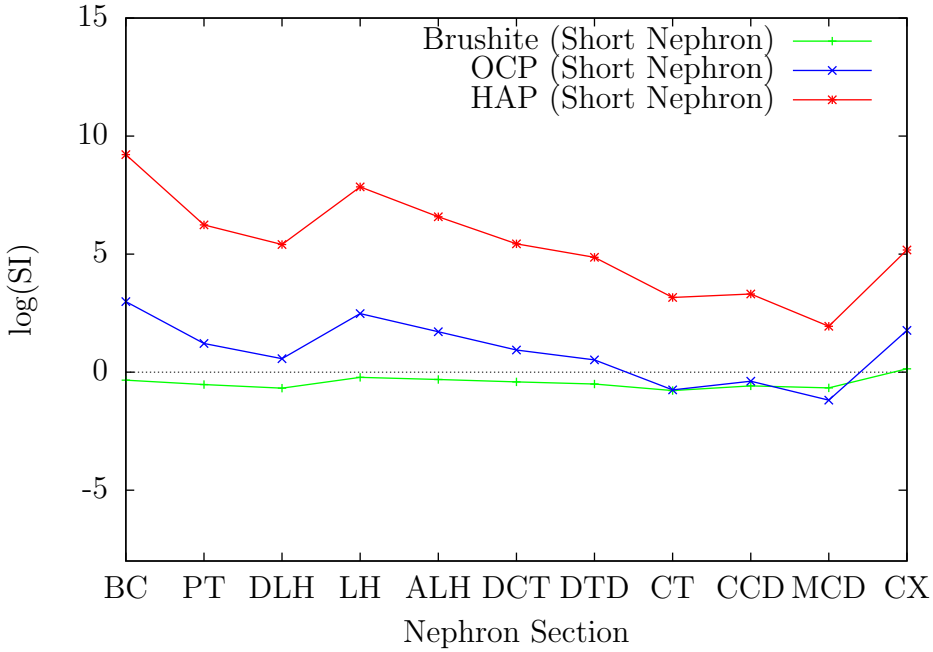

Figure 4.2: Profile 0: log(SI) Calcium Phosphates Short Nephron

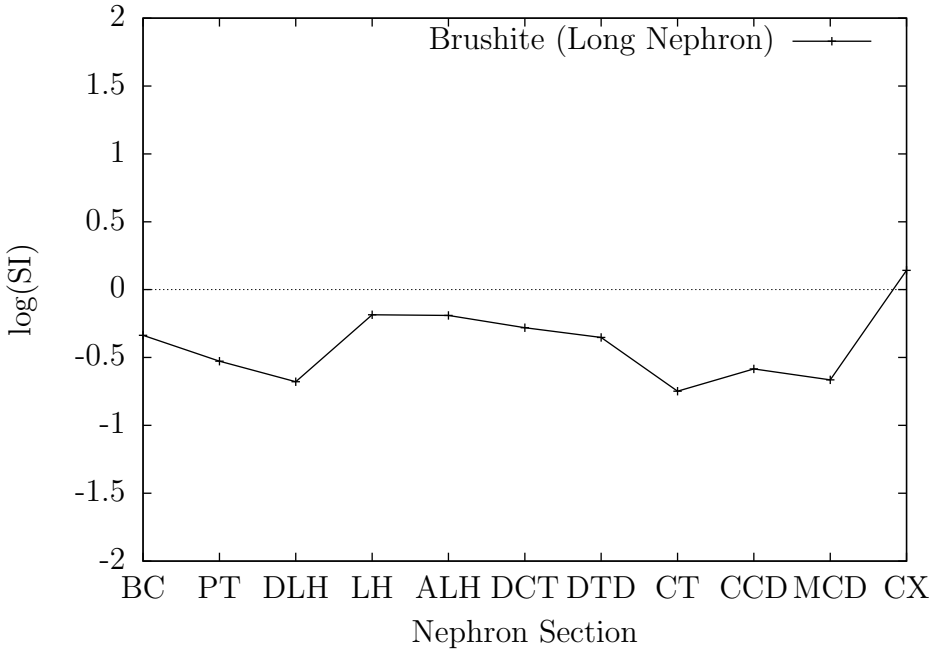

Figure 4.3: Profile 0: log(SI) Brushite Long Nephron

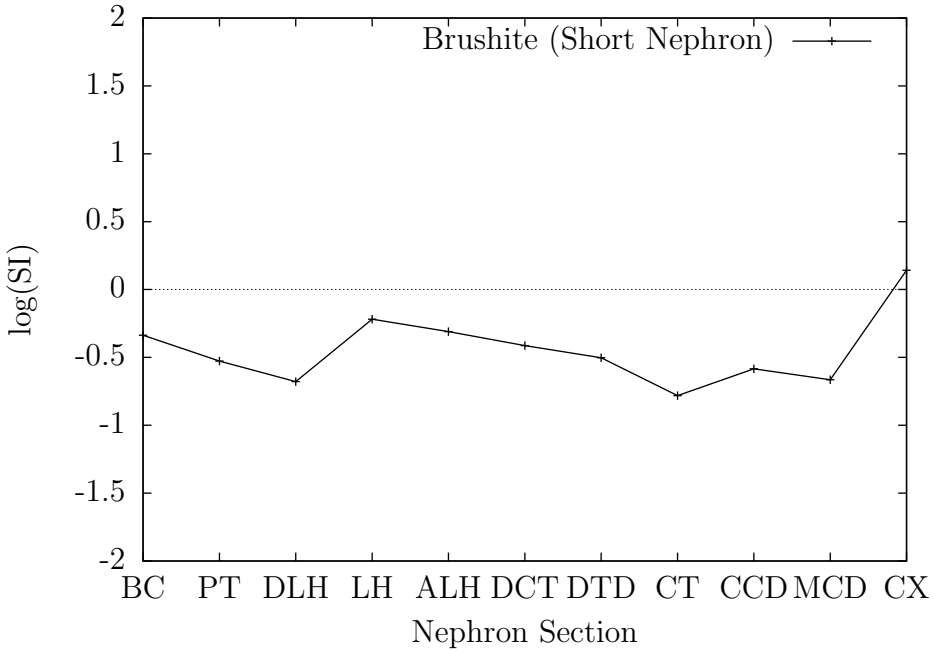

Figure 4.4: Profile 0: log(SI) Brushite Short Nephron

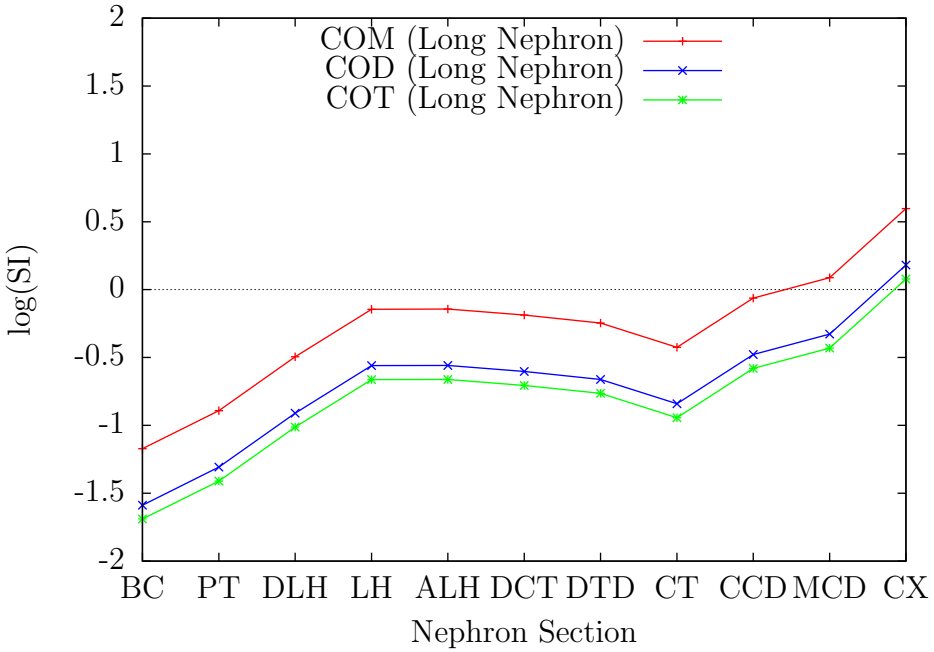

Figure 4.5: Profile 0: log(SI) Calcium Oxalates Long Nephron

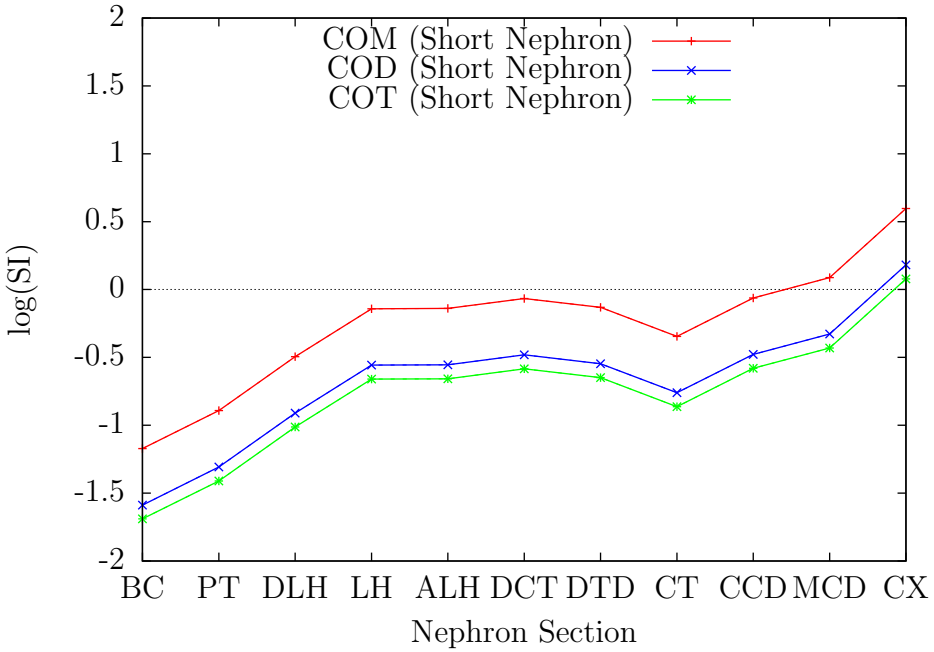

Figure 4.6: Profile 0: log(SI) Calcium Oxalates Short Nephron

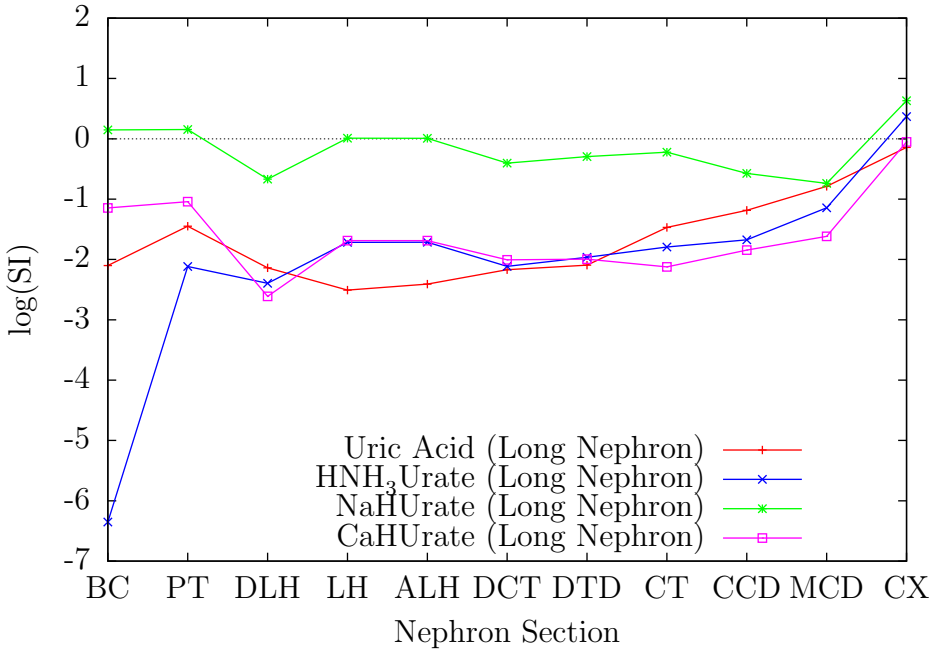

Figure 4.7: Profile 0: log(SI) Urates Long Nephron

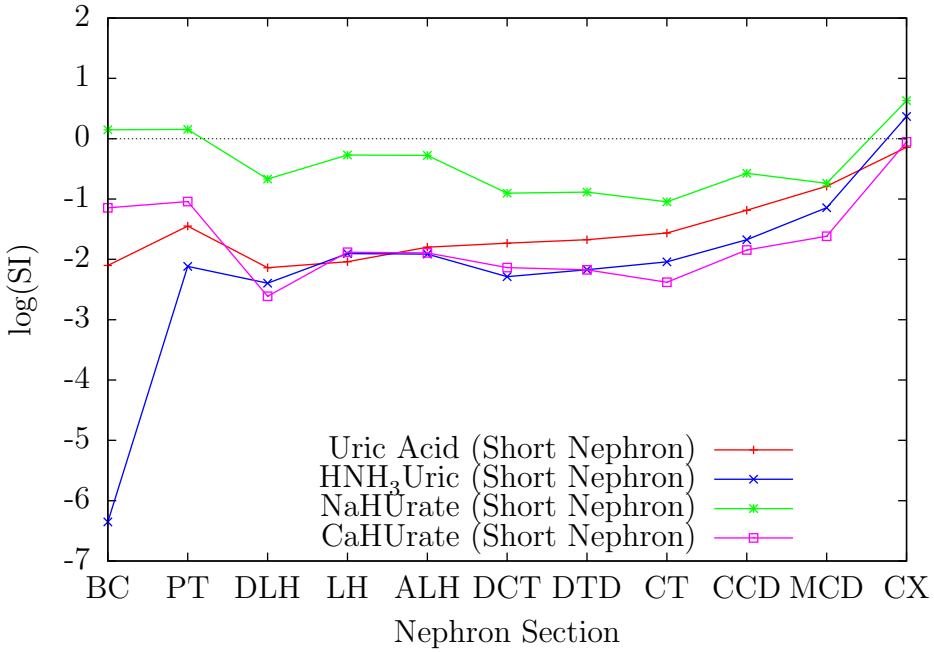

Figure 4.8: Profile 0: log(SI) Urates Short Nephron

Log(SI) of monosodium urate remains close to zero for the length of the nephron, ammonium hydrogen urate becomes supersaturated towards the end, calcium hydrogen urate hexahydrate remains unsaturated for the length of the nephron and uric acid remains below saturation all along the nephron, as illustrated in Figures 4.7 and 4.8

The results of the JESS calculations performed on the output of the model are in agreement with the conclusion of other studies in so far as they find that the calcium phosphates are more likely to precipitate than the calcium oxalates at nephron locations before the collecting duct [96AMC, 09TLF, 11RAJ, 15Rob].

Under normal conditions (Profile 0), the log(SI) values for the calcium phosphates are higher in the loop of Henle of the long nephron than in the short nephron, as expected, but the log(SI) values for the calcium oxalates are higher in the loop of Henle and distal tubule of the short nephron than they are in the long nephron. This result appears to be contrary to Le Châtelier's Principle, as the concentration is higher in the long loop, due the extra removal of water. However, this result is due to the difference in pH, and the resulting changes in chemical speciation.

Looking at the speciation of calcium and oxalate, it can be seen that there is a higher precentage of free Ca^{2+} and $Oxalate^{2-}$ under the conditions in the short (as opposed to the long) nephron. After the bend of the loop of Henle, in the long nephron, a greater amount of calcium is complexed as $CaHCO_3^+$.

Thus, the higher log(SI) value for the calcium oxalates is explained by the pH difference between the long and short nephrons. In the loop of Henle of the long nephron, the log(SI) values for brushite have a higher and longer peak than in the short nephrons. This pattern shows that if brushite crystals are going to form in this part of the nephron, it is much more likely to happen in a long nephron than in a short one.

4.2 Concentration Alterations

Reduced or increased plasma sodium level has a small calculated effect. Hyponatremia increases risk, and hypernatremia decreases risk up to the end of the distal tubule. Although the effect shown by the model is small, the change is in the right direction to agree with recent findings that have identified hyponatremia as a kidney stone risk factor [16TFM]. However, other biochemical relationships are certainly more important. In the case of hypernatremia, a higher level of plasma sodium concentration will increase levels of ADH and ANP and decrease levels of ALD, with hormone effect added, there is an increased risk in the collecting duct for both calcium phosphate and calcium oxalate precipitation, but still a slightly reduced risk in the early and mid sections of the nephron.

Low levels of plasma calcium do show a decreased level of risk, while higher levels show higher risk in a uniform manner along the length of the nephron. At a plasma calcium concentration of 3.0 mmol/L, log(SI) brushite is above zero in the loop of Henle, distal tubule and collecting duct. This indicates

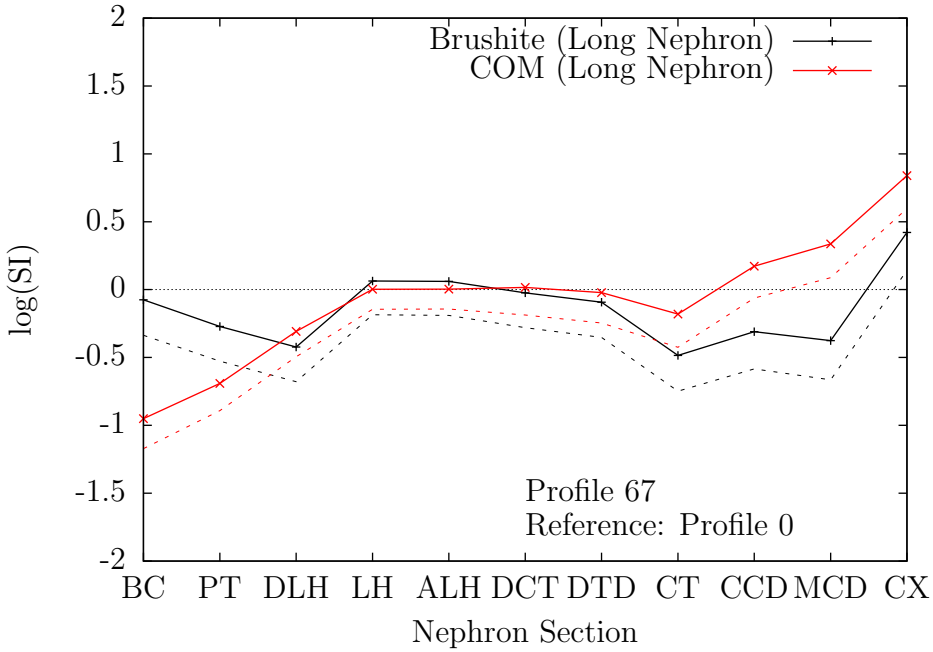

Figure 4.9: Profile 67 (Increased Plasma Calcium: 2.75 mmol/L): log(SI) Brushite and COM Long Nephron shown as solid lines with Profile 0 as a reference with dashed lines

that increased plasma calcium concentrations are a key factor risking brushite precipitation in the mid-nephron sections. Figure 4.9 shows the increases in log(SI) values for brushite and COM for an increased plasma calcium concentration of 2.75 mmol/L.

Lower levels of plasma phosphate result in a decrease in log(SI) values for the calcium phosphates and higher values cause an increase. Phosphate variations have little effect on log(SI) values of the calcium oxalates. The pattern of variation of supersaturation for OCP with increasing levels of phosphate produced by the model is in agreement with that illustrated by Robertson [15Rob].

Low plasma citrate shows a very small increase in risk, but high citrate does noticeably decrease risk toward the end of the nephron. This is significant in the case of brushite, where log(SI) remains below zero up to the end of the nephron. Increased citrate reduces risk for brushite all along the nephron. This interesting observation arises because changes in citrate concentration have a double effect: citrate has been shown to be a crystallization inhibitor [05CEW] as well as a calcium ion binder. Only the calcium binding effects are shown in the modelling results produced here so the actual effect of citrate concentration changes will be more significant.

The results of the present model accord with other experimental findings. An elevated oxalate level is more important than an elevated calcium level in increasing the risk of calcium oxalate precipitation [76RoN, 90Nan]. At low levels of plasma oxalate, there is a reduction in calculated log(SI) values for the calcium oxalates in a uniform manner all along the nephron. At higher oxalate levels (Profiles 88 and 89) the calcium oxalates can be seen to be supersaturated in early nephron segments. This is in agreement with observations that under high oxalate load, calcium oxalate crystals can form in these nephron segments [97Kok]. The calcium oxalates become increasingly supersaturated toward the end of the nephron. The pattern of variation of supersaturation for the calcium oxalates with increasing levels of oxalate produced by the model is in agreement with that illustrated by Robertson [15Rob].

Varying plasma concentrations of sulfate levels from 0.2 to 0.95 (Profiles 90 – 92, 190 – 192, 290 – 292) had little effect on the log(SI) values.

An increased plasma level of urate (Profiles 400 and 401) is the primary risk factor for the formation of uric acid stones. High plasma urate levels do not affect the risk of calcium phosphate or calcium oxalate precipitation due to the weak interaction of urate. A high plasma urate level alone (Profiles 400 and 401) does not result in a risk of uric acid stone formation. It is only when low pH is combined with a high urate concentration that the risk becomes noticeable [76RoN, 08Pak, 12GCG] (Profile 431). High pH removes the risk (Profile 438). Thus, model behaves as expected with changes in factors affecting the risk of uric acid stone formation.

4.3 Hormone Effects

In this section, the effect of hormones on the supersaturation of stone formng substances has been studied indirectly by exploiting their known action on the urine constituent concentrations. The following were considered: Antidiuretic Hormone (ADH), Aldosterone (ALD), Angiotensin II(AT2), Atrial Natriuretic Peptide (ANP) and Parathyroid Hormone(PTH).

4.3.1 ADH, ALD, AT2 and ANP

Antidiuretic hormone levels will increase in the situation of dehydration and it will have the effect of reducing water loss by lowering urine volume. The

urine will therefore beome more concentrated. As expected, simulating higher levels of ADH is found to increase the risk of crystal formation in the latter part of the nephron, while lower levels decrease the risk in these sections, as less water is being reabsorbed (Profiles 1 and 2). Aldosterone, angiotensin II and atrial natriuretic peptide all produce small effects toward the end of the nephron, as is to be expected from their actions in changing the solution concentrations.

4.3.2 Parathyroid Hormone

Hyperparathyroidism is a known risk for kidney stone formation [76PaH, 77Fin, 15EWC]. Parathyroid hormone changes do show the expected altered risk. High levels of PTH alone are sufficient to produce a clear risk for both calcium phosphate and calcium oxalate stone formation. At high plasma levels of both calcium and phosphate together with increased parathyroid hormone levels, brushite is supersaturated at the start of the nephron, falls below supersaturation in the proximal tubule, then becomes supersaturated in the loop of Henle and remains so throughout the distal tubule, falling to below supersaturation in the connecting tubule, and then becoming supersaturated again in the collecting duct. COM follows a similar pattern to brushite, becoming supersaturated toward the begining of the collecting duct. Figures 4.10 and 4.11 show the log(SI) values for the calcium phosphates for this scenario, with the values for Profile 0, shown as the dashed lines, as a reference. Figures 4.12 and 4.13 show the situation for brushite more clearly, together with the plot for calcium oxalate monohydrate for both

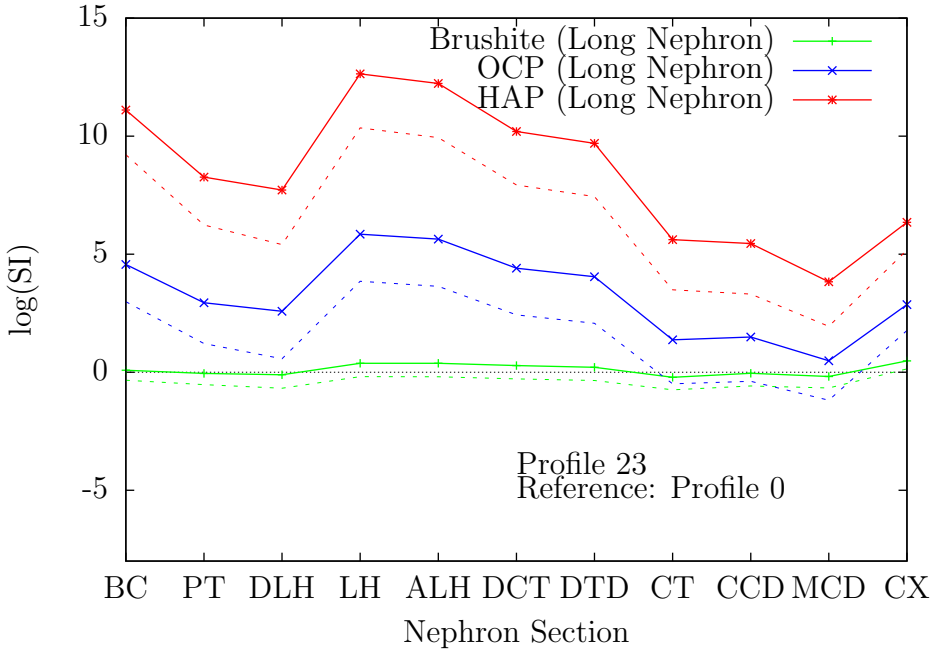

Figure 4.10: Profile 23 (Hyperparathyroidism): log(SI) Calcium Phosphates in a Long Nephron, Brushite, OCP and HAP shown as solid lines with Profile 0 as a reference with dashed lines

the long and short nephron. These figures illustrate the relative change in supersaturation of the two substances. In the collecting duct, the log(SI) of COM increases as that of brushite is falling, resulting in the situation where COM nucleation may be enhanced by the increase in free calcium ions produced by the dissolving brushite, thus supporting the 'Calcium Phosphate Hypothesis' of calcium oxalate stone formation.

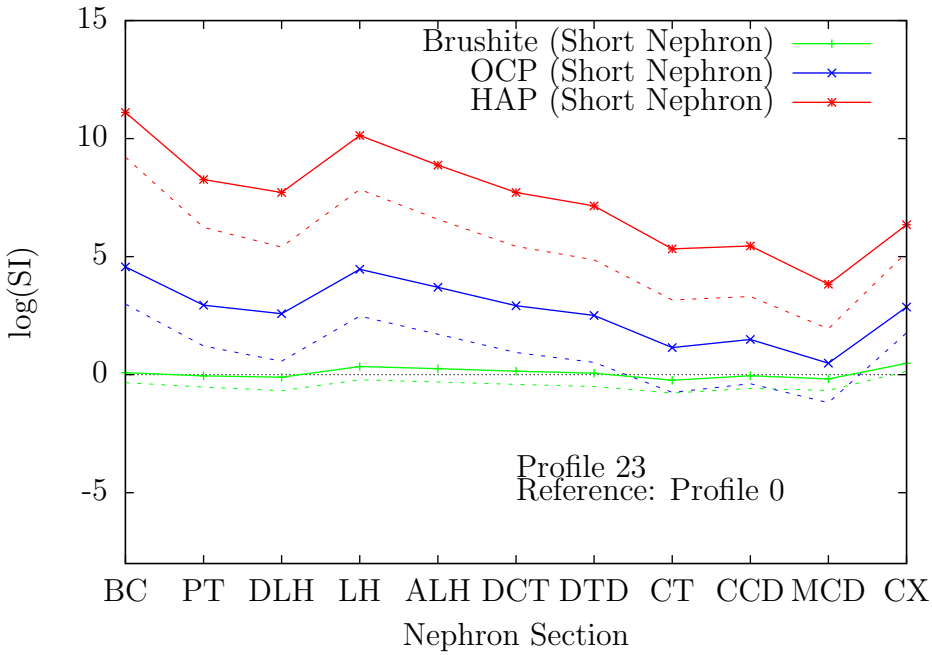

Figure 4.11: Profile 23 (Hyperparathyroidism): log(SI) Calcium Phosphates in a Short Nephron, Brushite, OCP and HAP shown as solid lines with Profile 0 as a reference with dashed lines

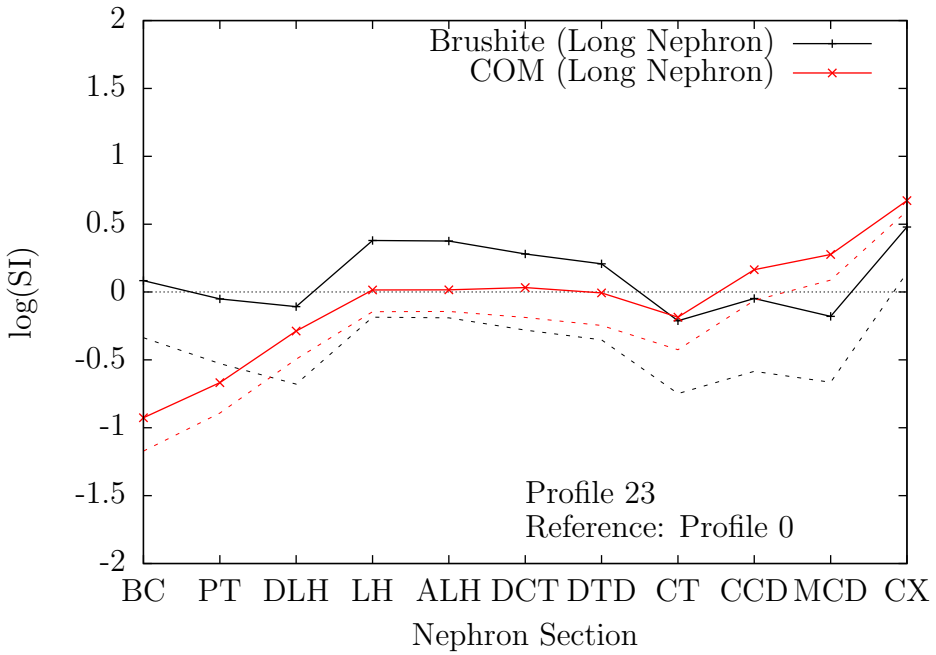

Figure 4.12: Profile 23 (Hyperparathyroidism): log(SI) Brushite and COM Long Nephron shown as solid lines with Profile 0 as a reference with dashed lines

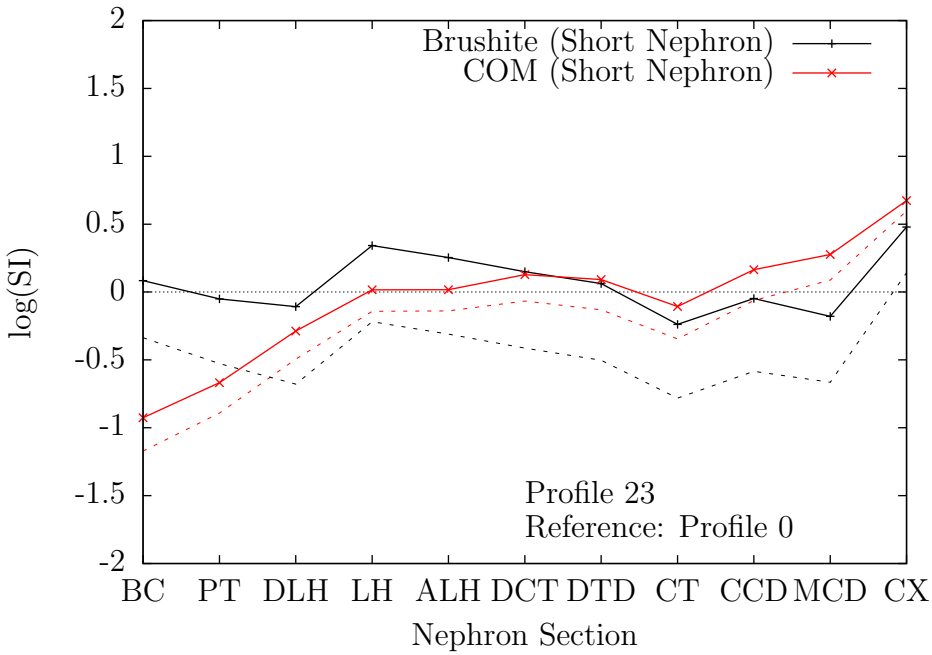

Figure 4.13: Profile 23 (Hyperparathyroidism): log(SI) Brushite and COM Short Nephron shown as solid lines with Profile 0 as a reference with dashed lines

4.4 Reduced Proximal Tubule Calcium Reabsorption

Figure 4.14 shows the difference between brushite log(SI) values and Figure 4.15 shows the differences for COM for normal reabsorption (Profile 0) and reduced proximal tubule calcium reabsorption (Profile 100) in both the long and short nephron. In the case of brushite, in both types of nephron, the log(SI) values in the pathological case diverge from the normal at the loop of Henle. The final supersaturation of brushite in the abnormal case (Profile 100) is much higher than in the normal case (Profile 0). In both situations, supersaturation is reached in the medullary collecting duct, but in the abnormal case, the final value is higher and supersaturation is attained earlier in the collecting duct.

There is a marked increase in the values for COM in both types of nephron after the loop of Henle in the case of the abnormal reabsorption. Final supersaturation is higher and supersaturation is reached earlier in the tubule than in the normal situation, giving more chance for formation of crystals in the tubule.

Figure 4.16 illustrates the situation in the case of both reduced proximal tubule calcium reabsorption and an increased level of PTH. The increased PTH level produces a large increase for the log(SI) value for brushite, resulting in supersaturation in the early parts of the nephron, particularly in the

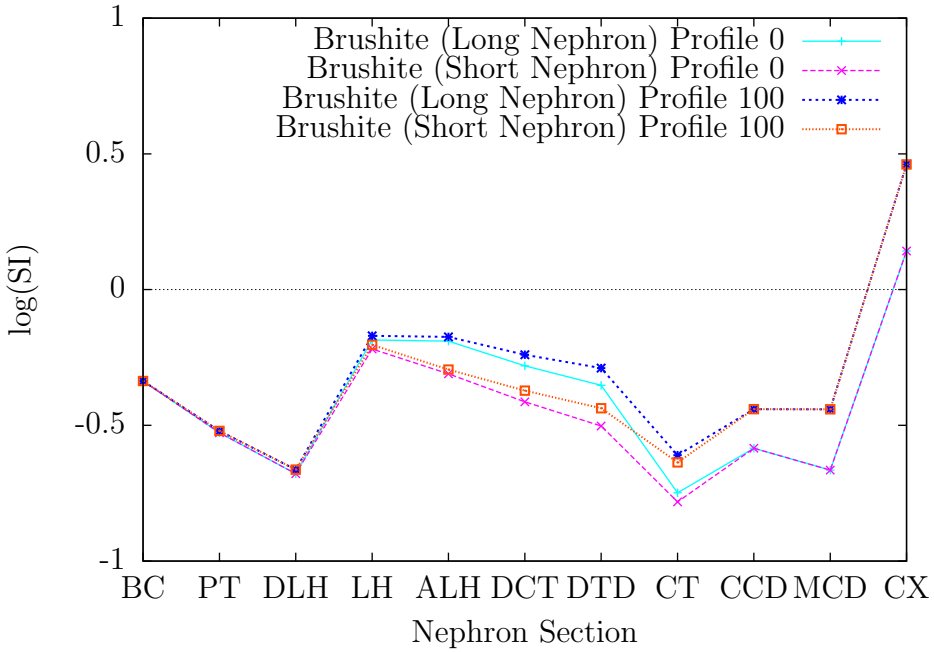

Figure 4.14: log(SI) Values for Brushite for Profile 0 (Normal) and Stone Former Profile 100 (Reduced PT Calcium Reabsorption)

loop of Henle. Thus, the model shows that an increase in PTH level, or an increase in sensitivity to PTH, can result in a significant increase in stone formation risk. Figure 4.17 illustrates the result of reduced proximal tubule calcium reabsorption and an increased plasma calcium level. This level of plasma calcium results in brushite becoming supersaturated in the loop of Henle, and also displays the the 'Calcium Phosphate Hypothesis' of calcium oxalate stone formation as brushite falls below supersaturation while COM reaches high levels of supersaturation in the collecting duct.

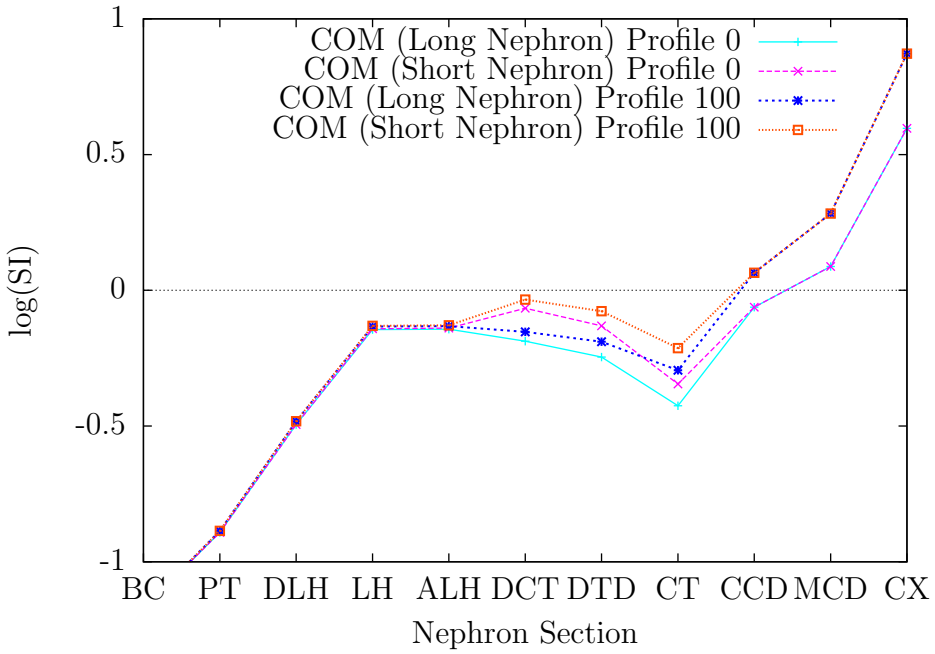

Figure 4.15: log(SI) Values for COM for Profile 0 (Normal) Stone Former Profile 100 (Reduced PT Calcium Reabsorption)

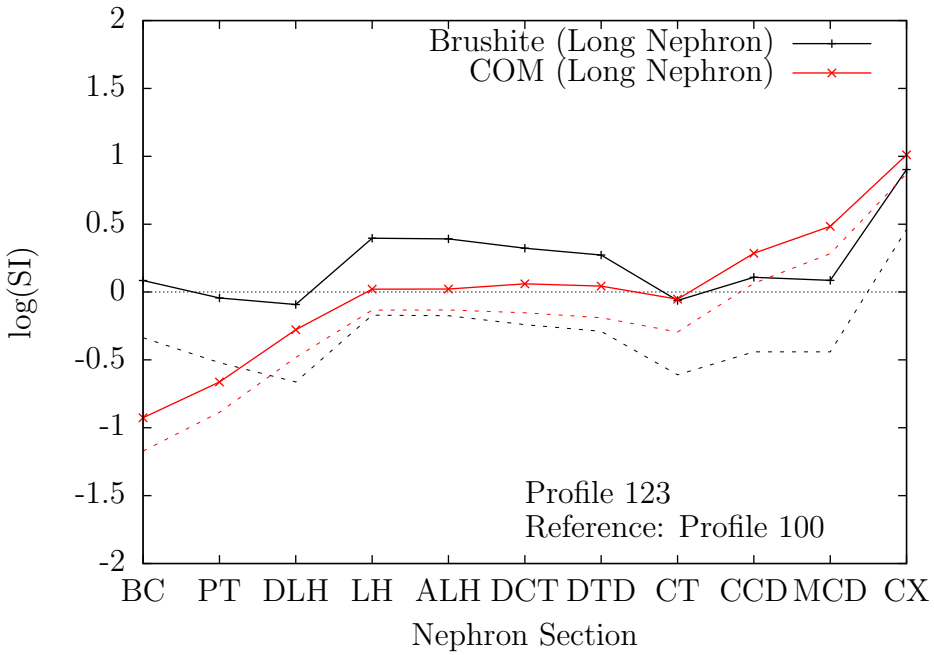

Figure 4.16: Profile 123 (Reduced PT Calcium Reabsorption and High PTH): log(SI) Brushite and COM Long Nephron shown as solid lines with Profile 100 as reference with dashed lines

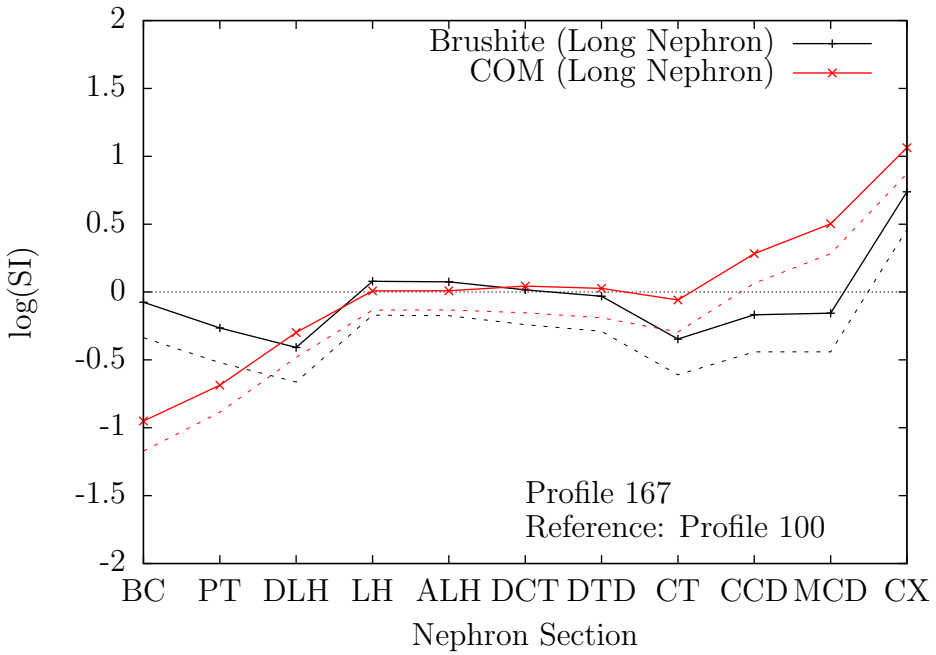

Figure 4.17: Profile 167 (Reduced PT Calcium Reabsorption and Increased Plasma Calcium): log(SI) Brushite and COM Long Nephron shown as solid lines with Profile 100 as reference with dashed lines

4.5 Reduced Distal Tubule Calcium Reabsorption

An important prerequisite for the precipition of the calcium phosphates is high pH [93DBJ]. This occurs in this case, as the reduced proximal tubule calcium reabsorption condition has an associated reduction in bicarbonate reabsorption [11CEW]. Figure 4.18 compares both the reduced proximal tubule calcium reabsorption (Profile 100) and the reduced distal tubule calcium reabsorption (Profile 200) with the normal situation for the log(SI) values of brushite, in the long nephron. In both of the pathological cases, the value diverges significantly starting in the loop of Henle. This is greater in the case of the reduced DT reabsorption abnormality (Profile 200), due to both the higher calcium concentration and the higher pH. Figure 4.19 compares both the reduced proximal tubule calcium reabsorption and the reduced distal tubule calcium reabsorption with the normal situation for the log(SI) values of COM. As in the case of brushite, Figure 4.18, the log(SI) values of COM for the two abnormal cases deviates upwards from the normal situation from the loop of Henle. The reduced distal tubule calcium reabsorption (Profile 200) has a higher value due to the higher calcium concentration.

Figure 4.20 shows the difference between brushite log(SI) values and Figure 4.21 shows the differences for COM for normal reabsorption (Profile 0) and reduced distal tubule calcium reabsorption (Profile 200) in both the long

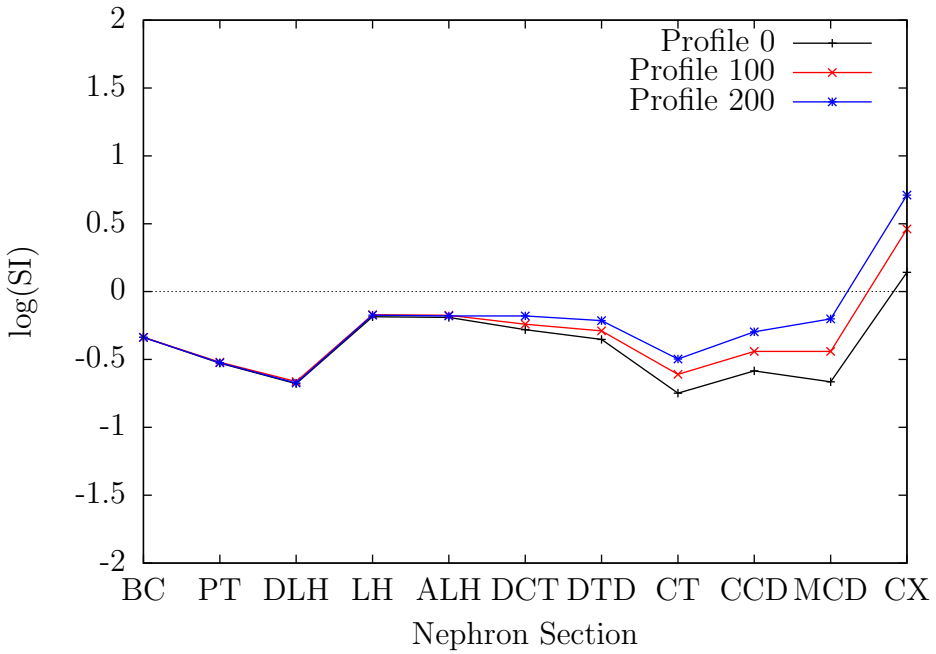

Figure 4.18: log(SI) Brushite: Normal and Stone Former Profiles (Long Nephron)

and short nephron. For the normal case in both the long and short nephrons, the log(SI) value of brushite decreases towards the end of the loop of Henle, while in the abnormal case, it remains at a higher level for longer before falling, but does not approach supersaturation in this part of the nephron. The increase is then greater and earlier in the abnormal case than in the normal case. For COM, the reduced calcium reabsorption in the ascending loop of Henle results in an increased log(SI) value from the end of the loop of Henle onwards in both lengths of nephron. Final supersaturation is higher, and supersaturation is reached earlier in the collecting duct than in the normal situation.

Figures 4.22 and 4.23 show the plots for increased PTH level and increased

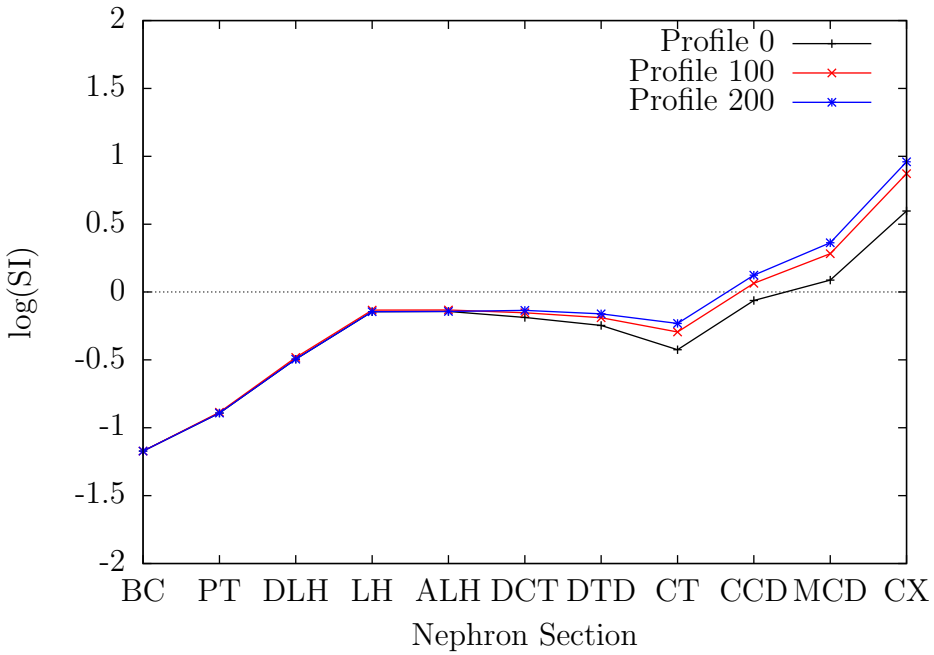

Figure 4.19: log(SI) COM: Normal (Profile 0) and Stone Former Profiles (Profile 100 – Reduced PT Calcium Reabsorption and Profile 200 – Reduced DT Calcium Reabsorption) (Long Nephron)

calcium plasma concentration in the situation of reduced distal tubule calcium reabsorption in comparison to Figures 4.16 and 4.17 showing same conditions in the case for reduced proximal tubule calcium reabsorption. The combination of increased plasma calcium and reduced proximal tubule calcium reabsorption (Profile 167) results in a greater increase in the supersaturation of brushite in the loop of Henle followed by a more rapid and bigger fall than in the reduced distal tubule reabsorption situation. The pattern for COM is similar for both, but COM log(SI) values are slightly higher in the reduced distal tubule reabsorption situation due to the higher calcium concentration. But it is the brushite that is of significance in the reduced proximal tubule calcium reabsorption case, as it does become supersaturated in the loop of Henle and then falls below supersaturation in the late sections of the nephron as the COM supersaturation is rising.

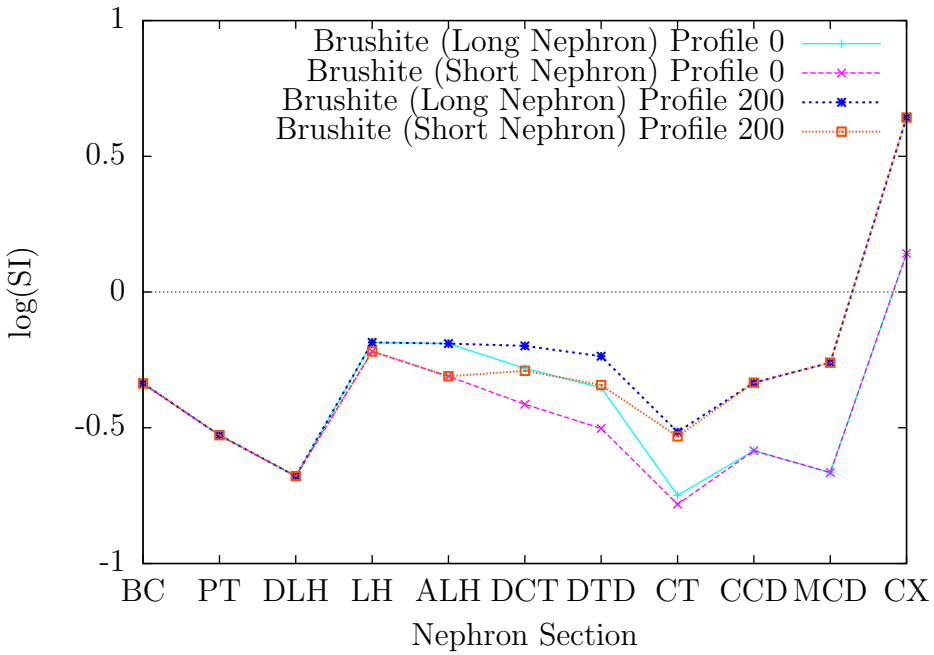

Figure 4.20: log(SI) Values for Brushite for Stone Former Profile 200 (Reduced PT Calcium Reabsorption) in both long and short nephrons compared to values in the normal case

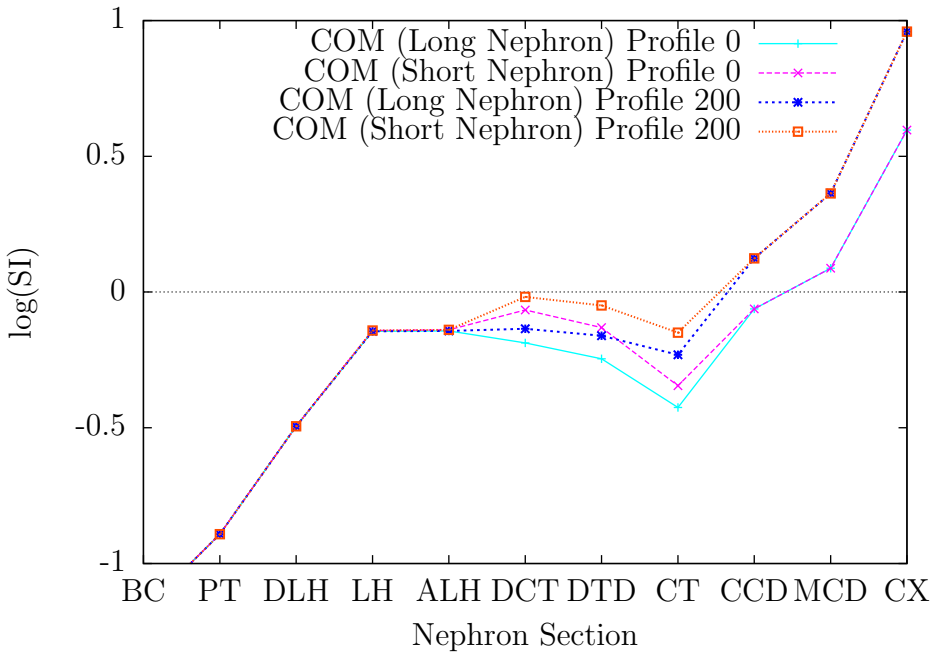

Figure 4.21: log(SI) Values for COM for Stone Former Profile 200 (Reduced DT Calcium Reabsorption) in both long and short nephrons compared to values in the normal case

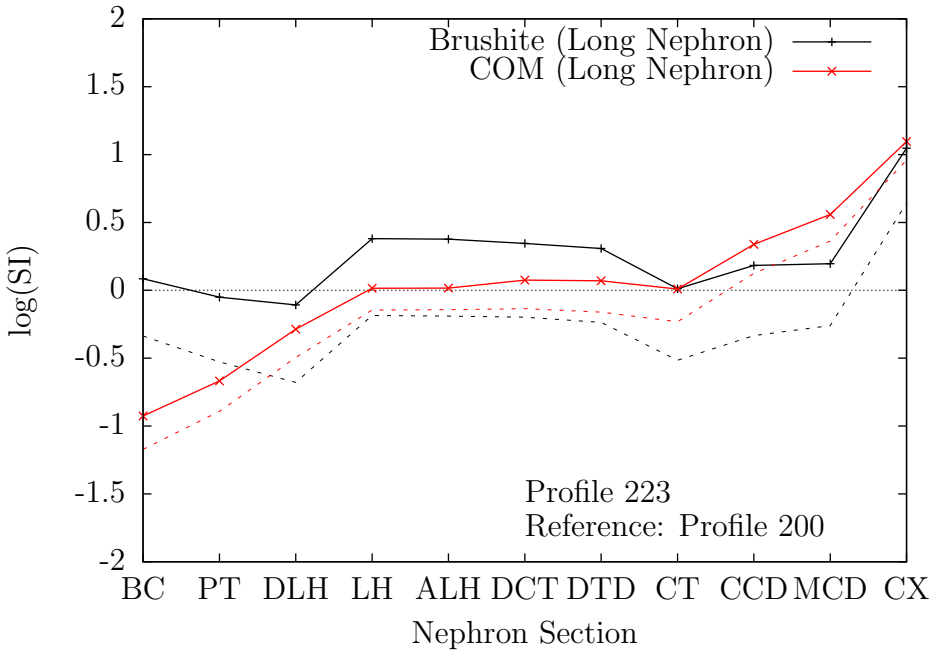

Figure 4.22: Profile 223 (Reduced DT Calcium Reabsorption and High PTH): log(SI) Brushite and COM Long Nephron

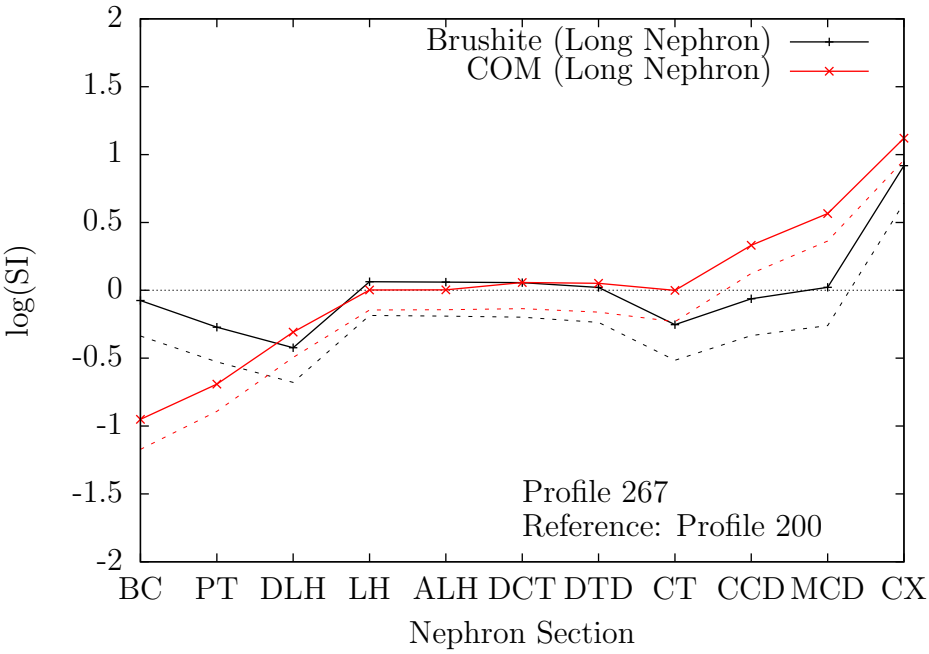

Figure 4.23: Profile 267 (Reduced DT Calcium Reabsorption and Increased Plasma Calcium): log(SI) Brushite and COM Long Nephron

4.6 Combinations

It is assumed that stone formation is initiated when a number of risk factors peak simultaneously, since there is seldom a single factor which is able to separate patients with idiopathic calcium urolithiasis from normal subjects [85WBS, 11Tis1, 14Rod, 17Rob]. In this section, a number of risk factors have been combined and the effect of the combination on risk increase noted.

4.6.1 Profile 301

This is a combination of Profiles 2, 66, 73, 87 and 96, simulating an increased level of ADH, increased plasma concentrations of calcium, phosphate and oxalate, and a reduced plasma concentration of magnesium.

This combination increases the brushite log(SI) to above zero in the loop of Henle and distal tubule, as well as raising log(SI) COM above zero at the end of the proximal tubule and keeping it there for the rest of the nephron, thus yielding a high risk of calcium oxalate stone formation. As shown in Figure 4.24, log(SI) brushite decreases towards the end of the distal tubule, as log(SI) COM starts to increase. This scenario could result in the situation where brushite crystallizes in the loop of Henle, and then dissolves in the early part of the collecting duct, in the region where COM supersaturation is increasing enhancing the formation of COM crystals, thus, illustrating the 'Calcium Phosphate Hypothesis.'

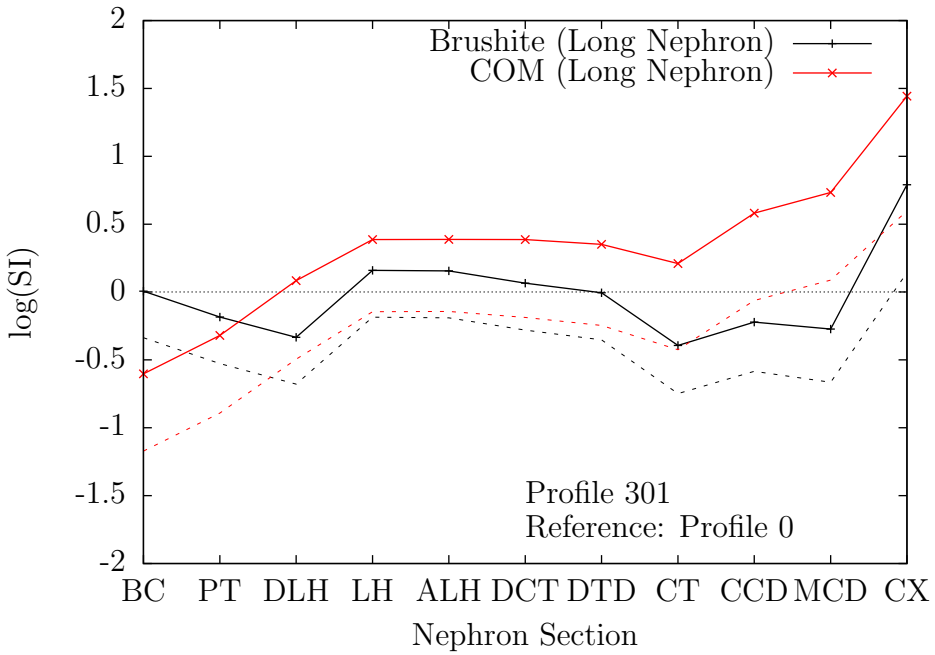

Figure 4.24: Profile 301 (High ADH, Increased Plasma Calcium, Increased Plasma Phosphate, Increased Plasma Oxalate, Decreased Plasma Magnesium): log(SI) Brushite and COM Long Nephron

4.6.2 Profile 311

This is a combination of Profiles 100, 2, 66, 73, 87 and 96, simulating an increased level of ADH, increased plasma concentrations of calcium, phosphate and oxalate, and a reduced plasma concentration of magnesium in addition to the reduced proximal tubule calcium reabsorption.

A similar pattern to Profile 301. Brushite is supersaturated in the loop of Henle and distal tubule, drops below supersaturation in the connecting tubule and cortical collecting duct and then supersaturation increases from the medullary collecting duct to the end of the nephron. COM becomes supersaturated early on in the nephron, rising to a high level toward the end. This is another scenario where brushite may dissolve in the connecting tubule and cortical collecting duct, enhancing the crystallisation of COM.

4.6.3 Profile 321

This is a combination of Profiles 200, 2, 66, 73, 86 and 96, simulating an increased level of ADH, increased plasma concentrations of calcium, phosphate and oxalate, and a reduced plasma concentration of magnesium in addition to the reduced distal tubule calcium reabsorption.

As in Profile 301, the calcium phosphate values are increased all along the nephron and the calcium oxalate values are also increased all along the nephron, and COM becomes supersaturated in the pars recta. In both the long and short nephrons, brushite is supersaturated in the loop of Henle. Brushite

drops below supersaturation at the end of the distal tubule, where the supersaturation of COM is high and increasing. This is another scenario where brushite crystals formed in the loop of Henle, may enhance the formation of COM crystals.

4.6.4 Profile 341

This is a combination of Profiles 100, 66, 86 and 97, simulating an increased plasma concentration of calcium and oxalate in addition to the reduced proximal tubule calcium reabsorption.

The calcium oxalate values are increased all along the nephron, with COM becoming supersaturated in the pars recta, and remaining so for the rest of the nephron. The value for brushite is increased all along the nephron, but only just reaches supersaturation in the loop of Henle in the long nephron. This situation displays an increased risk of COM crystal formation.

4.6.5 Profile 351

This is a combination of Profiles 200, 66, 73, 87 and 96 simulating an increased plasma concentration of calcium, phosphate and oxalate in addition to the reduced distal tubule calcium reabsorption.

There is an increase for the calcium phosphates all along the nephron. Brushite is hardly above supersaturation in the loop of Henle. COM becomes supersaturated in the pars recta. This scenario produces a high risk of COM

crystal formation, due to the high oxalate value.

4.7 Increased Risk due to Brushite Supersaturation

The log(SI) of brushite is greater than zero in the middle sections of a long nephron in the scenarios[1] when there is high plasma calcium levels, high plasma phosphate levels, and high pH combined with reduced calcium reabsorption in the proximal tubule.

In the set of scenarios[2] including increased plasma calcium levels, increased plasma phosphate levels, hyperparathyroidism and certain combinations of deviations from normal, the conditions exist where brushite exceeds supersaturation in the loop of Henle, and then falls below supersaturation further along in the nephron while in those sections COM supersaturation rises above normal values. These scenarios support the 'Calcium Phosphate Hypothesis' that COM precipitation may be enhanced by the brushite precipitation earlier along in the nephron and redissolution later. These relative changes in log(SI) values can be seen in Figures 4.9, 4.16, 4.17, 4.22, 4.23, 4.24, 4.25, 4.26 and 4.27. Only Profiles 67, 167 and 267 are shown in the figures here as Profiles 66, 68, 166, 168, 266 and 268 are similar.

[1]Profiles 23, 66, 67, 68, 74, 123, 138, 166, 167, 168, 174, 223, 266, 267, 268 and 274
[2]Profiles 66, 67, 68, 123, 166, 167, 168, 223, 266, 267, 268, 301, 311, 321 and 341

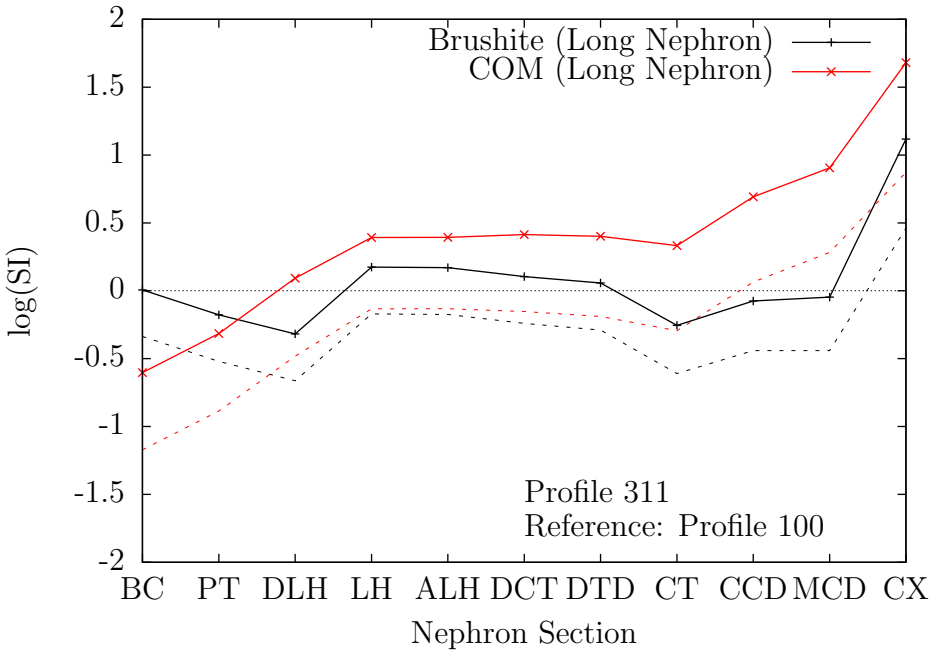

Figure 4.25: Profile 311 (Reduced PT Calcium Reabsorption and High ADH, Increased Plasma Calcium, Increased Plasma Phosphate, Increased Plasma Oxalate, Decreased Plasma Magnesium): log(SI) Brushite and COM Long Nephron

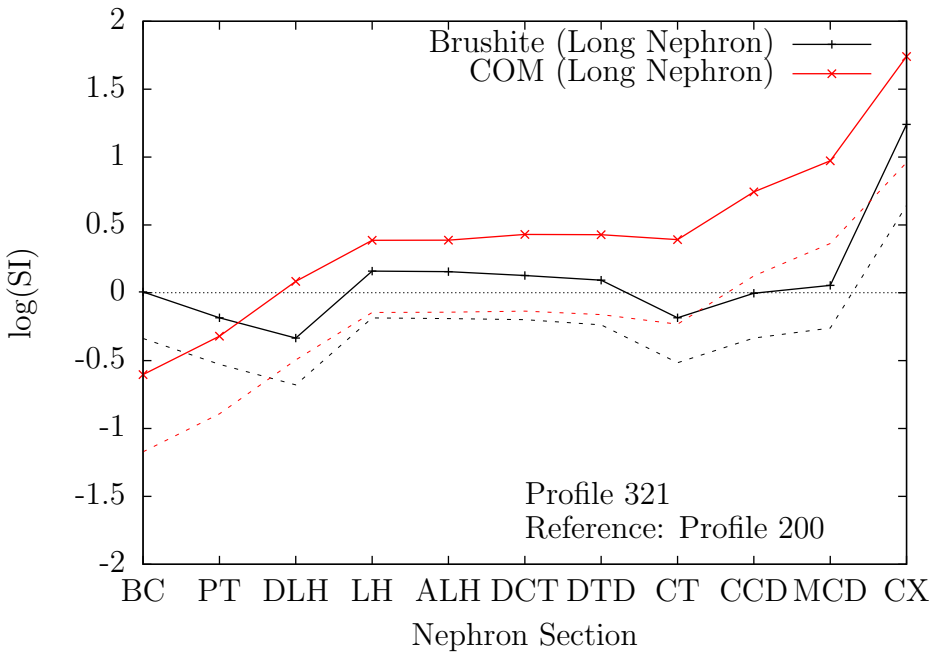

Figure 4.26: Profile 321 (Reduced DT Calcium Reabsorption and High ADH, Increased Plasma Calcium, Increased Plasma Phosphate, Increased Plasma Oxalate, Decreased Plasma Magnesium): log(SI) Brushite and COM Long Nephron

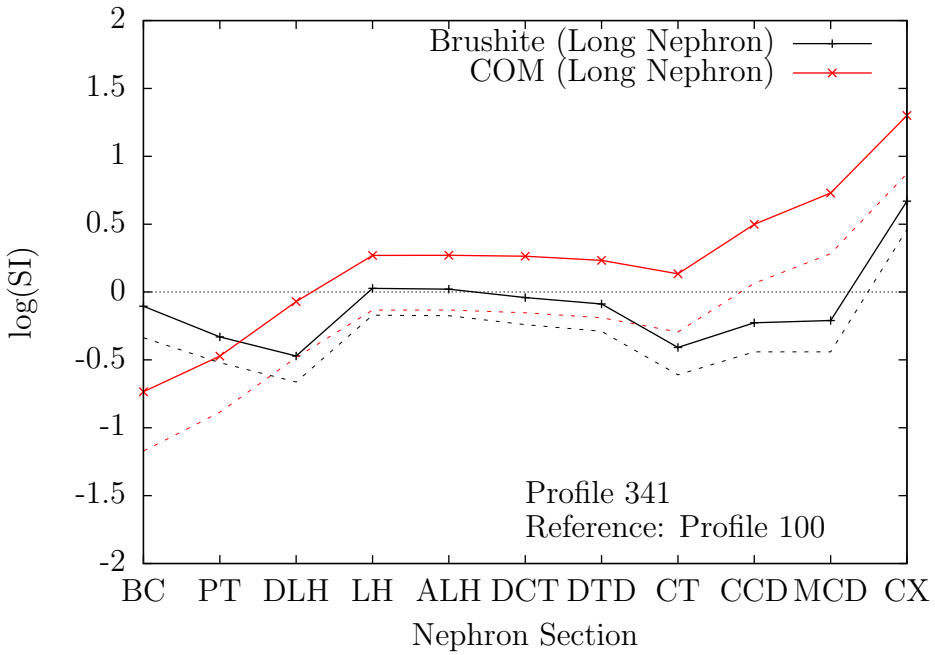

Figure 4.27: Profile 341 (Reduced PT Calcium Reabsorption and Increased Plasma Calcium, Increased Plasma Oxalate, Decreased Plasma Magnesium): log(SI) Brushite and COM Long Nephron

4.8 Calculating Nephron Fluid Concentrations from Specified Urine Concentrations

So far the model has been used where the various inputs have been adjusted and the end result has been the substance concentrations in final urine. Another way to use the model is to specify the concentrations of the resultant urine and make a proportional adjustment of the reabsorption values to fit the required output. By using this 'reverse engineering' model, a set of concentration values at the various locations in the nephron is produced from a set of blood and urine tests that allows details of the processes taking place in the nephron to be revealed. The model is therefore increasing the amount of information that can be obtained from the tests enhancing the clinician's ability to perform diagnoses and provide treatment.

Profile numbers 511, 512 and 513 have been constructed using blood plasma and urine values from Robertson(2015) [15Rob], as shown in Table D.6, for a set of values from normal subjects and sets from two different types of stone formers. The normal subjects are labelled UK N in the figures, and the two sets of recurrent stone formers are one set from the United Kingdom, labelled UK RSF, and one from the Kingdom of Saudi Arabia, labelled KSA RSF. Values for bicarbonate have not been specified in Table D.6 and so have been to set to the values used in Profile 0 of 24 mmol/L for blood plasma, and 338.3 mmol/L for urine. The differences between the three groups of log(SI)

values for brushite and COM along the length of the nephron are shown in Figures 4.28 and 4.29.

The stone type for the patients from Saudi Arabia is calcium oxalate [15Rob]. It can be seen in Figure 4.28 that brushite is well below supersaturation for most of the collecting duct, which fits the characteristics of this case. There is a sharp drop in the value in the early part of the collecting duct. The UK RSF group contains both CaOx and CaP stone formers [15Rob], hence the higher log(SI) values for brushite shown in the plot is as expected. In the case of COM, the value is higher for both sets of stone formers than that for the normal set, all along the nephron, with the values for the recurrent stone formers from the Kingdom of Saudi Arabia being higher than the United Kingdom set, especially in the middle parts of the nephron. In both sets of stone formers, the increase in the log(SI) value of brushite in the mid-nephron, followed by the sharp decrease in value in the collecting duct, where COM supersaturation is rising well above normal supersaturation values illustrated here is yet another scenario where brushite may dissolve in the collecting duct, enhancing the crystallisation of COM.

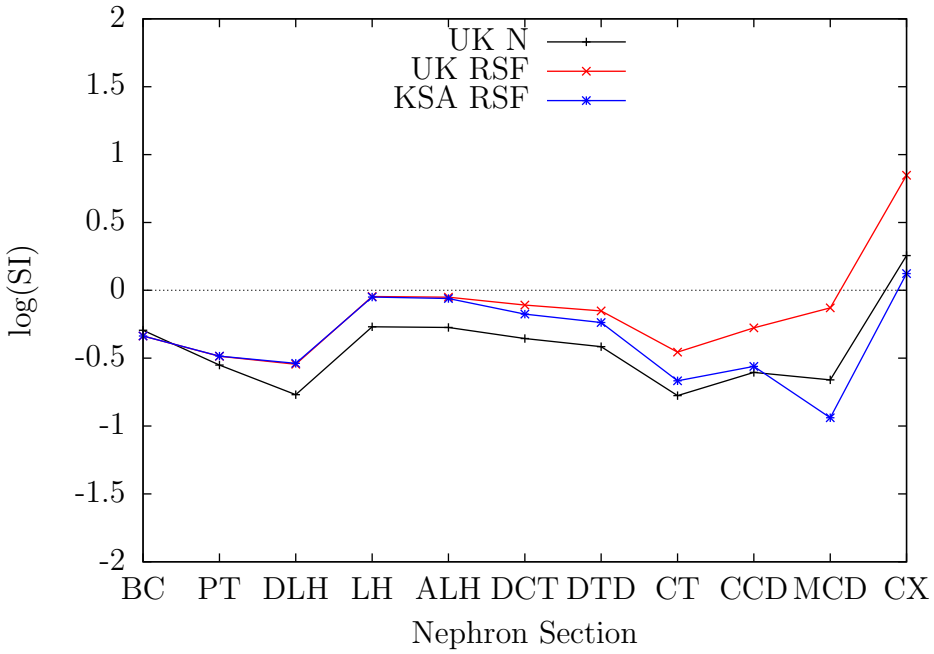

Figure 4.28: Profiles 511, 512 and 513 log(SI) Brushite: Normal and Stone Former Profiles (Long Nephron)

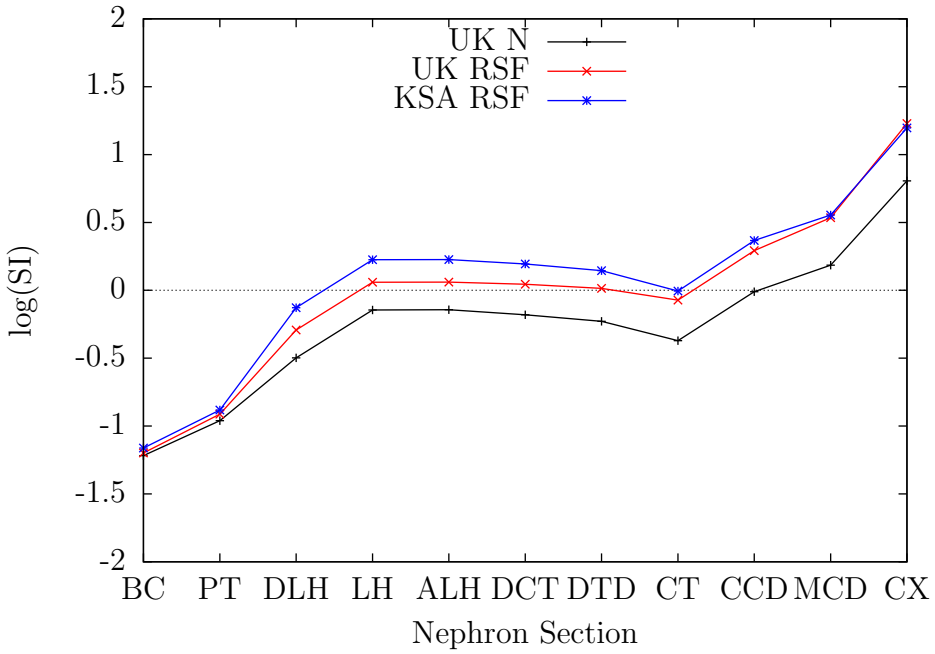

Figure 4.29: Profiles 511, 512 and 513 log(SI) COM: Normal and Stone Former Profiles (Long Nephron)

4.9 Model Testing

Figures E.1 to E.15 show the model output values and published values for substances included in the model. These plots show that the output from the model fits well with measured values.

The simple variations on Profile 0 of decreasing or increasing the ADH level (Profile 1 and Profile 2) produce the expected results due to the changes in concentration in the latter sections of the nephron and hence confirm the general reliability of the output. Similarly, changes in citrate concentration also show alterations which are known to occur.

While this study is primarily concerned with the formation of calcium-based stones, uric acid stone formation has been included for model testing purposes. The fact that the model behaves as expected in the case of uric acid stone formation demonstrates that the behaviour of the model is reasonable.

4.10 Model Limitations

The nephron simulation program, described in Section 3.2 and Appendix E, is based on details of physiology and reabsorption and secretion values from numerous sources. Many aspects of renal function are not fully understood and the values available regarding substance movement into and out of the various parts of the nephron are estimates and averages. Therefore the results produced by the simulation are approximations.

The thermodynamic modelling using JESS is very dependent on the data in the database. Some substances, such as citrate, are known to form complexes with calcium ions and thus reduce the supersaturation of stone forming solids. Other substances, such as sulfate, do not do this as well and still some others, such as urea, have little such effect. If information about some interactions is inaccurate or missing from the database, then the true effect will obviously not be reflected by the model. The thermodynamic modelling is not able to include any effects of macromolecules, as no data for these substances is available.

Chapter 5

Conclusion

In this work computing tools have been developed to gain insight into various aspects of the medical condition of urolithiasis. The main value of this modelling is that it can help clinicians predict risk in cases where there is increased likelihood of stone recurrence. In these cases a measure of supersaturation is highly relevant because it provides a single vector, directly related to the propensity for precipitation, which can be compared after the clinical diagnosis to monitor patient progression or regression.

A detailed analysis of various scenarios that can occur in the fluid of the nephron lumen has been performed by combining a simulation of nephron filtration model with calculations from the Joint Expert Speciation System. The combined model allows the composition of nephron fluid to be calculated under different conditions. Unlike other nephron fluid models in the literature, this model considers both long and short nephrons, and thus can

highlight resulting differences between the properties of the fluid. The model estimates supersaturation changes associated with variations in concentration of substances in blood plasma, pathological alterations in calcium reabsorption and changes in hormone levels. Variations in plasma concentrations of calcium, oxalate and phosphate are shown to be the main drivers of change in stone formation risk. The level of citrate is also important. Combinations of changes can produce significant synergistic effects. It is indeed considered likely that kidney stone initiation in general stems from co-incidental effects impacting together. The calculations performed showing how the composition of tubular fluid changes at various locations within the nephron under different clinical conditions, together with the indications regarding which stone forming salts may precipitate at particular sites, will help researchers better understand the pathogenesis of kidney stone formation. These developments may in turn lead to further improvements in the methodology of treatment of this disease.

A key outcome of this research is that the risk of calcium phosphate precipitation is found to be higher in long nephrons than short nephrons, due to the higher pH and higher concentrations. Brushite seems to be the phase of calcium phosphate most likely to initially precipitate. The 'Calcium Phosphate Hypothesis', attributes enhancement of calcium oxalate stone formation to an initial precipitation of calcium phosphate in the middle sections of the nephron. A number of scenarios have been illustrated in this work where the risk of brushite precipitation is seen in the middle of the nephron followed by conditions where it may then dissolve in the collecting duct, where calcium

oxalate supersaturation is simultaneously increasing. These support the validity of the 'Calcium Phosphate Hypothesis'.

The most common method for monitoring urolithiasis is urinalysis. Since the kidney stone formation process has it origin in the nephron, for the purpose of diagnosis of stone disease, nephron fluid composition is more important than urine composition. However, the measurement of the composition of fluid within nephrons is not clinically feasible. The so-called 'reverse model' developed here allows information about the processes and substance concentrations within the nephron to be extracted from the results of a urinalysis. In this way, the diagnostic value of urinalysis can be enhanced.

The effects of urinary macromolecules are not taken into account in the methods used here. However, while these substances may reduce or increase the risk of stone formation, the underlying physicochemical properties of the solution are thought to be the main factors driving any stone forming process that takes place. Thus, the quantitative results produced here are considered to be a valuable representation of the risk of stone disease.

Appendix A

Blood Plasma Composition and Concentrations

This chapter contains a collection of published values for the concentrations of various substances found in blood plasma. Different sources give different values, so for the purposes of construction of the model a single value has been selected as a reference value for each substance of interest. These values are shown as the "Value Used" at the end of each list of published values.

The following values are from the Documenta Geigy Scientific Tables [70Gei], unless otherwise indicated.

Water

945 g/L

90 to 93 g/100mL [68BDS]

Sodium, Na^+

144 mEq/L = 144 mmol/L

140 – 145 mEq/L [97GuH]

142 mEq/L [00GuH]

0.32 g/100mL [68BDS]

142 mmol/L [10BZC]

140 mmol/L [15Rob]

Value Used: 145 mmol/L

Potassium, K^+

3.7 mEq / L = 3.7 mmol/L

4.2 mEq/L [97GuH]

5 mEq/L [00GuH]

0.02 g/100mL [68BDS]

= 0.2 g/L = 0.0051 mol/L

Value Used: 4.2 mmol/L

Calcium, Ca^{2+}

A significant proportion of the calcium in plasma is bound to proteins. Only the unbound fraction is available for ultrafiltration

Total:

5.2 mEq/L = 2.6 mmol/L

Total Plasma Calcium:

5 mEq/L = 2.5 mmol/L [06GuH]

Calcium Ion Concentration:

2.4 mEq/L = 1.2 mmol/L [06GuH]

0.01 g/100mL = 2.5 mmol/L [68BDS]

8.7 – 10.2 mg/dL = 2.17 – 2.54 mmol/L [84NTM]

8.5 – 10.5 mg/dL = 2.12 – 2.62 mmol/L [08Sho]

Ultrafiltrable Calcium:

1.5 mmol/L [04Rob]

1.47 mmol/L [15Rob]

Value Used: 1.5 mmol/L

Magnesium, Mg^{2+}

1.7 mEq/L = 0.85 mmol/L

1.5 mEq / L [00GuH]

0.0025 g/100mL [68BDS]

0.025 g/L = 0.0103 mmol/L

Value Used: 0.4 mmol/L

Bicarbonate, HCO_3^-

24.9 mEq/L = 24.9 mmol/L

24 mEq / L [00GuH]

Value Used: 24 mmol/L

Chloride, Cl^-

106 mEq/L = 106 mmol/L

107 mEq / L [00GuH]

0.37 g/100mL [68BDS]

Value Used: 125 mmol/L

Phosphorus

112 mg/L total

33.6 mg of this is inorganic

Hydrogen Phosphate, HPO_4^{2-}

3 mEq/L [00GuH]

= 1.5 mmol/L

Phosphate, PO_4^{3-}

0.003 g/100 mL [68BDS]

PO_4^{3-}

2.5 to 4.5 mg/dl (15% is bound to proteins) [84NTM] : 0.26 to 0.47 mmol/L

0.81 - 1.45 mmol/L[08Sho]

Ultrafiltrable Phosphate: 1.0 mmol/L [15Rob]

Value Used: 1.5 mmol/L (as HPO_4^{2-})

Pyrophosphate

2 to 6 $\mu mol/L$ [77FlR]

Sulfur

780 mg/L total

740 mg in protein

Sulfate, SO_4^{2-}

15.7 mg inorganic sulfate

SO_4^{2-} 0.5 mEq/L [00GuH]

= 0.25 mmol/L

0.003 g/100mL [68BDS]

0.33 mmol/L [01BeS]

Value Used: 0.35 mmol/L (as SO_4^{2-})

Nitrogen

13.1 g/L total

240 mg/L nonprotein

Urea, $CO(NH_2)_2$

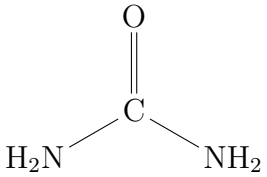

328 mg/L

= 5.46 mmol/L

0.03 g/100mL [68BDS]

4 to 10 mmol/L [12BaY]

Value Used: 5.46 mmol/L

Uric Acid, $C_5H_4N_4O_3$

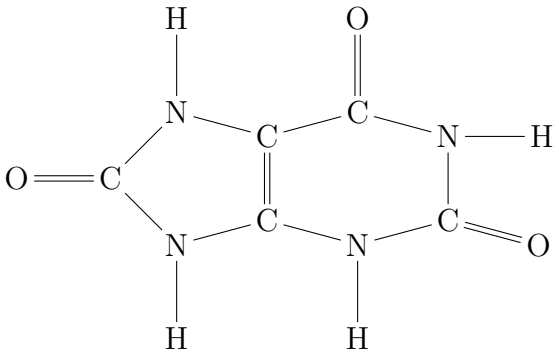

48.6 mg/L

0.002 g/100mL [68BDS]

0.25 mmol/L [90Lan]

Value Used: 0.25 mmol/L

Ammonia, NH_3 and Ammonium, NH_4^+

0.19 mg/L

0.0001 g/100mL [68BDS]

Value Used: 1.118E-02 mmol/L

Citrate, $C_6H_5O_7^{3-}$

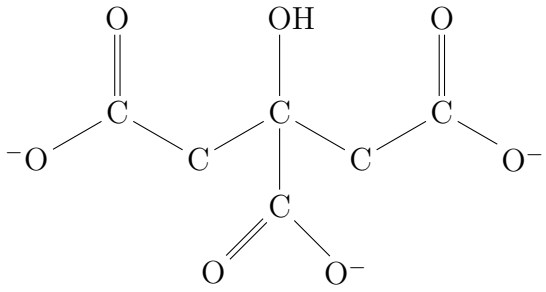

13 to 16.7 mg/L, as Citric Acid [70Gei] (0.07 to 0.09 mmol/L)

0.05 to 0.3 mmol/L [09ZuA]

Value Used : 0.3 mmol/L

Creatinine

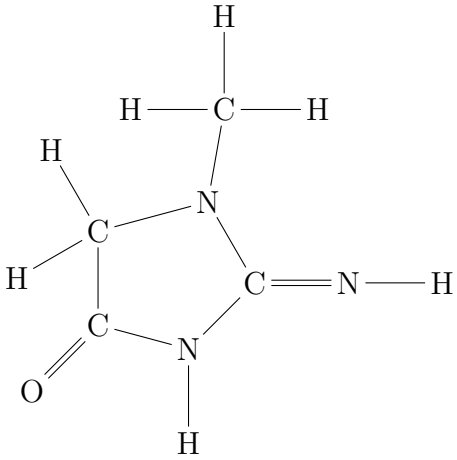

$C_4H_7N_3O$

12.4 mg/L = 0.000109 mmol/L

0.001 g/100mL [68BDS]

Value Used: 0.109 mmol/L

Oxalate, $C_2O_4^{2-}$

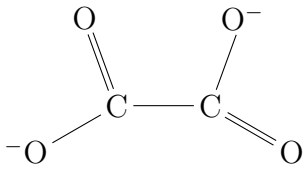

1 to 3 mg/L

100 - 235 μg per 100 mL [84NTM]

1 to 2 μmol/L [96AMC]

2 μmol/L [04Rob]

1.50 μmol/L [15Rob]

0.7 to 4 μmol per litre [97Kok]

1 to 5 μmol per litre [90Lan]

Stone Formers: 1.65 to 1.79 μmol/L [15Rob]

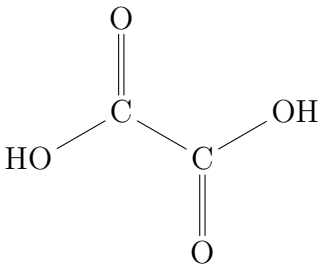

Oxalic Acid

Value Used : 1.75 μmol/L

Glucose

995 mg/L

0.1 g/100mL [68BDS]

= 5.6 mmol/L

Value Used: 5.6 mmol/L

Phytic Acid

Phytic Acid or Phytate.

Normal: 0.26 $\pm$ 0.03 mg/L (0.393μmol/L)

Low: 0.07 $\pm$ 0.01 mg/L (0.106μmol/L)

[01GSV]

Vitamins

A: 324 μg/L

D: 2000 IU/L

Ascorbic Acid (C): 4.76 mg/L

Copper

1.1 mg/L

Manganese

2 μg/L

Zinc

1.2 mg/L

Bromide, Br^-

2.8 mg/L

Fluoride, F^-

0.16 mg/L

Iodide, I^-

52.1 μg/L total

2.8 μg/L inorganic

48.1 μg/L protein bound

Thiocyanate

0.8 mg/l

Cobalt

0.29 μg/L

Iron

1.34 mg/L (Most of this is bound)

Aluminium

172 μg/L

370 nmol/L [10TGD]

Lead

29 μg/L

pH

7.38 – 7.42 [06Ath4]

Value Used: 7.4

Ionic Strength

0.15 mmol/L [15May]

Redox Potential

Eh = -83 mV [15May]

Trace Elements

Trace elements are dietary minerals required in very small quantities. They are essential for normal body function. Their most common function is as structural components of enzymes and cofactors. They are defined as each being less than 0.01 % body mass and collectively less than 1 % [10Str]. Trace elements include chromium, cobalt, copper, flourine, iodine, iron, manganese, molybdenum, selenium, zinc, boron, germanium and lithium [91GAB, 11Slo]. Of these, iron, copper, cobalt, manganese, molybdenum, and zinc are considered to be essential [67ElE]. A lack of them can result in numerous problems, including inadequate absorption of nutrients and failures in immune function, antioxidant defence and regulation of gene expression [10Str]. Iron is the most common trace element found in the body [95TaW]. Zinc is the second most common trace element [11Slo]. Increased concentrations of copper are found in the liver, kidney, heart and brain. It is an antioxidant. Copper and manganese urinary levels have been found to be lower in stone formers [11Slo]. A low concentration of boron has been reported in patients with cystine stones

[11Slo]. Selenium is found in some anti-oxidant and anti-inflammatory compounds [11Slo].

Trace elements have not been included in the model. Due to their low concentrations, the effects produced by them in the thermodynamic calculations would not be significant.

Appendix B

Urine Composition and Concentrations

The volume of urine produced per day is about 1 to 2 litres [68BDS, 06CMA, 07TaC]. The specific gravity is 1.001 to 1.040, representing the removal from the body of 40 to 60 g of dissolved salts in 24 h [68BDS]. The pH can vary from 4.5 to 8 and the concentration can vary over a range of 4 to 5 times average figures [97BrK]. As many as 150 different substances have been found in human urine [71MBR]. Saude *et al* [07SAR], highlight the difficulties in attempting to establish normal baseline values for the composition of urine. They have shown that large variations exist in both intra- and inter-subject concentrations of different metabolites identified and measured in urine. The composition of urine also varies according to the time of day [82SoK, 70Gei].

Table B.1 gives some mean values for an analysis of 330 samples of 24 h

Table B.1: Average Composition of 24 h Urine of Female Subjects, from [07TaC]. Range values are 10th to 90th percentile values.

Component	Mean Value	Range
Creatinine (mg)	1036	775 to 1326
Calcium (mg)	183	73 to 302
Oxalate (mg)	28	18 to 40
Citrate (mg)	686	332 to 1012
Uric acid (mg)	448	281 to 662
Sodium (mEq)	137	72 to 204
Potassium (mEq)	64	39 to 94
Magnesium (mg)	104	63 to 152
Phosphate (mg)	743	465 to 1040
Sulfate (mmol)	17	10 to 26
pH	6.08	5.42 to 6.71
Volume (L)	2.03	1.14 to 2.96

urine. In this study [07TaC] titratable acids and urinary ammonium were not measured. The results from some similar studies are shown in Table B.2 and Table B.3.

Table B.4 lists some other substances mentioned in the literature as being found in urine.

Values for the concentration of substances found in urine given in a number

Table B.2: Average Composition of 24 h Urine, from [06CMA]

Component	Value (per day)	Units
Volume	2.1	L
Uric Acid	500	mg
pH	6.05	–
Sulfate	37	mEq
Potassium	60	mEq
Ammonium	29	mEq
Citrate	11	mEq
Bicarbonate	4.7	mEq

Table B.3: Average Composition of 24 h Urine, from [10EES]

Component	Value (per day)	Units
Volume	2.3	L
Uric Acid	0.71	g
pH	6.14	–
Sodium	154	mmol
Calcium	186	mg
Sulphite	46	mg
Potassium	70	mmol
Magnesium	105	mg
Phosphorus	0.88	g
Citrate	488	mg
Oxalate	41	mg
Creatinine	1578	g

Table B.4: Other Substances Found in Urine

Substance	Range	Reference
Hippuric Acid	2 – 10 mmol/L	[93GAB]
Tamm-Horsfall Protein	1.1 – 19.8 mg/L	[00GHJ]
4-Hydroxyphenylacetate	0.02 – 0.24 mmol/L	[07SAR]
Alanine	0.04 –0.80 mmol/L	[07SAR]
Aspartate	0.00 – 0.34 mmol/L	[07SAR]
Creatine	0.00 – 2.05 mmol/L	[07SAR]
Formate	0.03 – 3.47 mmol/L	[07SAR]
Glutamate	0.00 – 0.59 mmol/L	[07SAR]
Histidine	0.01 – 1.35 mmol/L	[07SAR]
Lactate	0.03 – 9.79 mmol/L	[07SAR]
N-Methylhistidine	0.00 – 0.83 mmol/L	[07SAR]
Phenylalanine	0.01 – 0.33 mmol/L	[07SAR]
Tryptophan	0.02 – 0.28 mmol/L	[07SAR]
Tyrosine	0.01 – 0.29 mmol/L	[07SAR]

Table B.5: Typical Main Components of Urine [68BDS]

Substance	g/24 h
Urea	20 to 30 (9 to 14 g nitrogen)
Uric acid	0.6 (0.2 g nitrogen)
Creatinine	1.2 (0.4 g nitrogen)
Ammonia	0.5 to 0.9 (0.4 to 0.7 g nitrogen)
Sodium	6
Potassium	2
Calcium	0.2
Chloride	7
Phosphate	1.7
Sulfate (as H_2SO_4)	1.8
Free Amino Acids	1
Conjugated Amino Acids	2

of publications are listed below. As noted in Section 2.6, urine concentrations are very variable, therefore, as in the case of the blood plasma concentration values, one value for each substance has been selected as the "Value Used" as a basis for normal urine, so that the effects of alterations in the filtration process can be compared to it.

Sodium, Na^+

Should be > 20 mmol/L [11Sch]

Range: 120 to 220 mEq per 24 h [70Gei]

Male

Reference	Value per 24 h	Units	L / 24 h	Concentration (mmol/L)
[06RAJ]	222.7	mmol	1.477	151
[04SJH]	173	mmol	2.32	75
[70Gei]	177	mEq	1.015	174

Female

Reference	Value per 24 h	Units	L / 24 h	Concentration (mmol/L)
[06RAJ]	101.2	mmol	1.674	60.45
[07TaC]	137	mmol	2.03	67.49

128 mEq per 24 hrs (Range: 120 to 220 mEq per 24 hr) [70Gei]

137 mEq per 24 hrs (Range: 72 to 204 mEq per 24 hr) [07TaC]

Stone Formers

CaOx Stone Formers 91.29 mmol/L [14RGE]

CaP Stone Formers 88.75 mmol/L [14RGE]

Uric Acid Stone Formers 89.55 mmol/L [14RGE]

Cystine Stone Formers 89.10 mmol/L [14RGE]

Values for Male Stone Formers, grouped by BMI (Body Mass Index) quartiles (mmol per 24 hours) [10EES]:

BMI	22.0	24.8	27.5	33.4
mmol	154.0	156.6	189.1	206.8

Values for Female Stone Formers, grouped by BMI quartiles (mmol per 24 hrs) [10EES]:

BMI	22.0	24.8	27.5	33.4
mmol	129.1	134.1	160.6	189.8

Values for Male Stone Formers rated according to increasing score of DASH-Style diet (Dietary Approaches to Stop Hypertension) (mEq per 24 hrs (adjusted)) [10TSM]:

DASH Score	1	2	3	4	5
mEq	186	183	183	185	177

Values for Female Stone Formers (mEq per 24 hrs), (adjusted) and rated according to increasing score of DASH-Style diet [10TSM]:

DASH Score	1	2	3	4	5
mEq	152	148	155	152	150

Na^+:Value Used for Normal Urine: 125 mmol/L

Potassium, K^+

Male

Reference	Value per 24 h	Units	L / 24 h	Concentration (mmol/L)
[06RAJ]	47.24	mmol	1.477	32.0
[04SJH]	80	mmol	2.32	34.5
[70Gei]	57	mEq	1.015	56.2

57 mEq per 24 hrs (Range: 35 to 80 mEq per 24 hrs) [70Gei]

Female

Reference	Value per 24 h	Units	L / 24 h	Concentration (mmol/L)
[06RAJ]	42.92	mmol	1.674	25.6
[07TaC]	64	mEq	2.03	31.5
[70Gei]	47	mEq	0.989	47.5

64 mEq per 24 hrs (Range: 39 to 94 mEq per 24 hrs) [07TaC]

Stone Formers

CaOx Stone Formers 38.20 mmol/L [14RGE]

CaP Stone Formers 48.12 mmol/L [14RGE]

Uric Acid Stone Formers 48.82 mmol/L [14RGE]

Cystine Stone Formers 25.10 mmol/L [14RGE]

Values for Male Stone Formers, grouped by BMI quartiles (mmol per 24 hrs) [10EES]:

BMI	22.0	24.8	27.5	33.4
mmol	69.6	68.3	71.1	78.7

Values for Female Stone Formers, grouped by BMI quartiles (mmol per 24 hrs) [10EES]:

BMI	20.5	24.3	28.8	38.6
mmol	57.6	60.4	64.3	68.1

Values for Male Stone Formers, mEq per 24 hrs (adjusted) and rated according to increasing score of DASH-Style diet [10TSM]:

DASH Score	1	2	3	4	5
mEq	66	75	77	79	87

Values for Female Stone Formers, mEq per 24 hrs (adjusted) and rated according to increasing score of DASH-Style diet [10TSM]:

DASH Score	1	2	3	4	5
mEq	48	52	56	59	64

47 mEq per 24 hrs (Range: 35 to 80) [70Gei]

K^+: Value Used for Normal Urine: 30.4 mmol/L

Calcium, Ca^{2+}

11.5 mEq per 24 hrs (Range: 6.5 to 16.5) [70Gei] 7.8 mmol per 24 hrs = 5.2 mmol/L for 1.5 L

< 50 to > 500 mg per day

Average 130 to 170 mg daily for both genders [11CEW]

High: Over 250mg per 24 h [99GSC]

Hypercalciuria: 400 mg or more per 24h [04KYY]

Male

Reference	mmol per 24 h	L/24 h	mmol/L
[06RAJ]	3.33	1.477	2.25
[04SJH]	5.11	2.32	2.2
[70Gei]	5.75	1.015	5.7

Female

Reference	Value per 24 h	Units	L / 24 h	mmol/L
[07TaC]	183	mg	2.03	2.25

1.98 mmol per 24h hrs [06RAJ]

183 mg per 24 hrs (Range: 73 to 302 mg per 24 hrs) [07TaC]

Stone Formers

CaOx Stone Formers 2.61 mmol/L [14RGE]

CaP Stone Formers 2.86 mmol/L [14RGE]

Uric Acid Stone Formers 2.62 mmol/L [14RGE]

Cystine Stone Formers 1.54 mmol/L[14RGE]

Overnight: 6 mmol vs 2 mmol for normals [11CEW]

Values for Male Stone Formers, grouped by BMI quartiles (mg per 24 hrs) [10EES]:

BMI	22.0	24.8	27.5	33.4
mg	186.2	198.2	230.2	236.1

Values for Female Stone Formers, grouped by BMI quartiles (mg per 24 hrs) [10EES]:

BMI	22.0	24.8	27.5	33.4
mg	183.4	181.5	206.0	206.3

Values for Male Stone Formers, mg per 24 hrs (adjusted) and rated according to increasing score of DASH-Style diet [10TSM]:

DASH Score	1	2	3	4	5
mg	195	184	201	206	201

Values for Female Stone Formers, mg per 24 hrs (adjusted) and rated according to increasing score of DASH-Style diet [10TSM]:

DASH Score	1	2	3	4	5
mg	196	207	212	200	219

Ca^{2+}: Value Used for Normal Urine: 2.025 mmol/L

Magnesium, Mg^{2+}

High: Over 70 mg per 24 h [99GSC]

Hypomagnesuria: 75 mg or less per 24h [04KYY]

Male

Reference	Value per 24 h	Units	L / 24 h	Concentration
[06RAJ]	4.96	mmol	1.477	3.35
[04SJH]	5.05	mmol	2.32	2.18
[70Gei]	10.7	mEq	1.015	5.27

4.96 mmol per 24h hrs [06RAJ]

10.7 mEq per 24 hrs (Range: 4.7 to 16.7) [70Gei]

Female

Reference	Value per 24 h	L / 24 h	Concentration (mmol/L)
[07TaC]	4.28	2.03	2.11

Range: 63 to 152 mg per 24 hrs [07TaC]

2.37 mmol per 24h hrs [06RAJ]

8.8 mEq per 24 hrs (Range: 3.4 to 14.2) [70Gei]

Stone Formers

CaOx Stone Formers 6.63 mg/dL [14RGE]

CaP Stone Formers 5.66 mg/dL [14RGE]

Uric Acid Stone Formers 6.17 mg/dL [14RGE]

Cystine Stone Formers 5.03 mg/dL [14RGE]

Values for Male Stone Formers, grouped by BMI quartiles (mg per 24 hrs) (mg and not g as listed in the paper) [10EES]:

BMI	22.0	24.8	27.5	33.4
mg	104.6	108.4	121.7	123.5

Values for Female Stone Formers, grouped by BMI quartiles (mg per 24 hrs) (mg and not g as listed in the paper) [10EES]:

BMI	22.0	24.8	27.5	33.4
mg	94.5	95.5	95.9	105.3

Values for Male Stone Formers, mg per 24 hrs (adjusted) and rated according to increasing score of DASH-Style diet [10TSM]:

DASH Score	1	2	3	4	5
mg	115	120	122	127	135

Values for Female Stone Formers. mg per 24 hrs (adjusted) and rated according to increasing score of DASH-Style diet [10TSM]:

DASH Score	1	2	3	4	5
mg	90	96	100	105	105

Mg^{2+}: Value Used for Normal Urine: 2.1 mmol/L

Chloride

98.2 mmol/L (N) [13RAJ]

Reference	Value per 24 h	Units	L / 24 h	Concentration (mmol/L)
[06RAJ]	155	mmol	1.477	104.9
[04SJH]	188	mmol	2.32	81.0
[70Gei]	184	mEq	1.015	181.3

Male

155 mmol per 24h hrs [06RAJ] = 105 mmol/L

188 mmol per 24 hrs [04SJH] = 81 mmol/L

184 mEq per 24 hrs (Range: 120 to 240) [70Gei]

Female

Reference	Value per 24 h	Units	L / 24 h	Concentration (mmol/L)
[06RAJ]	111.1	mmol	1.674	66.4

111.1 mmol per 24h hrs [06RAJ]

Stone Formers

CaOx Stone Formers 88.87 mmol/L [14RGE]

CaP Stone Formers 97.57 mmol/L [14RGE]

Uric Acid Stone Formers 98.36 mmol/L [14RGE]

Cystine Stone Formers 81.20 mmol/L [14RGE]

106.7 mmol/L [13RAJ]

Cl^-: Value Used for Normal Urine: 81 mmol/L

Phosphorus

Reference	Value per 24 h	Units	L / 24 h	Concentration (mmol/L)
[70Gei]	0.8 – 2.0	g	0.989	26.12 – 65.30

Stone Formers

Values for Male Stone Formers, grouped by BMI quartiles (g per 24 hrs) [10EES]:

BMI	22.0	24.8	27.5	33.4
g	0.88	0.95	1.09	1.16

Values for Female Stone Formers, grouped by BMI quartiles (g per 24 hrs) [10EES]:

BMI	22.0	24.8	27.5	33.4
g	0.73	0.82	0.89	0.98

Phosphate

800 mg/day [84NTM]

Male

Reference	Value per 24 h	Units	L / 24 h	Concentration
[06RAJ]	29.39	mmol	1.477	19.9
[04SJH]	37.3	mmol	2.32	16.08

Female

19.36 mmol per 24h hrs [06RAJ]

743 mg per 24 hrs (Range: 465 to 1040) [07TaC]

Stone Formers

CaOx Stone Formers 61.60 mg/dL [14RGE]

CaP Stone Formers 57.00 mg/dL [14RGE]

Uric Acid Stone Formers 66.18 mg/dL [14RGE]

Cystine Stone Formers 38.50 mg/dL [14RGE]

Values for Male Stone Formers, mg per 24 hrs (adjusted) and rated according to increasing score of DASH-Style diet [10TSM]:

DASH Score	1	2	3	4	5
mg	1035	1066	1052	1107	1100

Values for Female Stone Formers, mg per 24 hrs (adjusted) and rated according to increasing score of DASH-Style diet [10TSM]:

DASH Score	1	2	3	4	5
mg	832	834	835	853	857

PO_4^{2-}: Value Used for Normal Urine: 19.9 mmol/L

Oxalate

15 to 50 mg/day [84NTM]

0.4 mmol per 24 hrs [90Lan]

Low Normal 0.031 mmol; Normal 0.44 mmol; High Normal 0.62 mmol; Acute High 0.89 mmol (per 24 h) [94KoK]

Hyperoxaluria: 45 mg or more per 24h [04KYY]

Male

Reference	Value per 24 h	Units	L / 24 h	Concentration (mmol/L)
[06RAJ]	0.160	mmol	1.477	0.108
[04SJH]	0.423	mmol	2.32	0.182
[04Rob]	0.470	mmol	1.5	0.313

Female

Reference	Value per 24 h	Units	L / 24 h	Concentration (mmol/L)
[07TaC]	28	mg	2.03	0.157

0.20 mmol per 24h hrs [06RAJ]

28 mg per 24 hrs (Range: 18 to 40) [07TaC]

Stone Formers

UK RSF 1.65 μmol/L [15Rob]

CaOx Stone Formers 1.68 mg/dL [14RGE]

CaP Stone Formers 1.37 mg/dL [14RGE]

Uric Acid Stone Formers 2.02 mg/dL [14RGE]

Cystine Stone Formers 0.98 mg/dL [14RGE]

In Primary Hyperoxaluria > 65 to 70 mg per day

Values for Male Stone Formers, grouped by BMI quartiles (mg per 24 hrs) [10EES]:

BMI	22.0	24.8	27.5	33.4
mg	40.5	39.8	43.4	42.6

Values for Female Stone Formers, grouped by BMI quartiles (mg per 24 hrs) [10EES]:

BMI	22.0	24.8	27.5	33.4
mg	33.1	38.3	37.7	40.8

Values for Male Stone Formers, mg per 24 hrs (adjusted) and rated according to increasing score of DASH-Style diet [10TSM]:

DASH Score	1	2	3	4	5
mg	38	39	40	39	45

Values for Female Stone Formers, mg per 24 hrs (adjusted) and rated according to increasing score of DASH-Style diet [10TSM]:

DASH Score	1	2	3	4	5
mg	27	26	28	28	28

Oxalate: Value Used for Normal Urine: 0.2 mmol/L

Citrate

350mg per 24 h [99GSC] Range 0.05 to 9.50 mmol/L [07SAR]

A value below 1.67 mmol per 24 hrs is considered to be Hypocitraturia [09ZuA].

Hypocitraturia: 320 mg or less per 24h [04KYY]

350 mg/day (male) 500mg/day (female) [05CEW]

Male

Reference	Value per 24 h	Units	L / 24 h	Concentration (mmol/L)
[06RAJ]	2.95	mmol	1.477	1.997
[04SJH]	2.262	mmol	2.32	0.975
[07SAR]	1.00	mmol	2.535	2.535

Female

Reference	Value per 24 h	Units	L / 24 h	Concentration (mmol/L)
[06RAJ]	2.91	mmol	1.674	1.74
[07TaC]	686	mg	2.03	1.76

mg per 24 hrs (Range: 332 to 1012) [07TaC]

Stone Formers

CaOx Stone Formers 32.81 mg/dL [14RGE]

CaP Stone Formers 30.39 mg/dL [14RGE]

Uric Acid Stone Formers 35.55 mg/dL [14RGE]

Cystine Stone Formers 27.72 mg/dL [14RGE]

Values for Male Stone Formers, grouped by BMI quartiles (mg per 24 hrs) [10EES]:

BMI	22.0	24.8	27.5	33.4
mg	448.1	535.3	623.1	656.8

Values for Female Stone Formers, grouped by BMI quartiles (mg per 24 hrs) :

BMI	22.0	24.8	27.5	33.4
mg	550.0	574.6	559.0	552.6

Values for Male Stone Formers, mg per 24 hrs (adjusted) and rated according to increasing score of DASH-Style diet [10TSM]:

DASH Score	1	2	3	4	5
mg	661	674	708	710	733

Values for Female Stone Formers,mg per 24 hrs (adjusted) and rated according to increasing score of DASH-Style diet [10TSM]:

DASH Score	1	2	3	4	5
mg	665	728	780	764	772

Citrate: Value Used for Normal Urine: 1.788 mmol/L

Uric Acid/Urate

2 to 5 mmol per 24 h

600mg per 24 h (Uric Acid) [82DeS]

3.49 mmol per 24h hrs [06RAJ] (Urate)

3.76 mmol per 24 hrs [04SJH]

Hyperuricosuria: 750 mg or more per 24h [04KYY]

Male

Reference	Value per 24 h	Units	L / 24 h	Concentration (mmol/L)
[06RAJ]	3.49	mmol	1.477	2.36
[04SJH]	3.76	mmol	2.32	1.62

Female

Reference	Value per 24 h	Units	L / 24 h	Concentration (mmol/L)
[06RAJ]	2.75	mmol	1.674	1.64
[07TaC]	448	mg	2.03	1.31

2.75 mmol per 24h hrs [06RAJ] (Urate)

448 mg per 24 hrs (Range: 281 to 662) [07TaC]

Stone Formers

Uric Acid

CaOx Stone Formers 47.27 mg/dL [14RGE]

CaP Stone Formers 29.54 mg/dL [14RGE]

Uric Acid Stone Formers 51.45 mg/dL [14RGE]

Cystine Stone Formers 23.60 mg/dL [14RGE]

Values for Male Stone Formers, grouped by BMI quartiles (g per 24 hrs) [10EES]:

BMI	22.0	24.8	27.5	33.4
g	0.71	0.67	0.78	0.76

Values for Female Stone Formers, grouped by BMI quartiles (g per 24 hrs) [10EES]:

BMI	22.0	24.8	27.5	33.4
g	0.54	0.59	0.66	0.70

Values for Male Stone Formers, mg per 24 hrs (adjusted) and rated according to increasing score of DASH-Style diet [10TSM]:

DASH Score	1	2	3	4	5
mg	601	607	623	610	645

Values for Female Stone Formers, mg per 24 hrs (adjusted) and rated according to increasing score of DASH-Style diet [10TSM]:

DASH Score	1	2	3	4	5
mg	503	504	506	522	518

Urate: Value Used for Normal Urine : 1.86 mmol/L

Urea

20.6 g per 24 hrs (Range: 12.6 to 28.6) [70Gei]

Urea: Value Used for Normal Urine: 338.3 mmol/L

Ammonium, NH_4^+

43.2 mmol per 24 hrs [04SJH]

0 to 50 mmol/L [06MMC]

High: Over 1100 mg per 24 h [99GSC]

Ammonia, NH_3

Male

680 mg per 24 hrs (Range: 340 to 1200) [70Gei]

40 mEq per 24 hrs (Range: 20 to 70) [70Gei]

Female

510 mg per 24 hrs (Range: 340 to 1200) [70Gei]

30 mEq per 24 hrs (Range: 20 to 70) [70Gei]

Ammonia: Value Used for Normal Urine: 18.6 mmol/L

Sulfate

Male

Reference	Value per 24 h	Units	L / 24 h	Concentration (mmol/L)
[04SJH]	28.2	mmol	2.32	12.16
[70Gei]	45	mEq	1.015	22.17

45 mEq per 24 hrs (Range: 30 to 70 mEq per 24 hrs) [70Gei]

Female

Reference	Value per 24 h	Units	L / 24 h	Concentration
[07TaC]	17	mmol	2.03	8.37

36 mEq per 24 hrs (Range: 30 to 70) [70Gei]

Stone Formers

Values for Male Stone Formers, mmol per 24 hrs (adjusted) and rated according to increasing score of DASH-Style diet [10TSM]:

DASH Score	1	2	3	4	5
mmol	22	24	23	24	25

Values for Female Stone Formers, mmol per 24 hrs (adjusted) and rated according to increasing score of DASH-Style diet [10TSM]:

DASH Score	1	2	3	4	5
mmol	16	17	17	17	18

Value Used for Normal Urine: 12.2 mmol/L

Sulfite

Stone Formers

Values for Male Stone Formers, grouped by BMI quartiles (mg per 24 hrs) [10EES]:

BMI	22.0	24.8	27.5	33.4
mg	46.1	44.1	48.1	50.4

Values for Female Stone Formers, grouped by BMI quartiles (mg per 24 hrs) [10EES]:

BMI	22.0	24.8	27.5	33.4
mg	33.9	36.8	38.8	41.1

Bicarbonate

4.7 mEq per 24 hrs[06CMA]

HCO_3^{2-}: Value Used for Normal Urine: 2.24 mmol/L

Creatinine

Range 1.78 to 20.4 mmol/L [07SAR]

Male

Reference	Value per 24 h	Units	L / 24 h	Concentration (mmol/L)
[04SJH]	17.22	mmol	2.32	7.4
[70Gei]	1.8	g	1.015	15.7

1.8 g per 24 hrs (Range: 1.1 to 2.5) [70Gei]

Female

Reference	Value per 24 h	Units	L / 24 h	Concentration (mmol/L)
[07TaC]	1036	mg	2.03	4.5

1036 mg per 24 hrs (Range: 775 to 1326) [07TaC]

1.17 g per 24 hrs (Range: 1.01 to 1.33) [70Gei]

Stone Formers

Average: 97.4 ml/min/1.73m^2 (Range: 24.3 – 144.8) (Male) [00GHJ]

Average: 81.3 ml/min/1.73m^2 (Range: 36.0 – 119.3) (Female) [00GHJ]

(Values are normalized for 1.73m^2 body surface area.)

CaOx Stone Formers 91.87 mg/dL [14RGE]

CaP Stone Formers 71.00 mg/dL [14RGE]

Uric Acid Stone Formers 107.82 mg/dL [14RGE]

Cystine Stone Formers 67.40 mg/dL [14RGE]

Values for Male Stone Formers, grouped by BMI quartiles (mg per 24 hrs) [10EES]:

BMI	22.0	24.8	27.5	33.4
mg	1577.5	1654.4	1868.9	1949.3

Values for Female Stone Formers, grouped by BMI quartiles (mg per 24 hrs) [10EES]:

BMI	22.0	24.8	27.5	33.4
mg	1040.9	1148.1	1289.5	1397.7

Creatinine: Value Used for Normal Urine: 7.4 mmol/L

Phytate

mg per 24 hours

Healthy Subjects: 3.27 mg

Stone Formers: 2.01 mg

Urine Volume:

Healthy Subjects 1.126 L

Stone Formers 1.828 L

Healthy Subjects: 2.94 mg/L

Stone Formers: 1.10 mg/L

Low : <0.610 μmol

Intermediate : 0.61 – 1.21 μmol

High : >1.21 μmol

[15FGP]

0.00445 mmol/L [00GMP]

Phytate: Value Used for Normal Urine: 0.00445 mmol/L

Tamm-Horsfall Protein

Normal

Min 7.5 Max 76.7 Mean 21.37 μg per day [01LGH]

40 to 50 mg per day [00GHJ]

Male

9.3 to 35.0 mg/day

(5th to 95th percentile)

Av 21.9 mg per day [00GHJ]

= 0.000158 mmol/L (1.635L and 85kDa)

Female

9.0 to 36.3 mg/day

(5th to 95th percentile)

Av 20.9 mg per day [00GHJ]

= 0.000131 mmol/L (1.873L and 85kDa)

Stone Formers

Min 7.8 Max 26.2 Mean 16.34 μg per day [01LGH]

THP: Value Used for Normal Urine: 1.58 x 10^{-7} mmol/L

Hippuric Acid

$C_6H_5CONHCH_2COOH$

0.5 to 2.5 g per L

or

2 to 10 mmol/L [93GAB]

25.4 mmol per day or 28.03 mmol/L in normal subjects

2.3 mmol per day or 2.9 mmol/L in Stone Formers [93GAB].

pH

4.5 to 8 [97BrK]

4.5 to 7.5 [95SoG]

Male

6.40 [06RAJ]

6.15 [04SJH]

5.7 (Range: 4.8 to 7.5) [70Gei]

Female

6.42 [06RAJ]

6.08 (Range: 5.42 to 6.71) [07TaC]

5.8 (Range: 4.8 to 7.5) [70Gei]

Stone Formers

CaOx Stone Formers 6.09 [14RGE]

CaP Stone Formers 6.42 [14RGE]

Uric Acid Stone Formers 5.92 [14RGE]

Cystine Stone Formers 6.65 [14RGE]

Values for Male Stone Formers, grouped by BMI quartiles [10EES]:

BMI	22.0	24.8	27.5	33.4
pH	6.14	6.05	6.01	5.93

Values for Male Stone Formers, rated according to increasing score of DASH-Style diet [10TSM]:

DASH Score	1	2	3	4	5
pH	5.8	5.8	5.9	5.9	5.9

Values for Female Stone Formers, grouped by BMI quartiles [10EES]:

BMI	22.0	24.8	27.5	33.4
pH	6.33	6.18	6.19	6.05

Values for Female Stone Formers, rated according to increasing score of DASH-Style diet [10TSM]:

DASH Score	1	2	3	4	5
pH	5.9	6.0	6.1	6.1	6.1

Ionic Strength

Average ionic strength of urine:

0.33 mol/L [95SoG]

0.3 mol/L[93GAB]

Volume per Day

Male

Reference	L / 24 h	Range
[06RAJ]	1.477	–
[04SJH]	2.32	–
[70Gei]	1.015	0.510 – 2.00
[00GHJ]	1.635	–
[94KoK]	1.44	0.6 – 16.7

2.052 litres [00GHJ]

Litres per day for Stone Formers, grouped by BMI quartiles [10EES]:

BMI	22.0	24.8	27.5	33.4
litres	2.3	2.1	2.0	2.2

Female

Reference	L / 24 h	Range
[06RAJ]	1.674	–
[07TaC]	2.03	1.14 – 2.96
[70Gei]	0.989	0.50 – 1.875
[00GHJ]	1.873	–

Stone Formers

2.196 litres [00GHJ]

Litres per day for Stone Formers, grouped by BMI quartiles [10EES]:

BMI	22.0	24.8	27.5	33.4
litres	2.1	2.0	2.1	2.2

Volume per day for Male Stone Formers (litres) and rated according to increasing score of DASH-Style diet [10TSM]:

DASH Score	1	2	3	4	5
litres	1.55	1.71	1.72	1.71	1.79

Volume per day for Female Stone Formers (Litres) and rated according to increasing score of DASH-Style diet [10TSM]:

DASH Score	1	2	3	4	5
litres	1.49	1.65	1.68	1.84	1.96

Healthy Subjects: 1.126 [00GMP]

Stone Formers: 1.828 [00GMP]

Redox Potential

32.2 mV [14GCF]

32 mV (COD Stone Formers) [15GCB]

55 mV (COM Stone Formers) [15GCB]

Notes

The range values given by Taylor and Curhan (2007) [07TaC], are 10th to 90th percentile ranges.

The range values given by [70Gei] for Calcium, Magnesium, Urea and Creatinine are 95% range values.

The DASH-Style diet (Dietary Approaches to Stop Hypertension) is high in fruit and vegetables and low in animal protein [10TSM]. More than 60% of the subjects in this study had a history of kidney stones.

Many of these values for the different substances are similar for each substance, but the volume per day is around 1 litre per day in some publications and around 2 litres per day in other publications, giving a difference in concentration of a factor of two, depending which total daily volume of urine is used.

Appendix C

Renal Anatomy and Physiology

This chapter describes the structure and function of the kidney to provide background information required to construct a model of the kidney filtration process.

C.1 Anatomy of the Kidney

The kidney consists of a pale outer region, called the cortex and a darker inner region, called the medulla. The renal interstitium is complex and consists of extracellular matrix, interstitial fluid, interstitial cells and filaments anchoring the structures to one another [87LeK, 15ZeK]. There is significant variation in the properties of the interstitium in the different sections of the kidney, it is most extensive in the inner medulla, in the deep medulla it can occupy up to 30 % of the volume. The medulla consists of 8 to 18 renal pyramids, which are conical in shape, with the base in the corticomedullary

boundry. The apex of each renal pyramid ends in a papilla, in one of the minor calyces. (See Figure C.1) The minor calyces drain into the major calyces and then into the ureter [99Ker]. A calyx is a space where the urine collects before leaving the kidney. Each kidney weighs between 120 g and 170 g [68BDS].

The kidney performs the functions of regulating:

- water, electrolyte and acid-base balance;
- body fluid osmolarity and electrolyte concentrations; and
- arterial pressure.

as well as

- secreting hormones;
- responding to hormones;
- excretion of metabolic wastes; and
- excretion of xenobiotics (for example drugs).

The renal arteries arise directly from the aorta, which means that the blood supply to the kidneys is at the highest possible pressure [68BDS]. The kidneys receive 20 % to 25 % of cardiac output [99Ker, 68BDS]. The renal circulatory system is unique, as it has two capillary beds [06GuH].

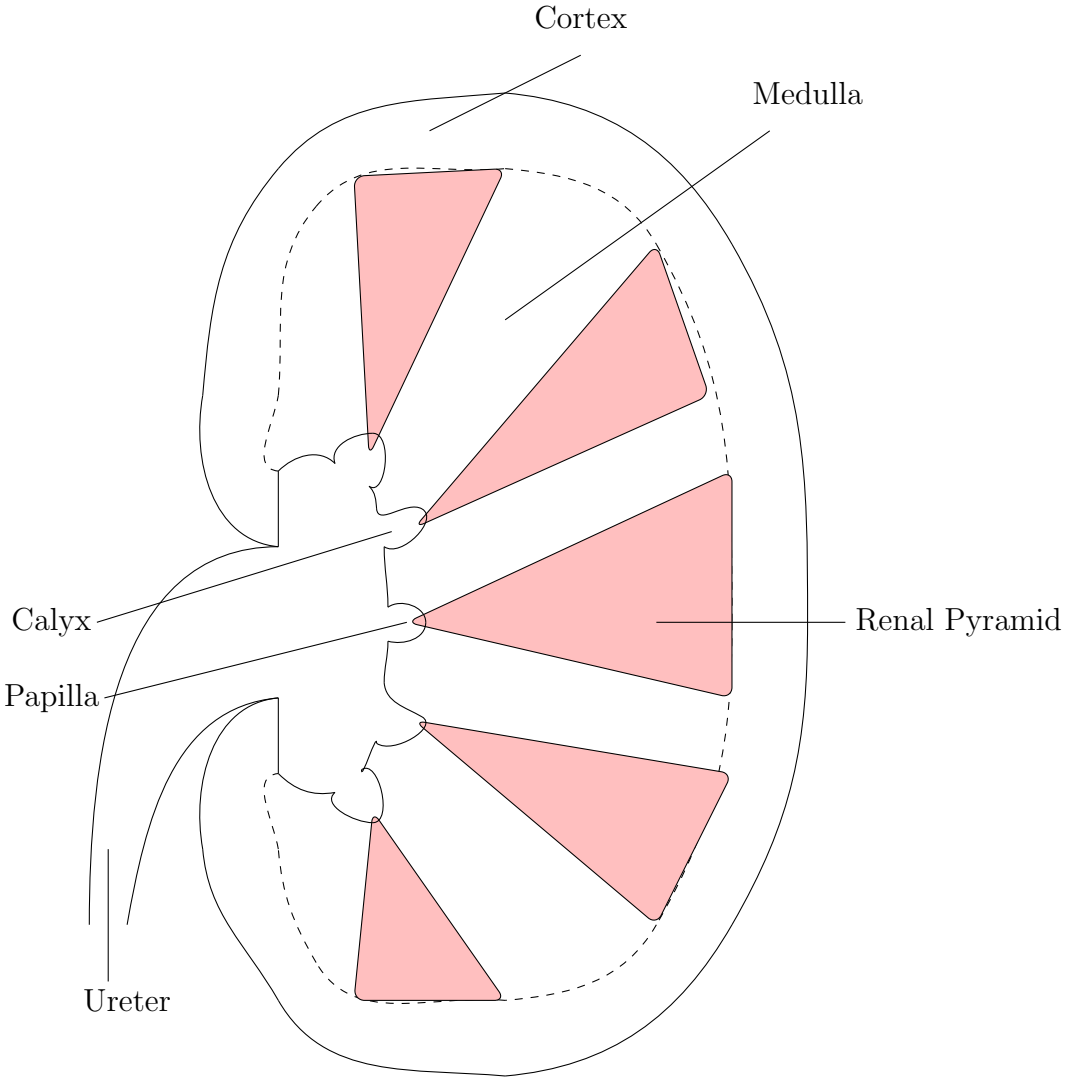

Figure C.1: Cross Section of a Kidney

The nephron is the functional unit of the kidney. It is estimated that each kidney contains an average of 600 000 nephrons, the range being estimated to be between 0.3 million to a million [99Ker, 68BDS]. Blood supply to a nephron is via an afferent arteriole, which branches into a capillary bed called the glomerulus, at the head of the nephron. After the glomerulus, the blood vessels then join to form the efferent arteriole, before branching again to form the peritubular capillaries. The nephron blood supply is shown in Figure C.2. In the average human, normal renal blood flow is 1200 mL per minute [68BDS] and approximately 20 % of the plasma flowing into the kidneys is filtered by the glomerular capillaries [06GuH], thus around 125 mL of glomerular filtrate (GF) is produced each minute, or 180 L/day [68BDS]. This volume is known as the Glomerular Filtration Rate (GFR). An increase in protein intake will increase the GFR [15WMS]. The total volume of extracellular fluid in the body is 15 litres, thus, this volume will pass through the kidneys every 2 hours [68BDS]. About 1 mL of urine is produced per minute. This means that most of the glomerular filtrate is reabsorbed [06GuH], resulting in large concentration changes for the solutes in the solution, especially with higher levels of water reabsorption.

A nephron is a closed end, epithelial lined tubule. The origin is in the renal cortex and end in a duct, a number of which join into the papillary tip of a renal pyramid [99Ker].

As shown in Figures C.3 and C.4, the nephron is made up of a number of sections:

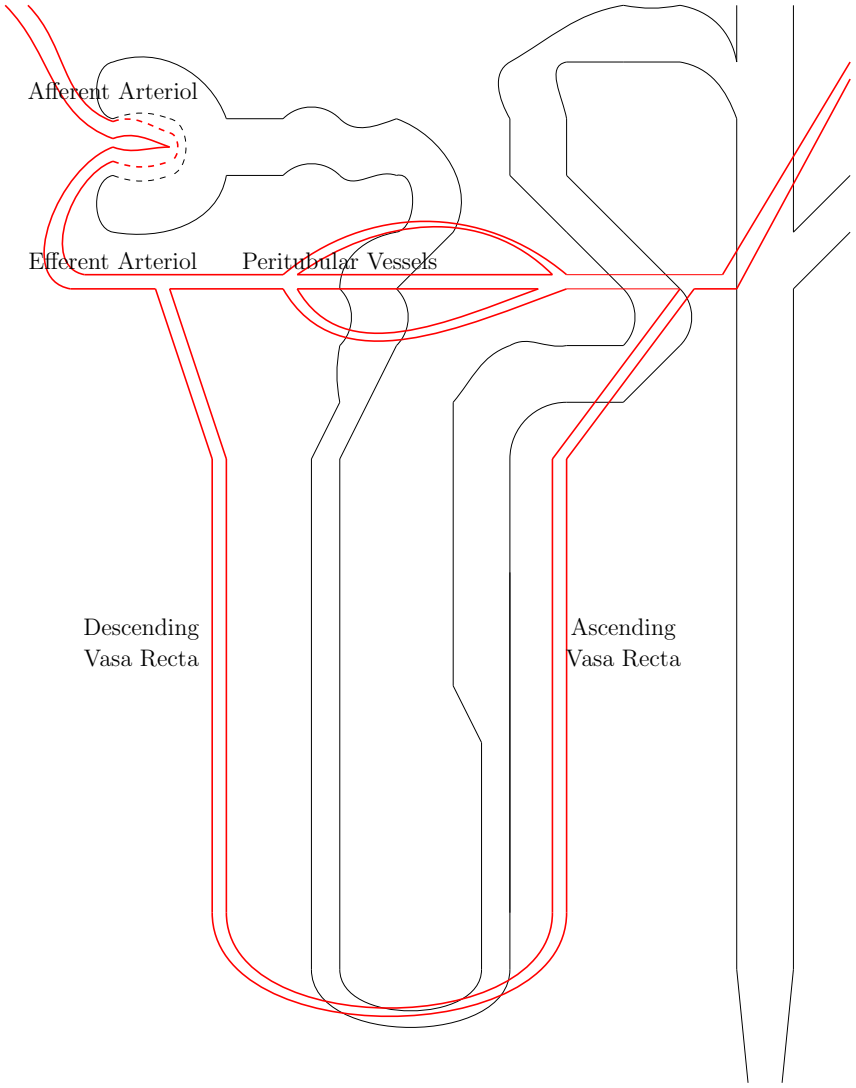

Figure C.2: Schematic Diagram of Nephron Blood Supply

- *Renal Corpuscle*,
- *Proximal Tubule*,
- *Thin Descending Limb of the Loop of Henle*,
- *Thin Ascending Limb of the Loop of Henle*,
- *Thick Ascending Limb of the Loop of Henle*,
- *Macula Densa of the Distal Tubule*,
- *Distal Convoluted Tubule*,
- *Connecting Tubule*,
- *Cortical Collecting Duct*,
- *Medullary Collecting Duct*,
- and *Duct of Bellini*.

There are two types of nephron: cortical and juxtamedullary, also known as short and long nephrons. Cortical nephrons are shorter and only enter the outer medulla, while juxtamedullary nephrons descend deep into the medulla and are responsible for the function of the concentration of urine. The loops of Henle differ between the short and long nephrons. The short type do not have a thin ascending limb [15WMS, 12BaY]. In humans, around 15 % of the nephrons are juxtamedullary.

It is at the point of the collecting tubules where the individual nephrons merge and thus, the collecting ducts will contain the output of multiple

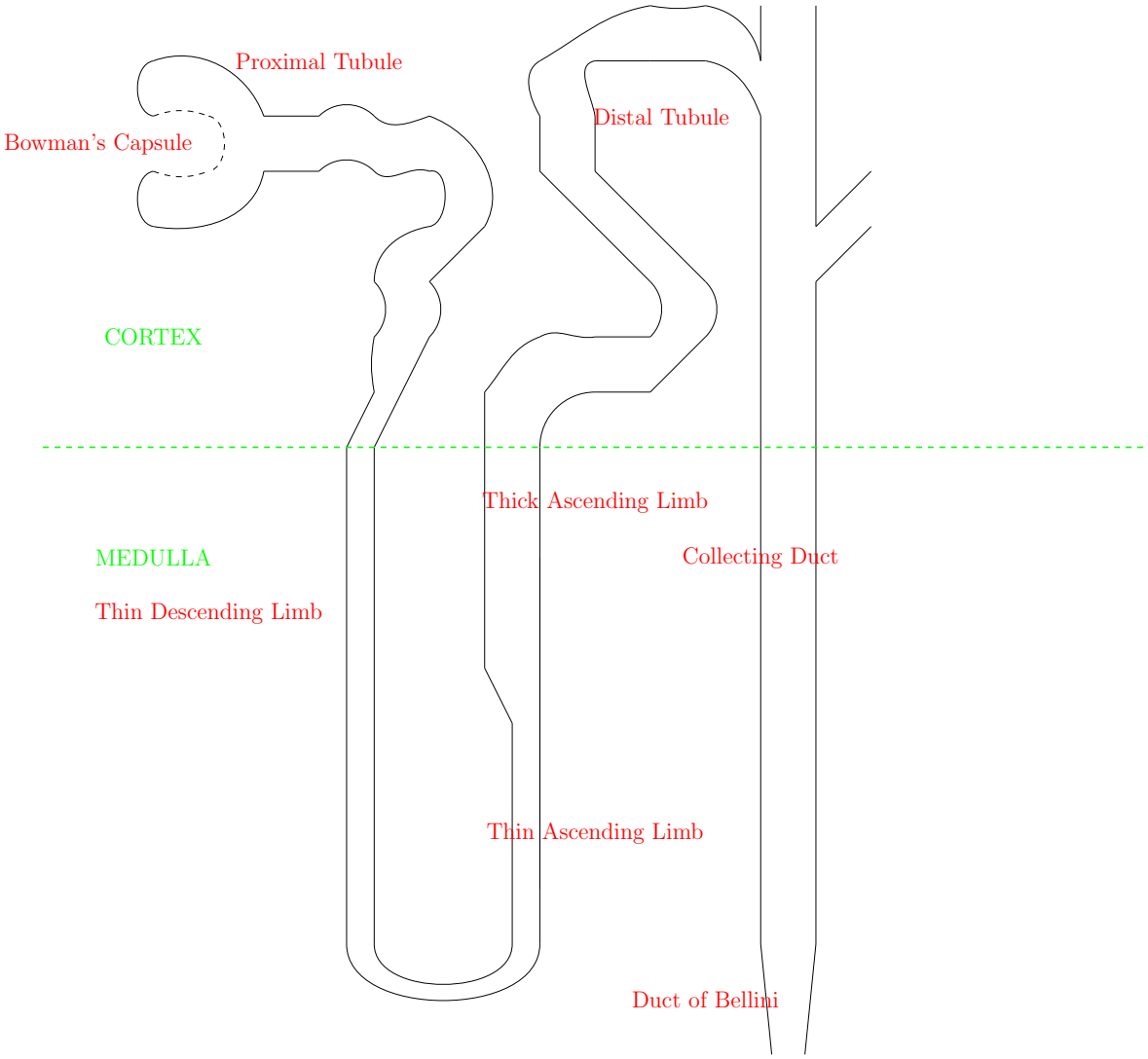

Figure C.3: Schematic Diagram of a Long Nephron. The Loop of Henle is a long structure, which descends deeply into the Medulla.

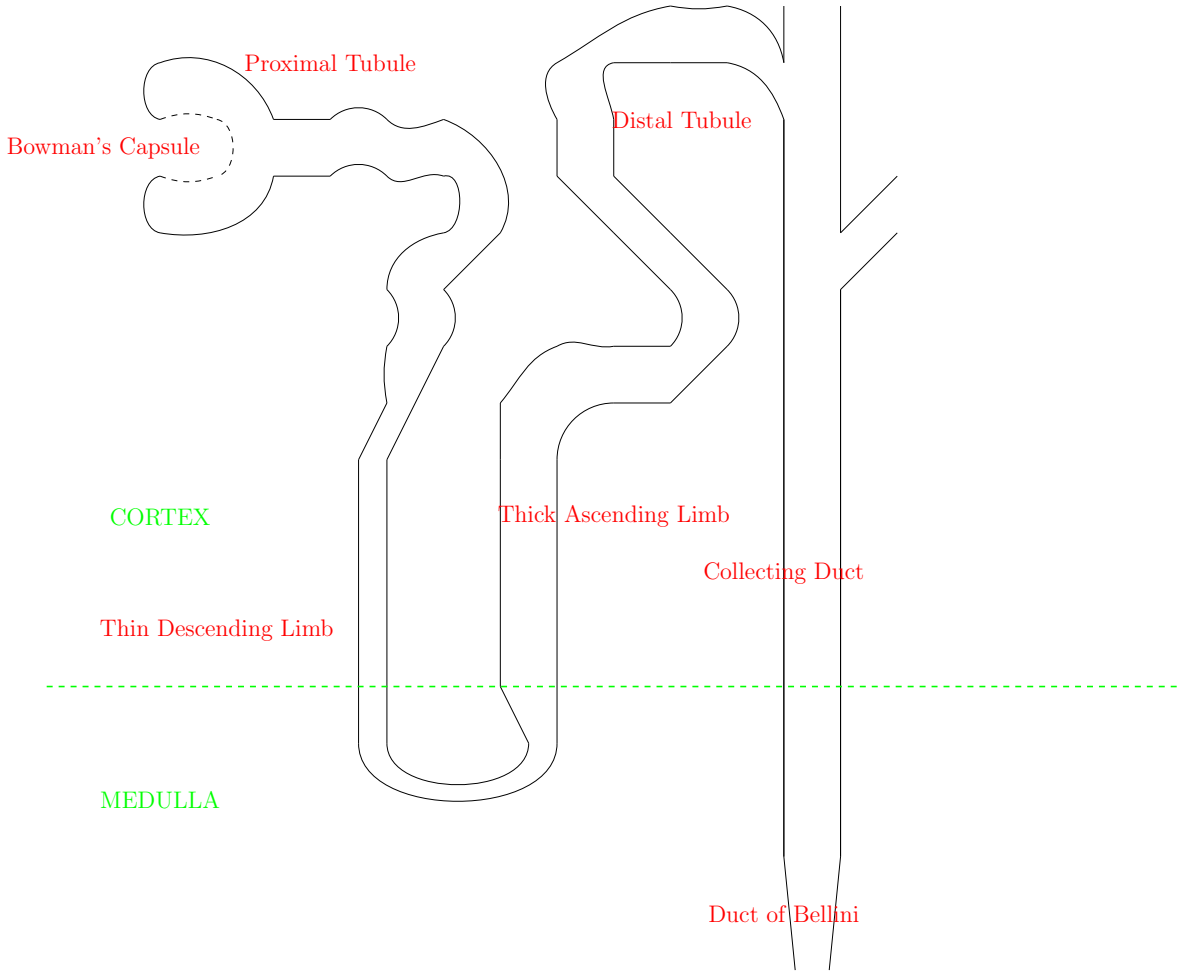

Figure C.4: Schematic Diagram of a Short Nephron. The Bowman's Capsule of the Short Nephron is higher up in the Cortex than in the case of the Long Nephron. The Loop of Henle only dips into the Medulla, and does not contain a Thin Ascending Limb.

nephrons [06GuH]. Approximately 4000 nephrons combine into a single collecting duct [97Kok]. At the end of the collecting duct is the duct of Bellini. The urine passes through the duct of Bellini into a calyx which is a space where the urine collects before leaving the kidney.

The medullary rays, located within the cortex, contain the straight parts of the proximal and distal tubules and the collecting ducts, all of which extend into the medulla [99Ker]. The renal corpuscle is made up of the glomerulus and the Bowman's capsule. The glomerulus is a tuft of capilliaries. At the junction between the two, the properties of the lining cells allow plasma to be filtered so that larger molecules, such as proteins and negatively charged larger molecules are excluded from being filtered into the Bowman's space [06Ath1]. Figure C.5 depicts a cross section of a nephron, showing how the lumen is a space surrounded by the epithelial cells which make up the wall of the nephron. The apical surface of the cell faces inward toward the lumen. The basolateral surface of the cell faces towards the interstitium or neighbouring cells.

The proximal tubule is initially highly convoluted in the cortex and becomes straight or spiral in the medulla [99Ker]. The portion following the convoluted section is also known as the pars recta [12BaY]. The proximal tubule undergoes a transition into the loop of Henle after entering the medulla. The juxtamedullary nephrons perform the function of setting up the conditions required to allow concentrating the urine to be performed further along the nephron in the collecting duct. The vasa recta are blood vessels which follow

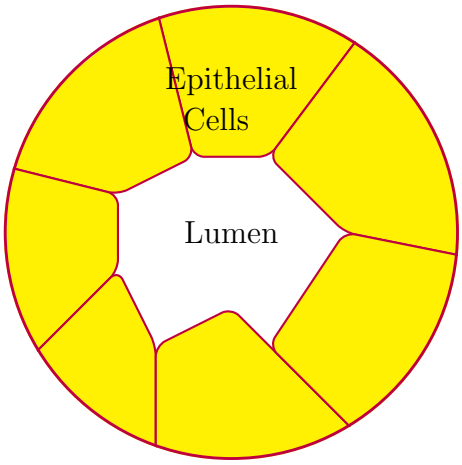

Figure C.5: Cross Section of a Nephron

the path of the loop of Henle into and out of the medulla, thus providing the loop of Henle a blood supply with which it can exchange solutes and water. Blood flow in the vasa recta is much lower than that in the cortex, with only 1 % to 2 % of the blood flow into the kidney entering the medulla [06GuH, 99Ker]. The cells of the lining epithelium of the descending loop of Henle are flat and have special permeability properties which maintain the hypertonicity of the medulla [99Ker]. These epithelal cells produce and secrete Tamm-Horsfall Protein, as do those of the distal tubule [97RNN]. The three sections of the loop of Henle have different transport and permeability properties [06Ath1]. (See Section C.2.3.) The collecting duct reabsorbs water, thus controlling the volume and concentration of urine [99Ker]. It has been estimated that the transit time for the fluid passing through the nephron is 3 to 4 minutes [04Rob].

C.2 Sections of the Nephron

C.2.1 Renal Corpuscle

The renal corpuscle, or glomerulus, consists of the Bowman's capsule, and its associated capilliary network and filtration membrane. The Bowman's space is the start of the nephron lumen. The glomerular filtrate is produced via the process of ultrafiltration. The total area of glomerular capillaries is about 1 m^2, so, with 125 mL of glomerular filtrate being produced per minute, 0.0125 mL is filtered per cm^2 per minute [68BDS].

C.2.2 Proximal Tubule

The proximal tubule reabsorbs water, sodium, potassium, calcium, chloride, bicarbonate, glucose and amino acids. It secretes hydrogen ions, organic acids and bases [06GuH] and ammonia [85GoK]. Reabsorption in the proximal tubule is unregulated. Fluid in the proximal tubule is isotonic with plasma. There is active reabsorption of glucose and sodium in the proximal tubule. Over 65 % of the reabsorption of water takes place in the initial convoluted section of the proximal tubule. In the proximal tubule, 65 % of the sodium and a slightly lower percentage of the chloride is reabsorbed [06GuH]. Of the solutes, those which are reabsorbed to a lesser extent are urea (50 %) and Mg^{2+} (20 %). A low intracellular Na^+ concentration provides the driving force for Na^+ movement across the membrane [68BDS]. The first part of the proximal tubule reabsorbs amino acids, glucose, the small amount of protein that passes through the filtration process and some of the filtered

phosphate. Sodium is reabsorbed uniformly along the proximal tubule and distal tubule [06Ath1]. Solute transport properties change along the proximal tubule for some substances. There is preferential reabsorption of HCO_3^-, HPO_4^{2-}, glucose and amino acids in the early part and for Cl^- in the second half. Acid loads reduce Cl^- reabsorption and increase HCO_3^- reabsorption in the proximal tubule [98WEA, 11CEW]. In acidosis, there will be a lower concentration of HCO_3^- in the glomerular filtrate, leading to an increased concentration of both sodium and chloride in the luminal fluid [98WEA].

C.2.3 Loop of Henle

The loop of Henle of a juxtamedullary nephron consists of three segments, the thin descending limb, the thin ascending limb and the thick ascending limb. In the case of a cortical nephron, the thin descending limb is much shorter, and there is no thin ascending limb. The thin segments have little metabolic activity. In the thick ascending limb, the tubule cells actively transport solutes [06GuH]. The loop of Henle reabsorbs about 20 % of the filtered water, almost all of this is in the thin descending limb, as the other parts are mainly impermeable to water [06GuH]. Fluid in the first part of the distal tubule is normally hypotonic. Thus, it can be seen that the loop of Henle, as a whole, absorbs sodium and chloride in preference to water. Even in the situation when small amounts of concentrated urine are being produced, the fluid in the distal part of the distal convoluted tubule is only isotonic with plasma. Thus, the final reabsorption of water to produce concentrated urine takes place in the collecting tubules or collecting ducts [68BDS].

The thin descending limb is moderately permeable to most solutes and has a high permeability to water through aquaporin 1 water channels and 15 % to 25 % of the filtered fluid is reabsorbed through water channels in this part. The thin ascending limb is impermeable to water [06GuH, 06Ath2] and does not transport solutes, but like the thin descending limb is permeable to solutes [87ITT, 99Ker]. The thick ascending limb is impermeable to water, but reabsorbs about 20 % to 25 % of Na^+, K^+, Ca^+, Cl^- and 60 % of Mg^{2+} through a mechanism of active transport [06GuH]. $HCO_3{}^-$ is also reabsorbed here [06Ath1] and hydrogen ions are secreted in this section [06GuH]. Thus, the fluid becomes dilute as it passes towards the end of the loop of Henle [06GuH].

C.2.4 Distal Tubule

The first part of this is the macula densa, which is a component of the juxtaglomerular complex that provides feedback control of glomerular filtration rate and bloodflow of the nephron. The cells in the macula densa sense changes to volume delivery to the distule tubule. A possible mechanism for this is via NaCl concentration [15Wei]. A decrease in the glomerular filtration rate will result in a lower flow rate in the loop of Henle, hence higher reabsorption of NaCl in the ascending limb. This decrease in NaCl concentration at the macula densa results in action to increase the glomerular filtration rate by dilating the afferent arterioles and constricting the efferent arterioles [06GuH].

The next part is the convoluted section, also known as the diluting segment, which is similar to the thick part of the loop of Henle in terms of reabsorptive characteristics, it reabsorbs ions, including sodium, chloride and potassium. It is impermeable to water and urea [06GuH, 99Ker]. The tubule then straightens out and two different types of lining cells are found in this section, principal cells and intercalated cells. The principal cells reabsorb sodium ions and secrete potassium ions. The intercalated cells reabsorb potassium ions and bicarbonate ions and secrete hydrogen ions. This section of the tubule is impermeable to urea, thus most of the urea that passes into this section will be excreted, although, some of it may pass out of the lumen into the medulla later on in the collecting duct. Water reabsorption is controlled by the level of antidiuretic hormone (ADH), which is produced in the posterior pituitary. The action of this hormone is to increase water reabsorption by increasing the permeability of the distal tubules and collecting ducts and hence increase urine concentration [68BDS, 06GuH]. The distal tubule employs active transport mechanisms to reabsorb Na^+, Ca^{2+}, Cl^-, Mg^{2+} and secrete H^+ and K^+. The reabsorption here accounts for about 5 % to 10 % [06GuH]. K^+ and H^+ both compete for the same transport mechanism and H^+ will be transported if its concentration is high.

C.2.5 Collecting Tubule

The collecting tubule lies with the cortex. As with the late section of the distal tubule, the collecting tubule is lined with principle cells and intercalating

cells and is impermeable to urea. The reabsorption and secretion properties of this section are the same as the late distal tubule [06GuH]. A number of collecting tubules join together and flow into a collecting duct.

C.2.6 Collecting Duct

The collecting duct starts within the cortex and descends through the medulla. The fluid becomes concentrated as it passes through the increasingly hypertonic environment of the medulla. Fine tuning of the final concentration of the urine is performed here [06GuH]. In the absence of ADH, the walls of the collecting ducts become impermeable to water and the urine thus remains dilute. ADH increases the permeability, thus allowing the urine to become more concentrated [68BDS]. Less than 10 % of the filtered water and sodium are reabsorbed here. This section is permeable to urea; thus, urea can permeate out of the lumen and into the medulla, helping to increase the hypertonicity of the medullary interstitium. Urea contributes about 40 % of the osmolarity of the medullary interstitium. As with the cortical collecting tubule, the medullary collecting duct is able to secrete hydrogen ions against a large concentration gradient. It is thus involved in the regulation of acid-base balance [06GuH]. Calcium and magnesium are reabsorbed in the collecting duct [97Tis]. The walls of the collecting duct are also made up of principle cells and intercalating cells. In the cortex there are both principle cells and intercalating cells, but in the medulla the intercalating cells disappear [99Ker]. Estimates for pH in the middle of the collecting duct are 5.00 to 6.25 [09TLF].

C.3 Differences Between Long Nephrons and Short Nephrons

The main differences between the two types of nephrons are the length of the loop of Henle and the absence of a thin ascending limb in the short nephrons. Another difference is their relative locations with respect to the boundry between the cortex and the medulla. The glomeruli of the short nephrons are higher up in the cortex, while those of the long ones are further down closer to the cortico-medullary boundry [99Ker].

C.4 Tamm-Horsfall Protein

Tamm-Horsfall Protein (THP) is the most abundant protein in human urine [01LGH, 05DDP]. THP is a glycoprotein with a molecular weight of 80 [90KuM], 85 [05DDP] or 95 [96ZRW] kilodaltons. THP is produced in the kidneys and secreted in the urine [97RNN]. The sites of production and secretion of THP are the ascending loop of Henle and the proximal part of the distal tubule [90KuM, 97Kok, 05CJR]. The relationship between THP and stones is unclear. Evidence exists for THP, and some other substances, being both involved in the formation of stones [01LGH] and the inhibition of stone formation [97HCK, 04MHZ, 14BaA]. THP has been found in calcium oxalate stones [97RNN]. One study concluded that calcium oxalate stone formers had a lower level of THP secretion [97RNN], which is supported by the fact that it is thought to inhibit the aggregation calcium oxalate crystals

Table C.1: Hormone Regulation of Tubule Reabsorption [06GuH]

Hormone	Site	Effect
ADH	DT CT CD	increase water reabsorption
ALD	DT CD	increase NaCl and water reabsorption increase potassium secretion
PTH	PT TAL DT	decrease phosphate reabsorption increase calcium reabsorption
AT2	PT TAL DT CT	increase NaCl and water reabsorption increase hydrogen ion secretion
ANP	DT CT CD	decrease NaCl reabsorption

[05DDP]. Both lower calcium concentration and lower pH, result in increased polymerization of THP [00GHJ, 01Kav]. Differences in structure have been found between THP of normal subjects and recurrent stone formers [02BGS]. THP is also called uromodulin.

C.5 Hormones

A number of hormones have an effect on the kidney filtration process. These include Antidiuretic Hormone, Aldosterone, Parathyroid Hormone, Angiotensin II and Atrial Natriuretic Peptide.

Antidiuretic Hormone (ADH), also known as vasopressin, is secreted by the pituitary gland and alters the volume of urine in order to maintain the total volume of extracellular fluid in the body at the desired level [06GuH]. It regulates osmolarity [09BoB]. ADH is released in response to increased extracellular osmolarity. Excessive ADH levels will not result in large increases in arterial pressure, as GFR will be increased and thus increase water excre-

tion, however sodium loss will result [06GuH]. ADH is an agonist of thick ascending limb transport [11CEW]. ADH levels will increase when water needs to be conserved and decrease with excess fluid intake.

Aldosterone (ALD), secreted by the adrenal cortex, acts on the principle cells of the CCT to increase sodium and water reabsorption and increase potassium secretion [06GuH, 09BoB]. It regulates extracellular volume, and hence blood pressure [09BoB]. An increase in plasma potassium concentration will stimulate aldosterone secretion [09BoB]. Low Aldosterone causes increased secretion of sodium and water [06GuH], and hence will reduce extracellular volume. Increased plasma potassium levels of 5.3 to 6.3 mmol/L are seen in hypoaldosteronism [08Ada].

Parathyroid Hormone (PTH) is secreted by the parathyroid glands, which are small structures attached to the thyroid gland [99Ker]. PTH levels will increase in reaction to a fall in plasma calcium concentration. Parathyroid hormone increases blood plasma concentrations of both calcium and phosphate by stimulating the process of bone resorption and increasing calcium absorption in the gut [06GuH]. PTH acts on the proximal tubule to inhibit the reabsorption of phosphate, as well as sodium, potassium, amino acids and bicarbonate and on the distal tubule and collecting duct to increase calcium reabsorption and reduce hydrogen ion and ammonia excretion [77Fin, 06GuH, 06Ath2]. PTH stimulates magnesium reabsorption in the thick ascending limb [06GuH].

The normal level of PTH in the blood is around 0.5 ng/mL and changes with variations of calcium concentration in a range of about 0 to 3 ng/mL [06GuH]. A fall in plasma calcium concentration will result in a rapid increase in PTH level [78MaH]. While increasing calcium reabsorption, PTH decreases phosphate reabsorption in order to remove the extra phosphate from the plasma which was mobilised from the bones along with the calcium [06GuH]. Higher plasma calcium concentrations will reduce the PTH level; thus, PTH levels decrease after eating [13WBG].

Hyperparathyroidism results in an increased risk of kidney stone formation, as the excess calcium and phosphate mobilised from the bones and diet must be excreted by the kidneys. This creates a risk for both calcium phosphate and calcium oxalate stones, as even with normal oxalate levels, the increased calcium level will promote calcium oxalate precipitation [06GuH]. Although PTH increases calcium reabsorption in the nephron, the calcium concentration in the urine will increase at high PTH levels due to the higher calcium levels in the blood that result from the high PTH level. An increase in the level of parathyroid hormone (PTH) reduces the glomerular filtration rate [92YaL].

Agiotensin II increases blood pressure [06GuH]. It is a vasoconstrictor, it reduces renal plasma flow and glomerular filtration rate [06Ath1]. Agiotensin II formation increases with low blood pressure or low extracellular fluid volume. It increases sodium and water reabsorption. Increased levels will result in the following actions: a stimulation of aldosterone secretion, con-

striction of the efferent arterioles, stimulation of sodium reabsorption in the PT, LH, DT and CT [06GuH, 06Ath2] and an increase in the level of ADH [06GuH, 06Ath3, 09BoB]. Angiotensin II increases tubular reabsorption into the peritubular capillaries, especially of sodium and water, and can reduce urine output to less than one fifth of normal [06GuH]. Angiotensin II stimulates ammonium excretion in the proximal tubule during acidosis [09Hye].

Atrial Natriuretic Peptide (ANP) decreases sodium and water reabsorption. ANP is excreted by cells of the cardiac atria in the situation of volume expansion and inhibits reabsorption of sodium and water in the renal tubules, especially in the collecting ducts. ANP also increases the glomerular filtration rate [06GuH]. The action of ANP is to reduce plasma volume and blood pressure, the opposite to those of aldersterone and angiotensin II [06Ath3, 09BoB]. ANP inhibits ADH secretion [06Ath3]. ANP secretion will be stimulated by reduced extracellular volume [09BoB]. Excess or insufficient levels are not a major problem, as blood pressure changes will compensate [06GuH].

Appendix D

Biochemistry Data Comparison

As noted in Section 2.9, differences can be seen between people who form kidney stones and those who do not. Lower pH levels have been seen in the urine of calcium oxalate stone formers [11Tis2]. This section contains tables of published data showing comparisons of biochemical data of stone forming patients and normal control individuals.

The data in Table D.6 contains values for an average normal male in the UK with no history of stone formation (Controls), an average untreated recurrent idiopathic calcium oxalate and calcium phosphate stone formers in the UK (SF1) and an average untreated recurrent idiopathic calcium oxalate and uric acid stone formers in the Kingdom of Saudi Arabia (SF2). These sets of data are used in Section 4.8 in the reverse usage of the model, where nephron concentrations are calculated from specified blood and urine concentrations.

Table D.1: Risk Factors [06GrC]

Serum	mg/dL	Urine	mg/24 h
Ca	>10.2	Ca	>250 (female) >300 (male)
P	>4.5	Mg	<70
Mg	<1.8	P	>1200
Uric Acid	>6.5	Uric Acid	>600 (f) >800 (m)
Creatinine	>1.2	Oxalate	>40
		Citrate	<350
		Phytate	<1.0
		Cystine	>20
		pH	<5.5 >6.0

Table D.2: Urine Chemistries of Stone Formers [14RGE]

Stone Type	units	CaOx	CaP	Uric Acid	Cystine
pH	–	6.09	6.42	5.92	6.65
Citrate	mg/dL	32.81	30.39	35.55	27.72
Oxalate	mg/dL	1.68	1.37	2.02	0.98
Sodium	mEq/L	91.29	88.75	89.55	89.10
Potassium	mEq/L	38.20	48.12	48.82	25.10
Calcium	mg/dL	10.45	11.45	10.49	6.16
Phosphate	mg/dL	61.60	57.00	66.18	38.50
Uric Acid	mg/dL	47.27	29.54	51.45	23.60
Chloride	mEq/L	88.87	97.57	98.36	81.20
Creatinine	mg/dL	91.87	71.00	107.82	67.40
Sulfate	mg/dL	111.06	77.62	141.39	50.86
Magnesium	mg/dL	6.63	5.66	6.17	5.03

Table D.3: Urine Chemistries of Controls and Stone Formers [08LRA]

	units	Control (n=90)	Stone Formers (n=198)
Sodium	mmol/L	75.67	60.37
Potassium	mmol/L	30.53	24.37
Calcium (total)	mmol/L	1.67	2.61
Calcium (ionized)	mmol/L	0.32	0.78
Magnesium	mmol/L	2.23	1.96
Ammonium	mmol/L	14.90	14.00
Chloride	mmol/L	73.55	64.55
Phosphate	mmol/L	13.35	13.22
Sulfate	mmol/L	9.79	7.72
Uric Acid	mmol/L	1.63	1.44
Oxalic Acid	mmol/L	0.16	0.24
Citric Acid	mmol/L	1.56	0.90
pH	–	6.19	6.23

Table D.4: Urine Chemistries of Controls and Stone Formers [03ELC]

	units	Control (n=4)	Stone Formers (n=15)
Sodium	mEq/day	188 ± 60	199 ± 61
Potassium	mEq/day	59 ± 18	55 ± 22
Phosphate	mg/day	862 ± 316	950 ± 256
Magnesium	mg/day	60 ± 17	117 ± 36
Creatinine	mg/day	1449 ± 811	1673 ± 370
Ammonia	mEq/day	34 ± 16	38 ± 33
Sulfate	mEq/day	42 ± 15	45 ± 15
Uric Acid	mg/day	585 ± 178	637 ± 164
Volume	L/day	1.86 ± 0.43	1.64 ± 0.6
pH	–	5.94 ± 0.48	5.89 ± 0.5

Table D.5: Urine Chemistries of Controls and Stone Formers [17Rod]

Variable	units	Control (n=15)	Stone Formers (n=10)
pH	–	6.16	5.97
Vol	mL	1337	1928
Calcium	mmol/24 h	2.55	4.46
Oxalate	mmol/24 h	0.26	0.24
Citrate	mmol/24 h	2.41	2.49
Magnesium	mmol/24 h	4.25	3.72
Urate	mmol/24 h	2.51	4.19
Sodium	mmol/24 h	86.1	122.1
Potassium	mmol/24 h	72.2	52.2
Phosphate	mmol/24 h	28.8	31.8
Chloride	mmol/24 h	119	179
Creatinine	mmol/24 h	13.3	16.8

Table D.6: Blood and Urine Data of Controls and Stone Formers [15Rob]

Substance	units	Controls	SF 1	SF 2
Blood				
Ultrafiltrable Calcium	mmol/L	1.47	1.50	1.47
Ultrafiltrable Phosphate	mmol/L	1.00	1.60	1.60
Oxalate	μmol/L	1.50	1.65	1.79
pH	–	7.38	7.38	7.38
Sodium	mmol/L	140	144	140
Potassium	mmol/L	4.0	4.2	4.0
Ultrafiltrable Magnesium	mmol/L	0.60	0.56	0.56
Citrate	μmol/L	100	66	35
Sulfate	μmol/L	400	500	550
Urate	μmol/L	280	380	490
Ammonium	μmol/L	100	100	100
Urine				
Volume	L	1.72	1.43	1.34
pH	–	5.97	6.15	5.38
Calcium	mmol/day	5.62	9.05	5.09
Phosphate	mmol/day	28.9	47.8	49.6
Oxalate	mmol/day	0.34	0.55	0.82
Magnesium	mmol/day	3.93	3.64	3.67
Sodium	mmol/day	156	159	156
Potassium	mmol/day	71	74	71
Ammonium	mmol/day	22	18	45
Citrate	mmol/day	2.89	1.90	1.01
Sulfate	mmol/day	20	25	27
Uric Acid	mmol/day	3.02	4.09	5.27

Table D.7: Average (Urine) Values of Controls and Stone Formers [90CRG]

Group	Citrate (mg/L)	Uric Acid (mg/100mL)	Calcium (mg/100mL)	Oxalate (mg/L)
Controls	517.6	32.88	14.96	23.83
Stone Formers A	301.4	29.20	12.71	19.21
Stone Formers B	317.9	28.92	17.09	18.81

Table D.8: Average (Urine) Values of Controls and Stone Formers [03ELC]

Group	Calcium (mg/24h)	Oxalate (mg/24h)	Citrate (mg/24h)
Controls	113 ± 67	32 ± 9	482 ± 193
Stone Formers	312 ± 89	40 ± 13	485 ± 278

Table D.9: Urine Chemistries of Different Stone Formers [15GCB]

	units	Papillary COM	COD
Volume	L/day	1.257 ± 0.166	1.306 ± 0.157
pH	–	5.93 ± 0.49	6.15 ± 0.76
Calcium	mmol/day	4.76 ± 2.16	7.52 ± 1.99
Magnesium	mmol/day	8.72 ± 10.68	7.51 ± 10.11
Phosphorus	mmol/day	30.47 ± 10.10	23.92 ± 11.71
Citrate	mmol/day	3.02 ±1.49	2.78 ± 1.79
Creatinine	mmol/day	12.27 ± 3.78	7.83 ± 0.93
Oxalate	mmol/day	0.44 ± 0.16	0.22 ± 0.06
Uric Acid	mmol/day	4.22 ± 1.46	2.96 ± 0.95
Phytate	μmol	0.40 ± 0.20	0.38 ± 0.24
Redox Potential	mV	55	32

Appendix E

Implementation of the Nephron Filtration Model

The nephron filtration model has been implemented using the programming language Ada.

E.1 Data Structures

The input to the model is a set of substance concentrations in blood plasma, values representing hormone levels and the reabsorption factors for each substance, and the output is a set of substance concentrations along the nephron.

$$Plasma = \begin{bmatrix} [Na] \\ [K] \\ : \end{bmatrix}$$

The reabsorption factors are stored in a matrix. Each substance is associated with a sequence of values representing the reabsorption quantity in each segment of the nephron.

$$R = \begin{bmatrix} Na(PT) & Na(tDL) & Na(tAL) & .. & Na(MCD) \\ K(PT) & K(tDL) & K(tAL) & .. & K(MCD) \\ \vdots & & & & \end{bmatrix}$$

E.2 Reabsorption Calculations

A function is used to work out the change in amount of substance in the fluid in the lumen using the values in the matrix.

$y_{s+1} = F(y_s, R[s,i])$

$= y_s - \frac{R[s,i]}{100} y_0$

where:

y_{s+1} is the amount of the substance in nephron section under consideration

y_s is the amount of the substance in the previous nephron section

$R[s,i]$ is the percentage of the substance reabsorbed in the interval under consideration

Values for ADH and PTH and other hormones are read in from files. Their effect is simulated by multiplying the RFMatrix value by a calculated effect due to the hormone level.

In the case where the urine concentration values are set to fixed values (the 'reverse model'), adjustments are made to the values in the reabsorption matrix to alter the final result for the urine values to the specified value. The result is a matrix which contains the values of the concentrations of the substances at the different locations in the nephron.

$$\begin{bmatrix} [Na(PT)] & [Na(tDL)] & [Na(tAL)] & .. \\ [K(PT)] & [K(tDL)] & [K(tAL)] & .. \\ \vdots & & & \end{bmatrix}$$

The program represents short and long nephrons. The ratio between the types are 85 % are short and 15 % are long. There are two output matrices, one for long nephrons and one for short nephrons. The difference is that the tDL and TAL are approximately 10 times longer in the long nephron than in the short nephron, and there is no tAL in the short nephron. A factor is used to increase the long loop reabsorption amount. The additional amount reabsorbed as a result of this is then subtracted from the amount reabsorbed in the short nephrons.

The long and short nephrons join at the collecting tubule segment. This is implemented by performing the reabsorption calculations on the long and short CT sections separately, and then adding the two values together. Thus for the next reabsorption calculation, the first common section, in the cortical collecting duct, the start value will be the combined CT value. In the tables below, the value for water is in millilitres and for all other substances, it is

in mmol.

E.2.1 Water

The initial value is 1 litre. Since the values for solutes are in mmol, the ratio of solute to water volume at any stage will give the result in a concentration of mmol per litre. The amount of water reabsorbed in the distal portions of the nephron is dependent on the level of ADH. This is implemented using a value ADHLevel, between 0 and 100. The value of ADHLevel is then multiplied by a factor for each of the affected segments, and the result is added to the reabsorption value for that segment. The implementation is described in Section E.3.1. ADH levels ranging from 0 to 100 give a final urine volume ranging from about 3 L to less than 0.5 L. The default ADH value is 50 which results in a final urine volume of 1.8 L per day.

From the data in Section 2.8.1:

Section	X Value	% Reabsorbed	Y Value (mL)
BC	0	0	$y(0)$ =1000.00
PT–PCT	$0 < x \leq 1$	46.00	540.00
PT–PR	$1 < x \leq 2$	24.00	300.00
LH-tDL	$2 < x \leq 3$	13.50	165.00
LH-tAL	$3 < x \leq 4$	0.00	165.00
LH-TAL	$4 < x \leq 5$	0.00	165.00
DCT	$5 < x \leq 6$	2.10	144.00
DTd	$6 < x \leq 7$	2.10	123.00
CT	$7 < x \leq 8$	4.00	83.00
CCD	$5 < x \leq 6$	2.75	55.50
MCD	$9 < x \leq 10$	4.55	10.00
CX	$x = 10$		y(10) = 10.00

The calculation of the reabsorption factor totals is done using the reference values for the substance in urine and blood plasma at the water reabsorption value of 99 %. Thus the initial water value will be 1 and the final value 0.01. This is obtained by setting an ADH level of 50, in a range of 0 to 100. The value shown in the last column in the tables for each substance below, is an amount. The concentration is calculated by dividing this figure by the corresponding water value in the table above. Thus, the final concentration for sodium is 125 mmol/L, as the water value at the end of the nephron is 0.01 L.

E.2.2 Sodium, Na^+

The plasma concentration of sodium is assumed to be 145 mmol/L and this is used as the initial concentration in the glomerulus here.

Sodium Values:

Blood: 145 mmol/L

Normal Urine: 125 mmol/L

From the data in Section 2.8.2:

Section	X Value	% Reabsorbed	Y Value (mmol)
BC	0	0	$y(0) = 145.00$
PT–PCT	$0 < x \leq 1$	45.50	79.02
PT–PR	$1 < x \leq 2$	23.50	44.95
LH-tDL	$2 < x \leq 3$	5.00	37.70
LH-tAL	$3 < x \leq 4$	0.00	37.70
LH-TAL	$4 < x \leq 5$	20.04	8.64
DCT	$5 < x \leq 6$	1.00	7.19
DTd	$6 < x \leq 7$	2.00	4.29
CT	$7 < x \leq 8$	0.30	3.86
CCD	$5 < x \leq 6$	1.80	1.25
MCD	$9 < x \leq 10$	0.00	1.25
CX	$x = 10$		y(10) = 1.25

E.2.3 Potassium, K^+

Potassium Values:

Blood: 4.2 mmol/L

Normal Urine: 30.4 mmol/L

From the data in Section 2.8.3:

Section	X Value	% Reabsorbed	Y Value (mmol)
BC	0	0	$y(0) = 4.20$
PT–PCT	$0 < x \leq 1$	75.00	1.05
PT–PR	$1 < x \leq 2$	0.00	1.05
LH-tDL	$2 < x \leq 3$	0.00	1.05
LH-tAL	$3 < x \leq 4$	0.00	1.05
LH-TAL	$4 < x \leq 5$	21.76	0.14
DCT	$5 < x \leq 6$	0.00	0.14
DTd	$6 < x \leq 7$	0.00	0.14
CT	$7 < x \leq 8$	-2.03	0.22
CCD	$5 < x \leq 6$	-2.03	0.31
MCD	$9 < x \leq 10$	0.00	0.31
CX	$x = 10$		y(10) = 0.31

E.2.4 Calcium, Ca^{2+}

Calcium Values:

Blood: 1.5 mmol/L

Normal Urine: 2.025 mmol/L

From the data in Section 2.8.4:

Section	X Value	% Reabsorbed	Y Value (mmol)
BC	0	0	$y(0) = 1.50$
PT–PCT	$0 < x \leq 1$	40.00	0.90
PT–PR	$1 < x \leq 2$	20.00	0.60
LH-tDL	$2 < x \leq 3$	0.00	0.60
LH-tAL	$3 < x \leq 4$	0.00	0.60
LH-TAL	$4 < x \leq 5$	25.00	0.22
DCT	$5 < x \leq 6$	5.50	0.14
DTd	$6 < x \leq 7$	5.50	0.06
CT	$7 < x \leq 8$	0.00	0.06
CCD	$5 < x \leq 6$	1.50	0.04
MCD	$9 < x \leq 10$	1.00	0.02
CX	$x = 10$		y(10) = 0.02

E.2.5 Magnesium, Mg^{2+}

Magnesium Values:

Blood: 0.4 mmol/L

Normal Urine: 2.1 mmol/L

From the data in Section 2.8.5:

Section	X Value	% Reabsorbed	Y Value (mmol)
BC	0	0	$y(0) = 0.40$
PT–PCT	$0 < x \leq 1$	12.55	0.35
PT–PR	$1 < x \leq 2$	12.55	0.30
LH-tDL	$2 < x \leq 3$	10.30	0.26
LH-tAL	$3 < x \leq 4$	0.00	0.26
LH-TAL	$4 < x \leq 5$	55.00	0.04
DCT	$5 < x \leq 6$	0.00	0.04
DTd	$6 < x \leq 7$	0.00	0.04
CT	$7 < x \leq 8$	0.00	0.04
CCD	$5 < x \leq 6$	5.40	0.02
MCD	$9 < x \leq 10$	0.00	0.02
CX	$x = 10$		y(10) = 0.02

E.2.6 Chloride, Cl^-

Chloride Values:

Blood: 125 mmol/L

Normal Urine: 81 mmol/L

From the data in Section 2.8.6:

Section	X Value	% Reabsorbed	Y Value (mmol/L)
BC	0	0	$y(0) = 125.00$
PT–PCT	$0 < x \leq 1$	34.00	82.50
PT–PR	$1 < x \leq 2$	45.35	25.81
LH-tDL	$2 < x \leq 3$	5.00	19.56
LH-tAL	$3 < x \leq 4$	0.00	19.56
LH-TAL	$4 < x \leq 5$	5.50	12.68
DCT	$5 < x \leq 6$	2.00	10.18
DTd	$6 < x \leq 7$	3.00	6.43
CT	$7 < x \leq 8$	3.00	2.68
CCD	$5 < x \leq 6$	1.25	1.12
MCD	$9 < x \leq 10$	0.00	1.12
CX	$x = 10$		y(10) = 1.12

E.2.7 Phosphate, PO_4^{3-}

Phosphate Values:

Blood: 1.5 mmol/L

Normal Urine: 19.9 mmol/L

The concentration value used here is for HPO_4^{2-}.

From the data in Section 2.8.7:

Section	X Value	% Reabsorbed	Y Value (mmol)
BC	0	0	$y(0) = 1.50$
PT–PCT	$0 < x \leq 1$	63.00	0.56
PT–PR	$1 < x \leq 2$	23.73	0.20
LH-tDL	$2 < x \leq 3$	0.00	0.20
LH-tAL	$3 < x \leq 4$	0.00	0.20
LH-TAL	$4 < x \leq 5$	0.00	0.20
DCT	$5 < x \leq 6$	0.00	0.20
DTd	$6 < x \leq 7$	0.00	0.20
CT	$7 < x \leq 8$	0.00	0.20
CCD	$5 < x \leq 6$	0.00	0.20
MCD	$9 < x \leq 10$	0.00	0.20
CX	$x = 10$		y(10) = 0.20

E.2.8 Oxalate, $C_2O_4^{2-}$

Oxalate Values:

Blood: 1.75μmol/L

Normal Urine: 0.2 mmol/L

From the data in Section 2.8.8:

Section	X Value	% Reabsorbed	Y Value (mmol)
BC	0	0	$y(0) = 1.75000\text{E-}03$
PT–PCT	$0 < x \leq 1$	10.00	1.57500E-03
PT–PR	$1 < x \leq 2$	-20.00	1.92500E-03
LH-tDL	$2 < x \leq 3$	0.00	1.92500E-03
LH-tAL	$3 < x \leq 4$	0.00	1.92500E-03
LH-TAL	$4 < x \leq 5$	0.00	1.92500E-03
DCT	$5 < x \leq 6$	0.00	1.92500E-03
DTd	$6 < x \leq 7$	0.00	1.92500E-03
CT	$7 < x \leq 8$	0.00	1.92500E-03
CCD	$5 < x \leq 6$	0.00	1.92500E-03
MCD	$9 < x \leq 10$	0.00	1.92500E-03
CX	$x = 10$		$\text{y}(10) = 1.92500\text{E-}03$

E.2.9 Sulfate, SO_4^{2-}

Sulphate Values:

Blood: 0.35 mmol/L

Normal Urine: 12.2 mmol/L

From the data in Section 2.8.9:

Section	X Value	% Reabsorbed	Y Value (mmol)
BC	0	0	$y(0) = 0.35$
PT–PCT	$0 < x \leq 1$	35.00	0.23
PT–PR	$1 < x \leq 2$	35.00	0.10
LH-tDL	$2 < x \leq 3$	0.00	0.10
LH-tAL	$3 < x \leq 4$	0.00	0.10
LH-TAL	$4 < x \leq 5$	0.00	0.10
DCT	$5 < x \leq 6$	0.00	0.10
DTd	$6 < x \leq 7$	0.00	0.10
CT	$7 < x \leq 8$	0.00	0.10
CCD	$5 < x \leq 6$	0.00	0.10
MCD	$9 < x \leq 10$	0.00	0.10
CX	$x = 10$		y(10) = 0.10

E.2.10 Citrate, $C_6H_5O_7^{3-}$

Citrate Values:

Blood: 0.3 mmol/L

Normal Urine: 1.788 mmol/L

Section	X Value	% Reabsorbed	Y Value (mmol/L)
BC	0	0	$y(0) = 0.30$
PT–PCT	$0 < x \leq 1$	94.04	0.02
PT–PR	$1 < x \leq 2$	0.00	0.02
LH-tDL	$2 < x \leq 3$	0.00	0.02
LH-tAL	$3 < x \leq 4$	0.00	0.02
LH-TAL	$4 < x \leq 5$	0.00	0.02
DCT	$5 < x \leq 6$	0.00	0.02
DTd	$6 < x \leq 7$	0.00	0.02
CT	$7 < x \leq 8$	0.00	0.02
CCD	$5 < x \leq 6$	0.00	0.02
MCD	$9 < x \leq 10$	0.00	0.02
CX	$x = 10$		y(10) = 0.02

E.2.11 Creatinine

Creatinine Values:

Blood: 0.109 mmol/L

Normal Urine: 7.4 mmol/L

Creatinine is not reabsorbed.

Section	X Value	% Reabsorbed	Y Value (mmol/L)
BC	0	0	$y(0) = 0.11$
PT–PCT	$0 < x \leq 1$	0.00	0.11
PT–PR	$1 < x \leq 2$	0.00	0.11
LH-tDL	$2 < x \leq 3$	0.00	0.11
LH-tAL	$3 < x \leq 4$	0.00	0.11
LH-TAL	$4 < x \leq 5$	0.00	0.11
DCT	$5 < x \leq 6$	0.00	0.11
DTd	$6 < x \leq 7$	0.00	0.11
CT	$7 < x \leq 8$	0.00	0.11
CCD	$5 < x \leq 6$	0.00	0.11
MCD	$9 < x \leq 10$	0.00	0.11
CX	$x = 10$		y(10) = 0.11

E.2.12 Urea, $CO(NH_2)_2$

Urea Values:

Blood: 5.46 mmol/L

Normal Urine: 338.3 mmol/L

From the data in Section 2.8.12:

Urea follows water. The reabsorption values for urea are approximately half those for water.

Section	X Value	% Reabsorbed	Y Value (mmol)
BC	0	0	$y(0) = 5.46$
PT–PCT	$0 < x \leq 1$	22.00	4.26
PT–PR	$1 < x \leq 2$	7.00	3.88
LH-tDL	$2 < x \leq 3$	5.00	3.60
LH-tAL	$3 < x \leq 4$	0.00	3.60
LH-TAL	$4 < x \leq 5$	5.00	3.33
DCT	$5 < x \leq 6$	1.00	3.28
DTd	$6 < x \leq 7$	1.50	3.19
CT	$7 < x \leq 8$	1.50	3.11
CCD	$5 < x \leq 6$	0.50	3.08
MCD	$9 < x \leq 10$	5.00	2.81
CX	$x = 10$		y(10) = 2.81

E.2.13 Uric Acid, $C_5H_4N_4O_3$

Urate Values:

Blood: 0.25 mmol/L

Normal Urine: 1.86 mmol/L

From the data in Section 2.8.13:

Section	X Value	% Reabsorbed	Y Value (mmol)
BC	0	0	$y(0) = 0.25$
PT–PCT	$0 < x \leq 1$	44.50	0.14
PT–PR	$1 < x \leq 2$	51.00	0.01
LH-tDL	$2 < x \leq 3$	0.00	0.01
LH-tAL	$3 < x \leq 4$	0.00	0.01
LH-TAL	$4 < x \leq 5$	0.00	0.01
DCT	$5 < x \leq 6$	0.00	0.01
DTd	$6 < x \leq 7$	0.00	0.01
CT	$7 < x \leq 8$	0.00	0.01
CCD	$5 < x \leq 6$	0.00	0.01
MCD	$9 < x \leq 10$	0.00	0.01
CX	$x = 10$		y(10) = 0.01

E.2.14 Ammonium, NH_4^+

Ammonia Values:

Blood: 0.01118 mmol/L

Normal Urine: 18.6 mmol/L

From the data in Section 2.8.14:

Section	X Value	% Reabsorbed	Y Value (mmol)
BC	0	0	$y(0) = 0.01$
PT–PCT	$0 < x \leq 1$	-55.00	0.10
PT–PR	$1 < x \leq 2$	-55.00	0.20
LH-tDL	$2 < x \leq 3$	0.00	0.20
LH-tAL	$3 < x \leq 4$	0.00	0.20
LH-TAL	$4 < x \leq 5$	70.00	0.07
DCT	$5 < x \leq 6$	0.00	0.07
DTd	$6 < x \leq 7$	0.00	0.07
CT	$7 < x \leq 8$	0.00	0.07
CCD	$5 < x \leq 6$	-25.00	0.12
MCD	$9 < x \leq 10$	-25.00	0.17
CX	$x = 10$		y(10) = 0.17

E.2.15 Bicarbonate, HCO_3^-

Bicarbonate Values:

Blood: 24 mmol/L

Normal Urine: 2.24 mmol/L

From the data in Section 2.8.15:

Section	X Value	% Reabsorbed	Y Value (mmol)
BC	0	0	$y(0) = 24.00$
PT–PCT	$0 < x \leq 1$	50.00	12.00
PT–PR	$1 < x \leq 2$	24.00	6.24
LH-tDL	$2 < x \leq 3$	11.00	3.60
LH-tAL	$3 < x \leq 4$	0.00	3.60
LH-TAL	$4 < x \leq 5$	10.00	1.20
DCT	$5 < x \leq 6$	0.00	1.20
DTd	$6 < x \leq 7$	0.00	1.20
CT	$7 < x \leq 8$	0.00	1.20
CCD	$5 < x \leq 6$	4.90	0.02
MCD	$9 < x \leq 10$	0.00	0.02
CX	$x = 10$		y(10) = 0.02

E.2.16 pH

The pH is set to a specified value for each nephron segment.

The pH at the tip of a long loop of Henle will be higher than the pH at the tip of a short loop of Henle, as a result of CO_2 diffusing out of the lumen with the water that is being reabsorbed [11RAJ]. Estimates for these values are 7.3 and 6.75. Ultrafiltrate has a pH of 7.38, in the proximal tubule, this falls to around 6.71, then rises until at the end of the DLH it has risen to 7.39 [15Rob].

Long Nephron				Short Nephron			
Section	Low	Normal	High	Section	Low	Normal	High
0	7.4	7.4	7.4	0	7.4	7.4	7.4
1	6.75	6.75	6.75	1	6.75	6.75	6.75
2	6.6	6.6	6.6	2	6.6	6.6	6.6
3	6.5	7.3	7.3	3	6.5	6.75	7.3
4	6.4	7.2	7.2	4	6.4	6.5	7.2
5	6.38	7.0	7.0	5	6.38	6.5	7.0
6	6.4	7.0	7.0	6	6.4	6.5	7.0
7	6.45	7.0	7.0	7	6.45	6.45	7.0
8	6.2	6.45	6.6	8	6.2	6.45	6.6
9	5	6.25	6.25	9	5	6.25	6.25
10	5.5	6.0	6.7	10	5.5	6.0	6.7

E.2.17 Glucose

In normal conditions all glucose is reabsorbed in the early part of the proximal tubule. Glucose has a transport maximum of 220 mg/min and a threshold of 125 mg/min. The final value will only be non-zero in hyperglycaemia.

E.2.18 Amino Acids

As with glucose filtered amino acids are reabsorbed in the early part of the proximal tubule.

E.2.19 Proteins

Proteins are also reabsorbed in the early part of the proximal tubule.

E.3 Representing Changes due to Hormones

Hormone levels are adjusted via a model parameter. Each hormone represented is assigned a value between 0 and 100, where 50 is considered to be the normal value. At the normal value of 50, no adjustments are made to the reabsorption calculations. For values below or above 50, proportional adjustments are made to simulate the changes in reabsorption caused by the change in hormone level.

E.3.1 Antidiuretic Hormone

A value for ADH, between 0 and 100, is read from a file and used to alter the water reabsorption in the descending loop of Henle, ascending loop of

Henle, distal tubule, and collecting duct. See Table E.1, which shows how the values are stored. The value "Total" represents the maximum change in reabsorption that the hormone can be responsible for. The default of 50 is normal, and at this level no adjustments are made, but for lower or higher values calculations are made to alter the values in the reabsorption matrix proportionally. The same values of 0 to 100, with 50 as normal are also used for Parathyroid Hormone, Aldosterone, Angiotensin II and Atrial Natriuretic Peptide.

The first line of the file adhlevel.dat contains the hormone level. The value in the next line is the magnitude of the effect of the hormone. For ADH there is a single value for water, since it only has an effect on the reabsorption of a single substance. The following 10 lines indicate which sections of the nephron are subjected to the effect of the hormone. A non-zero value indicates an effect in that section, and the magnitude of the effect is proportioned according to these values.

The volume range of urine output under the control of ADH in the implementation of this model is 0.32 to 3.25 L (per 24 hours). This is a percentage reabsorption range of 98.18 to 99.82. At ADH level = 50, 99 % is reabsorbed, thus a level of 100 increases this by 0.82, and a level of 0 decreases this by 0.82. The magnitude effect value in the file adhlevel.dat is 0.0164, 0.82 decrease + 0.82 increase, which is the total effect over the range 0 to 100, divided by 100, as the values are percentages.

E.3.2 Aldosterone

The values for Aldosterone is read from the file aldlevel.dat and used to alter sodium, potassium and water reabsorption in the DCT and CT. The magnitude for water will be proportional to the value for sodium. As in the case for ADH, the first line of the file pthlevel.dat contains the hormone level. The next two values are the magnitude of the effect of the hormone on the two substances that it has its effect on, calcium and phosphate. The following 10 lines to indicate which sections of the nephron are subjected to the effect of the hormone each have two values, one for calcium and one for phosphate. The values for ADH are shown in Table E.2.

E.3.3 Parathyroid Hormone

A value for PTH is read from a file and used to alter the calcium reabsorption in the distal tubule, collecting tubule and collecting duct, and phosphate reabsorption in the proximal tubule. See Table E.1.

As in the case for ADH, the first line of the file pthlevel.dat contains the hormone level. The next two values are the magnitude of the effect of the hormone on the two substances that it has its effect on, calcium and phosphate. The following 10 lines indicate which sections of the nephron are subjected to the effect of the hormone each have two values, one for calcium and one for phosphate.

Table E.1: Hormone Adjustment Values: ADH and PTH

	ADH	PTH	
	H2O	Ca	PO4
Total	0.0164	0.015	-0.01946
PCT	0	0	1.0
PR	0	0	0
tDL	1.0	0	0
tAL	0	0	0
TAL	0.0	1.0	0
MD	0	0	0
DCT	1.0	1.0	0
CT	1.0	0	0
CCD	1.0	1.0	0
MCD	1.5	0	0

E.3.4 Angiotensin II

A value for Angiotensin II is read from a file and used to increase sodium reabsorption in the PT, LH, DT and CT. The values for ADH are shown in Table E.2. If a high value for Angiotensin II is entered into the model, the value for Aldosterone is increased, as Angiotensin II stimulates Aldosterone secretion.

E.3.5 Atrial Natriuretic Peptide

A value for ANP is read from a file and used to alter sodium and water reabsorption in the CD.

Tables E.3, E.4,E.5,E.6 and E.7 show some resultant variations in values as a result of hormone level changes.

Table E.2: Hormone Adjustment Values: ALD, AT2 and ANP

	ALD			AT2		ANP	
	Na	K	H2O	Na	H2O	Na	H2O
	0.01316	0.078	0.01	0.01316	0.01	0.01316	0.01
PCT	1.0	0	0	0	0	0	0
PR	1.0	0	0	0	0	0	0
tDL	0	0	0	0	0	0	0
tAL	0	0	0	0	0	0	0
TAL	0	0	0	0	1.0	0	0
MD	0	0	0	0	0	0	0
DCT	0	0	0	0	1.0	0	0
CT	1.0	-1.0	1.0	0	0	0	0
CCD	0	0	0	0	0	1.0	1.0
MCD	0	0	0	0	0	1.0	1.0

Table E.3: ADH Effect

Hormone Level	0	50	100
Urine Volume	3.28	1.8	0.32

Table E.4: ALD Effect

Hormone Level	0	50	100
Urine Volume	2.70	1.8	0.9
Na	146.9	124.99	59.2
K	9.5	30.6	93.98

Table E.5: PTH Effect

Hormone Level	0	50	100
Ca	3.38	2.25	1.125
PO4	5.3	19.9	34.5

Table E.6: AT2 Effect

Hormone Level	0	50	100
Urine Volume	2.7	1.8	0.42
Na	146.9	124.99	44.48

Table E.7: ANP Effect

Hormone Level	0	50	100
Urine Volume	2.7	1.8	0.9
Na	146.9	124.99	59.16

E.4 Input Data

Listing E.1 shows the values in the standard reabsorption factor matrix. Listing E.4 shows the pH values.

Listing E.1: rfmatrix.dat - Reabsorption Factors

```
water:
46 24 13.5 0 0.0 2.1 2.1 4 2.75 4.55
sodium:
45.5 23.5 5 0 20.038 1 2 0.3 1.8 0
potassium:
75 0 0 0 21.762 0 0 -2.025 -2.025
calcium:
40 20 0 0 25 5.5 5.5 0 1.5 1
magnesium:
12.55 12.55 10.3 0 55 0 0 0 5.4 0
chloride:
34 45.352 5 0 5.5 2 3 3 1.25 0.0
phosphate:
63 23.73 0 0 0 0 0 0 0 0
oxalate:
```

```
10 -20 0 0 0 0 0 0 0 0
sulfate:
35 35 0 0 0 0
citrate:
94.04 0 0 0 0 0
creatinine:
0 0 0 0 0 0 0 0
urea:
22 7 5 0 5 1 1.5 1.5 0.5 5
urate:
44.5 51 0 0 0 0 0 0
ammonia:
-55 -55 0 0 70 0 0 0 -25 -25
hydrogen:
-10 80 0 0 0 0
bicarbonate:
50 24 11 0 10 0 0 0 4.9
glucose:
100
aminoacid:
100
protein:
100
```

Listing E.2: plasma.dat - Blood Plasma Concentrations (mmol/L)

water:

1000.0

sodium:

145.0

potassium:

4.2

calcium:

1.5

magnesium:

0.4

chloride:

125.0

phosphate:

1.5

oxalate:

1.79E–3

sulfate:

0.35

citrate:

0.3

creatinine:

0.109

urea:

5.46

urate:

0.25

ammonia:

1.118E−03

hydrogen:

3.28617

bicarbonate:

24.0

glucose:

0.6

aminoacid:

1.0

protein:

1.0

E.5 Program Output

E.5.1 Tables

Table E.8 shows the reabsorption factor matrix and the total for each line, which gives the overall proportion of the substance that is reabsorbed.

Table E.9 shows the substance concentrations in the various parts of the nephron. The line of figures after the substance name, are the amounts remaining in the different sections of the lumen, starting at the Bowman's

Table E.8: Reabsorption Factors

Subst	PCT	PR	tDL	tAL	TAL	MD	DT	CT	CCD	MCD	Total(%)
H_2O	0.46	0.24	0.14	0.00	0.00	0.02	0.02	0.04	0.03	0.05	99.00
Na^+	0.45	0.23	0.05	0.20	0.02	0.01	0.01	0.00	0.01	0.00	99.14
K^+	0.75	0.00	0.00	0.22	0.00	0.00	0.00	-0.02	-0.02	0.00	92.71
Ca^{2+}	0.65	0.10	0.00	0.00	0.20	0.01	0.01	0.00	0.01	0.00	99.18
Mg^{2+}	0.13	0.13	0.10	0.55	0.00	0.00	0.00	0.00	0.05	0.00	95.80
Cl^-	0.34	0.45	0.05	0.00	0.05	0.02	0.03	0.03	0.01	0.00	99.10
PO_4^{2-}	0.63	0.24	0.00	0.00	0.00	0.00	0.00	0.00	0.00	0.00	86.73
C_2O_2	0.10	-0.20	0.00	0.00	0.00	0.00	0.00	0.00	0.00	0.00	-10.00
SO_4^{2-}	0.35	0.35	0.00	0.00	0.00	0.00	0.00	0.00	0.00	0.00	70.00
Cit	0.94	0.00	0.00	0.00	0.00	0.00	0.00	0.00	0.00	0.00	94.04
Creat	0.00	0.00	0.00	0.00	0.00	0.00	0.00	0.00	0.00	0.00	0.00
Urea	0.22	0.07	0.05	0.00	0.05	0.01	0.01	0.01	0.00	0.05	48.50
$Uric^-$	0.44	0.51	0.00	0.00	0.00	0.00	0.00	0.00	0.00	0.00	95.50
NH_3	-0.50	-0.50	-0.10	0.10	0.70	0.00	0.00	-0.25	-0.25	0.00	-80.00
H^+	-0.95	0.00	0.00	0.00	0.00	0.00	0.00	-0.04	-0.04	0.00	-103.00
HCO_3	0.55	0.30	0.00	0.10	0.00	0.00	0.00	0.00	0.05	0.00	99.90
G	1.00	0.00	0.00	0.00	0.00	0.00	0.00	0.00	0.00	0.00	100.00
AA	1.00	0.00	0.00	0.00	0.00	0.00	0.00	0.00	0.00	0.00	100.00
Pr	1.00	0.00	0.00	0.00	0.00	0.00	0.00	0.00	0.00	0.00	100.00

Capsule (Position 0) and ending at the Minor Calyx (Position 10). The values for water are litres per day, the others are mmol/L, except H^+, highlighted with *, which are shown as pH values. The last figure on the line is the final concentration, in mmol/litre, in the urine at the end of the nephron.

E.5.2 Substance Data Files for GnuPlot

A set of files are written containing the data shown in Table E.9 for use by GnuPlot. For each substance, the file contains the nephron coordinate and the corresponding concentration value.

E.5.3 Plots

The figures E.2 to E.15 show the results from the simulation plotted against the data from concentration values from the literature [85GoK, 94LBF, 96AMC, 97Kok, 99HoT, 09TLF, 11RAJ]. These plots show how the model output compares with published values of concentrations within the nephron. These show that the values produced by the model are reasonable, as they fit in well with published values.

E.5.4 JESS Data Files

The data from Table E.9 is written to a set of files which are used as input to JESS. A file for each nephron segment contains the list of substances and their corresponding concentrations.

Table E.9: Concentrations

Subst	BC	PCT	PR	tDL	tAL	TAL	MD	DT	CT	CCD	MCD	Calyx
H_2O	180.00	99.00	55.80	33.75	33.75	29.70	25.92	22.14	14.94	9.99	1.80	1.80
Na^+	145.00	145.00	147.34	204.93	49.97	39.21	34.86	29.02	37.77	22.52	124.99	124.99
K^+	4.20	1.91	3.39	5.60	0.73	0.82	0.94	1.11	2.66	5.52	30.61	30.61
Ca^{2+}	2.50	1.59	1.98	3.27	3.27	0.68	0.61	0.51	0.60	0.37	2.04	2.04
Mg^{2+}	0.50	0.79	1.21	1.72	0.26	0.29	0.33	0.39	0.58	0.38	2.10	2.10
Cl^-	125.00	150.00	83.26	137.65	137.65	76.88	70.73	52.32	32.35	20.23	112.25	112.25
PO_4^{2-}	1.50	1.01	0.64	1.06	1.06	1.21	1.38	1.62	2.40	3.59	19.91	19.91
C_2O_2	0.00	0.00	0.01	0.01	0.01	0.02	0.02	0.02	0.03	0.05	0.25	0.25
SO_4^{2-}	0.25	0.30	0.24	0.40	0.40	0.45	0.52	0.61	0.90	1.35	7.50	7.50
Cit	0.30	0.03	0.06	0.10	0.10	0.11	0.12	0.15	0.22	0.32	1.79	1.79
Creat	0.11	0.20	0.35	0.58	0.58	0.66	0.76	0.89	1.31	1.96	10.90	10.90
Urea	5.46	7.74	12.51	20.68	20.68	21.84	24.65	28.19	40.79	60.50	335.79	335.79
$Uric^-$	0.25	0.25	0.04	0.06	0.06	0.07	0.08	0.09	0.14	0.20	1.13	1.13
NH_3	0.00	0.18	0.65	1.19	1.08	0.37	0.42	0.50	1.35	2.93	16.24	16.24
H^+	7.40*	7.40*	6.75*	6.75*	6.50*	6.50*	6.45*	6.45*	6.45*	6.25*	6.00*	6.00*
HCO_3	24.00	19.64	11.61	19.20	6.40	7.27	8.33	9.76	14.46	0.43	2.40	2.40
G	5.60	0.00	0.00	0.00	0.00	0.00	0.00	0.00	0.00	0.00	0.00	0.00
AA	1.00	0.00	0.00	0.00	0.00	0.00	0.00	0.00	0.00	0.00	0.00	0.00
Pr	1.00	0.00	0.00	0.00	0.00	0.00	0.00	0.00	0.00	0.00	0.00	0.00

Table E.10: Antidiuretic Hormone and Urine Volume

ADH Level	Urine Volume (L)
0	3.05
10	2.80
20	2.55
30	2.30
40	2.05
50	1.80
60	1.55
70	1.30
80	1.05
90	0.80
100	0.55

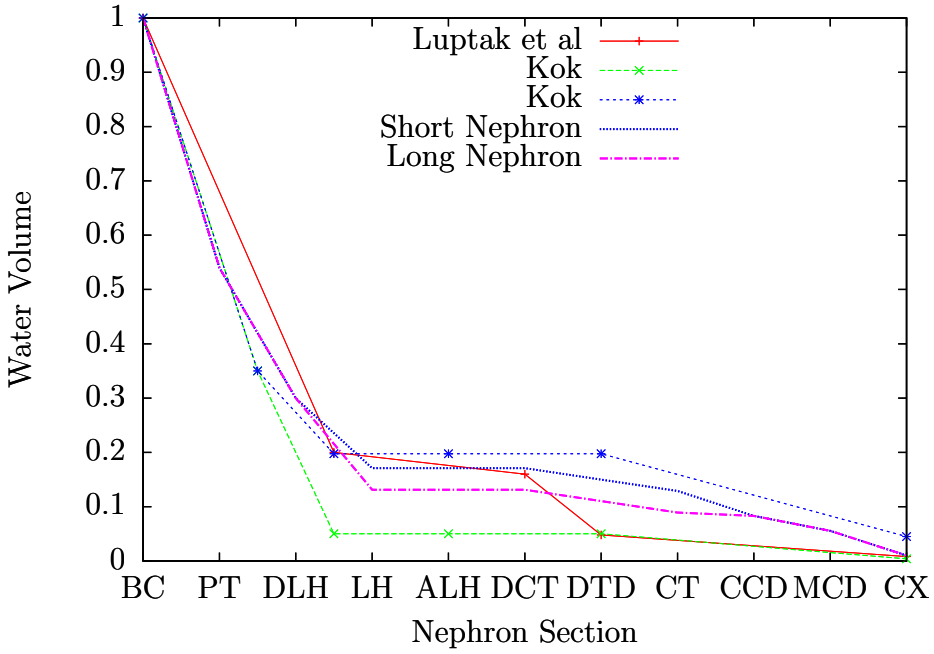

Figure E.1: Water Volume

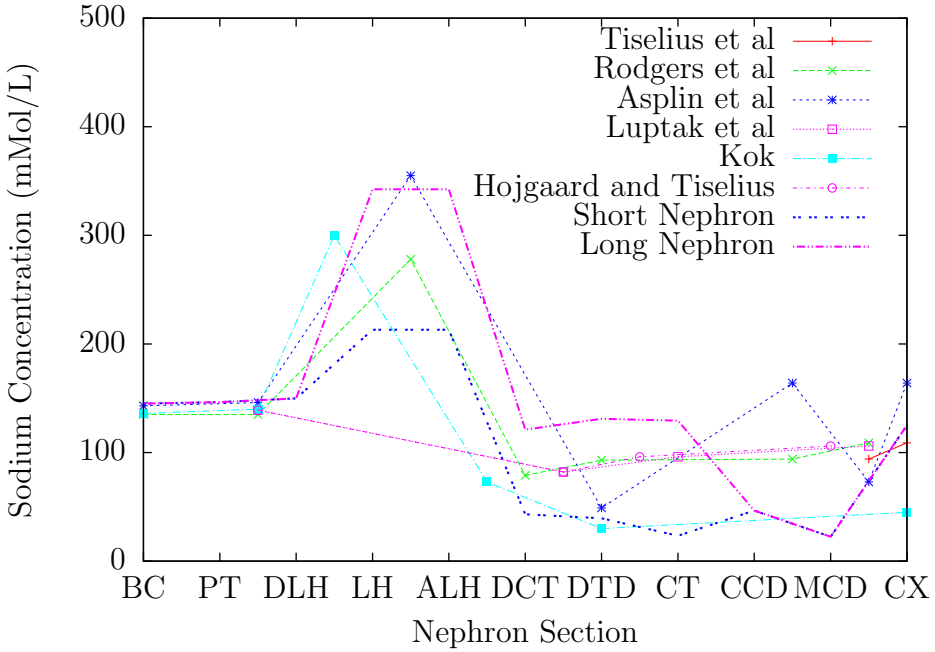

Figure E.2: Sodium Concentration (See Table 2.14)

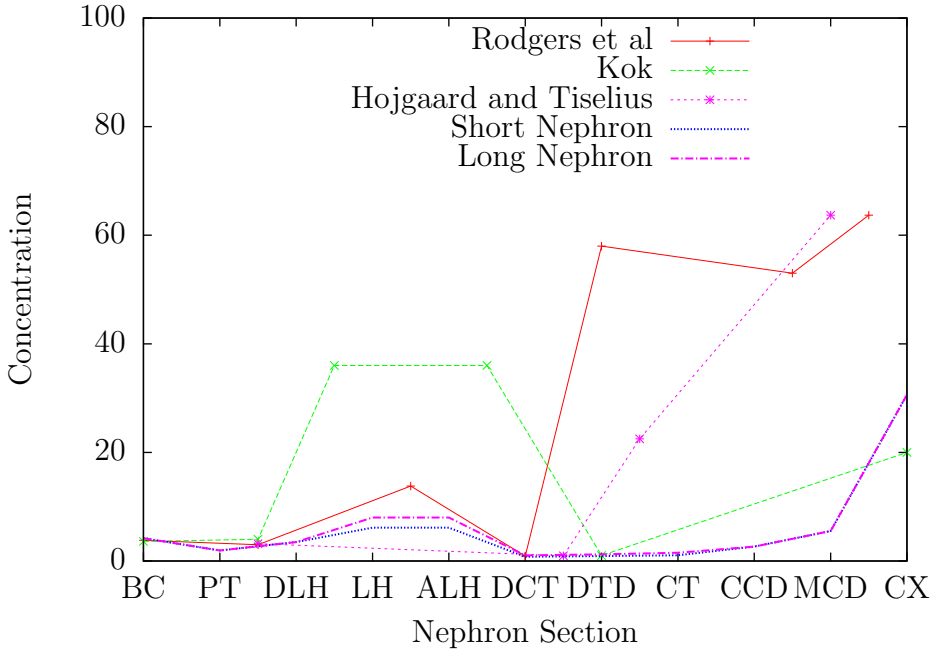

Figure E.3: Potassium Concentration (See Table 2.15)

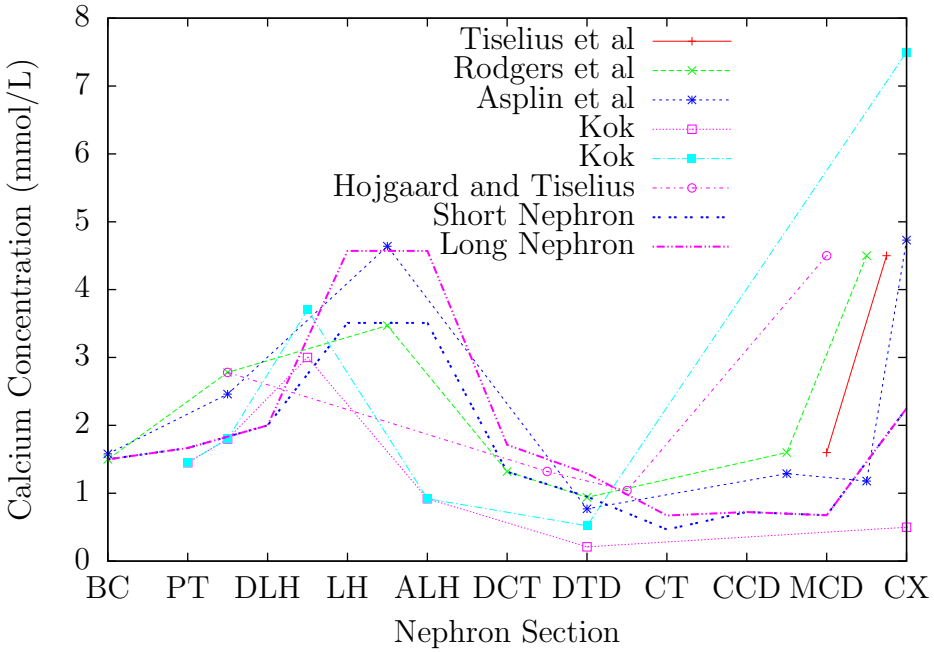

Figure E.4: Calcium Concentration (See Table 2.16)

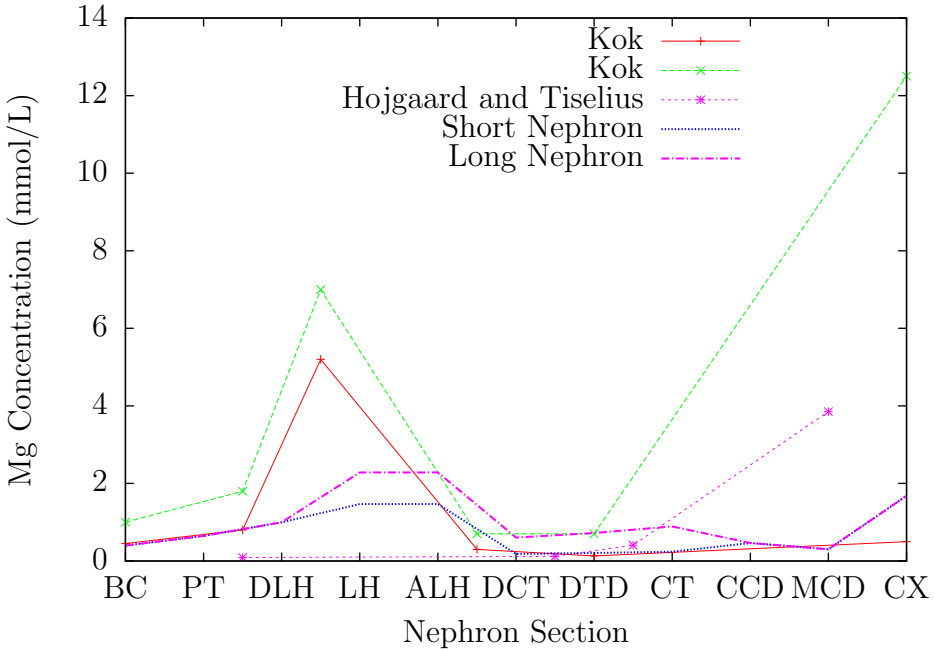

Figure E.5: Magnesium Concentration (See Table 2.17)

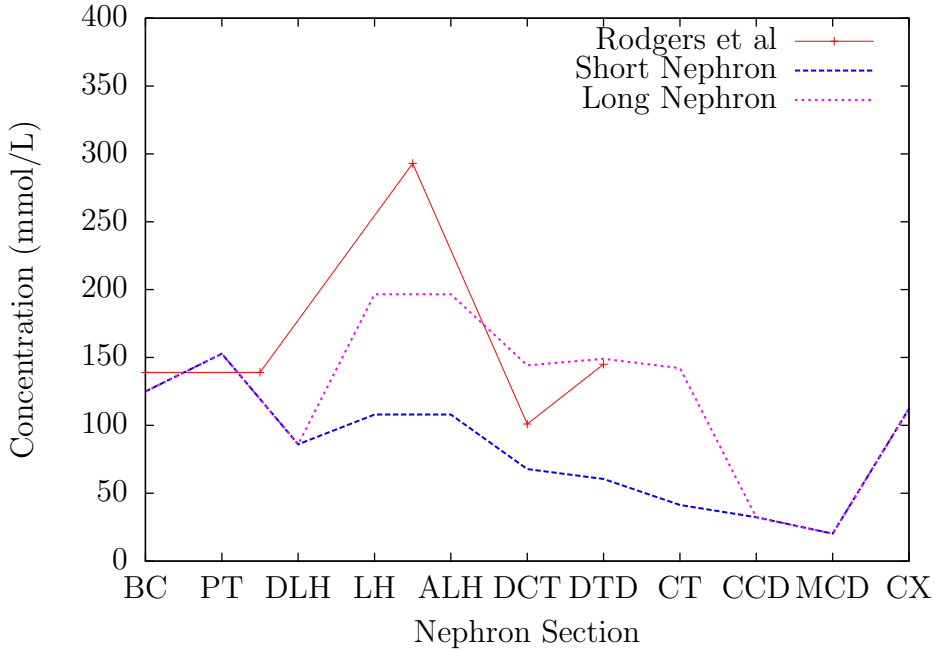

Figure E.6: Chloride Concentration (See Table 2.18)

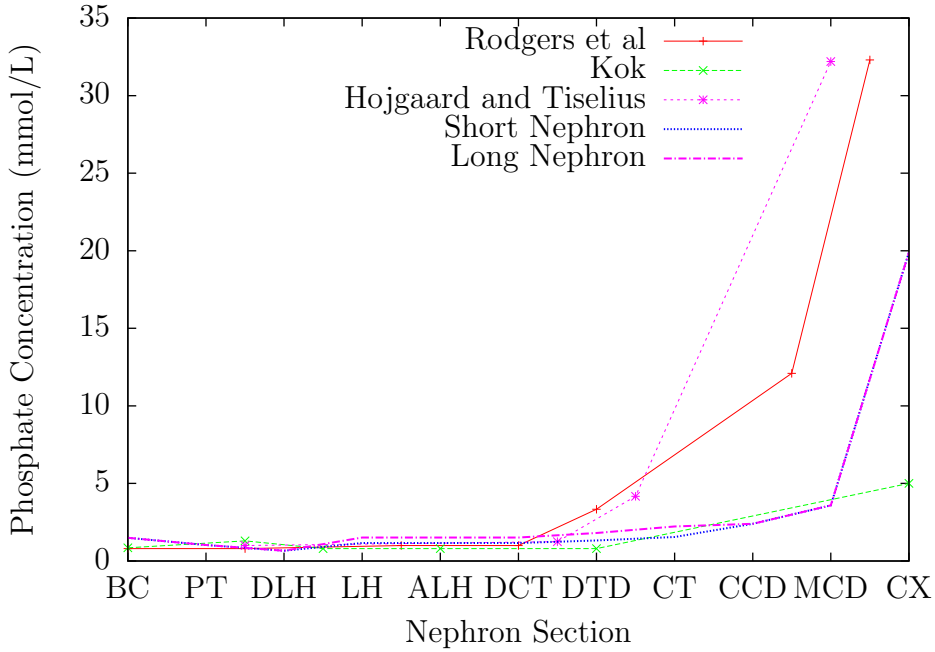

Figure E.7: Phosphate Concentration

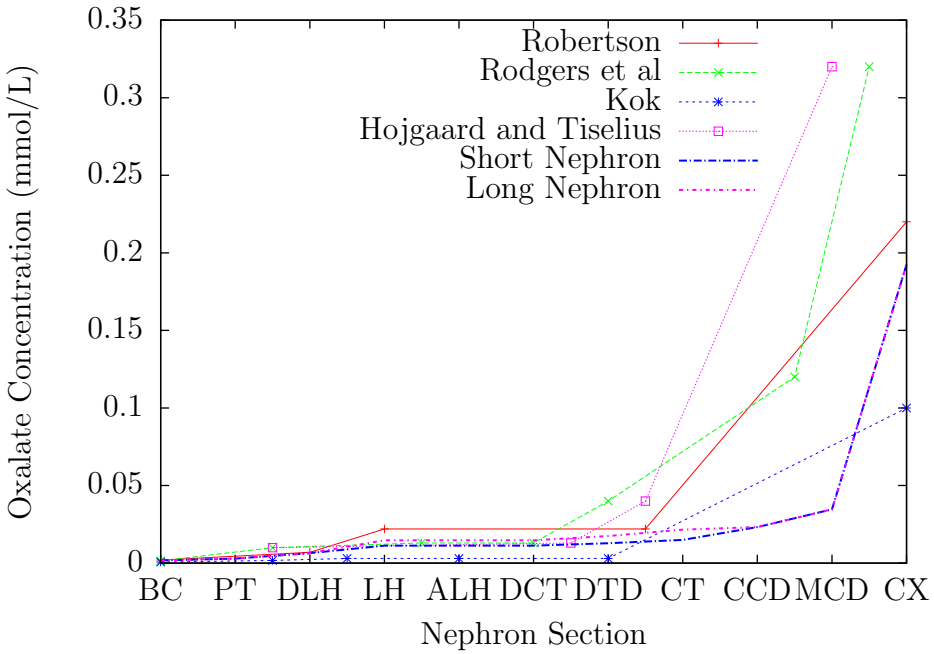

Figure E.8: Oxalate Concentration

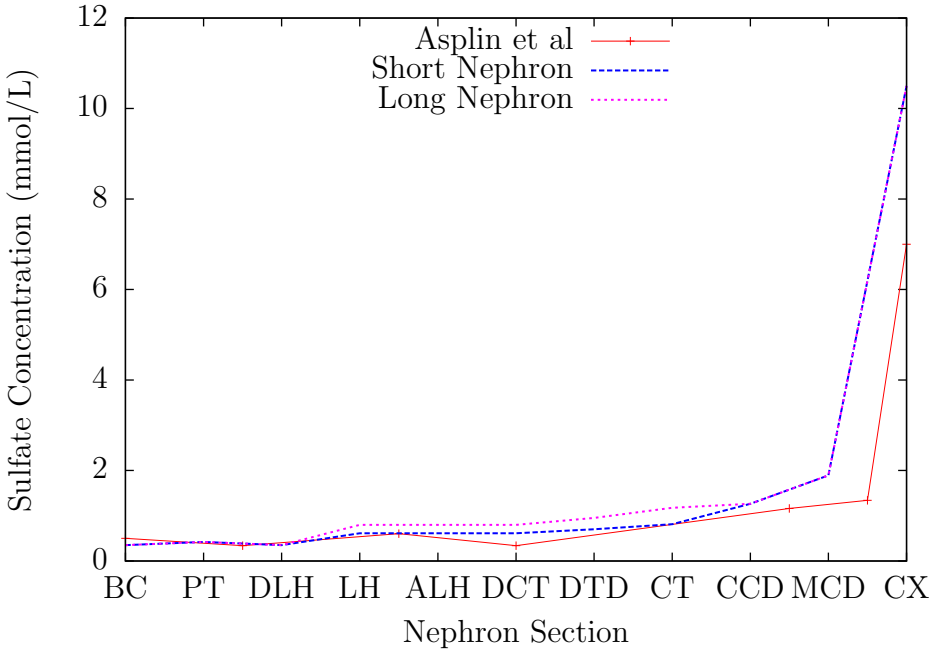

Figure E.9: Sulfate Concentration

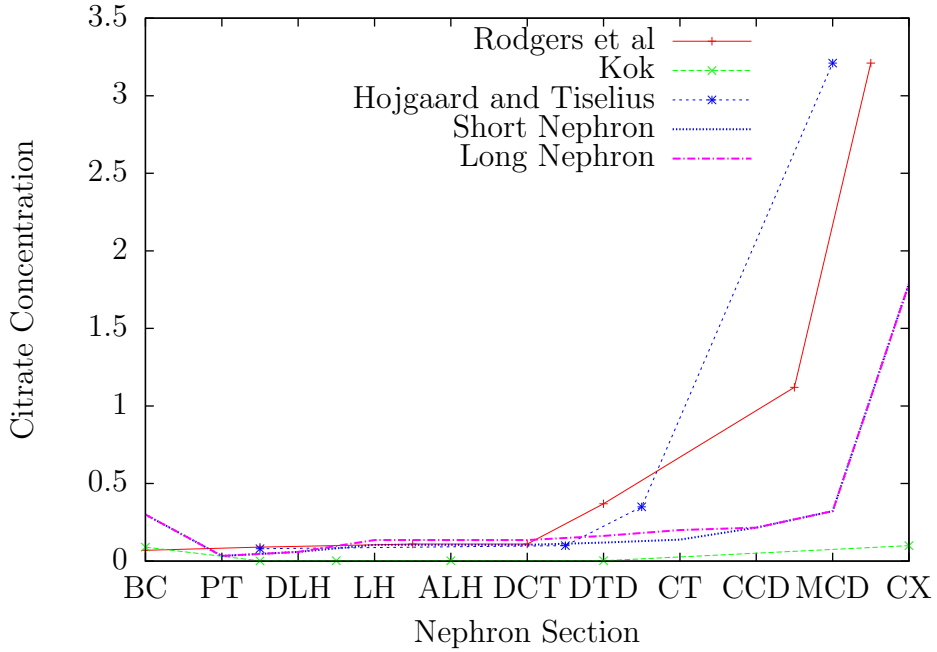

Figure E.10: Citrate Concentration

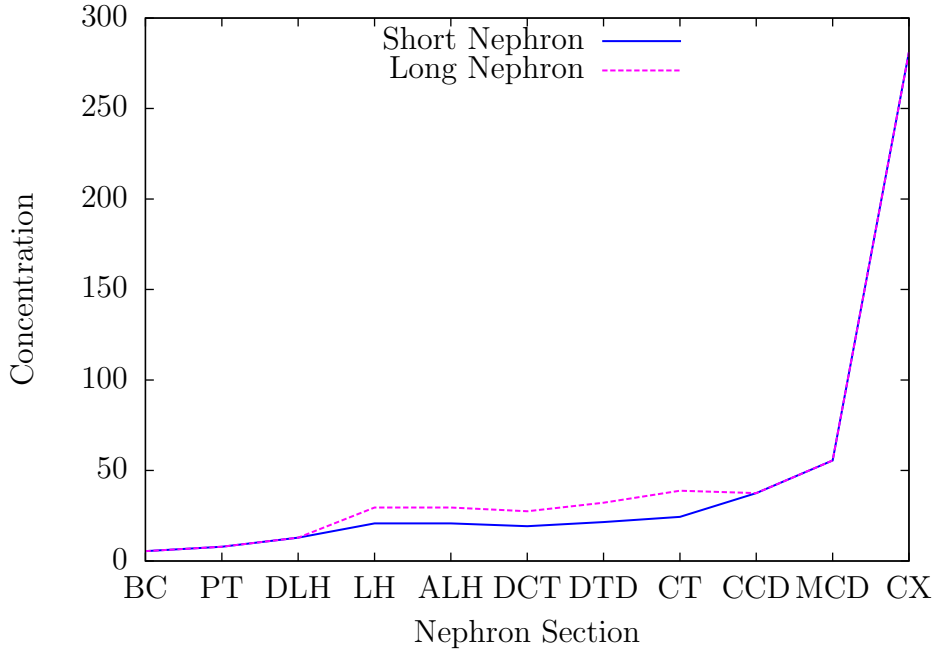

Figure E.11: Urea Concentration

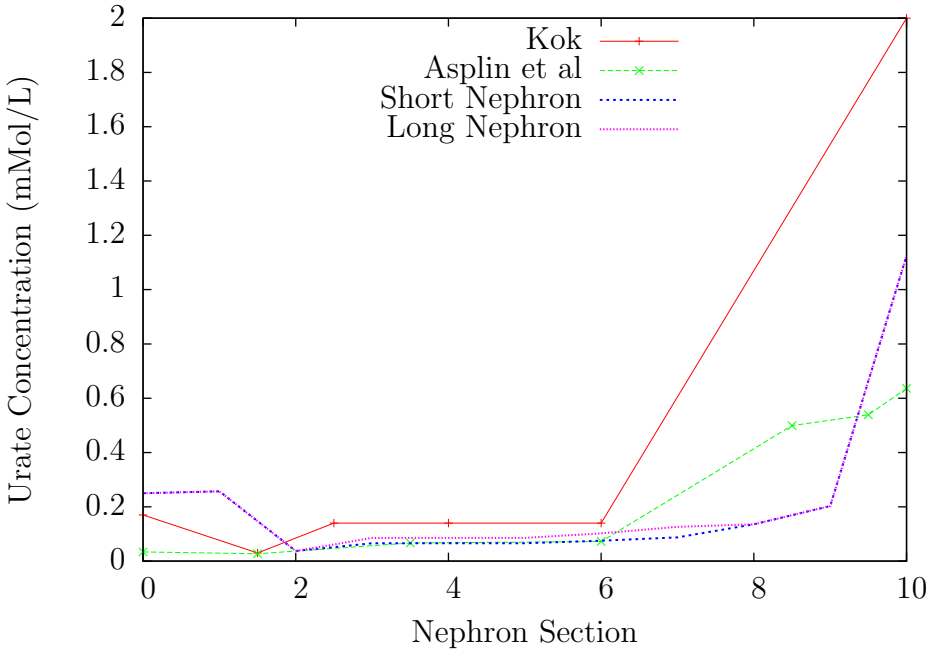

Figure E.12: Urate Concentration (See Table 2.23)

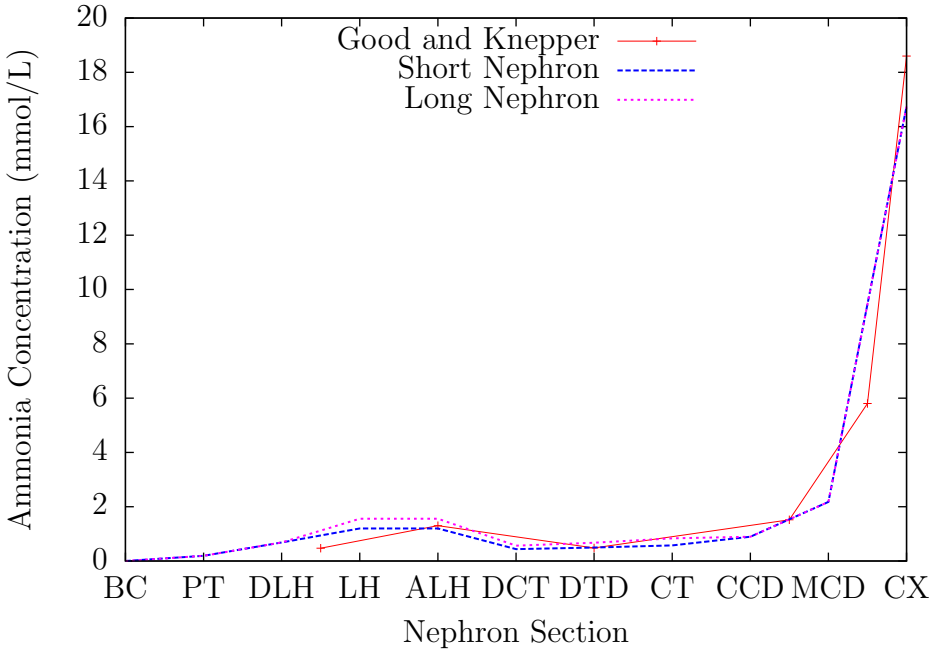

Figure E.13: Ammonia Concentration (See Table 2.24)

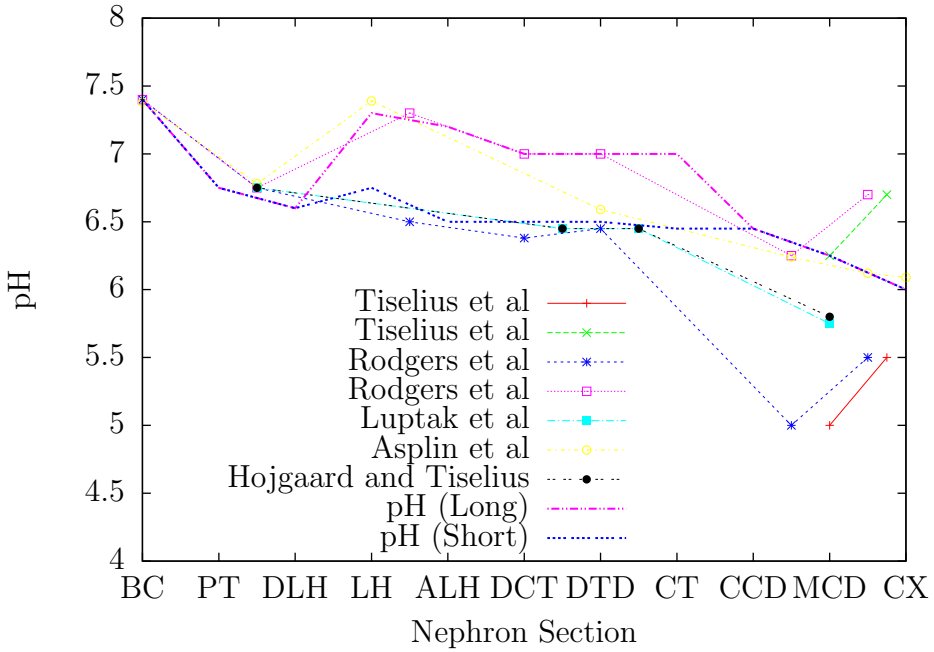

Figure E.14: pH

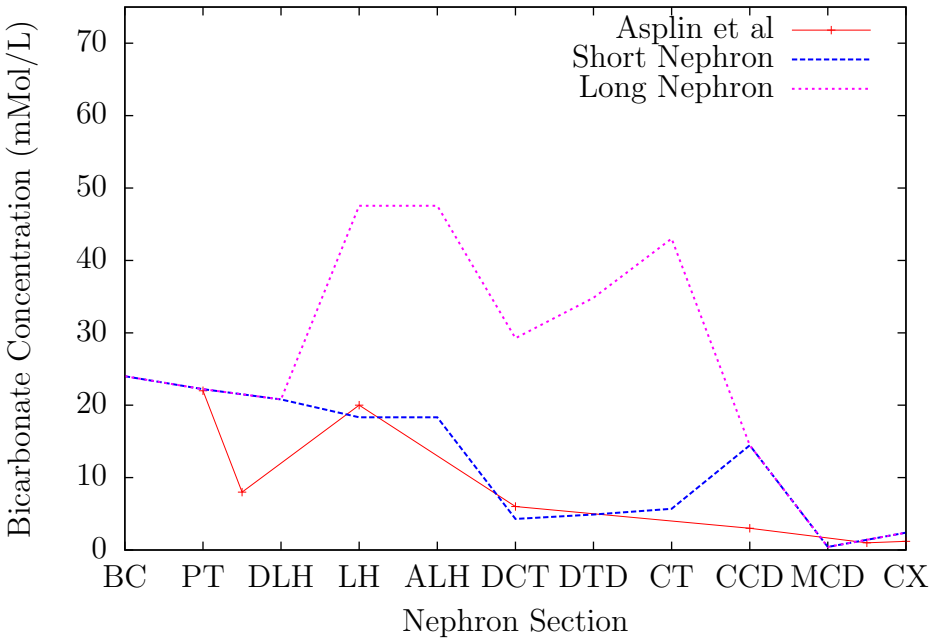

Figure E.15: Bicarbonate Concentration

Appendix F

Reabsorption Profiles

F.1 Profiles 0 to 98:

Normal Kidney Filtration

Profile 0

This is simulating normal kidney filtration, with no values out of range. The standard reabsorption matrix, as described in Section E.2, is used and all hormone levels, ADH, PTH, ALD and AT2, are set to 50, the normal level.

Profile 1

ADH 20

ADH conserves water by making urine more concentrated. Lower than normal ADH will result when fluid intake is high, resulting in a higher urine

volume. Saturation is reduced for all solids from the CT onwards. Reduced COM supersaturation in final urine, COD and COT remain unsaturated to the end of the nephron. The risk of COM precipitation is reduced.

Profile 2

ADH 80

Higher than normal ADH will result when fluid intake is low, resulting in a lower urine volume. Saturation is increased for all solids from the CT onwards. Increased COM supersaturation in the medullary collecting duct. The risk of COM precipitation is increased.

Profile 3

ALD 20

Aldosterone regulates blood pressure and blood volume. A low level of aldosterone will result from higher blood pressure and will result in more sodium and water being excreted.

Slightly reduced risk toward end of nephron.

Profile 4

ALD 80

A high level of aldosterone will result from lower blood pressure and will result in less sodium and water being excreted.

Slightly increased risk toward end of nephron.

Profile 5

AT2 20

Angiotensin II levels will decrease when blood pressure increases. Slightly reduced risk toward end of nephron.

Profile 6

AT2 80

Angiotensin II levels will increase when blood pressure decreases. Slightly increased risk toward end of nephron. (more than ANP)

Profile 7

ANP 20

ANP decreases sodium and water reabsorption. Low ANP will result when blood pressure is low. Supersaturation is slightly higher at the end, as more water is being reabsorbed.

Profile 8

ANP 80

High ANP will result when blood pressure is high. Supersaturation is slightly lower at the end.

Profiles 20 and 21

Hypoparathyroidism: PTH Level 20

Profile 20, low PTH with normal calcium and phosphate levels. Decrease for CaP PR to CCD and small increase for CaOx from PT onwards.

Profile 21, reduced plasma calcium value and increased phosphate value.

Ca_2^+ value used: 0.9 mmol/L

PO_4^{3-} value used: 1.94 mmol/L [08Sho]

CaP value is reduced all along the nephron. Brushite never reaches supersaturation. CaOx value is reduced all along the nephron. COM becomes supersaturated in the MCD.

Profiles 22 and 23

Hyperparathyroidism Values: PTH Level 80

Profile 22: Plasma calcium is the normal value of 1.5 mmol/L, plasma phosphate is the normal value of 1.5 mmol/L.

Small increase for CaP from the PR to the CT, and then a small decrease in the MCD. Brushite value is increased from the PR to the CCD and almost saturated in LH (Long). CaOx decreases toward end.

Profile 23: An ultrafiltrable plasma concentration of 2.8 mmol/L is likely for primary hyperparathyroidism [15Rob]. Plasma calcium is a high value of 3.0 and plasma phosphate is a high value of 2.0.

CaP increase. HAP up to around 13. Brushite is supersaturated in the BC, LH to DT and MCD. COM value > 0 CT onwards.

It can be seen in Figure F.1 the log(SI) value for brushite is increased to a value of up to 0.57, especially in the middle part of the nephron.

COM is supersaturated in DT - more so in short nephron.

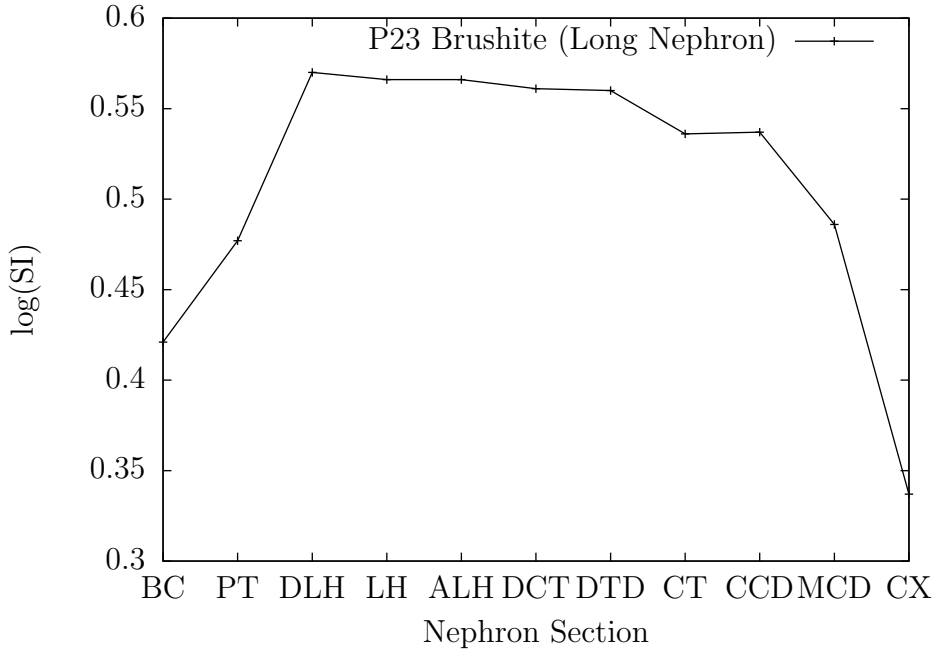

Figure F.1: Profile 23 (Hyperparathyroidism): Difference between log(SI) values of Brushite for Profile 0 and Profile 23 in the Long Nephron

Profiles 31 and 38: pH Variations

Profile 31 is low pH and Profile 38 is high pH.

Lower range for pH in the PCT is 6.7 and for urine it is 4.5 [06GuH]. The upper limit for the tip of a short loop is 7.0, the tip of a long loop may reach as high as 7.4 [11RAJ]. The upper limit for urine pH is 8.0 [06GuH].

Profile 38 has reduced HCO_3^- reabsorption all the way along the nephron.

The normal (Profile 0) bicarbonate reabsorption values are:

bicarbonate:

50 24 11 0 10 0 0 0 4.9

In Profile 38 this has been changed to:

bicarbonate:

25 12 5.5 0 5 0 0 0 2.5

P31 Long Nephron pH Values:

BC	PT	PR	tDL	tAL	TAL	MD	DT	CT	CD	CX
7.4	6.7	6.5	7.0	7.0	6.8	6.8	6.5	5.5	5.0	4.5

P31 Short Nephron pH Values:

BC	PT	PR	tDL	tAL	TAL	MD	DT	CT	CD	CX
7.4	6.7	6.5	6.7	6.4	6.4	6.2	5.8	5.5	5.0	4.5

P38 Long Nephron pH Values:

BC	PT	PR	tDL	tAL	TAL	MD	DT	CT	CD	CX
7.4	7.0	6.8	7.4	7.2	7.0	7.0	7.0	7.6	7.8	8.0

P38 Short Nephron pH Values:

BC	PT	PR	tDL	tAL	TAL	MD	DT	CT	CD	CX
7.4	7.0	6.8	7.0	7.0	7.0	7.0	7.0	7.6	7.8	8.0

Profile 31 Low pH:

HAP OCP values < 0 after DT.

COM COD COT little difference.

UA value > 0 in CD.

CaHUrate risk drops.

Profile 38 High pH:

HAP and OCP, large increase DT onwards (Long) and all along (Short).

Brushite - Converges with P0 plot from LH to DTD, above before and after (Long). Above all the way along for Short.

Reduces COM, COD and COT values toward end.

Profile 41 : Hyponatremia

Normal Values: Sodium 145 Chloride 125

In this case there is a decreased level of sodium, and also chloride, in the blood. Plasma sodium concentration 120 mmol/L and plasma chloride concentration 93 mmol/L.

Hyponatremia increases the risk of CaP precipitation from the LH to DT.

Profile 42 : Hyponatremia with Hormonal Response

Decreased plasma sodium will decrease levels of ADH and ANP, and increase levels of ALD. Values used here are:

P41 + ADH 25, ANP 25 and ALD 60

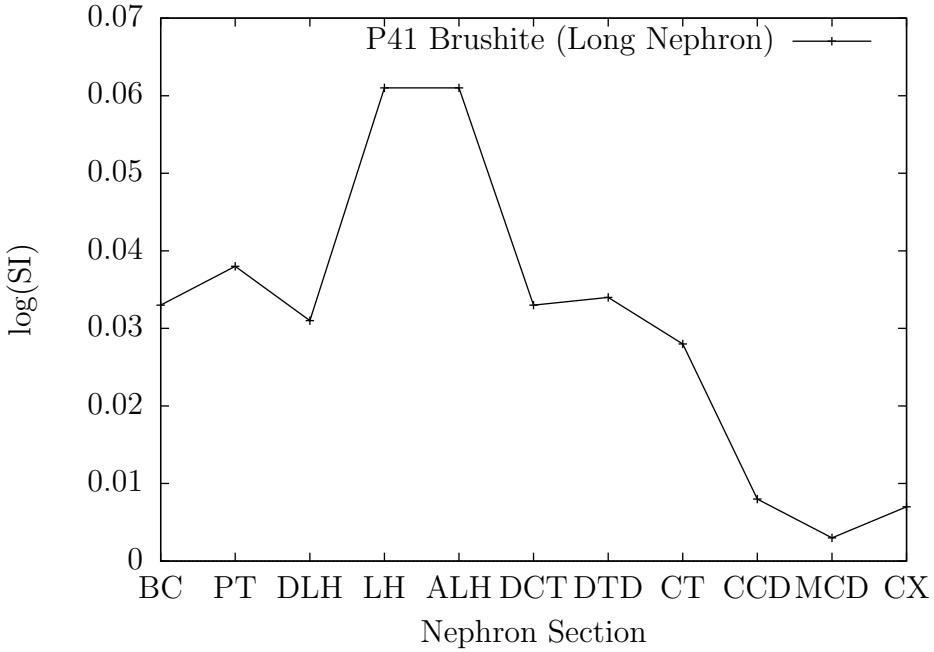

Figure F.2: Profile 41 (Hyponatremia): Differences in log(SI) Brushite values between Profile 41 and the Reference Profile 0

Both CaP and CaOx values are slightly increased up to the CT, and then reduced in the MCD. There is an increase for CaOx.

Profile 45 : Hypernatremia

An increased level of sodium, and also chloride, in the blood. Plasma sodium concentration 180 mmol/L [14Cha] and plasma chloride concentration 155 mmol/L.

Hypernatremia shows a small reduction in value up to the CT. This is greatest for brushite in the loop of Henle of the long nephron.

Profile 46 : Hypernatremia with Hormonal Response

Increased plasma sodium will increase levels of ADH and ANP and decrease levels of ALD. The values used here are:

P45 + ADH 75, ANP 75 and ALD 40

Small CaP and CaOx decrease from the start of the nephron until the CT, and then increase in the MCD for CaP and CaOx.

Profiles 47 and 48: Plasma Potassium Variations

Normal Value: 4.2 mmol/L

Lowering plasma potassium to 3.0 mmol/L or increasing it to 5.0 mmol/L showed no difference.

Profiles 50 to 58: Plasma Citrate Variations

Normal Value: 0.3

Profile	Plasma Citrate (mmol/L)	Urine Citrate (mmol/L)
50	0.05	0.30
51	0.10	0.60
55	0.30	1.79
57	0.50	2.98
58	0.80	4.77

High citrate levels lower the Ca^{2+} concentration, and thus reduce the risk.

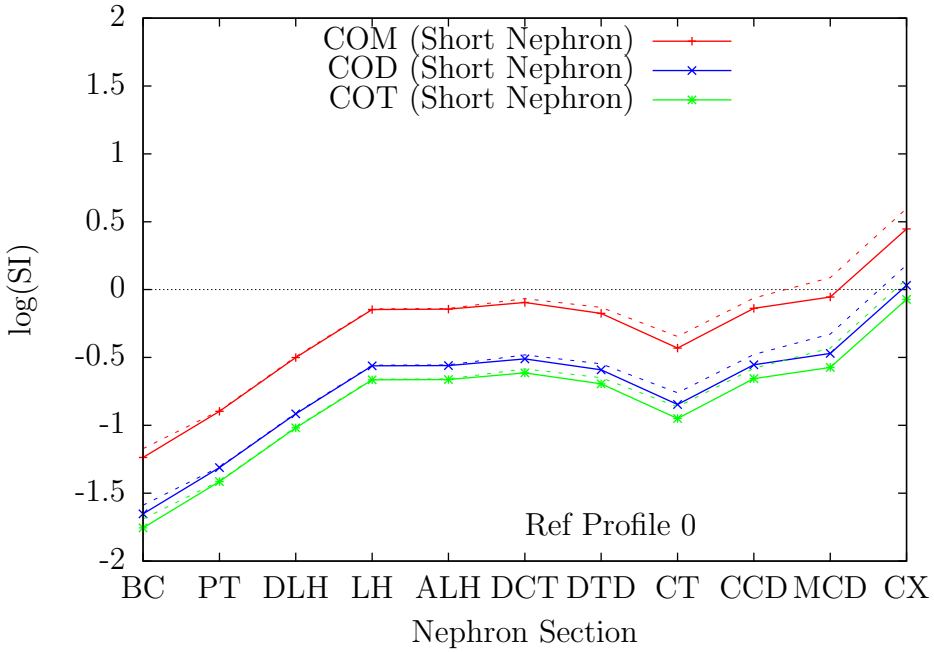

Figure F.3: Profile 74: log(SI) CaOx Short Nephron

Profiles 60 to 69: Plasma Calcium Variations

Normal Value: 1.5

Profile	Plasma Calcium (mmol/L)	Urine Calcium (mmol/L)
60	1.00	1.50
61	1.25	1.88
62	1.50	2.25
63	1.75	2.63
64	2.00	3.00
65	2.25	3.38
66	2.50	3.75
67	2.75	4.13
68	3.00	4.50

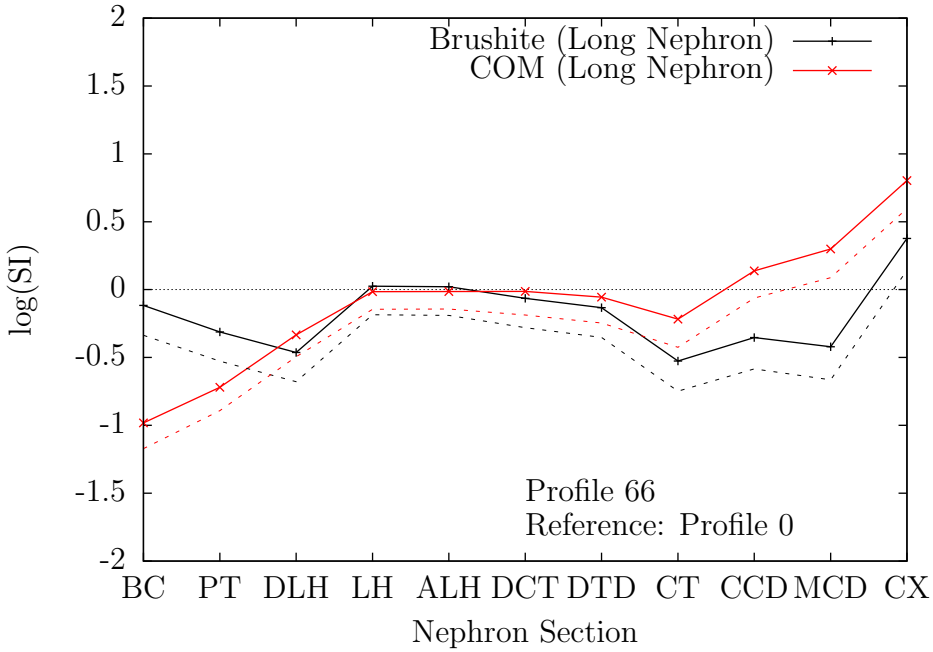

Figure F.4: Profile 66: log(SI) Brushite and COM Long Nephron

The high urine values exceed those listed in Appendix B, but this is to be expected, as they represent high peaks, that will not be measurable in the averaged concentrations seen in collected urine.

Low calcium reduces the values for CaP and CaOx.

With a simulated plasma calcium concentration of 2.25 mmol/L, COM exceeds supersaturation in the short nephron distal tubule, dipping below it in the collecting tubule before rising above it again the collecting duct. The pattern is the same for values of 2.5, 2.75 and 3.00 mmol/L, with increased supersaturation levels.

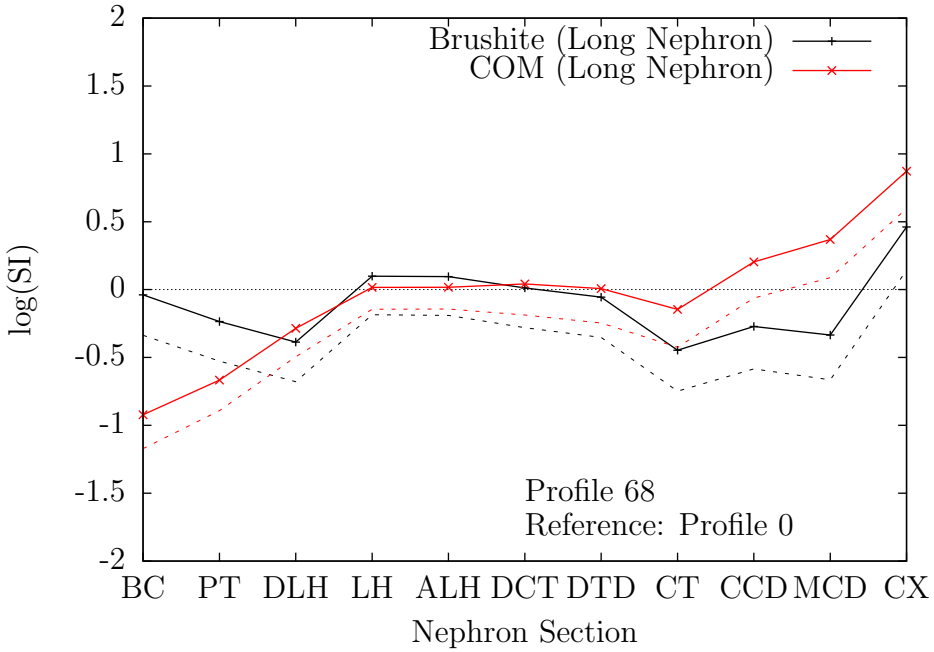

Figure F.5: Profile 68: log(SI) Brushite and COM Long Nephron

Profiles 70 to 74: Plasma Phosphate Variations

Normal Value: 1.5 mmol/L

Taken from an example in the paper by Robertson [15Rob].

Profile	Plasma Phosphate (mmol/L)	Urine Phosphate (mmol/L)
70	0.80	10.62
71	1.20	15.92
72	1.60	21.23
73	2.00	26.54
74	2.50	33.18
75	3.00	39.81

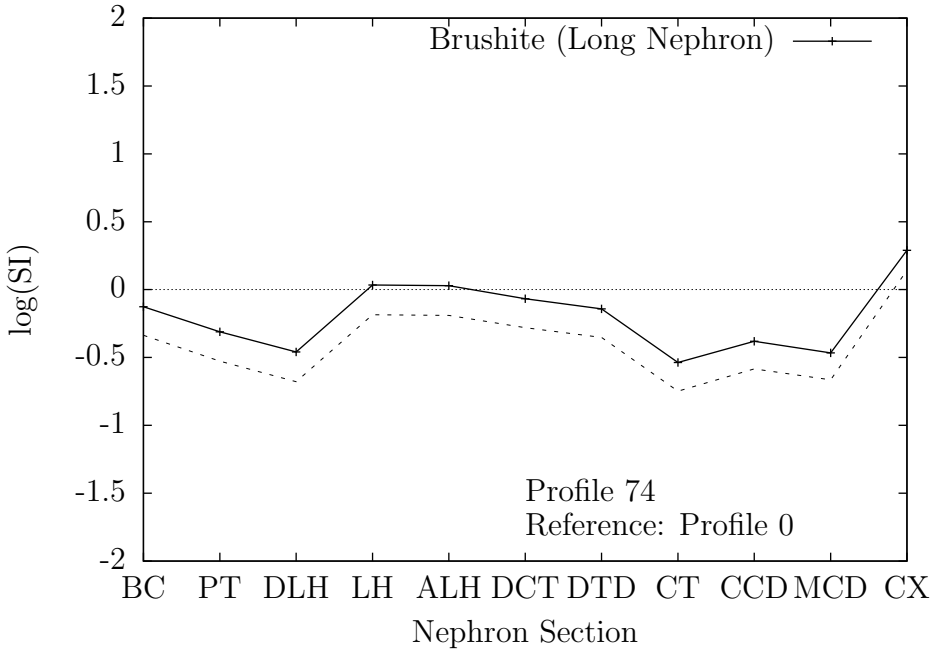

Figure F.6: Profile 74: log(SI) Brushite Long Nephron

Low phosphate reduces the values.

At a high plasma PO_4 level of 2.5 mmol/L brushite becomes supersaturated in the LH.

Profiles 80 to 89: Plasma Oxalate Variations

Normal Value: 1.75 μmol/L

Taken from an example in the paper by Robertson [15Rob] and data in [97Kok], which estimates that in stone formers, plasma oxalate may peak at 10.0 μmol/L.

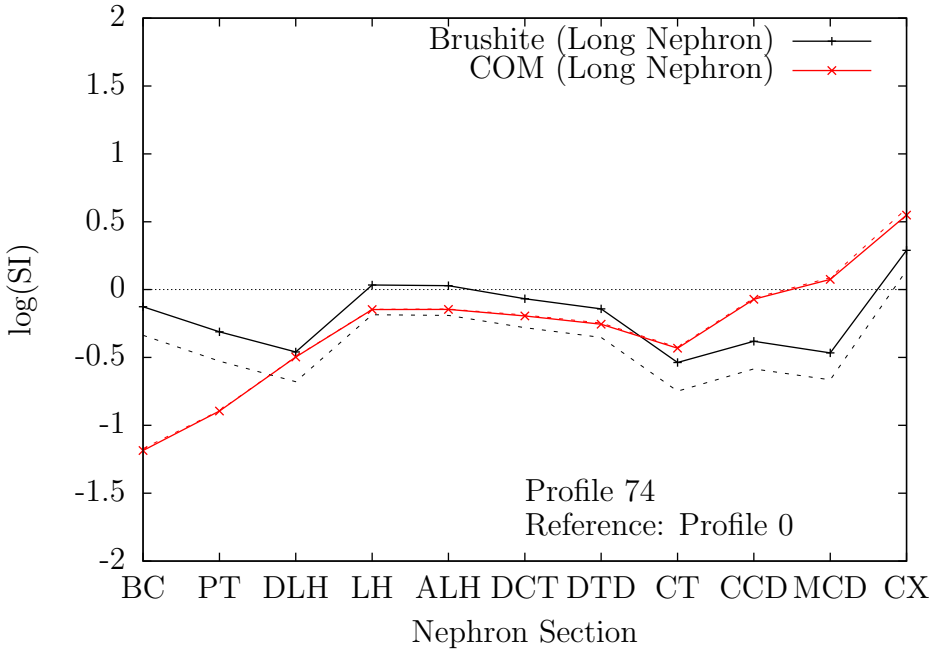

Figure F.7: Profile 74: log(SI) Brushite and COM Long Nephron

Profile	Plasma Oxalate (μmol/L)	Urine Oxalate (mmol/L)
80	1.25	0.14
81	1.50	0.17
82	1.75	0.19
83	2.00	0.22
84	2.25	0.25
85	2.50	0.28
86	3.00	0.33
87	4.00	0.44
88	5.00	0.55
89	10.00	1.10

With a simulated plasma oxalate concentration of 2.25μmol, COM exceeds

supersaturation in the short nephron distal tubule, dipping below it in the collecting tubule before rising above it again the collecting duct. At a value of 3.00 μmol/L supersaturation is reached by the bend of the loop of Henle and is exceeded in the long nephron also. At level 4.00 μmol/L supersaturation is achieved in the descending limb of the loop of Henle and maintained for the rest of the nephron.

Profiles 90 to 92: Plasma Sulfate Variations

Normal Value: 0.35 mmol/L

Sulfate reduces the risk of calcium stone formation [14RGE]. From the data in Appendix B, urine sulfate range is approximately 14.78 - 34.48 mmol/L, thus the the values tested here represent variations beyond those values considered normal, simulating transient peaks associated with stone formation.

Profile	Plasma Sulfate (mmol/L)	Urine Sulfate (mmol/L)
90	0.20	6.00
91	0.50	15.00
92	0.95	28.50
93	1.75	52.50

Increased levels of SO_4 show some reduction in risk, but this is small. Sulfate at 1.75 mmol/L (normal value 0.35 mmol/L) reduced both the CaP and CaOx values from the CT onwards and also the CaOx value from the CT onwards.

Profiles 96 to 98: Plasma Magnesium Variations

Normal Value: 0.4 mmol/L

Profile	Plasma Magnesium (mmol/L)	Urine Magnesium (mmol/L)
96	0.01	0.04
97	0.10	0.42
98	0.95	3.99

Low magnesium results in very little change in the CaP value, but a small increase in the value for CaOx all the way along, converging at the end. High magnesium results in reduced value for CaOx.

F.2 Profiles 100 to 198: Stone Former Reduced Calcium Reabsorption in Proximal Tubule

Profile 100

Profile 0 urine calcium value: 2.25 (mmol/L)

Profile 100 urine calcium value: 4.50 (mmol/L)

The calcium reabsorption values have been adjusted in the reabsorption matrix used to simulate the pathology of reduced calcium reabsorption in the proximal tubule.

RFMatrix (P0):

calcium:

40 20 0 0 25 5.5 5.5 0 1.5 1

RFMatrix (P100):

calcium:

39 19.5 0 0 25 5.5 5.5 0 1.5 1

CaP value is increased after LH. CaOx value is increased after LH.

Figure F.8 shows the log(SI) values for the calcium phosphates for the case of reduced proximal tubule calcium reabsorption, in comparison to the normal Profile 0. In the cases of Profiles 101 to 198, the comparison with respect to reduced or increased log(SI) values, and hence risk, is made to Profile 100, the reduced PT calcium reabsorption pathology.

Profile 101

P100 + P1 (Low ADH)

Values for CaP and CaOx are reduced at the end of the nephron.

Profile 102

P100 + P2 (High ADH)

Values for CaP and CaOx are increased at the end of the nephron. Brushite supersaturation increases at the end.

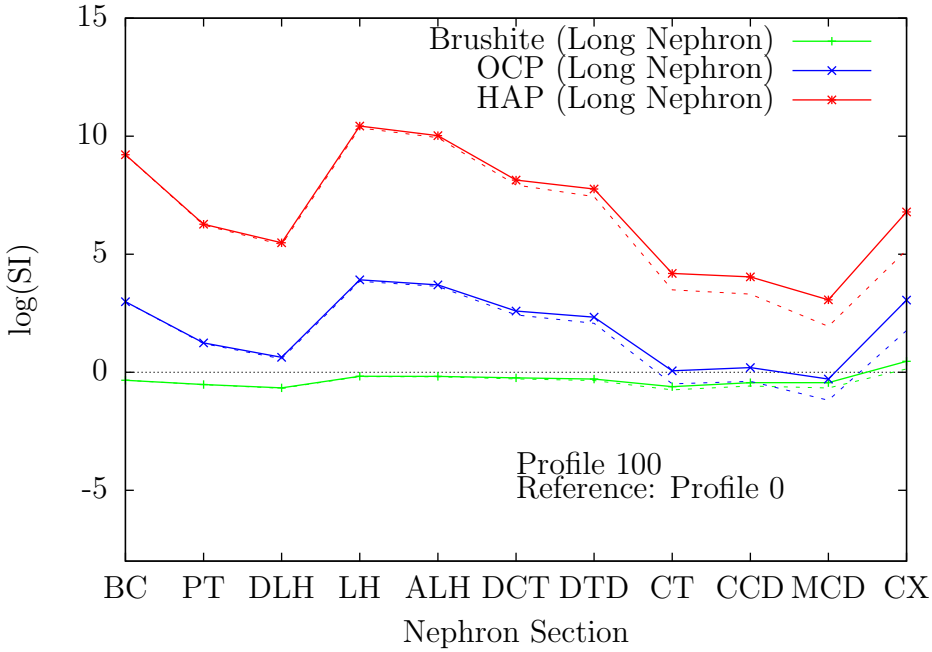

Figure F.8: Profile 100: log(SI) Calcium Phosphates Long Nephron

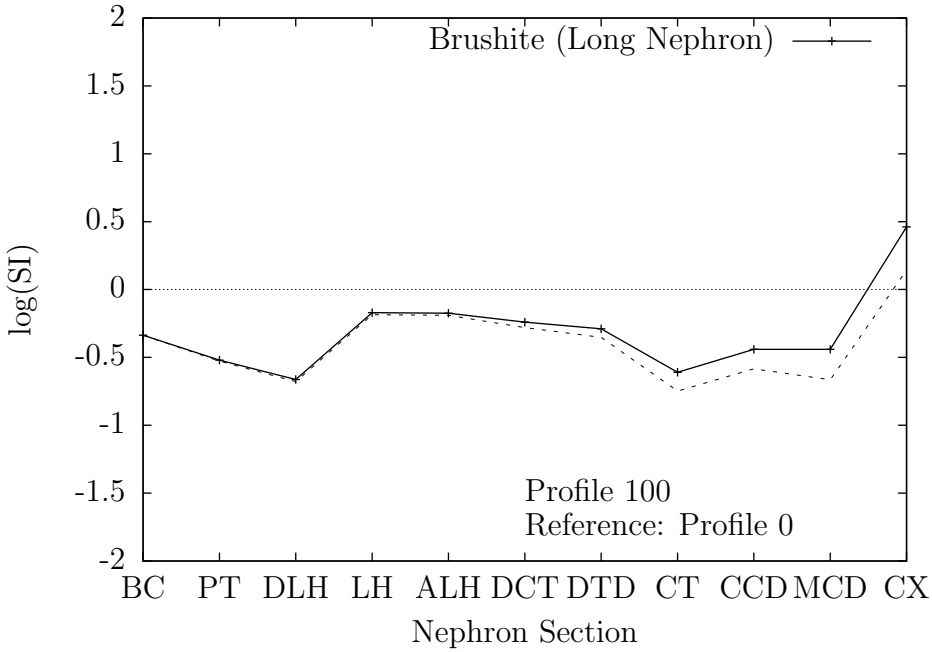

Figure F.9: Profile 100: log(SI) Brushite Long Nephron

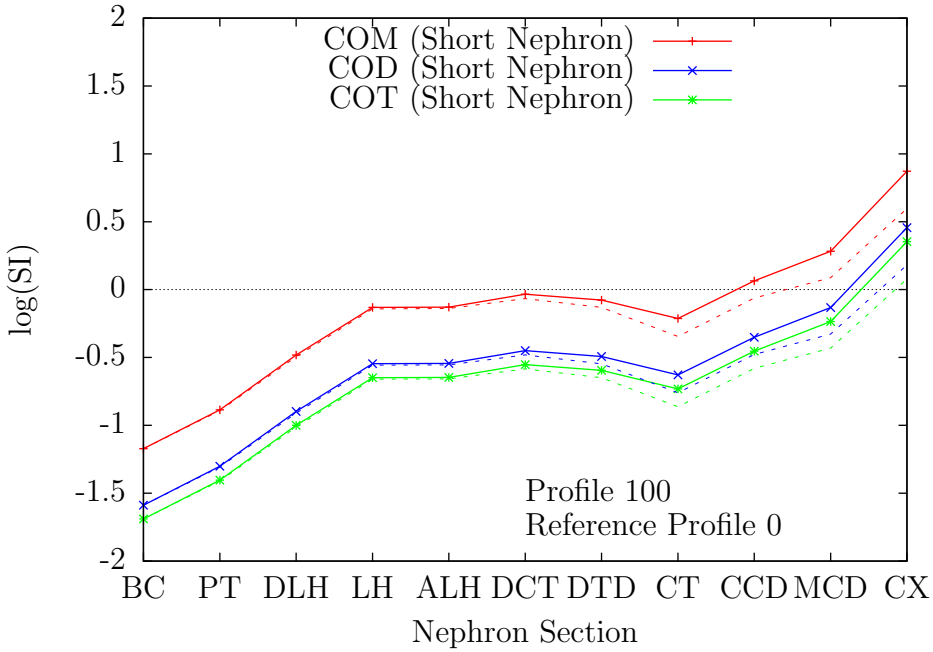

Figure F.10: Profile 100: log(SI) Calcium Oxalates Short Nephron

Profile 103

P100 + ALD 20

Reduced CaP and CaOx values in the MCD.

Profile 104

P100 + ALD 80

CaP and CaOx risk is increased in the CD.

Profile 105

P100 + AT2 20

CaP and CaOx slightly lower towards end. (Diverging from DT)

Profile 106

P100 + AT2 80

CaP and CaOx slightly lower towards end. (Diverging from DT)

Profile 107

P100 + ANP 20

CaP slightly higher risk MCD onwards. CaOx slightly higher risk MCD onwards.

Profile 108

P100 + ANP 80

CaP slightly lower risk MCD onwards. CaOx slightly lower risk MCD onwards.

Profile 120

P100 + PTH 20

CaP: Reduced risk from PR, almost converges with Profile 100 in MCD (more so for HAP).

CaOx: slightly increased from DT.

Profile 121

P100 + PTH 20 + low Ca

CaP and CaOx: reduced all the way along.

Profile 122

P100 + PTH 80

CaP: Small increase PR to CCD.

CaOx: Slight decrease DT onwards.

Profile 123

P168 + PTH 80

CaP: Increased value all the way along - COM value > 0 in DT, more so in the short nephron, log(SI) of brushite is above 0 from the DLH to the DTD, where it dips below 0 in the region of the CT, and then increases again, levelling off in the CCD and then rising rapidly in the MCD. CaOx: Higher value all the way along.

This supports the theory that CaP will precipitate in the LH, and then may dissolve again in the CT. At that point SI COM increases, thus solid CaOx may form. Increased $[Ca^{2+}]$ all along.

Profile 131

P100 + Low pH

Low pH. Reduced CaP especially towards the end. Insignificantly higher risk for CaOx towards the end. Increased value for uric acid in MCD.

Profile 132

P100 + Low pH and High plasma Ca

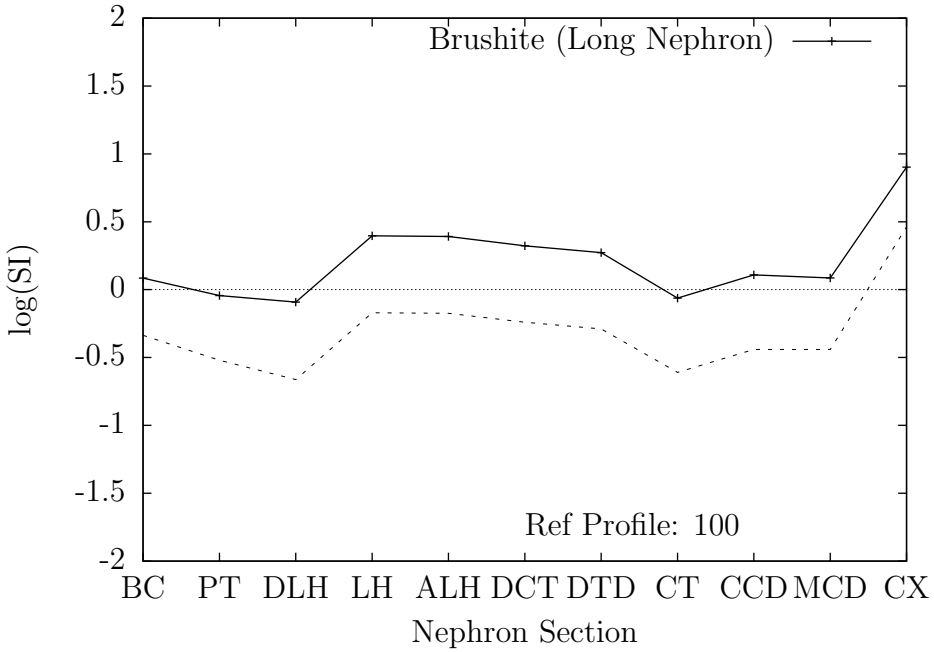

Figure F.11: Profile 123: log(SI) Brushite Long Nephron

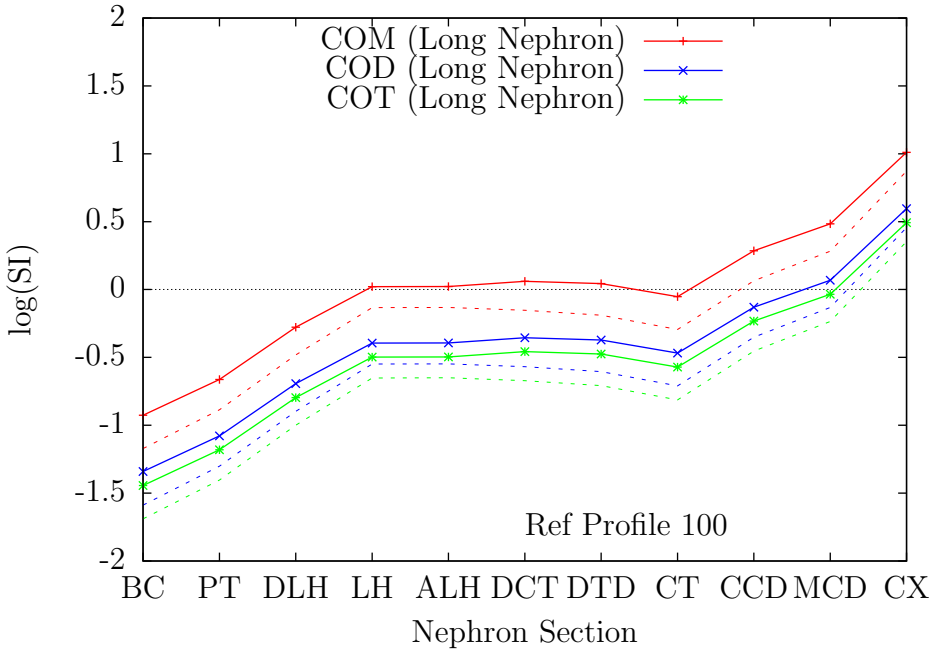

Figure F.12: Profile 123: log(SI) CaOx Long Nephron

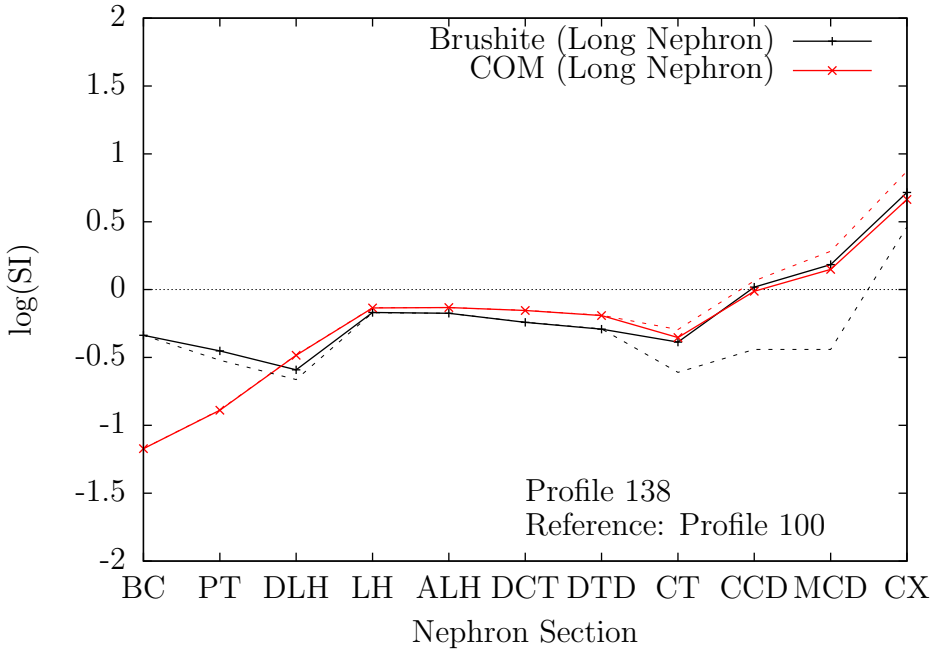

Figure F.13: Profile 138: log(SI) Brushite and COM Long Nephron

Increased value for CaP before CT, reduced after CT especially brushite in the long nephron. Bru > 0 LH in both. Increased CaOx all along.

Classic CaP Hypothesis CaOx stone formation.

Increased UA value toward end. Increased $[Ca^{2+}]$ especially toward end.

Profile 138

P100 + High pH

Increased CaP value towards end, brushite increased in CD. UA value decreased.

P141

P100 + P41 (Low sodium)

Less effect than in P41 (for brushite and HAP) except in the MCD, where it is slightly more. Very little effect for CaOx, and it converges with P100 after the CT.

Profile 142

P100 + P42 (Low sodium and adjusted hormone values)

CaP: Slightly increased to DTD, reduced in MCD.

Profile 145

P100 + P45 (High sodium)

Increased sodium results in CaP and CaOx risk slightly reduced in middle of the nephron.

Profile 146

P100 + P46 (High sodium and adjusted hormone values)

Brushite value decreases in middle. Brushite value increases towards end. CaOx increases toward end. $[Ca^{2+}]$ up in CD to LH level.

P146 vs P100 Brushite value slightly lower in middle, higher at end.

Profile 150

P100 + P50 (Low citrate)

Increased values for both CaP and CaOx.

Profile 158

P100 + P58 (High citrate)

Increased citrate reduces risk all along for brushite and CaOx.

P160

P100 + P60 (Lower calcium)

Lower Ca reduces risk all along CD for CaP and CaOx.

Profile 163

P100 + P60 (Higher calcium) Ca 1.75 mmol/L

CaP and CaOx values are increased all along the nephron. COM reaches supersaturation in the thick ascending limb.

Profile 165

Plasma Ca 2.25 mmol/L.

Brushite is close to supersaturation in the loop of Henle, but remains below, only becoming supersaturated in the MCD. COM is supersaturated in the DT.

Profile 166

Plasma Ca 2.5 mmol/L.

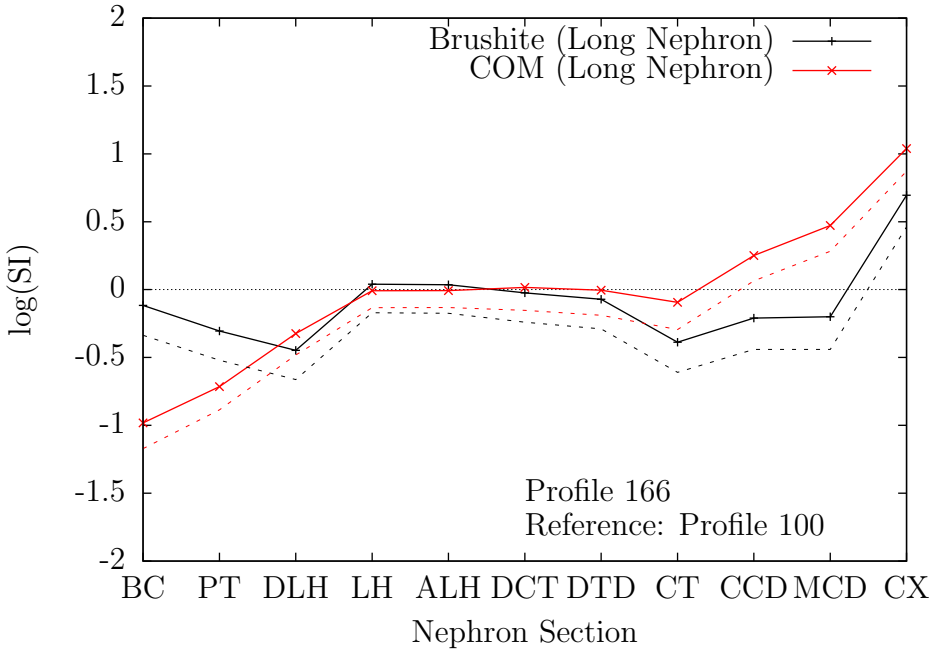

Figure F.14: Profile 166: log(SI) Brushite and COM Long Nephron

Bru > 0 in ALH (Long) (just above 0) COM > 0 from DT

Profile 167

At a plasma calcium concentration of 2.75, brushite becomes supersaturated in the ALH, dropping below supersaturation in the DT, and rises to supersaturation in the MCD.

Profile 170

P100 + P70 (Low phosphate)

Lower phosphate. Values are lowered all along the nephron for the calcium phosphates. No difference for the calcium oxalates.

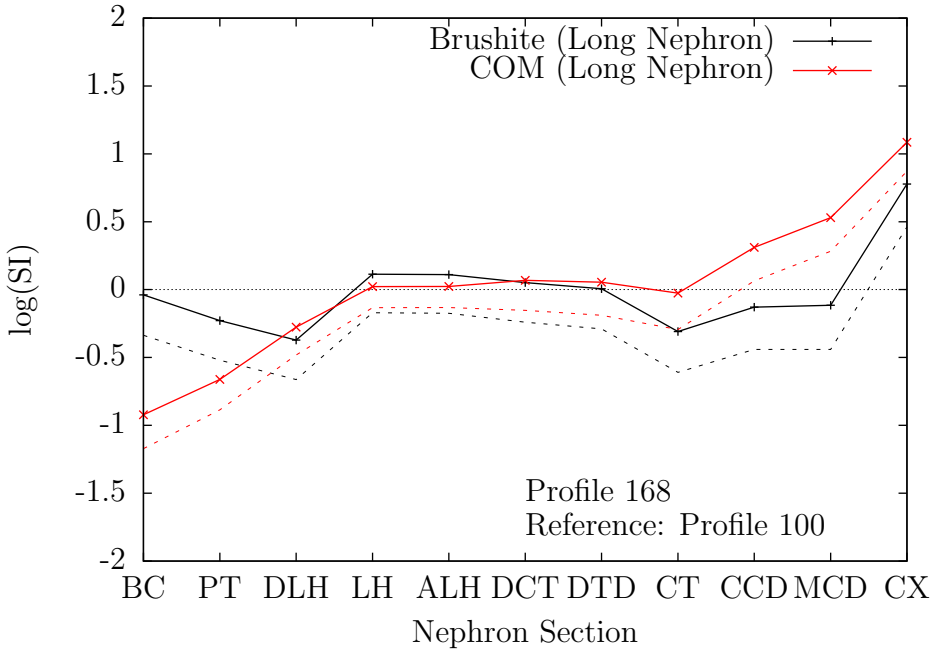

Figure F.15: Profile 168: log(SI) Brushite and COM Long Nephron

Profile 173

P100 + P73 (High phosphate: 2.0 mmol/L)

Values are higher all along the nephron for the calcium phosphates. Brushite almost reaches saturation in the ALH.

Profile 174

P100 + P74 (High phosphate)

Bru > 0 in the LH in both the long nephron and short nephron.

Profile 175

P100 + P75 (High phosphate)

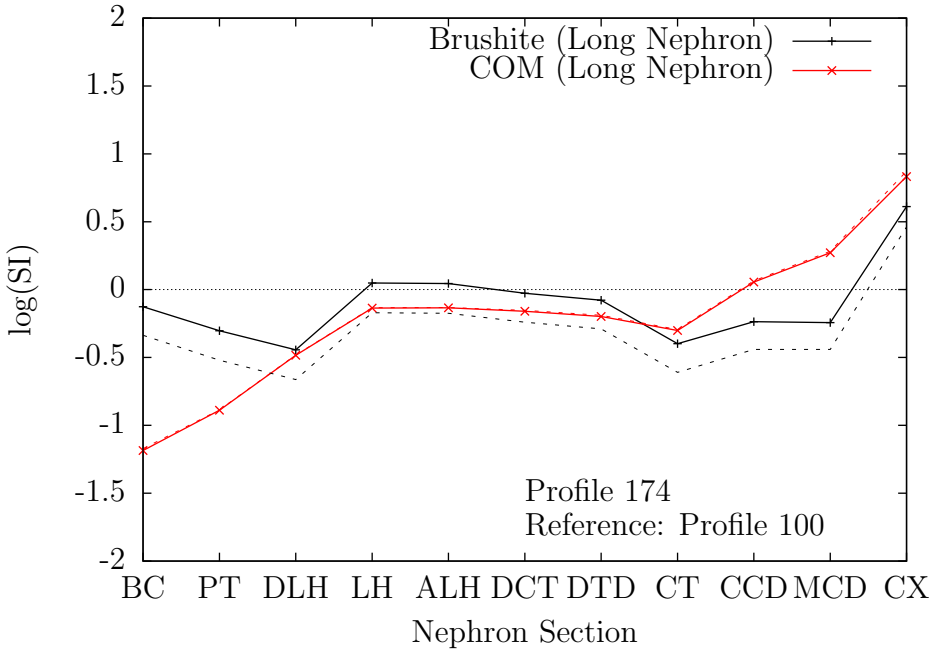

Figure F.16: Profile 174: log(SI) Brushite and COM Long Nephron

Phosphate 3.0 [1.5]

Bru > 0 in the LH in both the long and short nephron. In the long nephron, this is most of the loop of Henle.

Profiles 180 to 181

P100 + P80, P81 (Low oxalate)

Slightly lower Ox only reduces CaOx risk before DT.

Profile 188

P100 + P88 (High oxalate)

No difference for CaP values. CaOx values increased, with COM supersaturated from the tDL onwards. COD reaches supersaturation in the CT.

Profile 189

P100 + P89 (High oxalate)

COM supersaturated from the PR and COD supersaturated from the tDL.

Profile 190

P100 + P90 (Low sulfate – 0.2 mmol/L)

Very little effect.

Profile 191

P100 + P91 (High sulfate – 0.5 mmol/L)

Very little effect.

Profile 192

P100 + P92 (High sulfate – 0.95 mmol/L)

A decrease in value for CaP and CaOx from CT onwards.

Profile 193

P100 + P93 (High sulfate)

Sulfate 1.75 [0.35] reduces the value for both CaP and CaOx from the CT onwards.

Profile 196-7

P100 + P96, P97 (Low magnesium)

Lower Mg increases CaOx value slightly, no CaP effect.

Profile 198

P100 + P98 (High magnesium)

Higher Mg decreases CaOx risk slightly. No CaP effect.

F.3 Profiles 200 to 298: Stone Former Reduced Calcium Reabsorption in Distal Tubule

Profile 200

Profile 0 urine calcium value: 2.25 (mmol/L)

Profile 200 urine calcium value: 6.00 (mmol/L)

The reduction in calcium reabsorption is assumed to be in the Thick Ascending Limb. This is simulated by the adjusted calcium reabsorption values shown below.

RFMatrix (P0):

calcium:

40 20 0 0 25 5.5 5.5 0 1.5 1

RFMatrix (P200):

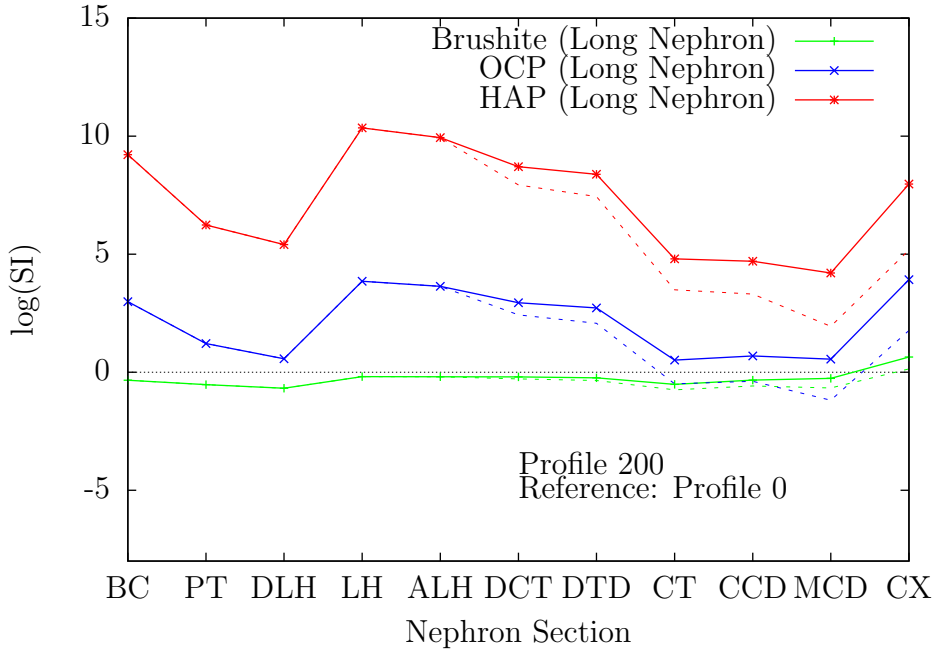

Figure F.17: Profile 200: log(SI) Calcium Phosphates Long Nephron

calcium:

40 20 0 0 22.5 5.5 5.5 0 1.5 1

There is also an associated reduction in bicarbonate reabsorption:

RFMatrix (P0):

bicarbonate:

50 24 11 0 10 0 0 0 4.9

RFMatrix (P200):

bicarbonate:

50 24 11 0 9 0 0 0 4.9

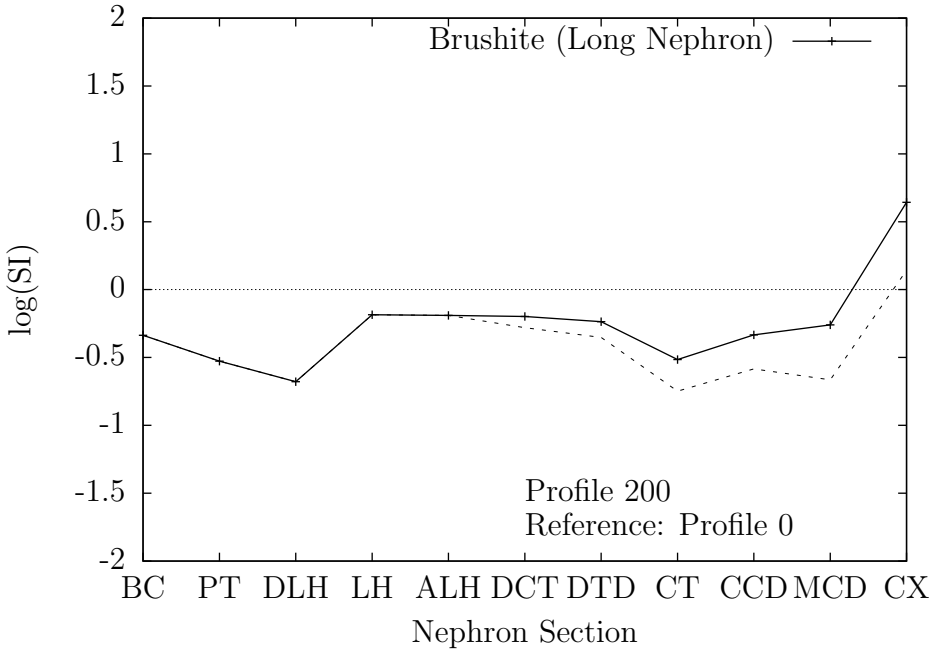

Figure F.18: Profile 200: log(SI) Brushite Long Nephron

Figure F.17 shows the log(SI) plot for the calcium phosphates for Profile 200 with the normal values (Profile 0) shown as a dotted line for reference. It can be seen that the values are increased from the loop of Henle onwards. In the cases of profiles 201 to 298, the comparison with respect to reduced or increased log(SI) values, and hence risk, is made to Profile 200, the reduced DT calcium reabsorption pathology.

Profile 201

P200 + P1 (Low ADH)

Reduced values in MCD, as expected due to lower concentrations.

Profile 202

P200 + P2 (High ADH)

Higher values in the in MCD due to increased concentrations.

$[Ca^{2+}]$ very high at end.

Profile 203

P200 + P3 (Low aldosterone)

Lower levels of aldosterone will result in decreased NaCl and H2O reabsorption and increased K reabsorption.

Slightly lower in CD.

Profile 204

P200 + P4 (High aldosterone)

Higher levels of aldosterone will result in increased NaCl and water reabsorption and decreased K reabsorption.

Slightly higher in MCD for all substances.

Profile 205

P200 + P5 (Low angiotensin II)

Very slightly lower from CT then diverges in MCD, for both CaP and CaOx.

Difference still small.

Profile 206

P200 + P6 (High angiotensin II, resulting in increased NaCl and H2O reabsorption)

Only just higher from CT then diverges in MCD. Brushite insignificantly higher from LH. Brushite difference in CX is fairly large.

Profile 207

P200 + P7 (Reduced atrial natriuretic peptide, resulting in increased NaCl and water reabsorption)

CaP: Only just higher from MCD onwards (insignificant difference from CCD). CaOx: Only just higher from MCD onwards as above.

Profile 208

P200 + P8 (Increased atrial natriuretic peptide, resulting in reduced NaCl and water reabsorption, to reduce BP) ANP action is the opposite of ALD and AT2.

Slightly lower from MCD onwards for CaP and CaOx.

Profile 220

P200 + P20 (Low PTH)

CaP: Starts to fall lower from the end of the PCT, then is lower for most of the way, but converges, only just lower from MCD onwards. For brushite there is more of a difference. CaOx: Insignificantly lower from DT onwards.

Profile 221

P200 + P21 (Low PTH 20 and low plasma calcium)

Lower all the way along (CaP and CaOx, more for CaP).

Profile 222

P200 + P22 (High PTH)

Increases PR to DCT then decreases from CD for HAP and OCP. Brushite is close to 0 in long nephron in ALH. Small decrease for CaOx starting from DT.

Profile 223

P200 + P23 (High PTH 80 and high plasma calcium, 3.0 mmol/L)

Clear risk. Higher all the way along for CaP starts to converge in MCD but still large difference by CX. Brushite precipitation risk in LH and DT which is not the case with P200.

CaOx greater all the way along but the difference starts to become less in the MCD. CD risk increased and shifted to beginning.

$[Ca^{2+}]$ very high in LH and MCD.

Profile 231

P200 + P31 (Low pH.)

Low pH reduces risk. CaP less than P200 all along especially at end, where it drops way down to about -6. Starts to diverge from P200 in PT. Falls

below 0 for HAP and OCP end of DT. Brushite never above 0. CaOx little difference.

Profile 238

P200 +P38 (High pH)

HAP and OCP: Above from PT to ALH, then falls below (P200) in DT increases sharply from the end of the DT. Brushite only > 0 in CD.

CaOx only slightly increased from CT but much greater risk with CaP.

Profile 241

P200 + P41 (Low sodium)

HAP, OCP and brushite small increase seen in LH to DCT.

CaOx increase hardly noticeable up to MCD, then no difference.

Profile 242

P200 + P42 (Low sodium and adjusted hormone values)

Same as P241.

Profile 245 and Profile 246

P200 + P45 (High sodium)

P200 + P46 (High sodium and adjusted hormone values)

HAP, OCP and brushite reduction all along the nephron.

CaOx reduced but not as much as CaP.

Profile 250

P200 + P50 (Low citrate: 0.05 mmol/L. Normal value is 0.3 mmol/L)
Very slightly higher in the PT. Higher (only slightly) DT to CX, more so in CCD for CaP. Same pattern for CaOx, but less difference.

Profile 251

P200 + P51 Low citrate: 0.1
As for P251.

Profile 257

P200 + P57 High citrate: 0.5
Slightly lower from CT onwards. More for CaP than CaOx. Increased citrate reduces CaP risk increasingly from DT.

Profile 258

P200 + P58 (High citrate: 0.8)
Small difference in PT. Slight difference from DT to CT. More for CaP than CaOx. Increased citrate at this level reduces CaP risk increasingly from CT. High citrate lowers CaP and CaOx risk CT onwards.

Profile 260 and 261

P200 + P60 (Lower calcium)
Low calcium: 1.0, 1.25

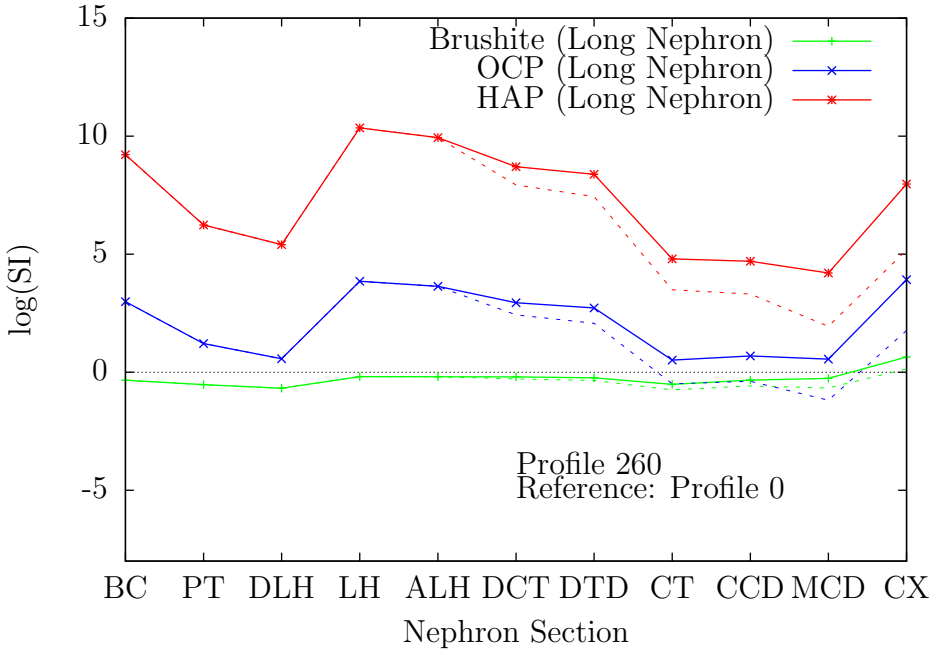

Figure F.19: Profile 260: log(SI) Calcium Phosphates Long Nephron

Even with lower plasma calcium the risk is still higher with abnormal calcium reabsorption, as shown in Figure F.19, where Profile 260 with a low plasma calcium value of 1.0 is plotted against the normal (Profile 0) as a reference. Little difference with respect to P200.

Profile 268

P200 + P68 (High calcium)

Bru $>$ 0 in LH DT high risk.

P268 vs P200 brushite is shifted above 0 in LH and DT in long, close to 0 in short but $>$ 0 at LH (bend) point.

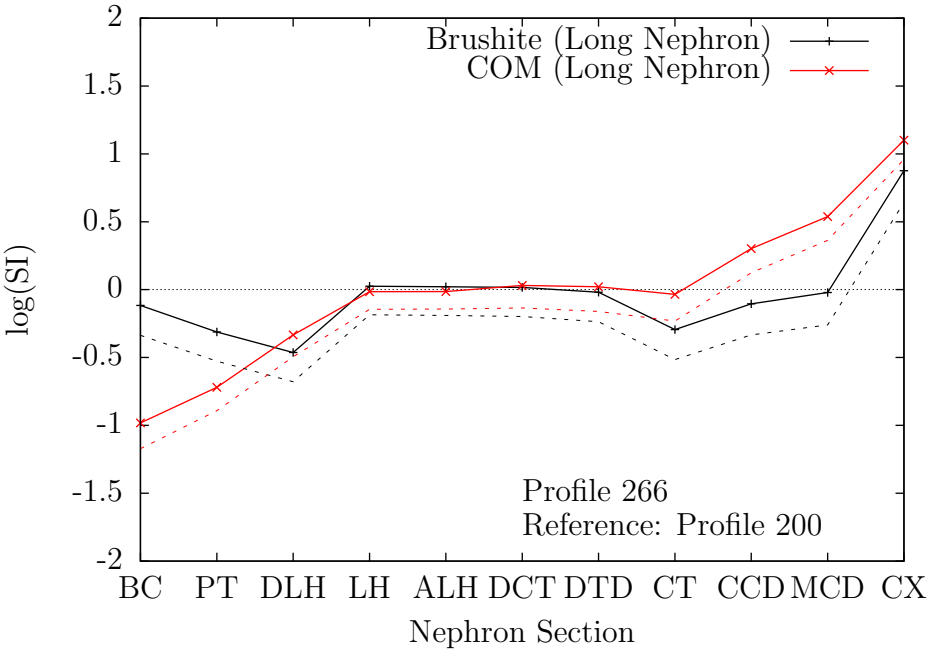

Figure F.20: Profile 266: log(SI) Brushite and COM Long Nephron

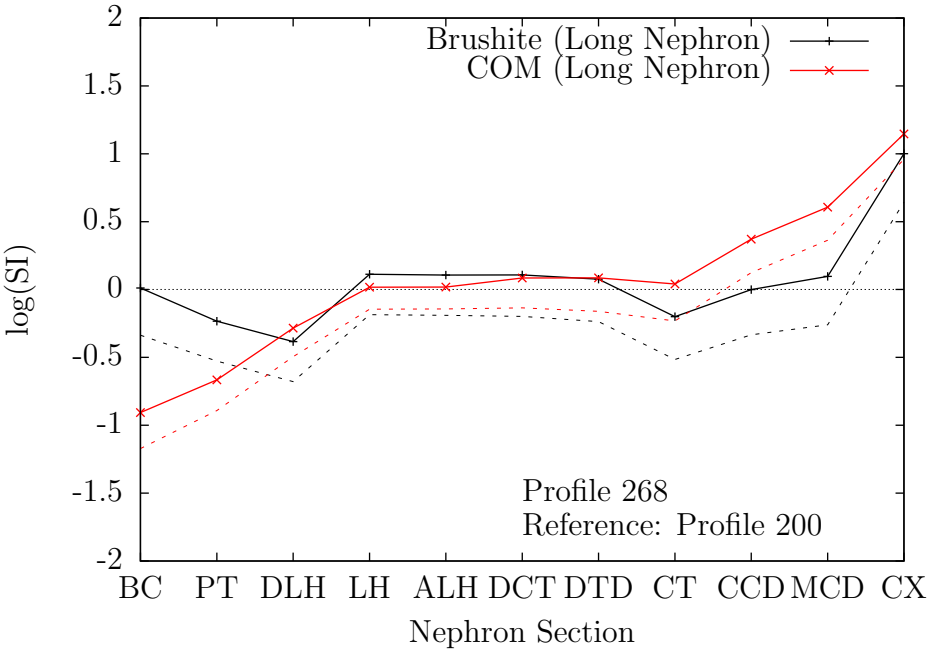

Figure F.21: Profile 268: log(SI) Brushite and COM Long Nephron

Profile 270

P200 + P70 (Low phosphate)

CaP values are reduced all along the nephron.

There is a very small increase in the CaOx values all along the nephron.

Profile 274

P200 + P74 (High phosphate)

High PO_4: 2.5 mmol/L instead of the normal value of 1.5 mmol/L.

CaP values are increased all along the nephron, but the difference with respect to Profile 200 becomes smaller at the end of the nephron. Brushite is (only just) supersaturated in the loop of Henle and also supersaturated in the MCD.

CaOx risk slightly lower from ALH onwards with higher phosphate.

Profile 275

P200 + P75 (High phosphate)

At a PO_4 value of 3.0 mmol/L brushite supersaturation is higher in the middle of the nephron than in P274. Brushite is supersaturated in the CCD and MCD. COM as for P274.

Profiles 280 and 281

P200 + P80, P81 (Low oxalate)

CaP - no difference. CaOx - lower all along the nephron.

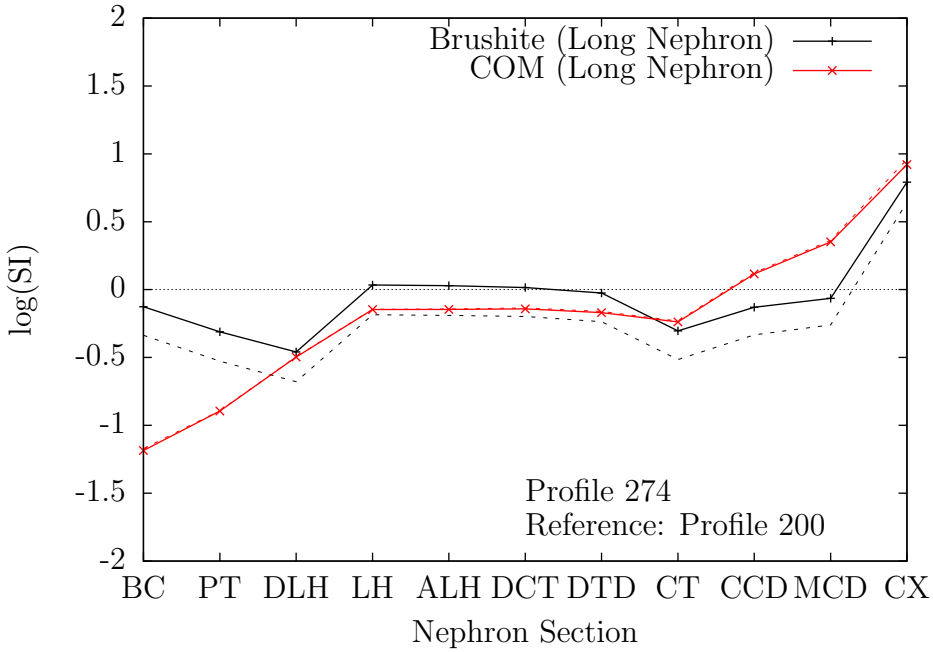

Figure F.22: Profile 274: log(SI) Brushite and COM Long Nephron

Profile 283 and 284

P200 + P83, P84 (High oxalate)

CaP - no difference. CaOx - higher all along the nephron. COM supersaturated from CT onwards.

Profile 285

P200 + P85 (High oxalate)

COM becomes supersaturated in the TDL, falls below supersaturation in the DT and then reaches it in the CT and maintains it to the end of the nephron.

Profile 286

P200 + P86 (High oxalate)

COM is supersaturated from the TDL.

Profile 289

P200 + P89 (High oxalate 10.0 μmol/L)

COM becomes supersaturated in the PR.

Profile 290

P200 + P90 (Low sulfate: 0.2 mmol/L. Normal value: 0.35 mmol/L)

Insignificant increase of risk in MCD for CaP and CaOx.

Profile 291 and 292

P200 + P91, P92 (High sulfate) (0.5 mmol/L and 0.95 mmol/L)

There is a lowering of values for both CaP and CaOx by the plasma sulfate increase.

Profile 293

Plasma Sulfate 1.75 mmol/L.

With high sulfate, risk is lowered all along, with the effect increasing after DT for both CaP and CaOx.

Profile 296

Lower Mg.

Value is slightly lower for CaP from DT onwards. CaOx value is slightly higher PT to LH, but converges after CT.

Profile 298

Higher Mg reduces CaOx risk slightly. Little effect on CaP risk.

Profiles 301 to 3XX:

Combinations of Risk Factors

Profile 301

P2+P66+P73+P87+P96

High ADH (80)

High Calcium (3.0)

High Phosphate (2.0)

High Oxalate (4.0)

Low Magnesium (0.01)

Increases CaP and CaOx values all the way along. Brushite is above supersaturation in the ascending loop of Henle and DT in the long nephron, and in the ascending loop of Henle in the short nephron. Brushite is highly supersaturated in the MCD. COM is supersaturated from the end of the proximal

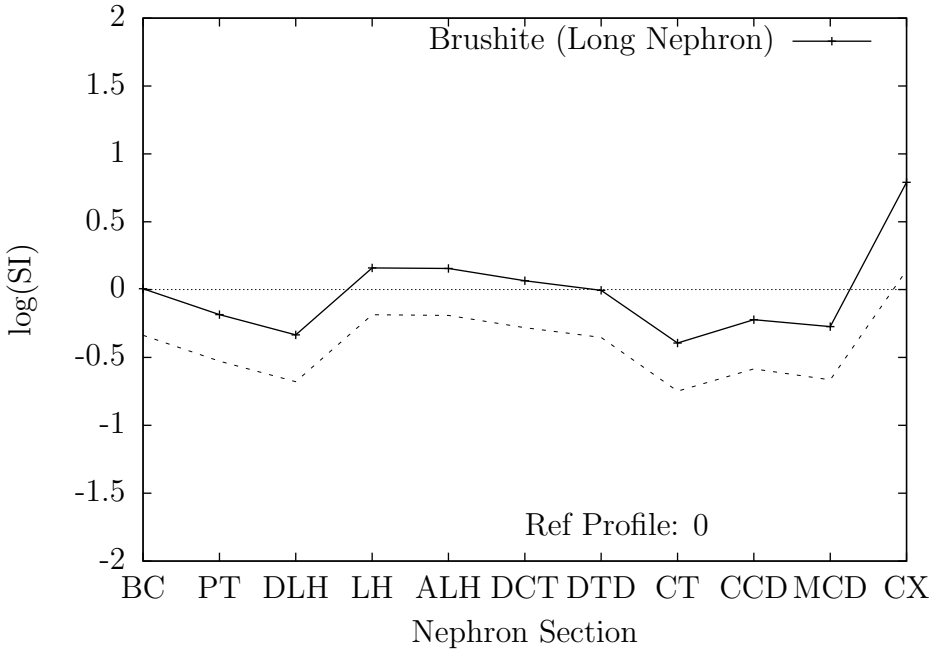

Figure F.23: Profile 301: log(SI) Brushite Long Nephron

tubule, becoming highly supersaturated in the CD.

Profile 311

P100+P2+P66+P73+P87+P96

High ADH

High Calcium (3.0)

High Phosphate (2.0)

High Oxalate (4.0)

Low Magnesium (0.01)

CaP and CaOx values are higher all the way along the nephron, in comparison to Profile 100. Brushite is as for Profile 301. COM follows the same pattern

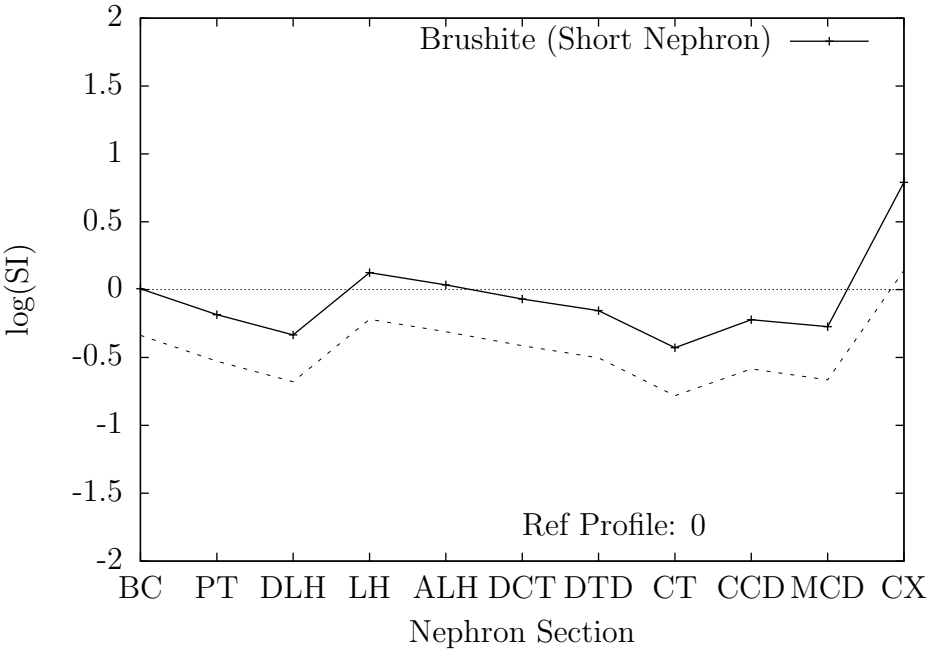

Figure F.24: Profile 301: log(SI) Brushite Short Nephron

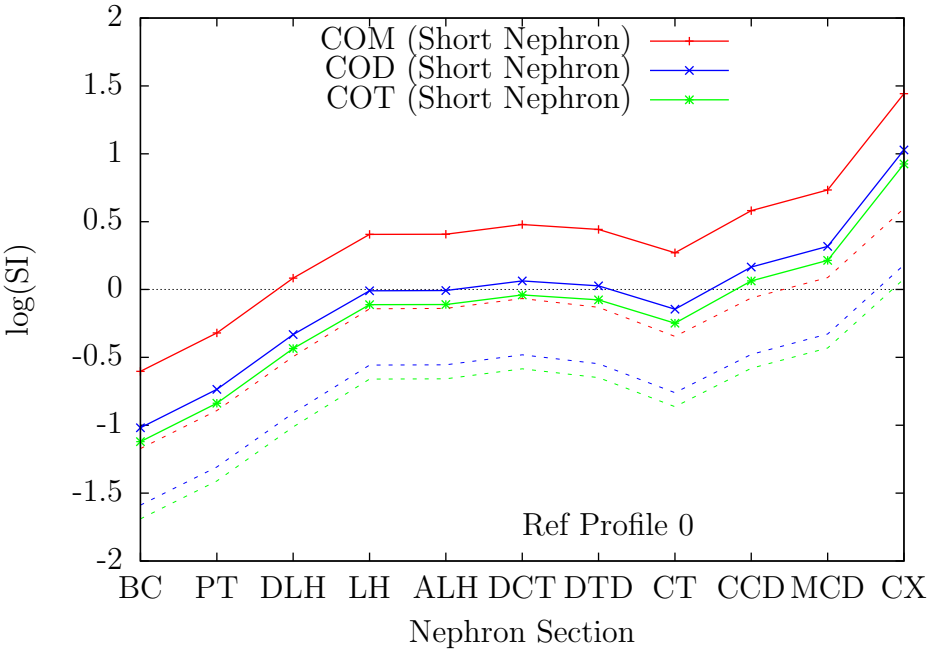

Figure F.25: Profile 301: log(SI) Calcium Oxalates Short Nephron

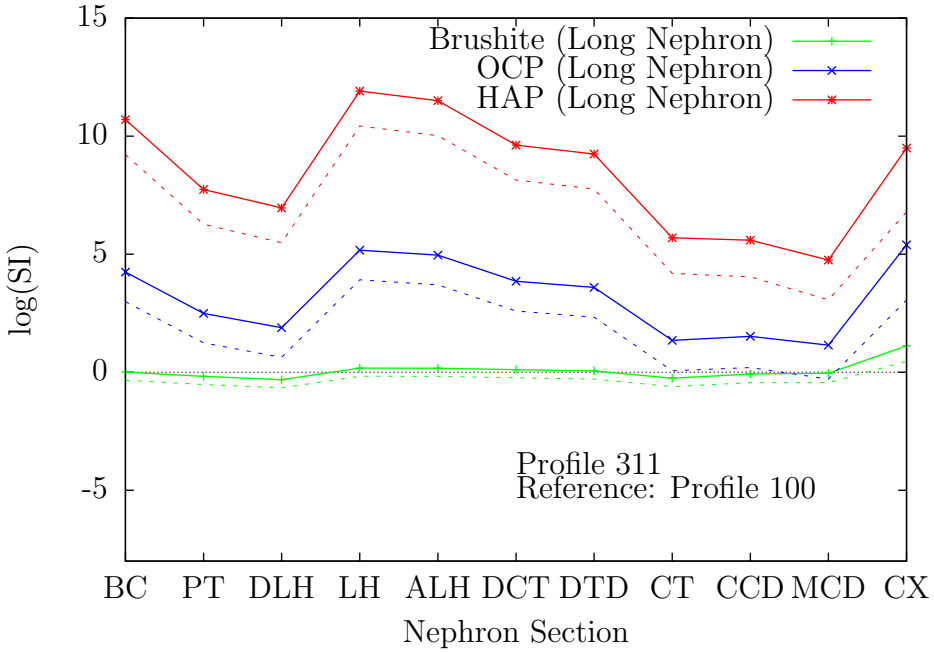

Figure F.26: Profile 311: log(SI) Calcium Phosphates Long Nephron

as in Profile 301. Brushite is supersaturated in the LH and DT, as well as in the CD. COM is supersaturated from the end of the PT onwards.

Profile 321

P200+P2+P66+P73+P87+P96

High ADH

High Calcium (3.0)

High Phosphate (2.0)

High Oxalate (4.0)

Low Magnesium (0.01)

The same pattern as in Profiles 301 and 311. Bru > 0 in mid-nephron. Com-

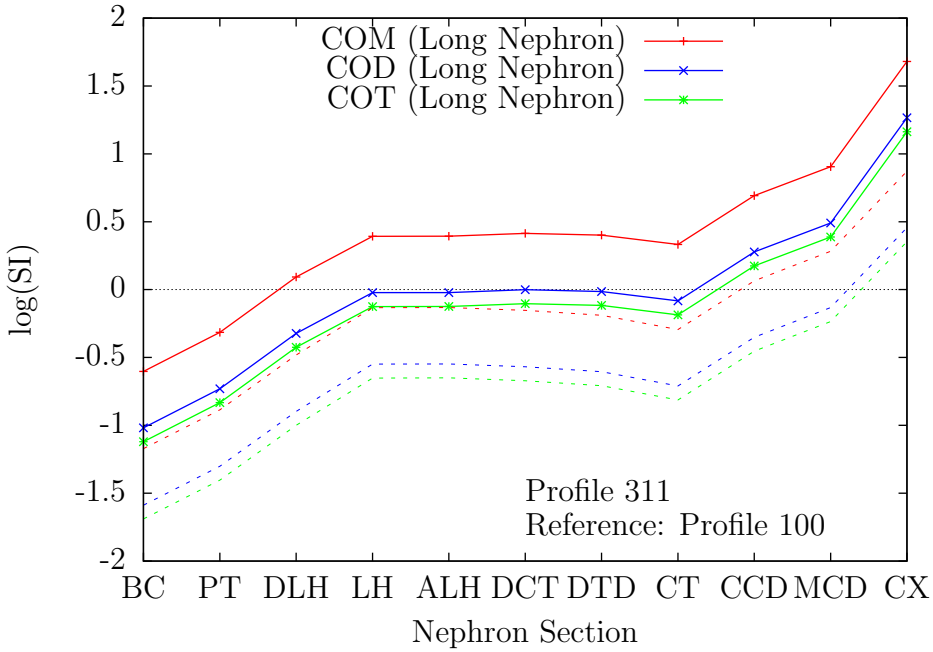

Figure F.27: Profile 311: log(SI) Calcium Oxalates Long Nephron

pared to Profile 311, the supersaturation values for the calcium phosphates and calcium oxalates are higher from the DT.

Profile 331

P66+P86+P97

High Calcium (3.0)

High Oxalate (3.0)

Low Magnesium (0.1)

Calcium oxalate values are increased more than calcium phosphate values, compared to Profile 0.

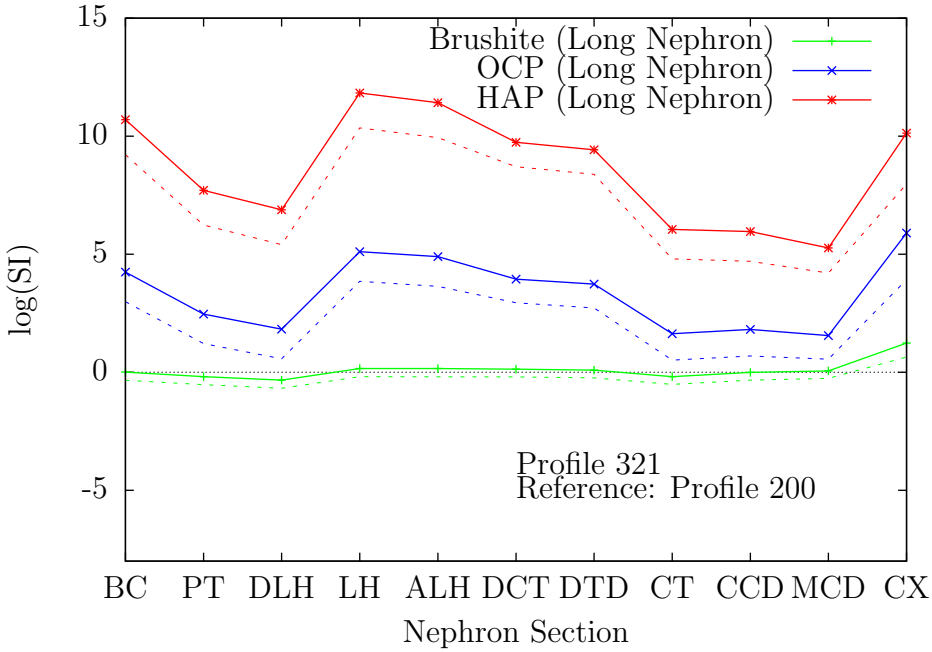

Figure F.28: Profile 321: log(SI) Calcium Phosphates Long Nephron

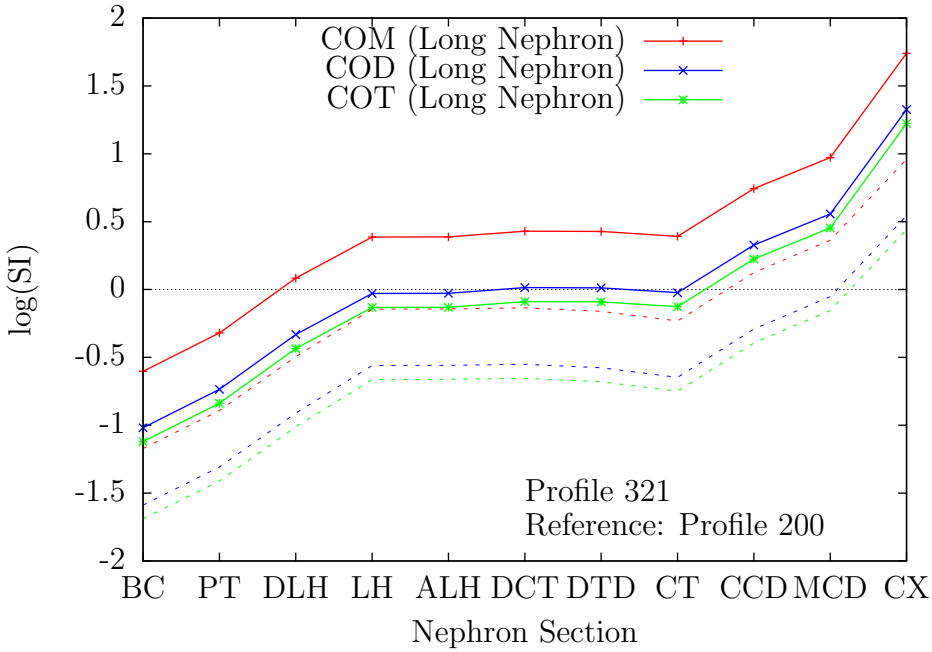

Figure F.29: Profile 321: log(SI) Calcium Oxalates Long Nephron

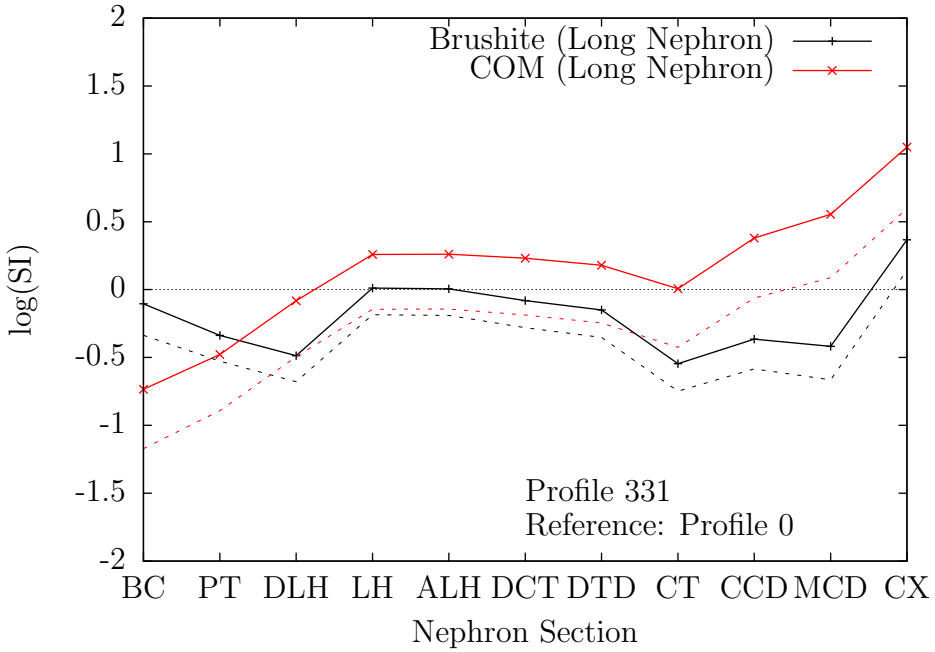

Figure F.30: Profile 331: log(SI) Brushite and COM Long Nephron

Profile 341

P100+P66+P86+P97

High Calcium (3.0)

High Oxalate (3.0)

Low Magnesium (0.1)

Compared to Profile 331, Bru only just > 0 in long mid-nephron. CaP and CaOx increasingly higher from LH.

Profile 351

P200+P66+P87+P97

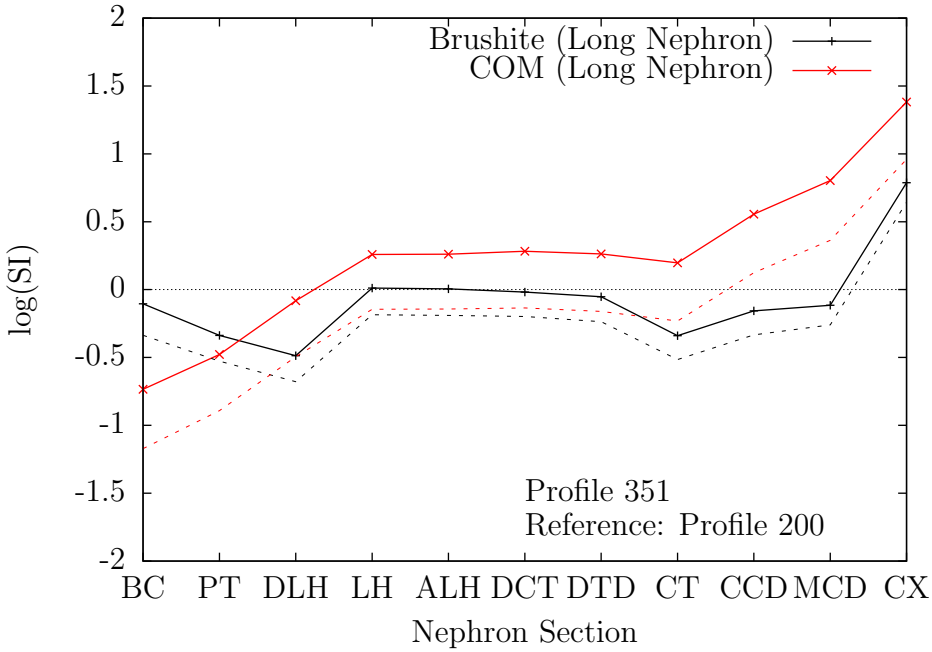

Figure F.31: Profile 351: log(SI) Brushite and COM Long Nephron

High Calcium (3.0)

High Oxalate (4.0)

Low Magnesium (0.1)

Compared to Profile 331, Bru only just > 0 in long LH. CaP and CaOx increasingly higher from DT.

F.4 Profiles 400 to 468: Increased Blood Urate

Normal urate value: 0.25 mmol/L

Increased urate levels used are those shown in Table D.6.

Profile 400

Blood Urate: 0.38 mmol/L (Normal Value: 0.25 mmol/L)

Increased urate makes no significant difference to the values for CaP and CaOx.

The supersaturation of sodium urate is increased in those nephron section where it is supersaturated under normal conditions (Profile 0).

Uric acid becomes only just supersaturated at the end of the nephron.

Profile 401

Blood Urate: 0.49 mmol/L

Similar to P400, but with uric acid more supersaturated at the end of the nephron.

Profile 431 : P401 + low pH

Uric acid becomes supersaturated at the end of the DT. High Urate + low pH needed to cause UA risk.

The supersaturation of sodium urate is increased.

Profile 438 : P401 + high pH

Uric acid remains undersaturated. High pH removes risk

Profile 441 : Hyponatremia

P400 + P41

The supersaturation of uric acid is decreased slightly at the end of the nephron.

The supersaturation of sodium urate is decreased slightly all along.

Profile 442 : Hyponatremia with Hormonal Response

P400 + P42

The decrease in supersaturation for uric acid is slightly less than in the case of P441. The same pattern for sodium urate as in P441, but the decrease in log(SI) value is lower.

Profile 445 : Hypernatremia

P400 + P45

Plasma sodium concentration 180 mmol/L [14Cha].

The supersaturation of sodium urate is increased.

The supersaturation of uric acid is increased slightly at the end of the nephron.

Profile 446 : Hypernatremia with Hormonal Response

P400 + P46

Increased plasma Na will increase levels of ADH ANP and decrease levels of ALD

P445 + ADH 75 ANP 75 ALD 40

The supersaturation of uric acid is increased at the end of the nephron.

Profile 468

Blood Urate: 0.49 mmol/L

Plasma calcium 3.0

No difference for uric acid.

Profile 511 to 513 : Specified Urine Concentrations

Profiles in the 500 range use an alternative mode of operation of the model that allows both the concentration of blood plasma and urine to be entered. Profiles 511, 512 and 513 use data from Robertson (2015) [15Rob]. Profile 511 contains the data set for the normal subjects, 512 represents the recurrent stone formers from the United Kingdom and 513 the recurrent stone formers from the Kingdom of Saudi Arabia.

References

[32HaJ] Hayman J and Johnston SM. The excretion of inorganic sulphates. *Journal of Clinical Investigation*, 1932. 11(3), 607–619.

[32Med] Medes G. Solubility of calcium oxalate and uric acid in solutions of urea. *Experimental Biology and Medicine*, 1932. 30(3), 281–284.

[58MVM] Miller GH, Vermeulen CW, and Moore JD. Calcium oxalate solubility in urine: Experimental urolithiasis XIV. *The Journal of Urology*, 1958. 79(3), 607–612.

[62Dav] Davies C. *Ion Association*. Butterworths, London, 1962.

[67ElE] Elliot JS and Eusebio E. Calcium oxalate solubility: The effect of trace metals. *Investigative Urology*, 1967. 4(5), 428–430.

[67LLL] Lemann J, Litzow JR, Lennon EJ, and Kelly OA. Studies of the mechanism by which chronic metabolic acidosis augments urinary calcium excretion in man. *Journal of Clinical Investigation*, 1967. 46(8), 1318–1328.

[68BDS] Bell GH, Davidson JN, and Scarborough H. *Textbook of Physiology and Biochemistry*. E and S Livingstone Ltd, Edinburgh and London, 7th edition, 1968.

[69Pak] Pak CYC. Physicochemical basis for formation of renal stones of calcium phosphate origin: Calculation of the degree of saturation of urine with respect to brushite. *The Journal of Clinical Investigation*, 1969. 48, 1914–1922.

[69Rob] Robertson W. Measurement of ionized calcium in biological fluids. *Clinica Chimica Acta*, 1969. 24, 149–157.

[70Gei] Diem K and Lentner C (Eds.) *Documenta Geigy Scientific Tables*. JR Geigy SA, Basle, 7th edition, 1970.

[71MBR] Mrochek JE, Butts WC, Rainey WT, and Burtis CA. Separation and identification of urinary constituents by use of multiple-analtical techniques. *Clinical Chemistry*, 1971. 17(2), 72–77.

[76PaH] Pak CYC and Holt K. Nucleation and growth of brushite and calcium oxalate in urine of stone-formers. *Metabolism*, 1976. 25, 665–673.

[76RoN] Robertson W and Nordin B. Physico-chemical factors governing stone formation. In DI Williams and GD Chisholm (Eds.) *Scientific Foundations of Urology*, chapter 37, 254–267. Heinemann Medical, London, 1976.

[77Fan] Fanelli GM. Urate excretion. *Annual Review of Medicine*, 1977. 28, 349–354.

[77Fin] Finlayson B. Calcium stones: Some physical and clinical aspects. In DS David (Ed.) *Calcium Metabolism in Renal Failure and Nephrolithiasis*, chapter 10, 337–382. Wiley and Sons, New York, 1977.

[77FlR] Fleisch H and Russell GG. Experimental and clinical studies with pyrophosphate and diphosphonates. In DS David (Ed.) *Calcium Metabolism in Renal Failure and Nephrolithiasis*, chapter 9, 293–336. Wiley and Sons, New York, 1977.

[77Met] Metzler DE. *Biochemistry: The Chemical Reactions of Living Cells*. Academic Press, New York, 1977.

[78Fin] Finlayson B. Physicochemical aspects of urolithiasis. *Kidney International*, 1978. 13, 344–360.

[78MaH] Mayer GP and Hurst JG. Sigmoidal relationship between parathyroid hormone secretion rate and plasma concentration in calves. *Endocrinology*, 1978. 109(4), 1036 – 1042.

[78Wil] Williams HE. Oxalic acid and the hyperoxaluric syndromes. *Kidney International*, 1978. 13, 410–417.

[79SWD] Sutton RAL, Wong NLM, and Dirks JH. Effects of metabolic acidosis and alkalosis on sodium and calcium transport in the dog kidney. *Kidney International*, 1979. 15, 520–533.

[80Hod] Hodgkinson A. Solubility of calcium oxalate in human urine, simulated urine, and water. *Investigative Urology*, 1980. 18(2), 123–126.

[80ToN] Tomazic BB and Nancollas GH. The kinetics of dissolution of calcium oxalate hydrates. *Investigative Urology*, 1980. 18(2), 97–101.

[81BDF] Backman U, Danielson BG, Fellström B, Johansson G, Ljunghall S, and Wikström B. The clinical importance of renal tubular acidosis in recurrent renal stone formers. In LH Smith, WG Robertson, and B Finlayson (Eds.) *Urolithiasis: Clinical and Basic Research*, 67–69. Plenum Press, New York, 1981.

[81Pak] Pak CYC. Potential etiologic role of brushite in the formation of calcium (renal) stones. *Journal of Crystal Growth*, 1981. 53, 202–208.

[81RSB] Robertson WG, Scurr DS, and Bridge CM. Factors influencing the crystallisation of calcium oxalate in urine - critique. *Journal of Crystal Growth*, 1981. 53, 182–194.

[81Tis] Tiselius HG. Urinary excretion of citrate in normal subjects and patients with urolithiasis. In LH Smith, WG Robertson, and B Finlayson (Eds.) *Urolithiasis: Clinical and Basic Research*, 39–44. Plenum Press, New York, 1981.

[82MFB] Marangella M, Fruttero B, and Linari F. Hyperoxaluria in idiopathic calcium stone disease: further evidence of intestinal hyperabsorption of oxalate. *Clinical Science*, 1982. 63, 381–385.

[82SoK] Sohtell M and Karlmark B. Thermodynamical aspects on the determination of bicarbonate in urine. *Upsala Journal of Medical Sciences*, 1982. 87, 151–161.

[82DeS] de Vries A and Sperling O. Uric acid stone formation: Concepts of aetiology and treatment. In GD Chisholm and DI Williams (Eds.) *Scientific Foundations of Urology*, chapter 39, 308–314. London Heinemann Medical, second edition, 1982.

[84NTM] Nath R, Thind SK, Murthy MSR, Talwar HS, and Farooqui S. Molecular aspects of idiopathic urolithiasis. *Molecular Aspects of Medicine*, 1984. 7, 1–176.

[84SmW] Smith L and Werness P. Hydroxyapatite–the forgotten crystal in calcium urolithiasis. *Transactions of the American Clinical and Climatological Association*, 1984. 95, 183–190.

[85GoK] Good DW and Knepper MA. Ammonia transport in the mammalian kidney. *American Journal of Physiology*, 1985. 248, F459–F471.

[85WBS] Werness PG, Brown CM, Smith LH, and Finlayson B. EQUIL2: A BASIC computer program for the calculation of urinary saturation. *The Journal of Urology*, 1985. 134, 1242–1244.

[86HCK] Hesse A, Classen A, Knoll M, Timmermann F, and Vahlensieck W. Dependence of urine composition on the age and sex of healthy subjects. *Clinica Chimica Acta*, 1986. 160, 79–86.

[86LiL] Linder PW and Little JC. Prediction by computer modelling of the precipitation of stone-forming solids from urine. *Inorganica Chimica Acta*, 1986. 123, 137–145.

[86Ros] Rose GA. Medical investigation and treatment of urinary stones: a search for new ideas. *Clinica Chimica Acta*, 1986. 160, 109–115.

[87ITT] Imai M, Taniguchi J, and Tabei K. Function of thin loops of Henle. *Kidney International*, 1987. 31, 565–579.

[87LeK] Lemley KV and Kriz W. Cycles and separations: The histotopography of the urinary concentrating process. *Kidney International*, 1987. 31, 538–548.

[89LGP] Lemann J, Gray RW, and Pleuss JA. Potassium bicarbonate, but not sodium bicarbonate, reduces urinary calcium excretion and improves calcium balance in healthy men. *Kidney International*, 1989. 35, 688–695.

[90BuL] Buck AC and Lote CJ. The renal handling of calcium. In JEA Wickham and AC Buck (Eds.) *Renal Tract Stone*, chapter 12, 165–182. Churchill Livingstone, Edinburgh, 1990.

[90CBK] Canzanello VJ, Bodvarsson M, Kraut JA, Johns CA, Slatopolsky E, and Madias NE. Effect of chronic respiratory acidosis on urinary calcium excretion in the dog. *Kidney International*, 1990. 38, 409–416.

[90CRG] Conte A, Roca P, Gianotti M, and Grases F. On the relation between citrate and calcium in normal and stone-former subjects. *International Urology and Nephrology*, 1990. 22(1), 7–12.

[90FKH] Finlayson B, Khan SR, and Hackett RL. Theoretical chemical models of urinary stones. In JEA Wickham and AC Buck (Eds.) *Renal Tract Stone*, chapter 10, 133–147. Churchill Livingstone, Edinburgh, 1990.

[90Ham] Hamm L. Renal handling of citrate. *Kidney International*, 1990. 38, 728–735.

[90KuM] Kumar S and Muchmore A. Tamm-Horsfall protein–uromodulin (1950–1990). *Kidney International*, 1990. 37, 1395–1401.

[90Lan] Lang F. Renal handling of oxalate, urate, citrate, phosphate and sulphate. In JEA Wickham and AC Buck (Eds.) *Renal Tract Stone*, chapter 13, 183–213. Churchill Livingstone, Edinburgh, 1990.

[90Nan] Nancollas GH. Physical chemistry of crystal nucleation, growth and dissolution of stones. In JEA Wickham and AC Buck (Eds.) *Renal Tract Stone*, chapter 6, 71–85. Churchill Livingstone, Edinburgh, 1990.

[91GAB] Gutzow I, Atanassova S, and Budevsky G. Kinetics of dissolution of calcium oxalate calculi in physiological solutions containing hippuric acid. *Crystal Research and Technology*, 1991. 26(5), 533–554.

[91MaM1] May PM and Murray K. JESS, A Joint Expert Speciation System - I. Raison d'être. *Talanta*, 1991. 38(12), 1409–1417.

[92BrP] Brown CM and Purich DL. Physical-chemical processes in kidney stone formation. In FL Coe and MJ Favus (Eds.) *Disorders of Bone and Mineral Metabolism*, chapter 29, 613–624. Raven Press Ltd, New York, 1992.

[92CPN] Coe FL, Parks JH, and Nakagawa Y. Inhibitors and promoters of calcium oxalate crystallization. their relationship to the pathogenesis and treatment of nephrolithiasis. In FL Coe and MJ Favus (Eds.) *Disorders of Bone and Mineral Metabolism*, chapter 35, 757–799. Raven Press Ltd, New York, 1992.

[92JoN] Johnsson MSA and Nancollas GH. The role of brushite and octacalcium phosphate in apatite formation. *Critical Reviews in Oral Biology and Medicine*, 1992. 3(1/2), 61–82.

[92YaL] Yanagawa N and Lee D. Renal handling of calcium and phosphate. In FL Coe and MJ Favus (Eds.) *Disorders of Bone and Mineral Metabolism*, chapter 1, 3–40. Raven Press Ltd, New York, 1992.

[93DBJ] Daudon M, Bader CA, and Jungers P. Urinary calculi: Review of classification methods and correlations with etiology. *Scanning Microscopy*, 1993. 7(3), 1081–1106.

[93FrG] Friedman PA and Gesek FA. Calcium transport in renal epithelial cells. *American Journal of Physiology*, 1993. 264, F181–F 198.

[93GAB] Gutzow I, Atanassova S, Budevsky G, and Neykov K. Solubility, inhibited growth and dissolution kinetics of calcium oxalate crystals in solutions, containing hippuric acid. *Urological Research*, 1993. 21, 181–185.

[93LNC] Lehninger AL, Nelson DL, and Cox MM. *Principles of Biochemistry*. Worth Publishers, New York, 2nd edition, 1993.

[94BAP] Brown C, Ackermann D, and Purich D. EQUIL93: a tool for experimental and clinical urolithiasis. *Urological Research*, 1994. 22, 119–126.

[94KoK] Kok DJ and Khan SR. Calcium oxalate nephrolithiasis, a free or fixed particle disease. *Kidney International*, 1994. 46, 847–854.

[94LBF] Luptak J, Bek-Jensen H, Fornander AM, Højgaard I, Nilsson MA, and Tiselius H. Crystallization of calcium oxalate and calcium phosphate at superstauration levels corresponding to those in different parts of the nephron. *Scanning Microscopy*, 1994. 8(1), 47–62.

[95SoG] Söhnel O and Grases F. Calcium oxalate monohydrate renal calculi. Formation and development mechanism. *Advances in Colloid and Interface Science*, 1995. 59, 1–17.

[95TaW] Taylor DM and Williams DR. *Trace Element Medicine and Chelation Therapy*. The Royal Society of Chemistry, Cambridge, 1995.

[96AMC] Asplin JR, Mandel NS, and Coe FL. Evidence for calcium phosphate supersaturation in the loop of Henle. *American Journal of Physiology*, 1996. 270(4-2), F604–F613.

[96DCM] Delatte LC, Cifuentes JM, and Medina JA. Randall and his plaque. *Urology*, 1996. 48(3), 343–346.

[96ZRW] Zimmerhackl L, Rostasy K, Wiegele G, Rasenack A, Wilhelm C, Lohner M, Brandis M, and Kinne R. Tamm-Horsfall protein as a marker of tubular maturation. *Pediatric Nephrology*, 1996. 10(4), 448–452.

[97BrK] Brooks T and Keevil C. A simple artificial urine for the growth of urinary pathogens. *Letters in Applied Microbiology*, 1997. 24, 203–206.

[97GVS] Grases F, Villacampa AI, Söhnel O, Königsberger E, and May PM. Phosphate composition of precipitates from urine-like liquors. *Crystal Research and Technology*, 1997. 32(5), 707–715.

[97GPS] Grenthe I, Plyasunow AV, and Spahiu K. Modelling in aquatic chemistry. In I Grenthe and I Puigdomènech (Eds.) *Modelling in Aquatic Chemistry*, chapter IX, 325–426. Nuclear Energy Agency, Organisation for Economic Co-operation and Development, 1997.

[97GuH] Guyton AC and Hall JE. *Human Physiology and Mechanisms of Disease*. WB Saunders Company, Philadelphia, 6th edition, 1997.

[97HCK] Hallson PC, Choong SK, Kasidas GP, and Samuell CT. Effects of Tamm-Horsfall Protein with normal and reduced sialic acid content upon the crystallization of calcium phosphate and calcium oxalate in human urine. *British Journal of Urology*, 1997. 80(4), 533–538.

[97Kok] Kok DJ. Intratubular crystallization events. *World Journal of Urology*, 1997. 15, 219–228.

[97KoT] Königsberger E and Tran-Ho LC. Solubility of substances related to urolithiasis - experiments and computer modelling. *Current Topics in Solution Chemistry*, 1997. 2, 183–202.

[97PCC] Parks JH, Coward M, and Coe FL. Correspondence between stone composition and urine supersaturation in nephrolithiasis. *Kidney International*, 1997. 51, 894–900.

[97RNN] Romero MC, Nocera S, and Nesse AB. Decreased Tamm-Horsfall Protein in lithiasic patients. *Clinical Biochemistry*, 1997. 30(1), 63–67.

[97Saw] Sawada K. The mechanisms of crystallization and transformation of calcium carbonates. *Pure and Applied Chemistry*, 1997. 69(5), 921–928.

[97Tis] Tiselius HG. Estimated levels of supersaturation with calcium phosphate and calcium oxalate in the distal tubule. *Urological Research*, 1997. 25, 153–159.

[98GCG] Grases F, Costa-Bauzá A, and Garcia-Ferragut L. Biopathological crystallization: a general view about the mechanisms of renal stone formation. *Advances in Colloid and Interface Science*, 1998. 74, 169–194.

[98MSG] March JG, M SB, Grases F, and Salvador A. Indirect determination of phytic acid in urine. *Analytica Chimica Acta*, 1998. 367, 63–68.

[98MBB] Milosevic D, Batinic D, Konjevoda NBP, Stambuk N, Votava-Raic A, Fumic VBK, Rumenjak V, Stavljenic-Rukavina A, Nizic L, and Vrljicak K. Determination of urine supersaturation with computer program Equil 2 as a method for estimation of the risk of urolithiasis. *Journal of Chemical Information and Computer Sciences*, 1998. 38, 646–650.

[98Pak] Pak CYC. Kidney stones. *The Lancet*, 1998. 351, 1797–1801.

[98STK] Streit J, Tran-Ho LC, and Königsberger E. Solubility of the three calcium oxalate hydrates in sodium chloride solutions and Urine-like liquors. *Monatshefte für Chemie*, 1998. 129, 1225–1236.

[98WEA] Wang T, Egbert AL, Aronson PS, and Giebish G. Effect of metabolic acidosis on NaCl transport in the proximal tubule. *American Journal of Physiology*, 1998. 274, F1015–F1019.

[99ABG] Ashby RA, Byrne JP, and György AZ. Urine is a saturated equilibrium and not a metastable supersaturated solution: evidence from crystalluria and the general composition of calcium salt and uric acid calculi. *Urological Research*, 1999. 27, 297–305.

[99APC] Asplin JR, Parks JH, Chen MS, Lieske JC, Toback FG, Pillay S, Nakagawa Y, and Coe FL. Reduced crystallization inhibition by urine from men with nephrolithiasis. *Kidney International*, 1999. 56, 1505–1516.

[99GSC] Grases F, Söhnel O, and Costa-Bauzá A. Renal stone formation and development. *International Urology and Nephrology*, 1999. 31(5), 591–600.

[99HoT] Højgaard I and Tiselius HG. Crystallization in the nephron. *Urological Research*, 1999. 27, 397–403.

[99Ker] Kerr J. *Atlas of Functional Histology.* Mosby, London, 1999.

[00GHJ] Glauser A, Hochreiter W, Jaeger P, and Hess B. Determinants of urinary excretion of Tamm-Horsfall protein in non-selected kidney stone formers and healthy subjects. *Nephrology Dialysis Transplantation*, 2000. 15, 1580–1587.

[00GCK] Grases F, Costa-Bauzá A, Königsberger E, and Königsberger LC. Kinetic versus thermodynamic factors in calcium renal lithiasis. *International Urology and Nephrology*, 2000. 32, 19–27.

[00GMP] Grases F, March JG, Prieto RM, Simonet BM, Costa-Bauzá A, García-Raja A, and Conte A. Urinary phytate in calcium oxalate stone formers and healthy people. *Scandinavian Journal of Urology and Nephrology*, 2000. 34, 162–164.

[00GuH] Guyton AC and Hall JE. *Textbook of Medical Physiology.* WB Saunders Company, Philadelphia, 10th edition, 2000.

[00KWK] Königsberger E, Wang Z, and Königsberger LC. Solubility of L-Cystine in NaCl and Artificial Urine Solutions. *Monatshefte für Chemie*, 2000. 131, 39–45.

[00LSH] Laube N, Schneider A, and Hesse A. A new approach to calculate the risk of calcium oxalate crystallization from unprepared native urine. *Urological Research*, 2000. 28, 274–280.

[00May] May PM. A simple, general and robust function for equilibria in aqueous electrolyte solutions to high ionic strength and temperature. *Chemical Communications*, 2000. 1265–1266.

[01BeS] Beck L and Silve C. Molecular aspects of renal tubular handling and regulation of inorganic sulfate. *Kidney International*, 2001. 59, 835 – 845.

[01GSV] Grases F, Simonet BM, Vucenik I, Prieto RM, Costa-Bauzá A, March JC, and Shamsuddin AM. Absorption and excretion of orally administered inositol hexaphosphate (IP_6 or phytate) in humans. *BioFactors*, 2001. 15, 53–61.

[01Kav] Kavanagh J. A critical appraisal of the hypothesis that urine is a saturated equilibrium with respect to stone-forming calcium salts. *BJU International*, 2001. 87, 589–598.

[01LGH] Laube N, Glatz S, and Hesse A. The relation of urinary Tamm-Horsfall-Protein on CaOx-crystallization under the scope of the Bonn-Risk-Index. *Urological Research*, 2001. 29, 45–49.

[02BGS] Barbas C, García A, Saavedra L, and Muros M. Urinary analysis of nephrolithiasis markers. *Journal of Chromatography B*, 2002. 781, 433–455.

[02GCR] Grases F, Costa-Bauzá A, Ramis M, Montesinos V, and Conte A. Simple classification of renal calculi closely related to their micromorphology and etiology. *Clinica Chimica Acta*, 2002. 322, 29–36.

[02Kok] Kok DJ. Clinical implications of physicochemistry of stone formation. *Endocrinology Metabolism Clinics of North America*, 2002. 31, 855–867.

[03ELC] Evan AP, Lingeman JE, Coe FL, Parks JH, Bledsoe SB, Shao Y, Sommer AJ, Paterson RF, Kuo RL, and Grynpas M. Randall's plaque of patients with nephrolithias begins in basement membranes of thin loops of Henle. *The Journal of Clinical Investigation*, 2003. 111, 607–616.

[03Sch] Scheinman SJ. Urinary calculi. *Medicine*, 2003. 31(6), 77–80.

[04KYY] Kato Y, Yamaguchi S, Yachiku S, Nakazono S, Hori JI, Wada N, and Hou K. Changes in urinary parameters after oral administration of potassium-sodium citrate and magnesium oxide to prevent urolithiasis. *Adult Urology*, 2004. 63, 7–12.

[04MHZ] Mo L, Huang HY, Zhu XH, Shapiro E, Hasty DL, and Wu XR. Tamm-Horsfall protein is a critical renal defense factor protecting against calcium oxalate crystal formation. *Kidney International*, 2004. 66, 1159–1166.

[04Rob] Robertson WG. Kidney models for calcium oxalate stone formation. *Nephron Physiology*, 2004. 98, 21–30.

[04SJH] Siener R, Jahnen A, and Hesse A. Influence of a mineral water rich in calcium, magnesium and bicarbonate on urine composition and the risk of calcium oxalate crystallization. *European Journal of Clinical Nutrition*, 2004. 58, 270–276.

[05Abd] Abdel-Halim R. Urolithiasis in adults: Clinical and biochemical aspects. *Saudi Medical Journal*, 2005. 26(5), 705–713.

[05AlR] Allie-Hamdulay S and Rodgers A. Prophylactic and therapeutic properties of a sodium citrate preparation in the management of calcium oxalate urolithiasis: randomized, placebo-controlled trial. *Urological Research*, 2005. 33, 116–124.

[05CJR] Capasso G, Jaeger P, Robertson WG, and Unwin RJ. Uric acid and the kidney: Urate transport, stone disease and progressive renal failure. *Current Pharmaceutical Design*, 2005. 11, 4153–4159.

[05CEW] Coe FL, Evan A, and Worcester E. Kidney stone disease. *The Journal of Clinical Investigation*, 2005. 115(10), 2598–2608.

[05DDP] Devuyst O, Dahan K, and Pirson Y. Tamm-Horsfall protein or uromodulin: new ideas about an old molecule. *Nephrology Dialysis Transplantation*, 2005. 20, 1290–1294.

[05ThH] Thomas B and Hall J. Urolithiasis. *Surgery*, 2005. 23(4), 129–133.

[06Ath2] Atherton JC. Function of the nephron and the formation of urine. *Anaesthesia and Intensive Care Medicine*, 2006. 7(7), 221–226.

[06Ath3] Atherton JC. Regulation of fluid and electrolyte balance by the kidney. *Anaesthesia and Intensive Care Medicine*, 2006. 7(7), 227–233.

[06Ath1] Atherton JC. Renal blood flow, glomerular filtration and plasma clearance. *Anaesthesia and Intensive Care Medicine*, 2006. 7(7), 216–220.

[06Ath4] Atherton JC. Role of the kidney in acid-base balance. *Anaesthesia and Intensive Care Medicine*, 2006. 7(7), 234–226.

[06CMA] Cameron MA, Maalouf NM, Adams-Huet B, Moe OW, and Sakhaee K. Urine composition in type 2 diabetes: Predisposition to uric acid nephrolithiasis. *Journal of the American Society of Nephrology*, 2006. 17, 1422–1428.

[06GrC] Grases F and Costa-Bauzá A. Mechanisms of renal and salivary calculi formation and development. In E Königsberger and LC Königsberger (Eds.) *Biomineralization - Medical Aspects of Solubility*, chapter 2, 39–69. Wiley, Chichester, UK, 2006.

[06GuH] Guyton AC and Hall JE. *Textbook of Medical Physiology*. Elsevier Saunders, Philadelphia, 11th edition, 2006.

[06KJA] Knight J, Jaing J, Assimos D, and Holmes R. Hydroxyproline ingestion and urinary oxalate and glycolate excretion. *Kidney International*, 2006. 70, 1929–1934.

[06KoK] Königsberger E and Königsberger LC. Solubility phenomena related to normal and pathological biomineralization processes. In E Königsberger and LC Königsberger (Eds.) *Biomineralization - Medical Aspects of Solubility*, chapter 1, 1–37. Wiley, Chichester, UK, 2006.

[06MMC] Magalhães MCF, Marques PAAP, and Correia RN. Calcium and magnesium phosphates: Normal and pathological mineralization. In E Königsberger and LC Königsberger (Eds.) *Biomineralization - Medical Aspects of Solubility*, chapter 3, 71–123. Wiley, Chichester, UK, 2006.

[06Moe] Moe OW. Kidney stones: pathophysiology and medical management. *The Lancet*, 2006. 367, 333–344.

[06Rob] Robertson WG. Is prevention of stone recurrence financially worthwhile? *Urological Research*, 2006. 34, 157–161.

[06RAJ] Rodgers A, Allie-Hamdulay S, and Jackson G. Therapeutic action of citrate in urolithiasis explained by chemical speciation: increase in pH is the determinant factor. *Nephrology Dialysis Transplantation*, 2006. 21, 361–369.

[07Bas] Bassi P. Stone formation. In M Epple and E Bäuerlein (Eds.) *Handbook of Biomineralization: Biological Aspects and Structure Formation*, chapter 21, 329– 348. Wiley, New York, 2007.

[07Hug] Hughes P. Kidney stones epidemiology. *Nephrology*, 2007. 12, S26–S30.

[07PCC] Pearle MS, Calhoun EA, and Curhan GC. Urolithiasis. In M Litwin and C Saigal (Eds.) *Urologic Diseases in America*, chapter 8, 283–319. US Department of Health and Human Services, Washington, DC, 2007. NIH Publication No. 07-5512.

[07SAR] Saude EJ, Adamko D, Rove BH, Marrie T, and Sykes BD. Variation of metabolites in normal human urine. *Metabolomics*, 2007. 3, 439–451.

[07TaC] Taylor EN and Curhan GC. Differences in 24-hour urine composition between black and white women. *Journal of the American Society of Nephrology*, 2007. 18, 654–659.

[08Ada] Adam WR. Hypothesis: A simple algorithm to distinguish between hypoaldosteronism and renal aldosterone resistance in patients with persistent hyperkalemia. *Nephrology*, 2008. 13, 459–464.

[08CoC] Cobelli C and Carson E. *Introduction to Modeling in Physiology and Medicine*. Academic Press, London, 2008.

[08LRA] Laube N, Rodgers A, Allie-Hamdulay S, and Straub M. Calcium oxalate stone formation risk - a case of disturbed relative concentrations of urinary components. *Clinical Chemistry and Laboratory Medicine*, 2008. 46(8), 1134–1139.

[08MGW] Miller NL, Gillen DL, Williams JC, Evan AP, Bledsoe SB, Coe FL, Worcester EM, Matlaga BR, Munch LC, and Lingeman JE. A formal test of the hypothesis that idiopathic calcium oxalate stones grow on Randalls plaque. *BJU International*, 2008. 103, 966–971.

[08MuM] Murray K and May PM. *JESS Primer*. Murdoch University, Perth, 2008.

[08Pak] Pak CYC. Pharmacotherapy of kidney stones. *Expert Opinion on Pharmacotherapy*, 2008. 9, 1509–1518.

[08PRP] Pak CYC, Rodgers K, Poindexter JR, and Sakhaee K. New methods of assessing crystal growth and saturation of brushite in whole urine: Effect of pH, calcium and citrate. *The Journal of Urology*, 2008. 180(4), 1532–1537.

[08Sho] Shoback D. Hypoparathyroidism. *The New England Journal of Medicine*, 2008. 359(4), 391 – 403.

[09BoB] Boron WF and Boulpaep EL. *Medical Physiology*. Saunders Elsevier, Philadelphia, 2nd edition, 2009.

[09Hye] Hye-Young K. Renal handling of ammonium and acid base regulation. *Electrolytes and Blood Pressure*, 2009. 7, 9–13.

[09Kar] Kardasz S. The function of the nephron and the formation of urine. *Anaesthesia and Intensive Care Medicine*, 2009. 10(6), 265–270.

[09PMR] Pak CYC, Maalouf NM, Rodgers K, and Poindexter JR. Comparison of semi-emperical and computer derived methods for estimating urinary saturation of calcium oxalate. *The Journal of Urology*, 2009. 182, 2951–2956.

[09TLF] Tiselius H, Lindbäck B, Fornander AM, and Nilsson MA. Studies on the role of calcium phosphate in the process of calcium oxalate crystal formation. *Urological Research*, 2009. 37, 181–192.

[09ZuA] Zuckerman JM and Assimos DG. Hypocitraturia: Pathophysiology and medical management. *Reviews in Urology*, 2009. 11(3), 134–144.

[10BZC] Bertazzo S, Zambuzzi WF, Campos DDP, Ogeda TL, Ferreira CV, and Bertran CA. Hydroxyapatite surface solubility and effect on cell adhesion. *Colloids and Surfaces B: Biointerfaces*, 2010. 78, 177–184.

[10BGK] Borissova A, Goltz GE, Kavanagh JP, and Wilkins TA. Reverse engineering the kidney: Modelling calcium oxalate monohydrate crystallization in the nephron. *Medical and Biological Engineering and Computing*, 2010. 48, 649–659.

[10CBJ] Carpentier X, Bazin D, Jungers P, Reguer S, Thiaudiere D, and Daudon M. The pathogenisis of Randall's plaque: a papilla cartography of Ca compounds through an ex vivo investigation based

on XANES spectroscopy. *Journal of Synchrotron Radiation*, 2010. 17, 374–379.

[10EES] Eisner BH, Eisenberg ML, and Stoller ML. The relationship between body mass index and quantitative 24-hour urine chemistries in patients with nephrolithiasis. *Urology*, 2010. 75(6), 1289–1293.

[10Eva] Evan AP. Physiopathology and etiology of stone formation in the kidney and the urinary tract. *Pediatric Nephrology*, 2010. 25, 831–841.

[10RAA] Romero V, Akpinar H, and Assismos DG. Kidney stones: A global picture of prevalence, incidence, and associated risk factors. *Reviews in Urology*, 2010. 12(2/3), e86–e96.

[10Str] Strachan S. Trace elements. *Current Anaesthesia and Critical Care*, 2010. 21, 44–48.

[10TGD] Taunton AE, Gunter ME, Druschel GK, and Wood SA. Geochemistry in the lung: Reaction-path modeling and experimental examination of rock-forming minerals under physiologic conditions. *American Mineralogist*, 2010. 95, 1624–1635.

[10TSM] Taylor EN, Stampfer MJ, Mount DB, and Curhan GC. DASH-Style diet and 24-hour urine composition. *Clinical Journal of the American Society of Nephrology*, 2010. 5, 2315–2322.

[11BZA] Bergsland KJ, Zisman AL, Asplin JR, Worcester EM, and Coe FL. Evidence for net renal tubule oxalate secretion in patients with calcium kidney stones. *American Journal of Physiology. Renal Physiology*, 2011. 300, F311–F318. doi: 10.1152/ajprenal.00411.2010.

[11CEW] Coe FL, Evan A, and Worcester E. Pathophysiology-based treatment of idiopathic calcium kidney stones. *Clinical Journal of the American Society of Nephrology*, 2011. 6, 2083–2092.

[11Fav] Favus MJ. The risk of kidney stone formation: the form of calcium matters. *American Journal of Clinical Nutrition*, 2011. 94, 5–6.

[11KLL] Kallidonis P, Liourdi D, and Liatsikos E. Medical treatment for renal colic and stone expulsion. *European Urology Supplements*, 2011. 10, 415–422.

[11RAJ] Rodgers AL, Allie-Hamdulay S, Jackson G, and Tiselius HG. Simulating calcium salt precipitation in the nephron using chemical speciation. *Urological Research*, 2011. 39, 245–251.

[11Sch] Schrier RW. Diagnostic value of urinary sodium, chloride, urea, and flow. *Journal of the American Society of Nephrology*, 2011. 22, 1610–1613.

[11Slo] Slojewski M. Major trace elements in lithogenisis. *Central European Journal of Urology*, 2011. 2(64), 58–61.

[11SoG] Söhnel O and Grases F. Supersaturation of body fluids, plasma and urine, with respect to biological hydroxyapatite. *Urological Research*, 2011. 39, 429–436.

[11Tis2] Tiselius HG. A hypothesis of calcium stone formation: an interpretation of stone research during the past decades. *Urological Research*, 2011. 39, 231–243.

[11Tis1] Tiselius HG. Who forms stones and why? *European Urology Supplements*, 2011. 10, 408–414.

[12BaY] Bankir L and Yang B. New insights into urea and glucose handling by the kidney, and the urine concentrating mechanism. *Kidney International*, 2012. 81, 1179–1198.

[12GCG] Grases F, Costa-Bauzá A, Gomila I, Ramis M, García-Raja A, and Prieto RM. Urinary pH and renal lithiasis. *Urological Research*, 2012. 40, 41–46.

[12KuE] Kuo IY and Ehrlich BE. Ion channels in renal disease. *Chemical Reviews*, 2012. 112, 6353–6372.

[12Rob1] Robertson WG. Methods for diagnosing the risk factors of stone formation. *Arab Journal of Urology*, 2012. 10, 250–257.

[12Rob2] Robertson WG. Stone formation in the Middle Eastern Gulf States: A review. *Arab Journal of Urology*, 2012. 10, 265–272.

[13AtG] Atanassova SS and Gutzow IS. Hippuric acid as a significant regulator of supersaturation in calcium oxalate lithiasis: The physiological evidence. *BioMed Research International*, 2013. doi: http://dx.doi.org/10.1155/2013/374950.

[13MRM] May P, Rowland D, and Murray K. *JESS Primer*. Murdoch University, Perth, 2013.

[13RDD] Rendina D, De Filippo G, De Pascale F, Zampa G, Muscariello R, De Palma D, Ippolito R, and Strazzullo P. The changing profile of patients with calcium nephrolithiasis and the ascendancy of overweight and obesity: a comparison of two patient series observed 25 years apart. *Nephrology Dialysis Transplantation*, 2013. 28, iv146–iv151.

[13RAJ] Rodgers AL, Allie-Hamdulay S, Jackson GE, and Durbach I. Theoretical modeling of the urinary supersaturation of calcium salts in healthy individuals and kidney stone patients: Precursors, speciation and therapeutic protocols for decreasing its value. *Journal of Crystal Growth*, 2013. 382, 67–74.

[13WBG] Worcester EM, Bergsland KJ, Gillen DL, and Coe FL. Evidence for increased renal tubule and parathyroid gland sensitivity to serum calcium in idiopathic hypercalciuria. *American Journal of Physiology. Renal Physiology*, 2013. 305(6), F853–F860.

[14BaA] Baumann JN and Affolter B. From crystaluria to kidney stones, some physicochemical aspects of calcium nephrolithiasis. *World Journal of Nephrology*, 2014. 3(4), 256–267.

[14Cha] Chao CT. Hypernatremia-related miliaria crystallina. *Clinical and Experimental Nephrology*, 2014. 18, 831 – 832.

[14GCF] Grases G, Colom MA, Fernandez RA, Costa-Bauzá A, and Grases F. Evidence of higher oxidative status in depression and anxiety. *Oxidative Medicine and Cellular Longevity*, 2014. doi: 10.1155/2014/430216.

[13HLN] Holt C, Lenton S, Nylander T, Sørensen ES, and Teixeira SC. Mineralisation of soft and hard tissues and the stability of biofluids. *Journal of Structural Biology*, 2014. 185, 383–396.

[JESS] May PM, Rowland D, and Murray K. JESS website. `http://jess.murdoch.edu.au`, 2014. Accessed: 2014-10-14.

[14Mor] Moran ME. *Urolithiasis: A Comprehensive History*. Springer, New York, 2014.

[14Mou] Mount DB. Thick ascending limb of the loop of Henle. *American Journal of Physiology. Renal Physiology*, 2014. 9, 1974–1986.

[14RGE] Rodgers A, Gauvin D, Edeh S, Shameez AH, Jackson G, and Lieske JC. Sulfate but not thiosulfate reduces calculated and measured urinary ionized calcium and supersaturation: Implications for the treatment of calcium renal stones. *PLoS ONE*, 2014. 9. doi:10.1371/journal.pone.0103602. E103602.

[14Rod] Rodgers AL. Urinary saturation: casual or causal risk factor in urolithiasis? *BJU International*, 2014. 114, 104–110.

[15EWC] Evan AP, Worcester EM, Coe FL, Williams JJ, and Lingeman JE. Mechanisms of human kidney stone formation. *Urolithiasis*, 2015. 43, S19 – S32.

[15FGP] Fernándes-Palomeque C, Grau A, Perelló J, Sanchis P, Isern B, Prieto RM, Costa-Bauzá A, Candés OJ, Bonnin O, Garcia-Raja A, Bethencourt A, and Grases F. Relationship between urinary level of phytate and valvular calcification in an elderly population: A cross-sectional study. *PLoS One*, 2015. 10(8).

[15GCB] Grases F, Costa-Bauzá A, Bonarriba CR, Pieras EC, Fernández RA, and Rodríguez A. On the origin of calcium oxalate monohydrate papillary renal stones. *Urolithiasis*, 2015. 43, S33 – S39.

[15May] May PM. JESS at thirty: Strengths, weaknesses and future needs in the modelling of chemical speciation. *Applied Geochemistry*, 2015. 55, 3–16.

[15Rob] Robertson WG. Potential role of fluctuations in the composition of renal tubular fluid through the nephron in the initiation of Randall's plugs and calcium oxalate crystalluria in a computer model of renal function. *Urolithiasis*, 2015. 43(Supplement 1), S93–S107.

[15RWH] Rodgers A, Webber D, and Hibberd B. Experimental determination of multiple thermodynamic and kinetic factors for nephrolithiasis in the urine of healthy controls and calcium oxalate stone formers: does a universal discriminator exist? *Urolithiasis*, 2015. 43, 479–487.

[15Tis] Tiselius HG. Should we modify the principles of risk evaluation and recurrence preventive treatment of patients with calcium oxalate stone disease in view of the etiologic importance of calcium phosphate? *Urolithiasis*, 2015. 43, S47 – S57.

[15WMS] Weiner D, Mitch WE, and Sands JM. Urea and ammonia metabolism and the control of renal nitrogen excretion. *Clinical Journal of the American Society of Nephrology*, 2015. 10, 1444 – 1458.

[15Wei] Weinstein AM. A mathematical model of rat proximal tubule and loop of Henle. *American Journal of Physiology. Renal Physiology*, 2015. 308, F1076–F1097.

[15ZeK] Zeisberg M and Kalluri R. Physiology of the renal interstitium. *Clinical Journal of the American Society of Nephrology*, 2015. 10, 1831–1840.

[16PrM] Prywer J and Mielniczek-Brzóska E. Chemical equilibria of complexes in urine. a contribution to the physicochemistry of infectious urinary stone formation. *Fluid Phase Equilibria*, 2016. 425, 282–288.

[16RTS] Rabadjieva D, Tepavitcharova S, Sezanova K, and Gergulova R. Chemical equilibria modeling of calcium phosphate precipitation and transformation in simulated physiological solutions. *Journal of Solution Chemistry*, 2016. 45, 1620–1633.

[16TFM] Tominaga N, Fernandez S, Mete M, Shara NM, and Verbalis JG. Hyponatremia is associated with increased kidney stones in a large U.S. health system population. In *Kidney Week 2016 Abstract Supplement*. American Society of Nephrology, 2016 469A. Poster presented at the 2016 Kidney Week meeting in Chicago, Nov. 15-20. Poster FR-PO458.

[17ARI] Arzoz-Fabregas M, Roca-Antonio J, Ibarz-Servio L, Jappie-Mahomed D, and Rodgers AL. Stress-stones-stress-recurrent stones: a self-propagating cycle? Difficulties in solving this dichotomy. *Urolithiasis*, 2017. doi:10.1007/s00240-017-0970-5.

[17HKM] Hill MG, Königsberger E, and May PM. Mineral precipitation and dissolution in the kidney. *American Mineralogist*, 2017. 102(4), 701–710.

[17MaR] May PM and Rowland D. JESS, a Joint Expert Speciation System - VI: thermodynamically-consistent standard Gibbs energies of reaction for aqueous solutions. *New Journal of Chemistry*, 2017. doi:10.1039/c7nj03597g.

[17Rob] Robertson WG. Do "inhibitors of crystallisation" play any role in the prevention of kidney stones? A critique. *Urolithiasis*, 2017. 45, 43–56.

[17Rod] Rodgers AL. Physicochemical mechanisms of stone formation. *Urolithiasis*, 2017. 45, 27–32.

[17RoJ] Rodgers AL and Jackson G. Determination of thermodynamic parameters for complexation of calcium and magnesium with chondroitin sulfate isomers using isothermal titration calorimetry: Implications for calcium kidney-stone research. *Journal of Crystal Growth*, 2017. 463, 14–18.

Index